THE ANTIPLASMODIAL, TOXICITY AND PHARMACOKINETIC PROPERTIES OF SYNTHETIC DERIVATIVES OF THE NATURAL PRODUCT CURCUMIN

by

FAITH APOLOT OKALEBO

Thesis presented for the Degree of

DOCTOR OF PHILOSOPHY

In the Division of Clinical Pharmacology

UNIVERSITY OF CAPE TOWN

June, 2008

Supervisors

ASS. PROF. PETER J. SMITH, PROF. KELLY CHIBALE, ASS. PROF. ANASTASIA N. GUANTAI

DECLARATION

I, Faith Okalebo, declare that the thesis, "The Antiplasmodial and Pharmacokinetic Properties of Synthetic Derivatives of the Natural Product Curcumin" is my own work and that all sources that I have used or quoted have been indicated and acknowledged by means of complete references.

I grant the University of Cape Town free license to reproduce this thesis in whole or in part for the purpose of research.

This thesis is presented for examination for the degree of Doctor of Philosophy

Faith Apolot Okalebo

Date

"There along the banks of the river, were very many trees, on one side and the other. Their fruit will be for food and their leaves for medicine and for the healing of the nations."

Ezekiel 47: 7, 12; Revelation 22: 2.

ACKNOWLEDGEMENTS

I would like to thank the following for their contributions towards the preparation of this thesis.

First and foremost, God Almighty and for His divine guidance, mercy and protection during my studies. I am grateful for the opportunity to pursue my post graduate studies.

I am indebted to my supervisors, Profs. Peter J. Smith, Kelly Chibale and Anastasia N. Guantai, for their enduring patience, guidance and support. I am also indebted to Mr. Bill Campbell who also provided supervisory guidance. I also wish to thank the herbalist, Mr. Muiruri for revealing the medicinal value of *Curcuma longa* and supplying me with samples which triggered my interest in the natural product curcumin.

My husband, David Kennedy Cherutich, for his untiring patience and for giving me permission to go away to pursue my studies. I wish to thank my parents, Prof. John Robert Okalebo and Mary Teresa Apolot for setting very high standards for me and all they have done for me. I wish to thank my grandmother, Grandma Asio, for bringing me up and for her quiet example of hard work, patience and endurance. I wish to thank Eva Apomo, Linet Akweny, Ivans Elaborot and my brother, Sammy Emasit, for taking care of my children during my long period of absence.

University Science, Humanities and Engineering Partnerships in Africa (USHEPiA) for their financial and logistic support that made my dream a reality. I wish to acknowledge the specific contributions of the following members of the team: Prof. Martin West, Leslie Shackleton, Nan Warner, Zubaida Zhattas, Caroline Ojwang, Rosemary Wolson, Saudin Mwakaje, Mohoto Masego and Humprey Webuye. I wish to thank the University of Nairobi for granting me study leave and financial support.

I wish to thank Noel Hendricks and Pete Roberts of the Department of Chemistry and Jean M. McKenzie of Stellenbosch University for running NMR spectra for me. I am grateful to Alicia Evans of the Division of Clinical Pharmacology, UCT and Tommie van der Merwe of the Mass Spectrometry Service, University of Witwatersrand for running the mass spectra. I wish to acknowledge Lubbe Weisner for his guidance and for running mass spectra for the pharmacokinetic study.

I wish to thank the following past and present postgraduate and post-doctoral students for sharing their expertise and for providing a stimulating academic environment: Dr. Malefa Tselanyane; Dr. Bongi Gumede; Dr. Natasha October; Dr. Susan Yeh; Dr. Claire Muhanji; Dr. Alex Chipeleme; Dr. Chitalu Musonda; Dr. Albert Ndakala; Carmen Lategan; Mamello Sekhoacha; Dale Taylor; Renate Hans; Linda Mbeki; Tzu-Shean Feng; Richard Gessner; Eric Guantai; Ze-ev Krein; Tanya Paquet; and Candice Soares de Melo

I thank Sumaya Salie and Noor Salie for their great kindness and assistance in numerous experiments. I wish to thank the Diana Steele, Seta Jackson, Noor Ismail and all the staff of Knowledge Commons (University of Cape Library) for training me on how to do literature searches, use Refworks™ and for assistance in editing and formatting this thesis.

I wish to acknowledge the kind services of Prof. C. Himonga, Patrick Rezandt, Veronica De Waal and the all staff of All Africa House for making my stay in Cape Town as comfortable as possible.

ABSTRACT

Malaria is the most devastating protozoal infection in humans. There is widespread resistance to existing antimalarial agents hence the need for new antimalarial drugs. Curcumin, a natural product isolated from *Curcuma longa/domestica*, was used as a scaffold for the synthesis of new compounds with antiplasmodial activity. Curcumin was selected because of its low toxicity and is commercially available at a low cost.. Derivatives of curcumin were designed to act against selected molecular targets in *Plasmodium falciparum*. It was hoped that the derivatives would have a better oral bioavailability and antiplasmodial activity than the parent compound. The derivatives were tested for *in vitro* antiplasmodial activity against the chloroquine sensitive (D10) and chloroquine resistant (K1) strains. In addition they were evaluated for their *in vitro* ability to inhibit the formation of beta- hematin which is the chemical equivalent of hemozoin which is responsible for the pathophysiological responses observed in malaria.

The classes of derivatives synthesized included: the azoles; sulfonylureas; aminoquinolines; thiosemicarbazones and *N*-acyl hydrazones. All classes of derivatives tended to show isomerism. In the case of the pyrazole derivative, hydrazinocurcumin, two tautomers were synthesized (**2.2.1a** and **b**). There was a 10 fold difference in the *in vitro* antiplasmodial activity of the tautomers.

Three isomers of the isoxazole derivative were synthesized and these had comparable *in vitro* activity. Sulfonylurea derivatives were highly cytotoxic and had improved activity against the chloroquine sensitive strain (CQS), D10. Unlike curcumin, all derivatives were less active against the chloroquine resistant strain except for the thiosemicarbazone derivatives and the *N*-acyl hydrazone derivative, **2.10.3**. All derivatives inhibited the formation of beta-hematin and in this regard were superior to chloroquine.

The isoxazole derivative, **2.2.2a**, the aminoquinoline derivative, **2.8.1**, and the *N*-acyl hydrazone derivative, **2.10.3,** were subjected to a pilot toxicological investigation performed on mice. They were more toxic than curcumin and may affect neurological function. The most toxic compound was the *N*-acyl hydrazone derivative, **2.10.3**. The findings of the toxicological investigation were used to select an optimal dose for the *in vivo* antimalarial test. A repeated dose of 25 mg/kg of body weight (bwt.) for 4 days was considered safe for the *in vivo* antimalarial test.

Five derivatives were tested for *in vivo* antimalarial activity in mice infected with the CQS *Plasmodium berghei* ANKA strain. All the test compounds suppressed parasitemia on Day 4 by over 50 % with the exception of the pyrazole derivative, **2.2.1b**, and the aminoquinoline derivative, **2.8.1**. There was a statistical significant difference in the levels of parasitemia of the test and control mice for animals treated with the isoxazole (**2.2.2a),** sulphonylurea (**2.5.4**) and *N*-acyl hydrazone (**2.10.3**) derivatives. However, their ability to suppress parasitemia was inferior to orally administered chloroquine (10 mg/kg of bwt) which suppressed parasitemia completely until the 8^{th} day of the study. The pyrazole (**2.2.1b**) and isoxazole (**2.2.2c**) derivatives prolonged survival of infected mice at a dose of 100 mg/kg of bwt.

The pyrazole derivative, hydrazinocurcumin (**2.2.1b**), was selected for the pharmacokinetic investigation, because of its high yields on synthesis. An LC-MS/MS method was developed for quantification of **2.2.1b** in murine and human blood. The method was validated and its precision and accuracy were within accepted limits. The lower limit of quantification was 0.625 µg/ml and the limit of detection was 0.156 µg/ml. The oral bioavailability of hydrazinocurcumin was affected by the pH of the vehicle. Hydrazinocurcumin was found to have a very short half-life of about 0.452 hours. The short half-life explained the poor *in vivo* antimalarial activity of pyrazole derivative in infected mice. Hydrazinocurcumin has a better oral bioavailability than curcumin.

In conclusion, synthetic derivatives with improved *in vitro* antiplasmodial activity were synthesized. The *in vivo* antimalarial activity of selected derivatives was inferior compared to chloroquine. In the case of one of the derivatives, hydrazinocurcumin, the poor *in vivo* activity was due to a short half-life. More chemical modifications are required to improve *in vitro* and *in vivo* antiplasmodial activity of these derivatives.

ABBREVIATIONS

δ	Chemical shift in parts per million
µg	Microgram(s)
µM	Micromolar
ACN	Acetonitrile
AIDS	Acquired Immunodeficiency Syndrome
ANOVA	Analysis of Variance
AUC	Area under the Curve
AUC_{all}	Area under the curve from the time of dosing to the last time point.
AUC_{last}	Area under the curve from the time of dosing to the last measurable concentration
$AUC_{0-t\infty}$	Area under the curve from the time of dosing to time extrapolated to infinity.
BLOQ	Below lower limit of quantification.
br	Broad
br s	Broad singlet
Bwt.	Body weight
^{13}C NMR	Carbon Nuclear Magnetic Resonance
CC_{50}	50 % Cytotoxic Concentration
CD_3OD	Deuteromethanol
CH_3CN	Acetonitrile
CHO	Chinese Hamster Ovarian cells
Cmax	Maximum observed drug concentration
CM	Complete medium
COSY	proton-proton homonuclear shift COrrelated SpectroscopY
CQ	Chloroquine
CQR	Chloroquine Resistant
CQS	Chloroquine Sensitive
Cys	Cysteine
d	Doublet

dd	Double doublet
CH_2Cl_2	Methylene chloride/Dichloromethane
DCM	Methylene chloride/Dichloromethane
DHFR	Dihydrofolate reductase
DHPS	Dihydropteroate synthetase
DMEM	Dulbecco's Modified Eagles' Medium
DMF	*N*, *N*-Dimethylformamide
DMSO	Dimethylsulfoxide
d-DMSO	Deutero dimethlysulfoxide
DNA	Deoxyribonucleic acid
EI	Electron Impact
ESI	Electro Spray Ionization
EtOAc	Ethyl acetate
EtOH	Ethanol
Eq.	Equivalent
FA	Formic Acid
FAB	Fast Atomic Bombardment
FCS	Fetal calf serum
FT-IR	Fourier Transform Infrared Spectroscopy
g	gram(s)
h	hour
HAMS	Ham's Nutrient Mixture F-12
^{1}H NMR	Proton Nuclear Magnetic Resonance
His	Histidine
HMQC	Heteronuclear Multiple Quantum Correlation
HPLC	High Performance Liquid Chromatography
HSQC	Heteronuclear Single Quantum Coherence
HRMS	High Resolution Mass Spectrometry
Hz	Hertz
IC_{50}	50 % Inhibitory Concentration
IR	Infrared spectroscopy
J	Coupling constant

LD_{50}	the statistically derived single dose that can be expected to cause death in 50% of the animals under specific conditions of the test
LLOQ	Lower limit of quantification
LC-MS/MS	Tandem mass spectrometry coupled to HPLC
LRMS	Low Resolution Mass Spectrometry
m	Multiplet
min	Minute(s)
mM	Millimolar
ml	Milliliter
M+	Molecular ion
MeOH	Methanol
MHz	Mega Hertz
mp	Melting Point
MTT	3-(4,5-dimethylthiazol-2-yl)-2-5-diphenyltetrazolium bromide
m/z	Mass to charge ratio
n	Sample size
ND	Not determined
NMR	Nuclear Magnetic Resonance
PBS	Phosphate-buffered saline
Pet ether	Petroleum ether
Ph	Phenyl
pLDH	parasite Lactate Dehydrogenase
ppm	parts per million
prep. TLC	Preparative Thin Layer Chromatography
q	Quartet
Q_1	First quadrapole
Q_3	Third quadrapole
RBC	Red Blood Cell
rcf	relative centrifugal force

R_f	Retention factor
RI	Resistance Index
RNA	Ribonucleic acid
rpm	revolutions per minute
rt	Room temperature
s	Singlet
SD	Standard Deviation
SI	Selectivity Index
t	Triplet
TLC	Thin Layer Chromatography
Tmax	Time taken to achieve maximum observed concentration
TMS	Trimethylsilyl
$t_{R'}$	Retention time
UV	Ultra violet
WHO	World Health Organization

TABLE OF CONTENTS

LIST OF TABLES

LIST OF SCHEMES

LIST OF FIGURES

CHAPTER ONE
INTRODUCTION AND LITERATURE REVIEW

1.1 Introduction

Malaria is the most important protozoal disease in humans and is a major killer in Africa and other tropical countries. Existing antimalarial agents have many shortcomings such as low efficacy due to drug resistance. There is need for new effective antimalarial agents. Plants have been a key source of new drugs since time immemorial. Unfortunately natural products often do not meet the level of activity and pharmacokinetic properties required of a drug. To overcome these challenges, natural products are subjected to chemical derivatization to improve their potency and pharmacokinetic properties. Chemical modifications often follow the principles of rational drug design which involves incorporation of pharmacophores with known activity against molecular targets. In this study curcumin was subjected to chemical modifications aimed at improving activity against the malaria parasite and the following presumed molecular targets: cysteine proteases; hemozoin formation; iron-dependent enzymes; parasite induced new permeability pathways (NPPs). This chapter describes these molecular targets and key structural features of known compounds that act on these sites. Finally, the study objectives are presented.

1.1.1 Aetiology and Epidemiology of Malaria

Malaria is an acute febrile illness characterized by shivering, muscle pains, headache and vomiting. In humans, malaria is caused by *Plasmodium falciparum*, *P. vivax*, *P. malariae* and *P. ovale*. *Plasmodium knowlesi*, which usually causes simian malaria, may infect humans [1]. The genus Plasmodium belongs to the phylum Apicomplexa which is characterized by obligate intracellular protozoa. The severity of an infection of malaria is dependent on the type of infecting strain and the immune status of the human host. Severe

complicated malaria involves a number of conditions such as: cerebral malaria; anemia; renal failure; and respiratory failure [2].

1.1.2 Transmission of malaria and the Lifecycle of Plasmodium

Malaria is transmitted by the female Anopheles mosquito which thrives in humid, warm climates at environmental temperatures of 20 to 30°C. The mosquito lays its eggs in water and subsequent larval development is determined by water salinity, water temperature, food quantity and the larval density [3]. The presence of large water masses and rainfall favors breeding of mosquitoes throughout the year.

Gametocytes, the sexual stage of Plasmodium, are critical for the transmission of malaria. They are produced in the human host during the asexual stage from the merozoites [4, 5]. The male gametocyte is smaller and is called the microgamete while the female gametocyte is called the macrogamete. Gametocytes are taken up by a female Anopheles mosquito during a blood meal [6] (Figure 1-1). Within the mosquito the blood meal is digested by mosquito proteases and within 60 minutes the macrogamete and microgamete fuse in the mid-gut to form the zygote[7].

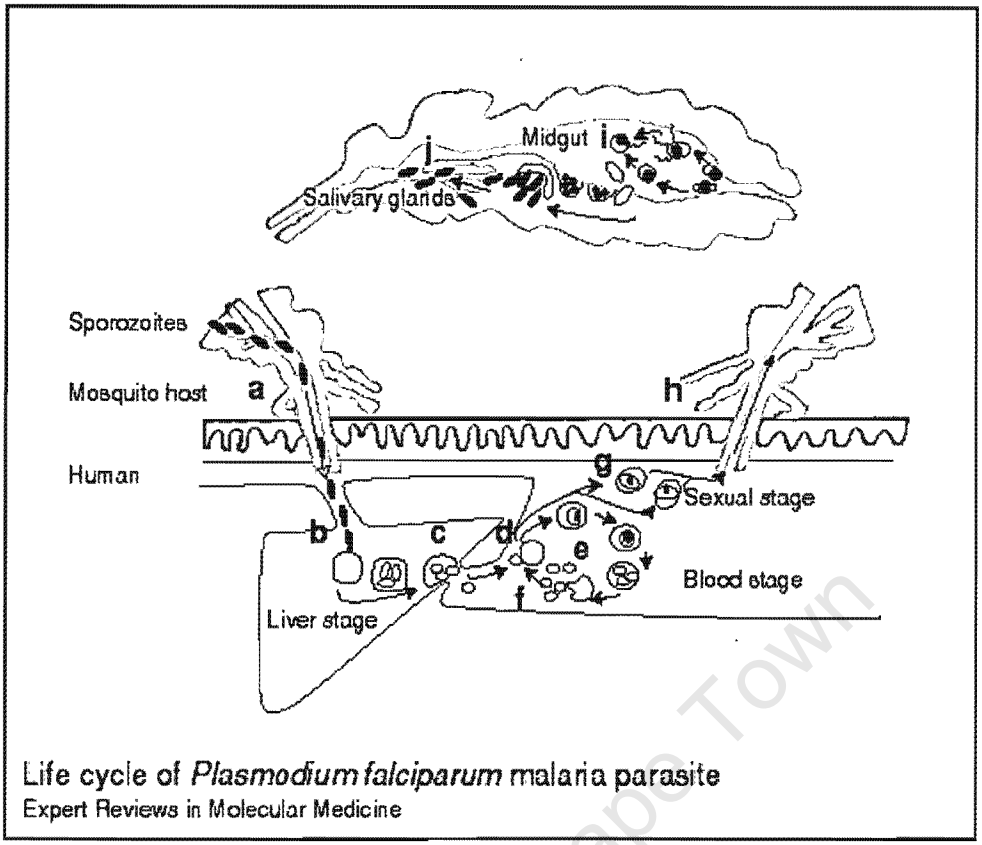

Figure 1 - 1: Life cycle of *PLASMODIUM FALCIPARUM* [8]

(a) An infected Anopheline female mosquito takes up a blood meal from a human host and injects infective sporozoites into the peripheral circulation.

(b) Invasion of hepatocytes in the liver by sporozoites where they undergo asexual multiplication for one week to produce merozoites.

(c) Rupture of the infected hepatocytes to release merozoites into peripheral circulation.

(d) The merozoites invade red blood cells (RBC).

(e) Multiplication in the RBC within 48–72 h leading to the production of 16–20 merozoites per RBC. Merozoites initially form rings/schizonts which mature to trophozoites which transform into merozoites.

(f) The released merozoites invade additional RBCs and carry on the cycle.

(g) Some invading merozoites do not divide, but differentiate into male (microgametocyte) and female (macrogametocyte) sexual forms.

(h) Sexual forms are taken from the bloodstream by a feeding female *Anopheles* mosquito.

(i) Fertilization in the mosquito midgut to form zygotes. These zygotes further differentiate into motile forms, called ookinetes, migrate through the mosquito gut wall and divide within oocysts on the external gut wall to form thousands of sporozoites.

(j) The infective sporozoites are released into the mosquito haemocoele and move to the salivary gland, where they await injection into another human host, thus completing the life cycle.

The zygote matures to form a flagellated ookinete which makes its way to the hemolymph located on the side of the mosquito mid-gut where it undergoes mitotic division to form sporozoites which are the infective form of the parasite [7]. The sporozoites are released into the human blood stream during the next blood meal of an infected mosquito. The sporozoites invade the heptatocytes in the liver where they form schizonts which differentiate and mature into merozoites. These are released into the blood stream. This marks the beginning of clinical disease. The merozoites invade red blood cells (RBC) and form rings within the cell. The ring stage matures into a trophozoite which undergoes cellular division to form schizonts. Forty eight hours after the invasion of the RBC, it ruptures to release merozoites which in turn infect more RBCs. The release of merozoites is associated with clinical signs such as fever, chills and vomiting.

1.1.3 The Epidemiology of malaria

The estimated average annual number of clinical attacks due to malaria is 515 (300 - 660) million of which 70 % occur in Africa [9]. The Democratic Republic of Congo and East Africa have the highest transmission rates of malaria in Africa [10, 11]. In sub-Saharan Africa, malaria is the leading cause of death in children aged between 0 to 4 years. It is the second leading cause of death amongst adults aged between 15 to 59 years [12]. About 80 % of the people at risk in Africa live in hyperendemic and haloendemic regions where the prevalence of malaria is over 50 %. The endemic distribution of malaria is presented in Figure 1-2 [13].

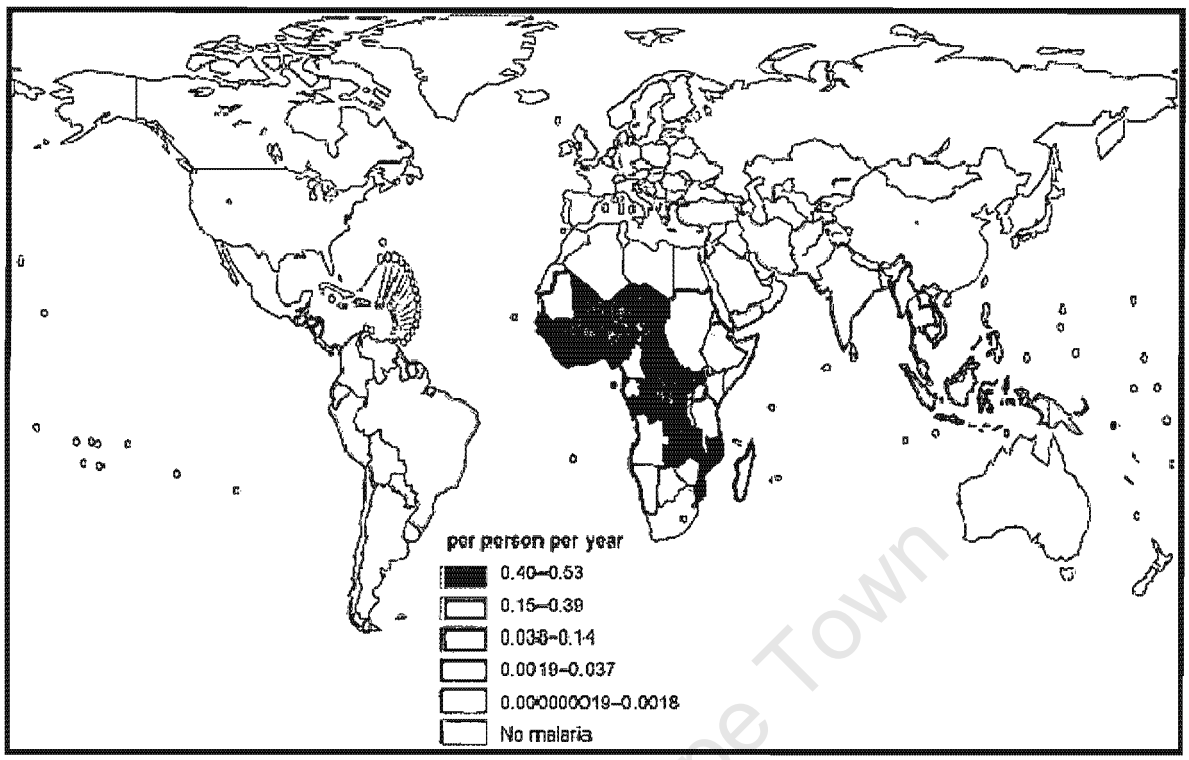

Figure 1 - 2: Geographic distribution of malaria [13]

Mortality and morbidity due to malaria have been increasing since 1970. Child mortality due to malaria has increased from 6.0 deaths per 1000 children in the 1990s to 8.0 deaths per 1000 children in 2001 [12]. Reasons for the increased morbidity and mortality due to malaria include: global warming; persistent use of ineffective drugs; human migration; deforestation; overcrowding; and resistance to insecticides [3, 11]. A one degree rise in global mean temperature due to global warming is expected to cause an additional 64, 475 deaths worldwide due to increased incidence of malaria and other mosquito borne infections [14].

Malaria is a disease of the poor and is restricted to low income countries [9]. Poor people in Africa are particularly susceptible to malaria because they cannot afford personal protective measures such as insecticide sprays and insecticide treated nets and lack access to effective health care [3, 11]. The additional burden of disease due to malaria and other vector borne diseases due to global warming is likely to have negative economic impacts and reduce economic growth in Africa by 13 % [15].

1.2 Antimalarial Agents in Clinical Use

Drugs are the mainstay for the management and prevention of malaria since there is no effective vaccine for malaria. It may not be technically feasible to produce an effective vaccine because Plasmodia produce many antigens [16, 17]. The antimalarials in clinical use are classified as: arylamino alcohols, 4- and 8-aminoquinolines, antifolates, endoperoxides and antibiotics.

1.2.1 An overview of Antimalarials in Clinical Use

The arylaminoalcohols include: quinine (**1.1**); mefloquine (**1.2**); halofantrine (**1.3**) and lumefantrine (**1.4**, Figure 1-3) [18].

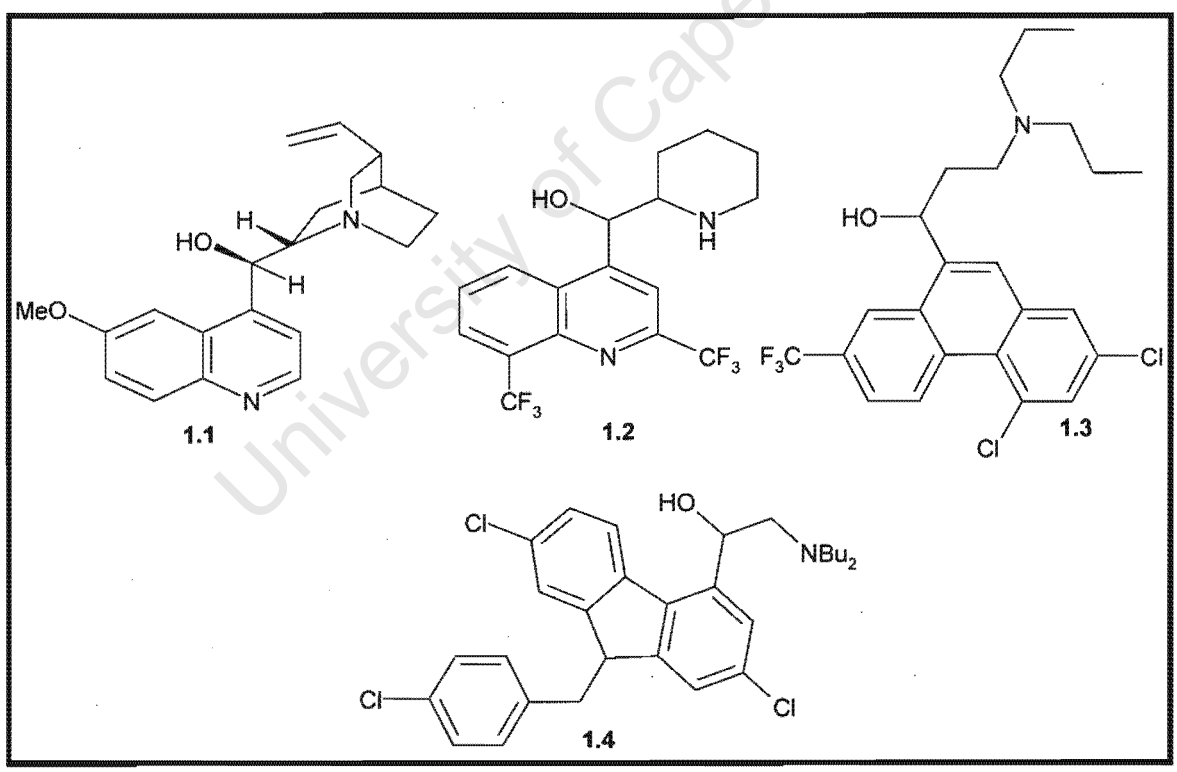

Figure 1 - 3: Chemical structures of the aryl amino alcohols: quinine (1.1), mefloquine (1.2), halofantrine (1.3) and lumefantrine (1.4).

Quinine (**1.1**) is the most widely used agent in this class and is used for the management of severe complicated malaria as a slow infusion. Mefloquine (**1.2**) and halofantrine (**1.3**) are second line drugs for management of chloroquine-resistant uncomplicated malaria [18]. Lumefantrine (**1.4**) is used in drug combinations such as CoArtem™ which is currently the first line drug for the management of uncomplicated malaria [19].

The 4-aminoquinolines include chloroquine (**1.5**), amodiaquine (**1.6**) and isoquine (**1.7**) while the 8-aminoquinolines include primaquine (**1.8**, Figure 1-4) [18].

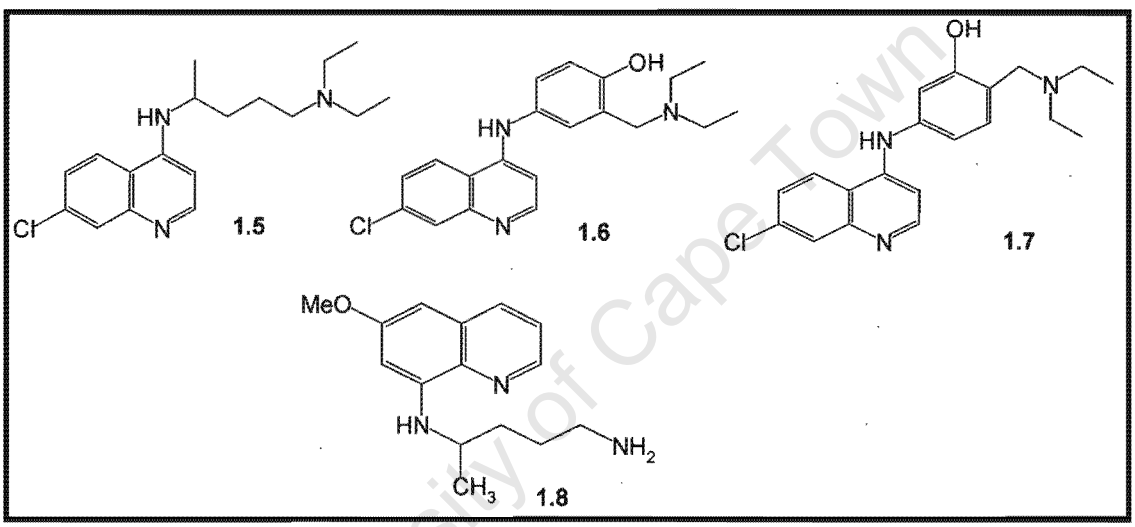

Figure 1 - 4: Chemical structures of chloroquine (1.5), amodiaquine (1.6), isoquine (1.7) and primaquine (1.8)

Chloroquine (**1.5**) was the first line drug for the management of uncomplicated malaria for a long time but its use was discontinued due to widespread resistance [20, 21]. Amodiaquine (**1.6**) is active against chloroquine resistant malaria but its use is restricted due to its propensity to cause hepatotoxicity and agranulocytosis. Isoquine (**1.7**) is an isomer of amodiaquine and is less toxic because it is not metabolized to a quinoneimine [22]. Primaquine (**1.8**), is active against the hepatic forms of the parasite and is used to eradicate dormant parasites and as a chemoprophylactic agent [18].

The antifolates include: biguanides; 2-aminopyridimidines; sulfonamides; and sulfones [18]. Antifolates inhibit the *de novo* synthesis of folic acid by the parasite. The biguanides include proguanil (**1.9**) and chlorproguanil (**1.10**). The 2-aminopyrimidines include trimethoprim (**1.11**) and pyrimethamine (**1.12**). The sulphonamides used for the treatment of malaria include sulfamethoxazole (**1.13**) and sulfadoxine (**1.14**) while the sulfones are represented by dapsone (**1.15**, Figure 1-5).

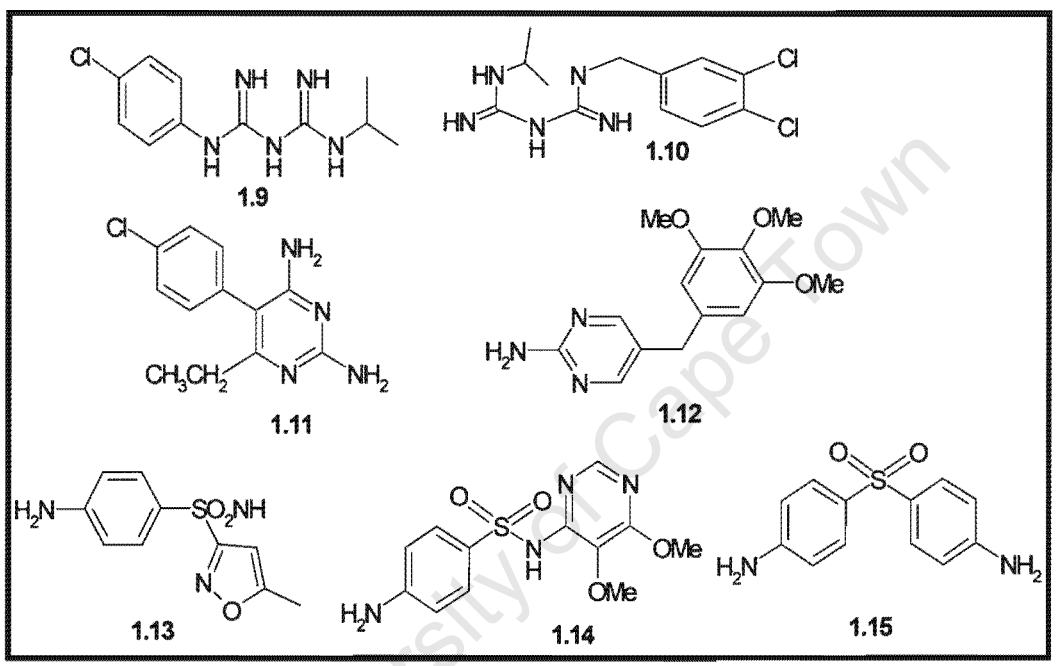

Figure 1 - 5: Chemical structures of antifolate antimalarial agents

Biguanides and 2-aminopyrimidines inhibit the enzyme dihydrofolate reductase (DHFR) which is responsible for the reduction of dihydrofolate to tetrahydrofolate. Sulphonamides and sulfones inhibit the enzyme dihydropteroate reductase. The antifolates are slow acting against the erythrocytic stages of the parasite. Antifolates are used as drug combinations such as the combination pyrimethamine and sulfadoxine and the combination chlorproguanil and dapsone [19].

The endoperoxide antimalarials include artemisinin (**1.16,** Figure 1-6), artesunate (**1.17**) and artemether (**1.18**). Artemether-lumefantrine

(coartemether or CoArtem™) is a fixed dose combination which is the WHO recommended first line drug for the management of uncomplicated malaria [23].

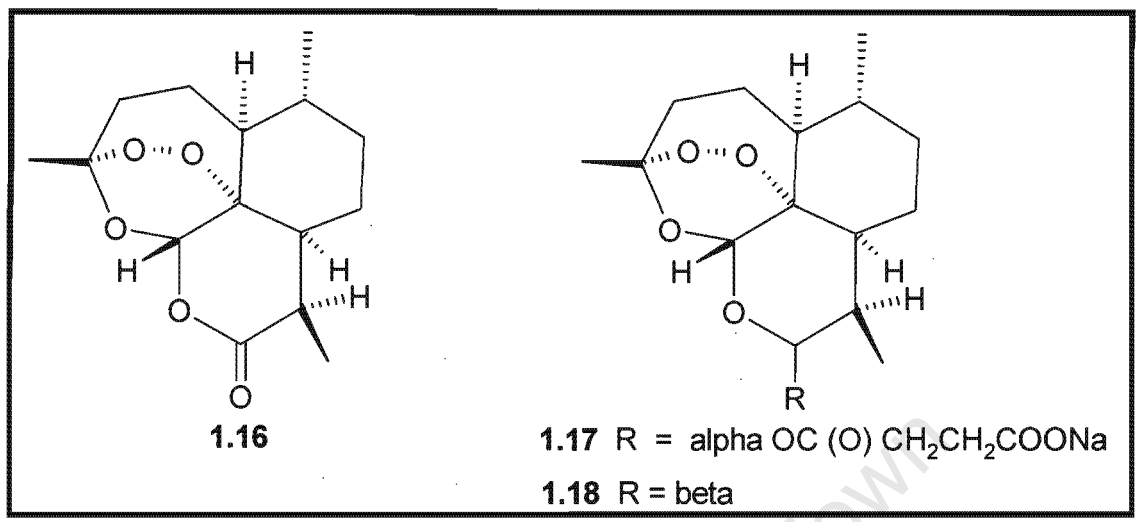

Figure 1 - 6: Chemical structures of Artemisinin (1.16) and first generation endoperoxide derivatives.

Atovaquone (**1.19**, Figure 1-7) is a napthoquinone and is a structural analogue of coenzyme Q. It acts on the mitochondrial electron transport chain leading to collapse of the organelle's membrane potential. It is not widely used because of its high cost and resistance developed soon after its introduction. It is used in combination with proguanil for the prophylaxis of malaria [18].

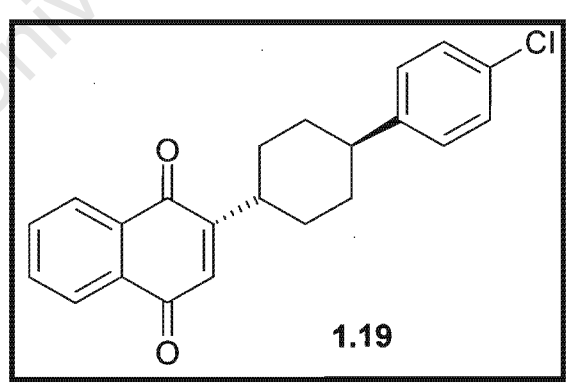

Figure 1 - 7: Chemical structure of Atovaquone (1.19)

Antibiotics are not widely used for the management of malaria because they have a slow and modest antimalarial effect. They include tetracycline (**1.20**, Figure 1-8), doxycycline (**1.21**) and clindamycin (**1.22**)[18].

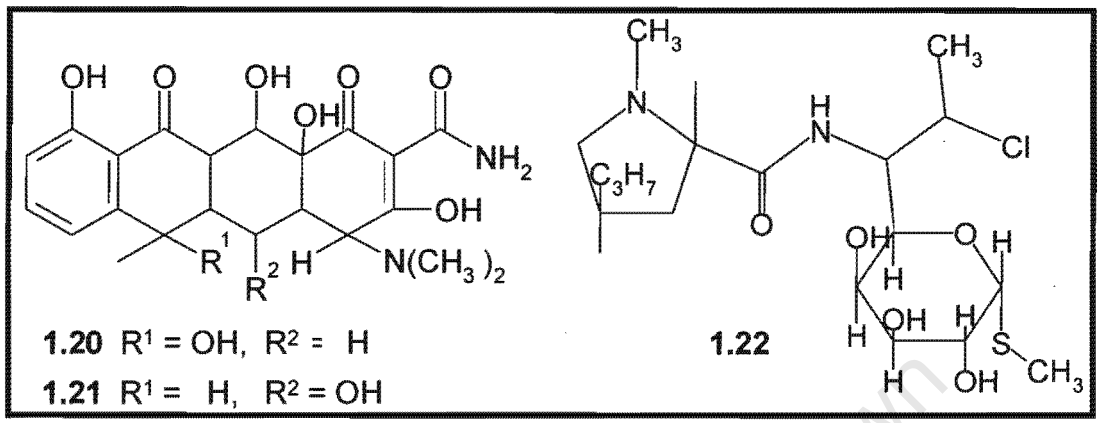

Figure 1 - 8: Chemical structures of Tetracycline (1.20), Doxycycline (1.21) and Clindamycin (1.22).

1.2.2 Short comings of Antimalarials in Clinical Use

An ideal antimalarial agent should have good *in vivo* efficacy and a rapid onset of action. It should produce a radical cure by acting against the asexual parasites in the liver. The half-life should be short enough so that residual levels of the drug do not persist. Antimalarial agents with long half-lives such as sulfadoxine are associated with persistent residual drug levels which provide selection pressure for the development of resistance [24, 25]. On the other hand, the half-life should be long enough to allow a low dosing frequency which is associated with improved adherence [26]. Artemisinin derivatives have short half-lives and therefore require frequent dosing leading to poor adherence. They are associated with high rates of recrudescence [27]. An ideal antimalarial drug should have a low potential for the development of resistance. Compounds to which resistance develop rapidly usually act at a single molecular target and are structurally related to compounds to which drug resistance is established [28, 29]. Rapid resistance developed to antifolates and atovaquone because they act at one point of the metabolic cycle of

Plasmodium [25, 30]. Resistance developed rapidly to mefloquine and halofantrine because of cross resistance to quinine. Since malaria is mainly restricted to poor tropical countries, an antimalarial agent should be affordable. Drugs that can be .synthesized on a large scale in a few steps tend to have a low cost. Artemisinin derivatives are very costly because the starting material is costly since it is obtained from plants in very low yields. An ideal antimalarial drug should have good oral bioavailability so that adequate plasma levels are achieved on routine use. In addition there should be the option for formulation of the drug for parenteral use for severe complicated malaria [27, 31]. An ideal antimalarial agent should have a low toxicity profile [29, 31, 32]. To reduce transmission of malaria, antimalarial agents should be active against the gametocyte stage of the parasite. The only two agents that meet this criterion are artemisinin derivatives and primaquine. All antimalarial agents in clinical use do not meet the criteria of an ideal antimalarial agent. The key advantages and shortcomings of the most widely used agents are summarized in Table 1-1.

Table 1- 1: Short Comings of Antimalarial Drugs in Clinical Use [27-29]

DRUG	KEY ADVANTAGES	KEY LIMITATIONS
Quinine	Effective in severe complicated malaria.	Highly toxic – tinnitus, Short half life, Poor Adherence Drug resistance in Asia
Chloroquine	Low cost, Long half-life, Rapidly acting, Good adherence	Wide spread drug resistance
Amodiaquine	Active against chloroquine resistant strains (CQR), Low cost, Long half -life	Toxicity - agranulocytosis
Mefloquine	Active against CQR strains	Cross-resistance with quinine, Toxicity – neuropsychiatric disorders, High cost
Halofantrine	Active against CQR strains	Cardiac arrhythmias, Cross resistance with quinine, High cost
Artemisinin derivatives	Not toxic, Rapidly acting Partially gametocidal Low chances of resistance	Short half lives Frequent dosing High cost
Lumefantrine	Long half-life , active against resistant strains	High cost, Ototoxicity Erratic absorption
Sulphadoxine-Pyrimethamine	Low toxicity, low cost	Slow acting, Wide spread drug resistance
Atovaquone	Good prophylactic agent	High cost, Rapid development of resistance, erratic absorption

1.3 Drug Resistance to Antimalarials

Drug-resistant malaria is defined as "an infection that survives a deliberate attempt to eradicate it using a standard drug protocol" [25]. Levels of drug resistance range from low to high-level resistance. Most worrying is the phenomenon of Accelerated Resistance to Multiple Drugs (ARMD) whereby certain *P. falciparum* strains are capable of developing resistance to multiple unrelated drugs [33, 34]. Though drug combinations are likely to slow the development of resistance, resistance to drug combinations such as atovaquone and cycloguanil (Malarone™) developed soon after their introduction [35, 36].

Drug resistance has resulted in epidemics of malaria in areas of highland areas where there is low endemicity and low partial immunity [37]. Drug resistant malaria causes more severe illness with higher mortality rates and increased rates of recrudescence. However, in some cases, the mutant drug resistant parasites are less virulent than the wild-type and cause less severe disease [38]. Drug resistance has forced many African countries to switch to more expensive antimalarial drugs such as artemisinin-lumefantrine. The increased case loads have overburdened the health systems [37].

The earliest record of drug resistance was resistance to quinine in 1908 in Brazil and later in 1938 in German railway workers returning from Brazil [20]. Today there are varying degrees of resistance to quinine worldwide. Fortunately, high-level resistance to quinine is restricted to South East Asia. The gene responsible for quinine resistance is *P. falciparum* Na^+/H^+ *exchanger-1* (*pfnhe-1*) which codes for the Na^+/H^+ exchanger located on the food vacuole [39].

Chloroquine was synthesized in 1944 and marketed in 1945. It was the most widely used antimalarial agent until the late 80s because of its low cost. Unlike many antimalarial drugs that were subsequently introduced, resistance to chloroquine took a long time to develop. Resistance to chloroquine began

to appear around 1960 and gradually spread to South East Asia and South America. There was a considerable delay in the appearance of chloroquine resistant strains in Africa where it only appeared from 1979 to 1984. Today, high level resistance to chloroquine is now widespread through out the world and it is no longer a first line agent for the management of uncomplicated malaria [20, 21].

Chloroquine resistance is associated with low drug concentrations in the food vacuole which is the site of action of chloroquine. There is lack of agreement as to whether the low drug concentrations in the food vacuole is caused by increased transporter mediated efflux [40, 41] or decreased uptake into the vacuole by transporter proteins [42]. Some researchers argue that reduced accumulation in the food vacuole is not transporter mediated but is a result of change in the pH gradient between the cytosol and food vacuole due to the presence of dysfunctional proton pumps which are incapable of maintaining the acidity of the food vacuole [43-46]. The resultant increase in vacuolar pH prevents chloroquine influx by ion trapping.

While most of the proposed mechanisms focus on chloroquine transport across the food vacuole membrane, a diverging view is that resistance is a result of increased energy-dependent efflux of chloroquine from the cytoplasm resulting in decreased levels in the food vacuole [47-50].

The two main genes implicated in quinoline resistance are *P. falciparum multi-drug resistance1* (*pfmdr1*) and *P. falciparum chloroquine resistance transporter* (*pfcrt*). The *pfcrt* gene codes for a transporter called *P. falciparum* Chloroquine Resistance Transporter (PfCRT) which is a trans-membrane protein with 424 amino acid residues. Replacement of the charged lysine residue at codon K76T with uncharged threonine reduces the ability of PfCRT to maintain the acidity of the food vacuole [51, 52]. The gene, *pfmdr1*, codes for a protein called P-glycoprotein homologue 1 (Pgh1) which causes the efflux of drugs from the cytoplasm and is responsible for cross resistance across the quinolines [53, 54].

Antifolates replaced chloroquine as the first line agents for the management of uncomplicated malaria in the early 90s. Unfortunately resistance to the combination sulfadoxine-pyrimethamine spread so fast that in less than 5 years it was no longer the first line drug for the treatment of malaria [55]. It was quickly replaced by lumefantrine-artemether combination. About 5 amino acid changes on dihydropteroate reductase are responsible for resistance to sulfadoxine and dapsone. About 13 amino acid changes in dihydrofolate reductase have been identified in mutants resistant to pyrimethamine, chlorproguanil and trimethoprim [56-59].

There are early warnings that resistance to the most recently introduced antimalarial agents may develop soon. Tolerance to the lumefantrine component of artemether-lumefantrine combination has been reported [60]. The mutation responsible for *in vitro* resistance to artemisinin is S76N which abolishes the ability of the drug to inhibit (Plasmodium falciparum adenosine triphosphotase) PfATPase which is one of the targets of artemisinin [61]. Resistance to atovaquone appeared shortly after its introduction and was caused by point mutations which caused changes at amino acid Y268S/N of cytochrome b [35, 62, 63].

1.4 Natural Products as Sources of New Drugs

In view of the fact that existing antimalarial agents have many shortcomings and there is widespread resistance, there is an urgent need to develop efficacious new agents. Since time immemorial plants have been used for the treatment of disease in both man and animals in their crude form as decoctions, infusions and powders. Empirical studies showed that natural products are more likely to make it to the market compared to purely synthetic molecules because they have molecular properties required of drug molecules [64, 65]. Natural products are used as starting materials in medicinal chemistry to produce more efficacious compounds.

1.4.1 Antimalarials from Plants

In antimalarial chemotherapy, the most important source of lead compounds is plants. A series of clinical trials have proven the *in vivo* efficacy of a number of medicinal plants used for the management of malaria [66]. The first antimalarial drug, quinine, is obtained from the bark of *Cinchona officinalis* (Rubiaceae family) and other minor species such as: *C. calisaya*; *C. pubescens* (*C. succirubra*); and *C. ledgeriana* [67]. Since quinine had a short half-life and its supply was erratic, it was replaced by synthetic quinoline based antimalarials such as chloroquine, mefloquine and halofantrine. These derivatives have a better pharmacokinetic profile compared to quinine.

The most recent addition to antimalarial drugs is artemisinin and its synthetic derivatives. Artemisinin was isolated from the Qinghaosu plant (*Artemisia annua*) in 1971. Artemisinin derivatives are the recommended first line drugs for the management of both uncomplicated and complicated malaria. It is a sesquiterpene lactone. Due to the fact the artemisinin had low water solubility, more water soluble semi-synthetic derivatives such as sodium artesunate were developed [68]. Recently, much simpler endoperoxide containing compounds such as G1 (**1.23**, Figure 1-9) have been isolated from *Eucalpytus grandis* and related species [69-71]. These compounds have *in vitro* antiplasmodial activity.

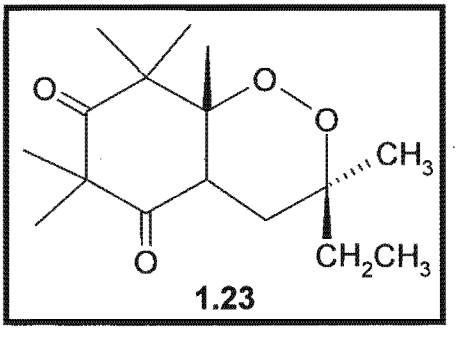

1.23

Figure 1 - 9: Chemical structure of G-1 (1.23), a natural product with an endoperoxide group.

Tazopsine (**1.24,** Figure 1-10), a morphinan isolated from the stem bark of *Strychnopsis thouarsii*, is a very interesting lead compound because it is active against the hepatic stage of Plasmodium but is totally inactive against the erythrocytic stage [72]. Its *N*-alkyl derivative, *N*-cyclopentyl-tazopsine (**1.25**) is less toxic. These compounds are promising leads for the development of prophylactic antimalarial agents and drugs that can produce a radical cure.

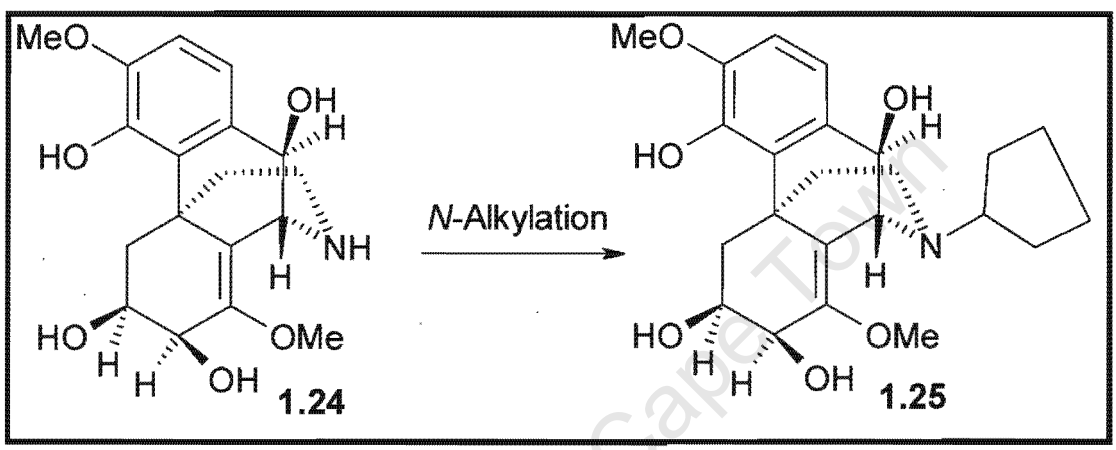

Figure 1 - 10: Chemical structures of Tazopsine (**1.24**) and *N*-cyclopentyl-tazopsine (**1.25**).

1.4.2 Lead Optimization of Natural Products

Unfortunately, natural products often lack the required pharmacokinetic, potency, selectivity and toxicological profile required of drug molecules. They are often structurally complex and hence are not amenable to commercial large scale synthesis [73]. To overcome these challenges promising natural products are subjected to the developmental processes outlined in Figure 1-11.

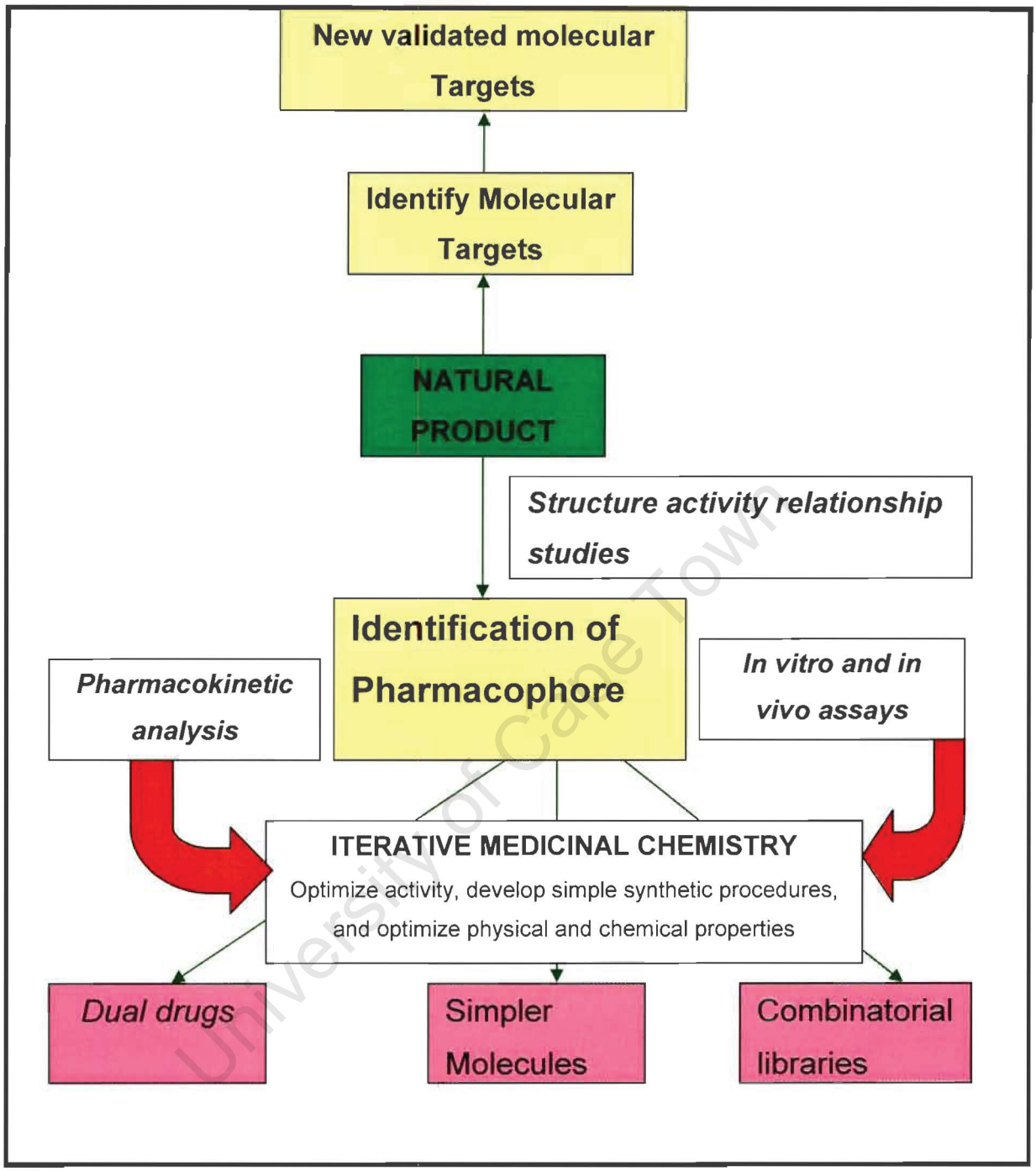

Figure 1 - 11: The process of lead optimization of natural products.

1.5 The Role of Stereoisomerism in Antimalarial Drug Development

Stereoisomers are compounds that have the same structure but differ in the spatial arrangement in selected or whole parts of the molecule. Different stereoisomers differ qualitatively and quantitatively in their pharmacological and pharmacodynamic properties [74, 75]. Twenty five percent of drugs in clinical use are racemic mixtures of stereoisomers. Stereoisomers are classified into two categories: geometric and optical isomers. The latter are more widely known. Geometrical isomerism is usually found in cyclic molecules or across double bonds [74]. In addition, a given stereoisomer may exist in 2 or more conformations. Different conformers arise from the ability of parts of a molecule to rotate along a single bond and therefore adopt different spatial arrangements. The most thermodynamically stable conformer is the most abundant and it can be predicted using quantum mechanical calculations.

During drug development, it is necessary to identify the possible stereoisomers of a compound and to identify possible differences in their pharmacokinetic and pharmacodynamic profiles. Where there are significant differences, the cost of drug development is likely to increase due to costs of separating the isomers [76]. Techniques used for the identification of stereoisomers include X-ray crystallography, NMR, gas- and liquid chromatography-mass spectrometry (GC-MS) 77[-79]. Duplicate NMR signals may be a sign of geometric isomerism or slowly interconverting conformers [74].

An example of an antimalarial agent that exhibit stereoisomerism is chalcones. The E-isomer of chalcone (**1.26a,** Figure 1-12) has greater antiplasmodial activity than the Z-isomer (**1.26b**) [80].

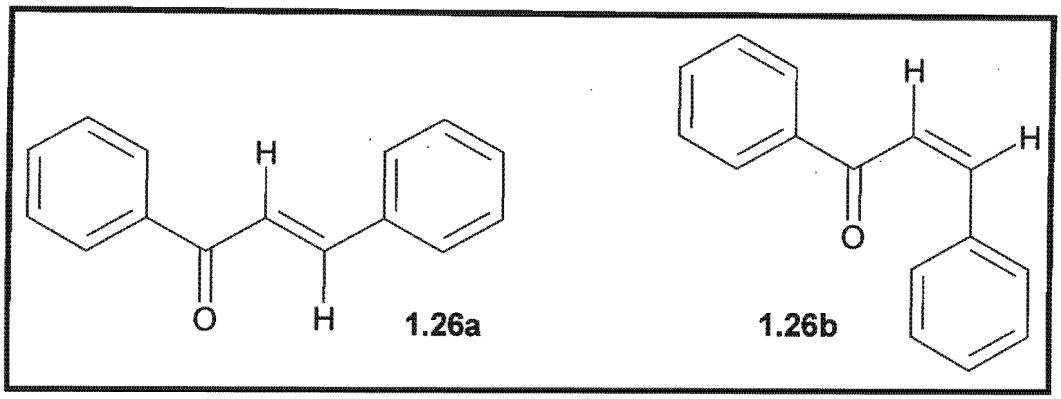

Figure 1 - 12: The stereoisomers of chalcone (1.26A and 1.26B).

1.6 Selected Molecular Targets within *Plasmodium falciparum*

Rational structure-based drug discovery is "the design of lead compounds that selectively inhibit a well characterized molecular target such as an enzyme on the basis of knowledge gained from previous structure activity relationship studies (SAR)" [81]. Structure-based rational drug design has been used in the design of new antimalarial targets [82]. In this study the potential molecular targets of interest were: cysteine proteases; hemozoin formation; iron-dependent enzymes; parasite induced new permeability pathways (NPPs). This section describes these molecular targets and the structural features or pharmacophores of known inhibitors. Some of these pharmacophores were subsequently incorporated in the natural product of interest, curcumin.

1.6.1 Hemozoin formation

1.6.1.1 Hemoglobin Degradation by Parasitic Proteases

The parasite degrades about 80% of the host's hemoglobin in the parasite food vacuole [83, 84]. Hemoglobin degradation creates space for the parasite within the RBC and supplies essential amino acids [85]. Hemoglobin degradation begins with invagination of the parasitophorous and plasma membranes of the parasite to form a double membrane transport vesicle [84].

The transport vesicle, containing part of the host's cytoplasm and hemoglobin, fuses with the parasite food vacuole which is highly acidic and rich in oxygen. Within the parasite food vacuole, hemoglobin is degraded by parasitic proteases to release free amino acids and a lipophilic prosthetic group called ferrous heme (**1.28**, Figure 1-13).

Heme is an iron-protoporphyrin complex in which 4 pyrrole groups are linked by –C=C-H bridges. Heme is electrically neutral and highly hydrophobic [86; 87].

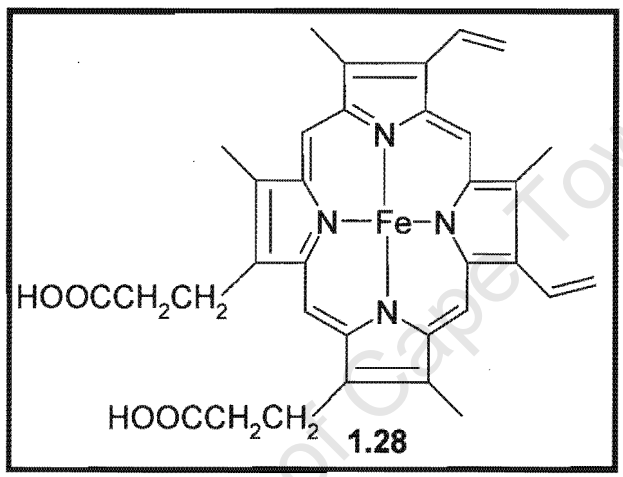

1.28

Figure 1 - 13: Structure of heme (1.28) (Ferroprotoporphyrin).

The ferrous moiety within heme undergoes oxidation in the oxygen rich environment of the food vacuole to form ferric heme which is also called ferriprotoporphyrin or hemin. It is positively charged and is associated with a chloride ion. Ferric heme is toxic to the parasite and human host. Heme causes oxidative stress and direct cellular death. Heme is oxidatively active and causes the formation of free radicals called Iron-derived reactive oxygen species (ROS). The free radicals cause peroxidation of DNA, membranes, lipoproteins and proteins [84 88]. Because of its toxicity, the heme is detoxified by the parasite and this process is the molecular target of chloroquine and related antimalarial agents. By disrupting heme detoxification, chloroquine increases levels of heme which causes death of the parasite.

Heme detoxification by the parasite is proposed to take place by 5 different mechanisms. These mechanisms include: complexation with histidine-rich protein 2 (HRP2) [89]; detoxification by cystolic proteins called peroxiredoxins [90]; destruction of the porphyrin ring by peroxidation with hydrogen peroxide [91] ; and glutathione mediated heme detoxification [92, 93]. The most widely accepted mechanism for heme detoxification is hemozoin formation.

1.6.1.2 Heme Detoxification by Hemozoin Formation

The main route of heme detoxification is formation of triclinic crystals called hemozoin. Hemozoin is a brown-black pigment which is insoluble in water. About 70 to 95 % of free heme is converted to hemozoin and about 200 µg/mol of hemozoin are released during the erythrocytic phase of the parasite's life cycle [94-96]. Hemozoin is chemically, structurally, biologically and spectroscopically identical to β-hematin which is synthesized in the lab under acidic conditions [97].

Hemozoin formation begins with the dimerization of heme by reciprocal bonding of the propyl carboxylate group of one heme molecule with the ferric moiety of a second heme molecule to form an iron-carboxylate bond. The heme dimers undergo stacking to form hemozoin [98 95]. Although hemozoin is often referred to as a polymer, it is made up of dimers of heme linked together by hydrogen bonding of free propyl carboxylic acid groups. The exact mechanism by which hemozoin crystals are formed is rather controversial and 5 different mechanisms have been proposed.

It has been proposed that hemozoin formation is the result of spontaneous crystallization of heme dimers. However, this may not be the case since this process is too slow at physiological conditions [96]. The autocatalytic mechanism proposes that preformed hemozoin acts as a catalyst for heme formation. However, this proposal does not explain how the initial hemozoin is formed [84, 99]. Hemozoin formation might be mediated by two proteins with heme polymerase activity called Histdine Rich Proteins II and III (HRP II and

III) [84, 100]. It has been proposed that hemozoin formation is mediated by saturated fatty acids such as arachidonic acid and oleic acid, which tend to concentrate heme and maintain it in a state favorable for dimerization [101, 102]. This mechanism may not be plausible since the reaction efficiency is too low (0.5 – 20 %) to allow for rapid hemozoin formation *in vivo* [99]. Secondly, the stoichiometry of the reaction demands equimolar amounts of heme and lipids which cannot be achieved intracellularly [93, 103]. Hempelmann *et al.* [103] put forward the membrane sacrifice mechanism. They proposed hemozoin formation takes place in parasite transport vesicles whose membranes act as a scaffold for the growth of hemozoin crystals. This mechanism is supported by the fact that hemozoin is usually associated with membrane fragments. Alternatively, hemozoin formation may take place by biomineralization which is a spontaneous crystallization process mediated by lipids. This process has been demonstrated *in vitro* and is fast enough to allow for hemozoin formation *in vivo* [104].

1.6.1.3 Role of Hemozoin in the Pathophysiology of Malaria

Hemozoin was initially thought to be inert but it has been recently shown to induce detrimental immunological responses in the human host. It causes over activation of the cellular component of the immune system leading to increased production of cytokines which cause end organ damage observed in complicated malaria [105, 106]. Hemozoin causes activation of neutrophils and macrophages leading to chemotaxis and increased expression of Tumor Necrosis Factor alpha (TNF-α) and other inflammatory agents [107-109]. Hemozoin increases the immune response of dendritic and splenic cells [110]. When hemozoin binds to Toll-like receptor 9 (TLR9), located on a sub-type of dendritic cells, a cascade of signaling reactions is triggered and this leads the eventual production of inflammatory agents [111].An acute infection with *P. falciparum* may be followed by a state of immunosuppression. The immuno-suppressive effects of the parasite may be mediated by hemozoin which acts by suppressing maturation of dendritic cells *in vitro* [112].

1.6.1.4 Antimalarial Agents that Inhibit Hemozoin Formation

Drugs that accumulate in the parasite food vacuole tend to interfere with hemozoin formation. Such drugs include: artemisinin and other antimalarial peroxides and 4-arninoquinolines and aryl alcohol antimalarials [113]. High concentrations of artemisinin and other related endoperoxide antimalarial derivatives inhibit β-hematin formation [114]. They may inhibit hemozoin formation by forming complexes with HRP2 and 3 [115] or by forming covalent bonds with free heme [116]. Despite the fact that they inhibit hemozoin formation, this is not the main mechanism through which endoperoxide antimalarials act [117].

It is widely accepted that 4-aminoquinoline antimalarials act by inhibiting hemozoin formation. However, they may exert their antimalarial effects through other mechanisms. Quinoline antimalarials reversibly reduce the rate of beta-hematin formation *in vitro* [118]. Other agents that inhibit beta hematin formation *in vitro* include: hydroxanthones (2, 3, 4, 5, 6-pentahydroxyxanthone (**1.29,** Figure 1-14) [119]; clotrimazole (**1.30**) [120]; and cyproheptadine (**1.31**) [121].

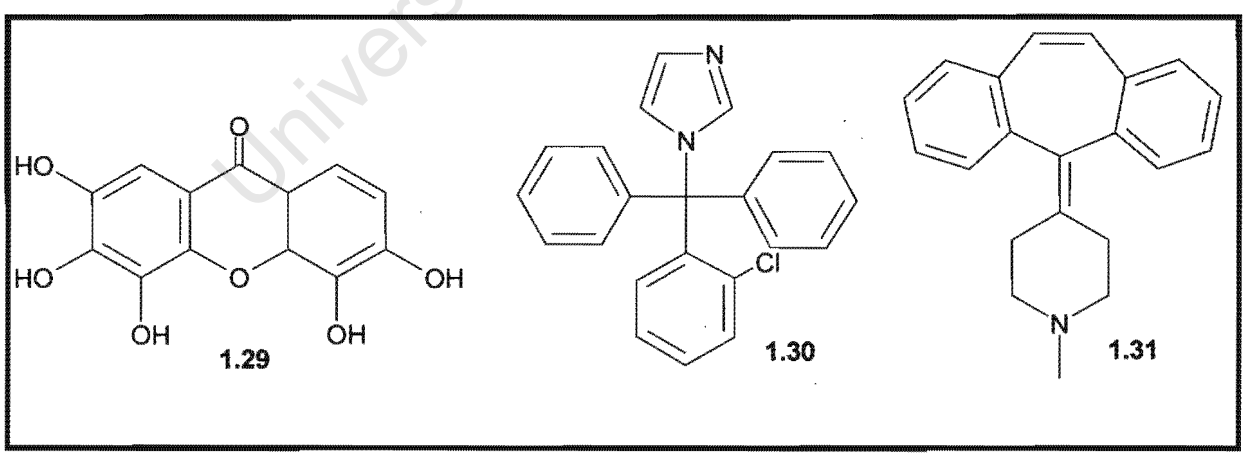

Figure 1 - 14: Structures of compounds that inhibit beta-hematin formation: pentahydroxyxanthone (**1.29**), clotrimazole (**1.30**) and cyproheptadine (**131**).

A common feature of these compounds is the presence of delocalized π electrons that interact with the π electrons of the porphyrin rings in heme. This results in the formation of a complex with heme which prevents the subsequent formation of hemozoin [122, 123]. The formation of the complex is called π- π stacking. Cationic- π interactions may also occur between the ferric moiety and the edge of the quinoline ring that contains the N and C8 [124, 125]. The structure of the quinoline-ferriheme complex is unknown since no crystals are available. Recent models show that the stacking is not entirely planar and is tilted [124, 126].

While it is widely accepted that quinoline antimalarial agents inhibit hemozoin formation by complexing with heme, alternative mechanisms have been proposed. Quinolines may act by inhibiting glutathione and hydrogen-peroxide dependent heme detoxification [91, 93]. This has been demonstrated *in vitro* but has never been observed in *vivo*. Quinolines may also act by masking lipids which are involved in hemozoin formation [102, 127].

1.6.1.5 Structure Activity Relationship of 4-aminoquinolines

The structural features of chloroquine essential for its antimalarial activity are summarized in Figure 1-15.

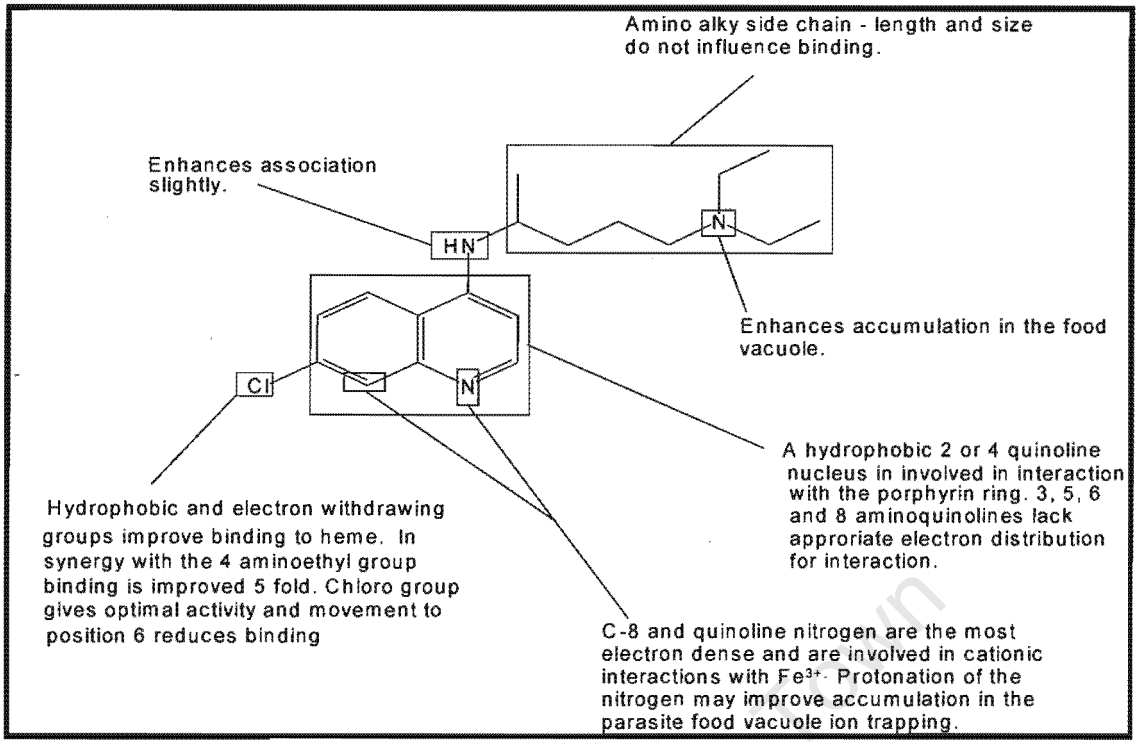

Figure 1 - 15: Summary of the structure activity relationship of 4 aminoquinoline antimalarials [128].

The quinoline ring N is essential for binding to heme to occur [129]. Since the nature of interaction of quinoline is electronic, substitutions that cause changes in the electron density reduce or abolish the ability to complex with heme [129-131]. The electron density distributions of 3, 5, 6 and 8 aminoquinolines do not allow them to interact with ferric heme [132].

The 7-chloro group and the alkyl group on the amino group independently do not improve binding to hematin significantly [128, 130]. However, the 7-chloro group and the terminal amino-ethyl side chain synergistically improve binding to ferric heme five fold [133]. A terminal ethyl group in CQ is critical for the synergistic effect.

The strength of ferric heme complexes is mainly determined by the hydrophobicity of the molecule. Hydrophobic substituents at position 7 increase the strength of association between ferric heme and the quinoline [134]. Although the amino alkyl side chain is not directly involved in hematin

binding, shortening or increasing the length of this side chain abolishes resistance in CQR strains [135]. In 4-aminoquinoline derivatives, the 7-chloroquine ring is weakly correlated with cross-resistance with CQ. The length and nature of the basic side chain is the determinant of activity against chloroquine-resistant parasite strains [136].

1.6.2 Cysteine proteases as Molecular Targets in Plasmodium

Proteases are a family of enzymes found in eukaryotes and prokaryotes and are involved in proteolysis, which is the break down of proteins to peptides and amino acids. Cysteine proteases, also called thioproteases, belong to the Clan CA of the papain family of proteins [137, 138]. In this clan the amino acid residue, Cysteine 25 and Histidine159 are highly conserved as the principle amino acids at the site of action. They are involved in hemoglobin degradation, erythrocyte invasion by the merozoites and rupture of the infected RBC [139, 140]. The recombinant cysteine proteases isolated from *P. falciparum* include: falcipains and Pf68. Pf68 is responsible for erythrocyte rupture by the mature schizonts. Four types of falcipains have been identified: falcipain-1 (FP-1); falcipain 2A (FP-2A); falcipain 2B (FP-2B); and falcipain 3 (FP-3) [141-144]. The falcipains are closely related and genes coding for them are located on chromosome 11 of the parasite. The falcipains are mainly involved in haemoglobin degradation and are located in the parasite food vacuole.

FP-2 cleaves the erythrocyte membrane proteins ankyrin and protein 4 during rupture of the infected RBC [145, 146]. FP-2 is responsible for over 90% of the cysteine protease activity in the trophozoite stage. Falcipain 2A is a product of duplication of the gene encoding for FP-2B [142]. The two have the same substrate specificity and similar kinetic properties [144, 147, 148]. FP-2B may be involved in RBC rupture. Falcipain 1 is distantly related to the other falcipains and its biological role is unknown. It may be involved in oocyst release in the mosquito mid-gut or may be involved in red blood cell invasion and cleavage of Pfs230 during gametogenesis [149-151].

1.6.2.1 Mechanism of inhibition of the cysteine proteases

The active site of cysteine proteases contains cysteine which has a highly active thiol group. The activity of the enzyme is dependent on His-159 which is in close proximity with the cysteine residue [138]. The close proximity of the two residues results in the deprotonation of the thiol group. At neutral and slightly acidic pH, the two residues exist as a highly nucleophilic thiolate-imidazolium ion pair. An amino acid at position S149 is critical for activity and mutations at this site completely abolish activity of falcipains [144]. The exact role of this amino acid is unknown. S149 is more critical for the activity of FP-2A compared to FP-2B.

The mechanism of the proteolytic action of cysteine proteases is presented in Figure 1-16.

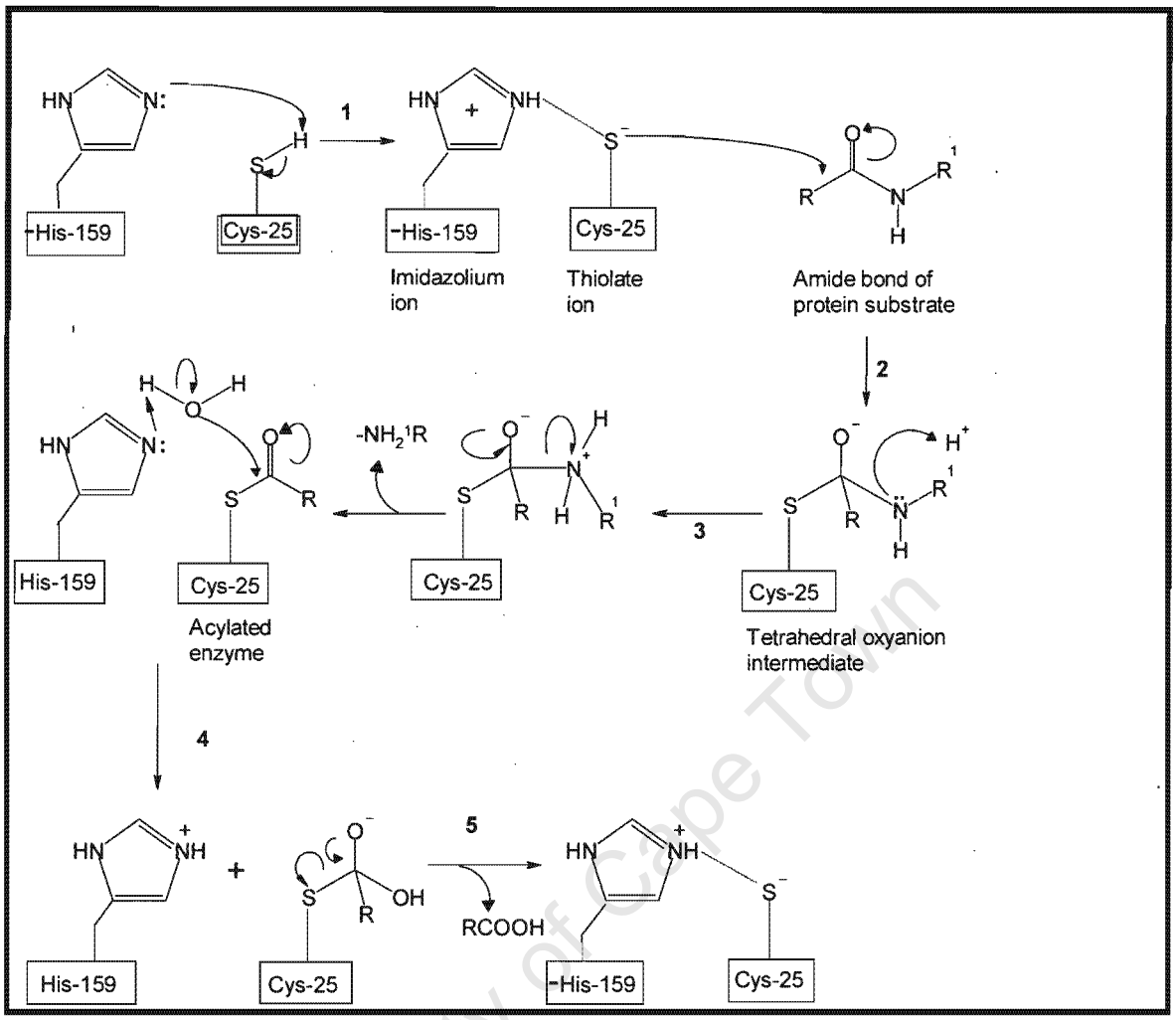

Figure 1 - 16: Mechanism of proteolysis by cysteine proteases [138, 152]

1. Deprotonation of the thiol group on Cys-25 by His-159 to form the thiolate and imidazolium ion pair.
2. The highly nucleophilic thiolate ion attacks the carbonyl bond of scissile amide bond resulting in the formation of an Oxyanion intermediate. This intermediate is stabilized by hydrogen bonding with NH and NH_2 of Cys.-25 and Gln-19 respectively.
3. Protonation of the amine group within the oxyanion with electronic rearrangement leading to lysis of the amino end of the protein and formation of acylated cysteine protease enzyme. The proton is supplied by the imidazolium ion.
4. Nucleophilic attack on the carbonyl of the acylated enzyme by water or a base leading to the formation of a tetrahedral intermediate.
5. Regeneration of the thiolate-imidazolium ion pair with loss of the acyl group.

1.6.2.2 Inhibitors of Cysteine Proteases

Most inhibitors contain an electrophilic center such as a carbonyl or thiocarbonyl group which is attacked by the negatively charged active site thiolate group of the cysteine residue [153]. Compounds with an α, β unsaturated ketone have a great affinity for the thiol in cysteine compared to amino and hydroxyl nucleophiles [154, 155].

Ideally, an inhibitor of the falcipains should be active against all the 4 isoforms of falcipain because selective reduction of the activity of any one of the isoforms results in compensatory over expression of the other isoforms [156]. To minimize toxicity, the inhibitor should be selective for the parasitic cysteine proteases and should not inhibit human cysteine proteases such as cathepsin L [144]. Inhibitors that bind to the amino acids at positions S149 and either position I85 or A151 of the falcipains are unlikely to interact with the human protease analogue [144].

Inhibitors block the rupture of the infected RBC leading to the accumulation of mature schizonts in RBC [157, 158]. They also cause accumulation of native hemoglobin and swelling of the food vacuole [159]. They inhibit gametogenesis *in vitro* [160].

Inhibitors are classified into three categories: irreversible; slow turnover; and the reversible inhibitors. The irreversible inhibitors form stable covalent bonds with cysteine proteases. They include epoxides (**1.32**), α, β-unsaturated ester Michael acceptors (**1.33**) and vinyl sulfones (1.34, Figure 1-17) [161]. Though irreversible cysteine protease inhibitors inhibit human cysteine proteases, undue toxicity has not been demonstrated in rodents and dogs because mammals have large reserves of cysteine proteases.

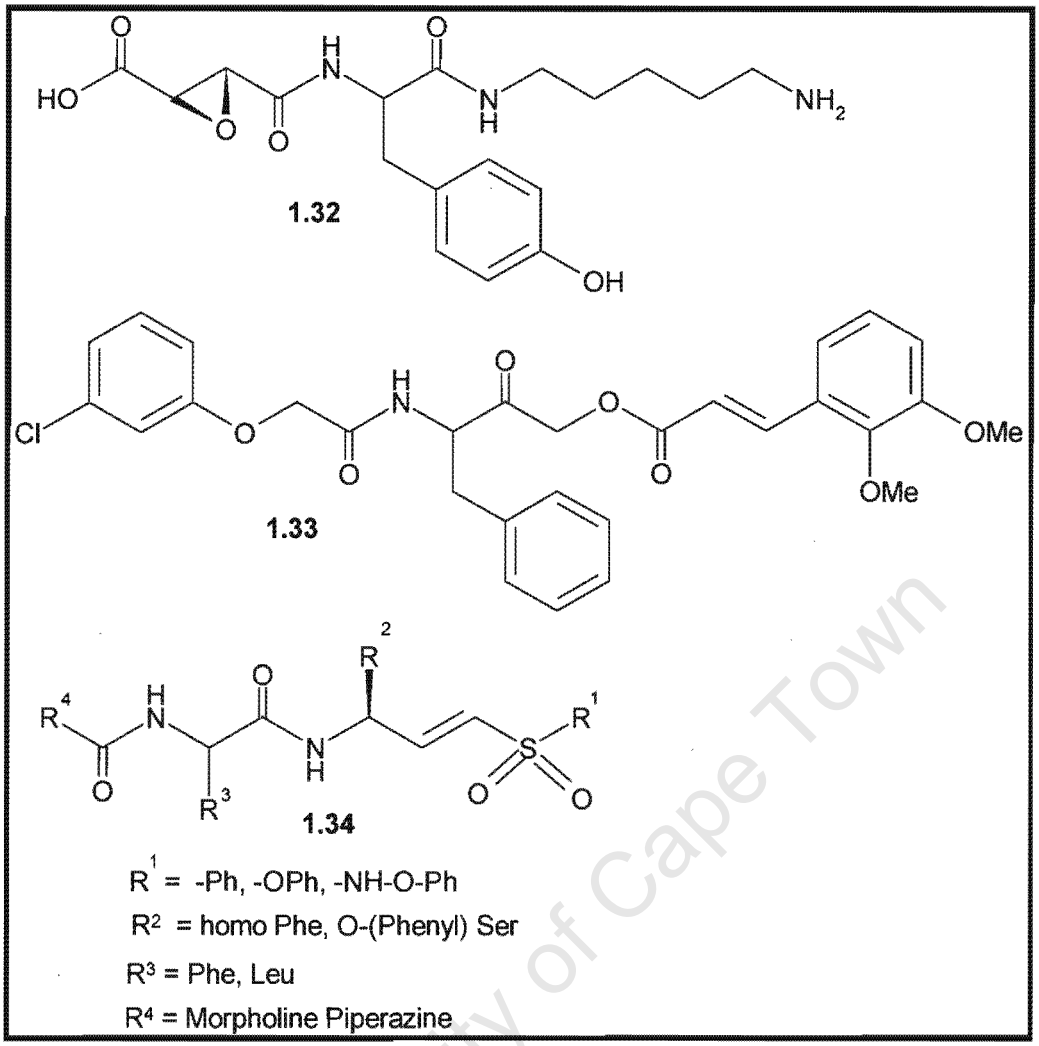

Figure 1 - 17: Structures of irreversible cysteine protease inhibitors.

Slow turn-over inhibitors form stable thioacyl complexes with cysteine proteases that hydrolyze slowly with time. The reversible inhibitors form a reversible transition state intermediate with cysteine proteases [162]. Slow turn-over inhibitors are made up of aza-substituted peptides such as peptidyl carbazate ester (**1.35,** Figure 1-18) [163] while reversible inhibitors include ketone based peptide derivatives (**1.36**) [162] and pyrazolines (**1.37**) [164].

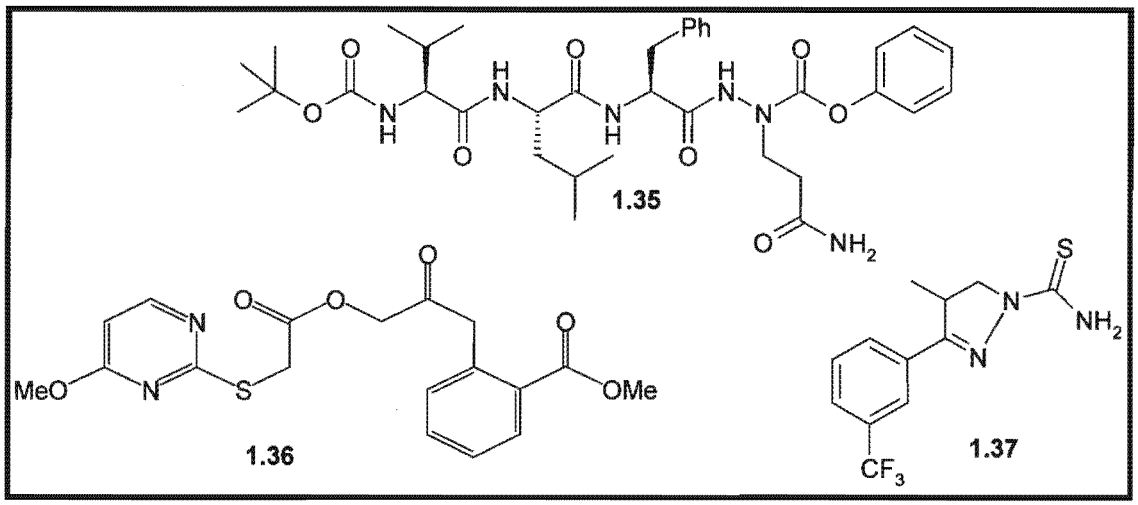

Figure 1 - 18: Structures of slow turnover and reversible inhibitors of cysteine proteases: a peptidyl carbazate ester (1.35); a ketone based peptide derivative (1.36); and a pyrazoline (1.37).

1.6.3 Antimalarial Activity of Iron Chelators

Iron chelators such as desferrooxamine (DFO) (**1.38**, Figure 1-19), have antimalarial activity [165]. Desferrooxamine inhibits the erythrocytic and hepatic phases of the parasite. Clinical trials showed it is effective in non-complicated malaria [166, 167].

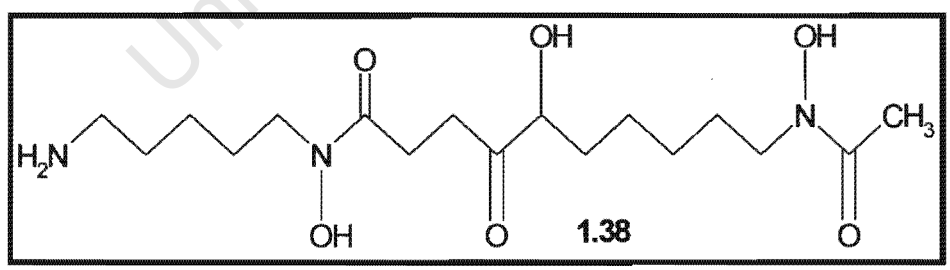

Figure 1 - 19: Chemical structure of desferroxamine (1.38).

Iron chelators act by forming chelates with iron thus withholding iron from iron-dependent enzymes. Some chelators, such as 8-hydroxyquinoline and 2, 2'-Bipyridyl, form toxic complexes with iron [168]. The parasite is more sensitive to

iron deprivation than mammalian cells. The metabolic processes in the parasite that are dependent on iron are presented in Table 1-2.

Table 1- 2: Iron-dependent enzymes in Plasmodium[169]

Enzyme	Metabolic Processes catalyzed by the enzyme
Ribonucleotide reductase	DNA synthesis[170]
Dihydroorotate dehydrogenase	Pyrimidine synthesis [171, 172]
Phosphoenol pyruvate carboxykinase	Carbon dioxide fixation [171]
Delta-aminolevulinate synthase	Heme synthesis [173]
Cytochrome oxidase, cytochrome b	Mitochondrial electron transport [174, 175]
Glycolytic enzymes	Pentose phosphate shunt [176, 177]

Iron chelators with antimalarial activity are highly lipophilic and this enables them penetrate RBCs [169, 178]. They have a high affinity for iron [179] and are relatively selective for iron compared to other divalent cations such as zinc and calcium [178]. The ability to accumulate and persist in the infected RBCs improves the activity of the iron chelators [180]. The structures and afffinity constants of selected iron chelating agents are presented in Table 1-3.

Table 1- 3: The affinity constants of iron chelators with antimalarial activity.

IRON CHELATOR	STRUCTURE	Affinity constant (K_a)
Desferrooxamine (DFO) [165]	**1.38,** Figure 1-19	10^{31}
Acetomethoxy-calcein (**1.39**) [181, 182]	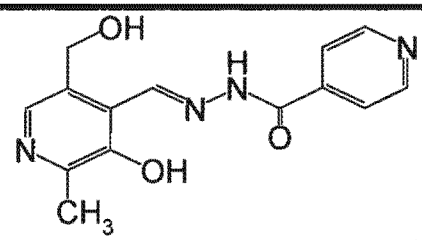	10^{24}
Hydroxyl pyridine-4-one (**1.40**)[178]	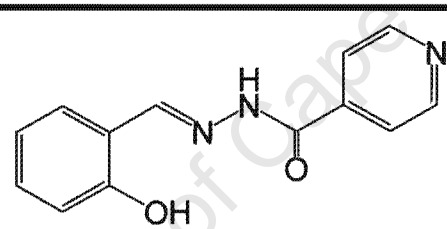	10^{36}
8-hydroxyquinoline (**1.41**) [183]	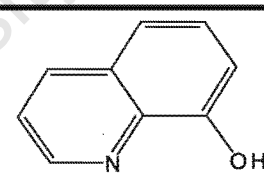	10^{38}

1.6.4 New Permeability Pathways as Potential Drug Targets

Following infection of the red blood cell, new pathways appear on the red blood cell membrane that differ biochemically from the host's cells native pathways. These pathways are called new permeability pathways (NPPs) and are produced 15 hours after RBC invasion [184]. They increase the permeability of the infected RBCs to electrolytes and other molecular currents [185]. Some of the NPPs are native to the RBC and are activated on infection [186-188]. Other NPPs are encoded by the parasite and are transported to the surface of the

RBC. They are synthesized during the ring phase and appear at the RBC surface only at the mid-trophozoite stage [189].

The functions of these pathways are still unclear but they may be responsible for entry of essential nutrients such as pantothenate, glucose and choline [190-192]. Other nutrients that are acquired through the NPPs include: purine and pyrimidine nucleosides; isoleucine; small carbohydrates such as pentitols, pentose, and hexitols; and polyamines [193, 194]. The NPPs are used for the excretion of metabolic wastes such as lactic acid [195, 196]. NPPs are involved in the regulation of the volume of infected RBCs by the extrusion of amino acids that accumulate after hemoglobin degradation. They regulate the intracellular concentrations of sodium and potassium ions [197].

The NPPs have pharmacological and biochemical properties that are distinct from mammalian transporters. This enables the design of drug molecules that specifically target the NPPs. They are not inhibited by the classical inhibitors that inhibit corresponding mammalian transporters [193, 198]. They are not saturable and show a preference for hydrophobic solutes [199, 200]. Selectivity for parasite encoded NPPs can be improved by improving the lipophilicity of an inhibitor [192]. They are not stereospecific and transport both the levo and dextro enantiomers of solutes [201, 202].

The anion transporters are the most predominant NPPs. They have very broad substrate specificity and transport monovalent anions and cations, amino acids, sugars and nucleosides [201, 203]. Due to their broad specificity, anionic transporters are ideal targets for antimalarial drugs.

1.6.4.1 Anionic Transporters as Potential Drug Targets

The most common anionic transporters in nature are the chloride channels. They are ubiquitous in nature. The chloride channels are involved in cell volume regulation, transportation of salt and water and maintenance of the electrical excitability of a cell [204]. Anionic transporters in an infected RBC have a greater preference for anions over cations and they tend to be inward

rectifying [185, 191]. There are about 5 different types of anionic channels in the infected RBC. Two of these anionic channels are Volume-Activated Anion channel and Small Conductance Channel (SCC) [186, 187, 205].

The anionic channel that has been validated as a potential drug target is the Plasmodial Surface Anion Channels (PSAC). It is encoded by the parasite and is a chloride transporter but is also permeable to purines, amino acids and vitamins [206]. It is located on the external surface of the infected RBC [207, 208]. PSAC is a good potential drug target for malaria since its biochemical properties are different from that of the mammalian anionic channel. This implies that inhibitors that are specific for PSAC are unlikely to bind to mammalian anionic channels thus minimizing the chances of toxicity. Its location on the external surface of the RBC implies that there is no need to design drugs that penetrate the RBC and this reduces the potential for drug resistance developing [209]. This target has been validated and known antagonists of this channel inhibit parasite growth *in vitro* [191, 210]. The IC_{50}s of compounds that inhibit anionic channels are presented in Table 1-4.

Table 1- 4: The antiplasmodial activity of selected anionic channel inhibitors.[198, 202]

Inhibitor	Structure	IC_{50} (Inhibition of choline transport) (μM)	IC_{50} (Inhibition of parasite growth) (μM)
Phlorozin and its aglycone (**1.42**)	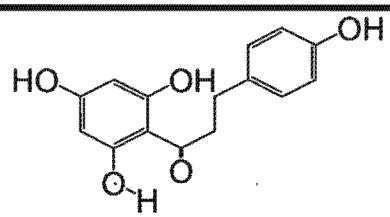	3	3 -17
Piperine (**1.43**)	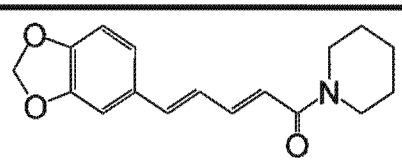	13	3 - 50
Furosemide (**1.44**)	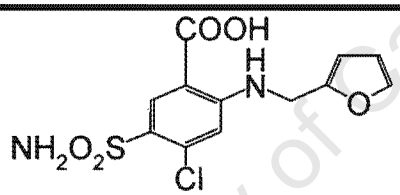	1	0.04 - 9
5-Nitro-2-(3-phenyl-propyamino) benzoic acid NPPB (**1.45**)	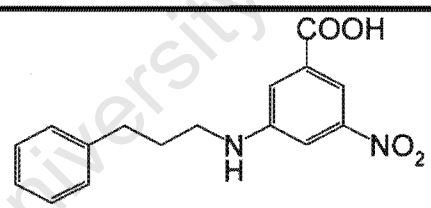	0.8	0.1 - 11

Anionic channel inhibitors tend to have an anionic head ($-COO^-$) and an uncharged hydrophobic tail end. Increasing the hydrophobicity of the tail end improves the anion channel inhibition. Interaction between the inhibitor and the anionic channels is stereospecific and R-enantiomers tend to be more potent inhibitors [211]. The *in vitro* antiplasmodial effects of these compounds may be mediated through other mechanisms unrelated to ion channel inhibition [210].

1.7 The Antiplasmodial and Anti-Inflammatory Activities of the Natural Product Curcumin

Curcumin, also called 1, 7-bis-(4-hydroxy-3-methoxyphenyl)-1, 6-heptadiene-3, 5-dione) (**1.46**, Figure 1-20), is a yellow-orange pigment isolated from turmeric powder which is the dried rhizome of the plant *Curcuma longa/domestica* L.
(Zingiberaceae).

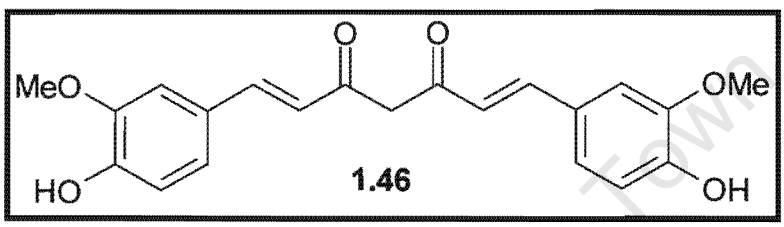

Figure 1 - 20: Chemical structure of the natural product curcumin (1.46).

Curcumin is a promising lead molecule for the development of anticancer, anti-inflammatory and antimicrobial agents because of its low toxicity, low molecular mass and ease of synthesis. Curcumin has a wide range of activities such as antiprotozoal, anticancer, anti-inflammatory and antioxidant [212]. Curcumin was selected for chemical modification because it is easily available at a low cost. Moreover, the presence of hydroxyl and carbonyl groups on the molecule provide chemical diversity sites. Curcumin has a favorable toxicity profile and moderate antiplasmodial activity. The IC_{50} values of curcumin and its naturally occurring analogues, demethoxycurcumin and bis-demethoxycurcumin, against a chloroquine sensitive strain of *P. falciparum* are of 3.5, 4.2 and 3.0 µg/ml respectively [213]. The *in vitro* activity of curcumin against a chloroquine resistant strain of *P. falciparum* is about 5 µM [214]. An oral dose of 100 mg/kg of body weight reduced parasitemia and improved survival in rodents infected with *P. berghei* [214]. A curcumin - α, β arteether combination was found to improve survival of *P. berghei* infected mice compared to either agent administered alone [215]. A combination of

arteminisinin and curcumin the delayed appearance of parasitemia compared to either agent used alone in artemisinin-resistant *Plasmodium chabaudi* infected mice [216]. Curcumin did not appear effective in reversing resistance to artemisinin [216]. In addition to its antiplasmodial activity, curcumin has also been reported to have antileishmanial [213, 217-222] and antitrypanosomal activities [223].

1.7.1 Proposed mechanisms of the antimalarial activity of curcumin

Curcumin may cause its antimalarial effects by intercalating with DNA [214]. Since curcumin has α, β-unsaturated carbonyl groups, it may also have the ability to inhibit cysteine proteases. Compounds with an α, β-unsaturated ketone group have a great affinity for the thiol groups in the active site of cysteine proteases [154, 155]. The antimalarial activity of curcumin may also be due to its ability to chelate iron. The affinity of curcumin for Fe^{3+} is similar to that of desferroxamine [224]. Because of its iron chelating ability curcumin reduces the enzymatic activity of iron-dependent enzymes [225]. The iron chelating properties of curcumin are due to the di-ketone and phenolic hydroxyl groups. However, alkylation of the phenolic groups does not abolish the iron chelating ability of curcumin. Curcumin may share the same mechanism of action with artemisinin since it inhibits human sarcoplasmic reticulum Ca^{2+} ATPase (SERCA) which is the orthologue of *P. falciparum* Ca^{2+} ATPase (PfATP6) [226]. Curcumin has not been demonstrated to inhibit the NPPs. However, its structural similarity to chalcones indicates that it may inhibit NPPs. Dimethoxy- and methoxychalcones (**1.47**, Figure 1-21) are potent inhibitors of NPPs [227].

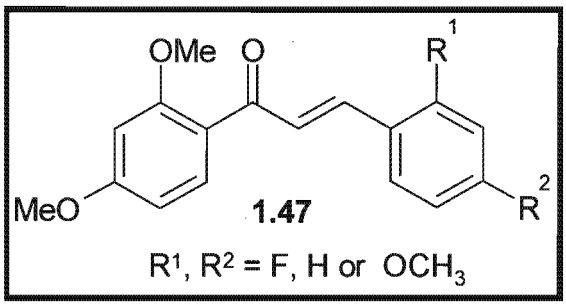

Figure 1 - 21: General structure of chalcones that inhibit new permeability pathways[227]

Curcumin has potent anti-inflammatory activity which is a useful property in the management of malaria [228, 229]. Part of the antimalarial activity of chloroquine and artemisinin is due to their anti-inflammatory activity. Chloroquine and artemisinin derivatives inhibit the production of pro-inflammatory cytokines and increase the production of interleukins 10 (IL-10) and 12 (IL-12) which confer protection against intracellular parasitic infection [230-232]. Curcumin inhibits both cyclooxygenase and lipoxygenase which are involved in the generation of inflammatory agents [233, 234]. It down-regulates the expression of pro-inflammatory agents such as COX2 [235, 236], LOX, inducible nitric oxide synthase (iNOS) [237, 238]; matrix metalloproteinase-9/gelatinase B (MMP-9) [239], TNF-α [240] and chemokines such as IL- 1β, IL-6, IL 8, ICAM-1 [241].

1.7.2 Disadvantages of Curcumin

One of the major draw backs in the clinical use of curcumin is its poor water solubility which results in low oral bioavailability. It is poorly absorbed when taken orally. Over 75 % of an orally administered dose is excreted unchanged in feces [242, 243]. Secondly, curcumin has a short half life because it is rapidly metabolized in the liver. Due to its short half-life, curcumin cannot be used clinically for management of malaria because it has to be administered frequently and this will reduce adherence. In clinical trials, curcumin has to be administered frequently and at very high doses to overcome its poor pharmacokinetic properties. Compared to agents like chloroquine, curcumin has a low antimalarial potency.

1.8 Aim and Objectives of the Study

The main aim of the study was to improve the antimalarial potency and pharmacokinetics properties of the natural product curcumin by chemical modifications targeted at specific biochemical pathways in *Plasmodium falciparum*.

The specific objectives of the study were:

1. Synthesis of derivatives of curcumin by incorporating moieties known to target specific biochemical pathways within *P. flaciparum*.
2. Improvement of the oral bioavailability and half-life of curcumin through chemical modifications aimed at increasing water solubility and reducing rate of metabolism.
3. Determination of the *in vitro* antiplasmodial activity of the derivatives against chloroquine sensitive and resistant strains of *P. falciparum*
4. Determination of the ability of the derivatives to inhibit hemozoin formation.
5. Determination of the cytotoxicity of the derivatives against Chinese Hamster Ovarian (CHO) cells.
6. Establishment of an optimal dose for *in vivo* antimalarial studies by pilot single and repeated dose oral toxicity studies in mice.
7. Evaluation of *in vivo* efficacy of selected derivatives in murine model of malaria.
8. Evaluation of the effect of chemical modification on the pharmacokinetic parameters of a selected derivative in mice.

References

(1) Vythilingam, I.; Tan, C. H.; Asmad, M.; Chan, S. T.; Lee, K. S.; Singh, B. *Trans. R. Soc. Trop. Med. Hyg.* **2006**, *100*, 1087-1088.

(2) Nguyen, C.; Day, N. P.; Pram, T. D.; Ferguson, D. J. P.; White, N. J. *Trans. R. Soc. Trop. Med. Hyg.* **1995**, *89*, 200-204.

(3) Khasnis, A. A.; Nettleman, M. D. *Arch. Med. Res.* **2005**, *36*, 689-696.

(4) Talman, A. M.; Domarle, O.; McKenzie, F. E.; Ariey, F.; Robert, V. *Malar J.* **2004**, *3*, 24-24.

(5) Baton, L. A.; Ranford-Cartwright, L. C. *Trends Parasitol.* **2005**, *21*, 573-580.

(6) Drakeley, C.; Sutherland, C.; Bousema, J. T.; Sauerwein, R. W.; Targett, G. A. T. *Trends Parasitol.* **2006**, *22*, 424-430.

(7) Sinden, R. E. *Parassitologia* **1999**, *41*, 139-148.

(8) Carucci, D. J.; Gardner, M. J.; Tettelin, H.; Cummings, L. M.; Smith, H. O.; Adams, M. D.; Hoffman, S. L.; Venter, C. *Exp. Rev. Mol. Med.* Centre for Applied Research in Educational Technologies (CARET), Ed.; Cambridge University Press: Cambridge, U.K. http://www-ermm.cbcu.cam.ac.uk/dcn/fig001dcn.htm

(9) Snow, R. W.; Guerra, C. A.; Noor, A. M.; Myint, H. Y.; Hay, S. I. *Nature* **2005**, *434*, 214-217.

(10) Hay, S. I.; Shanks, D.; Stern, D. I.; Snow, R. W.; Randolph, S. E.; Rogers, D. J. *Trends Parasitol.* **2005**, *21*, 52-53.

(11) Olumese, P. *Acta Trop.* **2005**, *95*, 265-269.

(12) Lopez, A. D.; Mathers, C. D.; Ezzati, M.; Jamison, D. T.; Murray, C. J. L. *Lancet* , *367*, 1747-1757.

(13) World Health Organization **2005**, *WHO/HTM/MAL/2005.1102*.

(14) Patz, J. A.; Olson, S. H. *Proc. Natl. Acad. Sci. U. S. A.* **2006**, *103*, 5635-5636.

(15) Bosello, F.; Roson R.; Tol, R. S. J. *Ecol. Econ.* **2006**, *58*, 579-591.

(16) Malkin, E.; Dubovsky, F.; Moree, M. *Trends Parasitol.* **2006**, *22*, 292-295.

(17) Plebanski, M.; Lopez, E.; Proudfoot, O.; Cooke, B. M.; Itzstein, M. v.; Coppel, R. L. *Methods* **2006**, *40*, 77-85.

(18) Rosenthal, P. J.; Goldsmith, R. S. Antiprotozoal Drugs; Katzung, B. G., Ed.; In *Basic and Clinical Pharmacology*; Lange Medical Books/McGraw-Hill: New York, U. S. A., 2001; Vol. 8, pp 882.

(19) Edwards, G.; Biagini, G. A. *Br. J. Clin. Pharmacol.* **2006**, *61*, 690-693.

(20) Gregson, A.; Plowe, C. V. *Pharmacol. Rev.* **2005**, *57*, 117-145.

(21) Hyde, J. E. *FEBS J.* **2007**, *274*, 4688-4698.

(22) Edwards, G.; Biagini, G. A. *Br. J. Clin. Pharmacol.* **2006**, *61*, 690-693.

(23) World Health Organization (WHO) **2005**, *WHO/HTM/MAL/2005.1102.*

(24) Watkins, W. M.; Sibley, C. H.; Hastings, I. M. *Am. J. Trop. Med. Hyg.* **2005**, *72*, 163-173.

(25) Hastings, I. M.; Watkins, W. M. *Trends Parasitol.* **2006**, *22*, 71-77.

(26) Ridley, R. G. *Nature* **2002**, *415*, 686-693.

(27) Ridley, R. G. *Nature* **2003**, *424*, 887.

(28) Ridley, R. G. *Microbes Infect.* **2002**, *4*, 155.

(29) Ridley, R. G. *Nature* **2002**, *415*, 686.

(30) Hastings, I. M.; Watkins, W. M. *Acta Trop.* **2005**, *94*, 218-229.

(31) Nwaka, S.; Hudson, A. *Nat. Rev. Drug Discov.* **2006**, *5*, 941-955.

(32) Nwaka, S.; Ridley, R. G. *Nat. Rev. Drug Discov.* **2003**, *2*, 919-928.

(33) Rathod, P. K.; McErlean, T. *Proc. Natl. Acad. Sci. U. S. A.* **1997**, *94*, 9389.

(34) Osman, M. E.; Mockenhaupt, F. P.; Bienzle, U.; Elbashir, M. I.; Giha, H. A. *Infect. Genet. Evol.* **2007**, *7*, 52-59.

(35) Wichmann, O.; Muehlen, M.; Gruss, H.; Mockenhaupt, F. P.; Suttorp, N.; Jelinek, T. *Malar J.* **2004**, *3*, 14-14.

(36) Wichmann, O.; Jelinek, T. *J. Infect. Dis.* **2005**, *191*, 822-823.

(37) Björkman, A.; Bhattarai, A. *Acta Trop.* **2005**, *94*, 163-169.

(38) Giha, H. A.; Elbashir, M. I.; A-Elbasit, I. E.; A-Elgadir, T. M. E.; ElGhazali, G. E.; Mackinnon, M. J.; Babiker, H. A. *Acta Trop.* **2006**, *97*, 181-187.

(39) Ferdig, M. T.; Roland A. Cooper; Mu, J.; Deng, B.; Joy, D. A.; Su, X.; Wellems, T. E. *Mol. Microbiol.* **2004**, *52*, 985-997.

(40) Fitch, C. D. *Proc. Natl. Acad. Sci. U. S. A.* **1969**, *64*, 1181-1187.

(41) van Schalkwyk, D. A.; Egan, T. J. *Drug Resist. Updat.* **2006**, *9*, 211-226.

(42) Ridley, R. G. *Curr. Biol.* **1998**, *8*, R346-9.

(43) Krogstad, D. J.; Schlesinger, P. H.; Gluzman, I. Y. *Prog. Clin. Biol. Res.* **1989**, *313*, 53-59.

(44) Ginsburg, H.; Stein, W. D. *Biochem. Pharmacol.* **1991**, *41*, 1463-1470.

(45) Bray, P. G.; Howells, R. E.; Ritchie, G. Y.; Ward, S. A. *Biochem. Pharmacol.* **1992**, *44*, 1317-1324.

(46) Bray, P. G.; Howells, R. E.; Ward, S. A. *Biochem. Pharmacol.* **1992**, *43*, 1219-1227.

(47) Sanchez, C. P.; Stein, W.; Lanzer, M. *Biochemistry)* **2003**, *42*, 9383-9394.

(48) Sanchez, C. P.; McLean, J. E.; Stein, W.; Lanzer, M. *Biochemistry 2004, 43*, 16365-16373.

(49) Sanchez, C. P.; McLean, J. E.; Rohrbach, P.; Fidock, D. A.; Stein, W. D.; Lanzer, M. *Biochemistry (N. Y.)* **2005**, *44*, 9862-9870.

(50) Sanchez, C. P.; Stein, W. D.; Lanzer, M. *Trends Parasitol.* **2007**, *23*, 332-339.

(51) Johnson, D. J.; Fidock, D. A.; Mungthin, M.; Lakshmanan, V.; Sidhu, A. B. S.; Bray, P. G.; Ward, S. A. *Mol. Cell.* **2004**, *15*, 867-877.

(52) Tran, C. V.; Saier, M. H., *Microbiology* **2004**, *150*, 1-3.

(53) Price, R. N.; Cassar, C.; Brockman, A. *Antimicrob. Agents Chemother.* **1999**, *43*, 2943-2949.

(54) Durrand, V.; Berry, A.; Sem, R.; Glaziou, P.; Beaudou, J.; Fandeur, T. *Mol. Biochem. Parasitol.* **2004**, *136*, 273-285.

(55) Thapa, S.; Hollander, J.; Linehan, M.; Cox-Singh, J.; Bista, M. B.; Thakur, G. D.; Davis, W. A.; Davis, T. M. E. *Am. J. Trop. Med. Hyg.* **2007**, *77*, 423-430.

(56) Arav-Boger, R.; Shapiro, T. A. *Annu. Rev. Pharmacol. Toxicol.* **2005**, *45*, 565-C-1.

(57) Uhlemann, A. C.; Krishna, S. *Curr. Top. Microbiol. Immunol.* **2005**, *295*, 39-53.

(58) Maïga, O.; Djimdé, A. A.; Hubert, V.; Renard, E.; Aubouy, A.; Kironde, F.; Nsimba, B.; Koram, K.; Doumbo, O. K.; Le Bras, J.; Clain, J. *J. Infect. Dis.* **2007**, *196*, 165-172.

(59) Sandefur, C. I.; Wooden, J. M.; Quaye, I. K.; Sirawaraporn, W.; Sibley, C. H. *Mol. Biochem. Parasitol.* **2007**, *154*, 1-5.

(60) Sisowath, C.; Ferreira, P. E.; Bustamante, L. Y.; Dahlström, S.; Mårtensson, A.; Björkman, A.; Krishna, S.; Gil, J. P. *Trop. Med. Int. Health* **2007**, *12*, 736-742.

(61) Jambou, R.; Legrand, E.; Niang, M.; Khim, N.; Lim, P.; Volney, B.; Ekala, M. T.; Bouchier, C.; Esterre, P.; Fandeur, T.; Mercereau-Puijalon, O. *Lancet* **2005**, *366*, 1960-1963.

(62) Korsinczky, M.; Chen, N.; Kotecka, B.; Saul, A.; Rieckmann, K.; Cheng, Q. *Antimicrob. Agents Chemother.* **2000**, *44*, 2100-2108.

(63) Fivelman, Q. L.; Butcher, G. A.; Adagu, I. S.; Warhurst, D. C.; Pasvol, G. *Malar J.* **2002**, *1*, 1-1.

(64) Feher, M.; Schmidt, J. M. *J. Chem. Inf. Comput. Sci.* **2003**, *43*, 218-227.

(65) Balunas, M. J.; Kinghhorn, D. *Life Sci.* **2005**, *78*, 431-441.

(66) Wilcox, M.; Bodeker, G. An overview of clinical studies on traditional herbal antimalarials; Wilcox, M., Bodeker, G., Eds.; In *Traditional medicinal plants and malaria*; CRC Press: London, U.K., **2004**.

(67) Bruce-Chwatt, L. J. *Br. Med. J. (Clin. Res. Ed)* **1988**, *296*, 1486-1487.

(68) Wright, C. W. *J. Ethnopharmacol.* **2005**, *100*, 67-71.

(69) Baltas, M.; Benbakkar, M.; Gorrichon, L.; Zedde, C. *J. Chromatogr. A,* **1992**, *600*, 323-326.

(70) Najjar, F.; Fréville, F.; Desmoulin, F.; Gorrichon, L.; Baltas, M.; Gornitzka, H.; Tzedakis, T.; André-Barrès, C. *Tetrahedron Lett.,* **2004**, *45*, 6919-6922.

(71) Najjar, F.; Gorrichon, L.; Baltas, M.; André-Barrès, C.; Vial, H. *Org. Biomol. Chem.* **2005**, *3*, 1612-1614.

(72) Carraz, M.; Jossang, A.; Franetich, J.; Siau, A.; Ciceron, L.; Hannoun, L.; Sauerwein, R.; Frappier, F.; Rasoanaivo, P.; Snounou, G.; Mazier, D. *PLoS Med.* **2006**, *3*, e513.

(73) Newman, D. J.; Cragg, G. M.; Snader, K. M. *J. Nat. Prod.* **2003**, 1022-1037.

(74) Casy, A. F. *The steric factor in medicinal chemistry: disymmetric probes of pharmacological receptors;* Springer-Verlag: New York, U. S. A., 1993.

(75) Cordato, D. J.; Mather, L. E.; Herkes, G. K. *J. Clin. Neurosci.* **2003**, *10*, 649-654.

(76) Federsei, H. *Endeavour* **1994**, *18*, 163-172.

(77) Kulikov, N. S.; Bobyleva, M. S. *Pure and Appl. Chem.* **1989**, *61*, 2059-2060.

(78) Kulikov, N. S.; Bobyleva, M. S. *Chem. Soc., Perkin Trans.* **2000**, 2, 571-576

(79) Suzuki, T.; Beuzenberg, V.; Mackenzie, L.; Quilliam, M. A. *J. Chromatogr. A* **2003**, *992*, 141-150.

(80) Larsen, M.; Kromann, H.; Kharazmi, A.; Nielsen, S. F. *Bioorg. Med. Chem. Lett.* **2005**, *15*, 4858-4861.

(81) Adam M. *Stud. Hist. Phil. Biomed. Sci.* **2004**, *36*, 513-537.

(82) Keenan, S. M.; Geyer, J. A.; Welsh, W. J.; Prigge, S. T.; Waters, N. C. *Comb. Chem. High Throughput Screen.* **2005**, *8*, 27-38.

(83) Sullivan, D. J.; Gluzman, I. Y.; Goldberg, D. E. *Science* **1996**, *271*, 219-222.

(84) Sullivan, D. *Int. J. Parasitol.* **2002**, *32*, 1645-1653.

(85) Francis, S. E.; Sullivan, D. J. *Annu. Rev. Microbiol.* **1997**, *51*, 97.

(86) Adams, P.; Berman, P. M.; Egan, T.; Marsh, P.; Silver, J. *J. Inorg. Biochem.* **1996**, *63*, 69-77.

(87) Egan, T. *Inorg. Biochem.* **2006**, *100*, 916-926.

(88) Kumar, S.; Bandyopadhyay, U. *Toxicol. Lett.* **2005**, *157*, 175-188.

(89) Papalexis, V.; Siomos, M. A.; Campanale, N.; Guo, X.; Kocak, G.; Foley, M.; Tilley, L. *Mol. Biochem. Parasitol.* **2001**, *115*, 77-86.

(90) Kawazu, S.; Ikenoue, N.; Takemae, H.; Komaki-Yasuda, K.; Kano, S. *FEBS J.* **2005**, *272*, 1784-1791.

(91) Loria, P.; Miller, S.; Foley, M.; Tilley, L. *Biochem. J.* **1999**, *339 (Pt 2)*, 363-370.

(92) Atamna, H.; Ginsburg, H. *Eur. J. Biochem.* **1997**, *250*, 670-679.

(93) Ginsburg, H.; Famin, O.; Zhang, J.; Krugliak, M. *Biochem. Pharmacol.* **1998**, *56*, 1305-1313.

(94) Sherry, B. A.; Alava, G.; Tracey, K. J.; Martiney, J.; Cerami, A.; Slater, A. F. *J. Inflamm.* **1995**, *45*, 85-96.

(95) Pagola, S.; Stephens, P. W.; Bohle, D. S.; Kosar, A. D.; Madsen, S. K. *Nature* **2000**, *404*, 307-310.

(96) Egan, T. *J. Inorg. Biochem.* **2002**, *91*, 19-26.

(97) Bohle, D. S.; Kosar, A. D.; Stephens, P. W. *Acta Crystallogr. D Biol. Crystallogr.* **2002**, *58*, 1752-1756.

(98) Slater, A. F. *Exp. Parasitol.* **1992**, *74*, 362-365.

(99) Rathore, D.; Jani, D.; Nagarkatti, R.; Kumar, S. *Drug Discov. Today: Ther. Strat.* **2006**, *3*, 153-158.

(100) Schneider, E. L.; Marietta, M. A. *Biochemistry* **2005**, *44*, 979-986.

(101) Fitch, C. D.; Cai, G. Z.; Chen, Y. F.; Shoemaker, J. D. *Biochim. Biophys. Acta* **1999**, *1454*, 31-37.

(102) Fitch, C. D. *Life Sci.* **2004**, *74*, 1957.

(103) Hempelmann, E.; Motta, C.; Hughes, R.; Ward, S. A.; Bray, P. G. *Trends Parasitol.* **2003**, *19*, 23-26.

(104) Egan, T. J.; Chen, J. Y.; de Villiers, K. A.; Mabotha, T. E.; Naidoo, K. J.; Ncokazi, K. K.; Langford, S. J.; McNaughton, D.; Pandiancherri, S.; Wood, B. R. *FEBS Lett.* **2006**, *580*, 5105-5110.

(105) Chen, L.; Zhang, Z. -.; Sendo, F. *Clin. Exp. Immunol.* **2000**, *120*, 125-133.

(106) Chen, L.; Sendo, F. *Parasitol. Int.* **2001**, *50*, 139-143.

(107) Carney, C. K.; Schrimpe, A. C.; Halfpenny, K.; Harry, R. S.; Miller, C. M.; Broncel, M.; Sewell, S. L.; Schaff, J. E.; Deol, R.; Carter, M. D.; Wright, D. W. *J. Biol. Inorg. Chem.* **2006**, *11*, 917-929.

(108) Parroche, P.; Lauw, F. N.; Goutagny, N.; Latz, E.; Monks, B. G.; Visintin, A.; Halmen, K. A.; Lamphier, M.; Olivier, M.; Bartholomeu, D. C.; Gazzinelli, R. T.; Golenbock, D. T. *Proc. Natl. Acad. Sci. U. S. A.* **2007**, *104*, 1919-1924.

(109) Schumann, R. R. *Proc. Natl. Acad. Sci. U. S. A.* **2007**, *104*, 1743-1744.

(110) Coban, C.; Ishii, K. J.; Kawai, T.; Hemmi, H.; Sato, S.; Uematsu, S.; Yamamoto, M.; Takeuchi, O.; Itagaki, S.; Kumar, N.; Horii, T.; Akira, S. *J. Exp. Med.* **2005**, *201*, 19-25.

(111) Engwerda, C. R.; Good, M. F. *Curr. Opin. Immunol.* **2005**, *17*, 381-387.

(112) Skorokhod, O. A.; Alessio, M.; Mordmüller, B.; Arese, P.; Schwarzer, E. *J. Immunol.* **2004**, *173*, 4066-4074.

(113) Kumar, S.; Guha, M.; Choubey, V.; Maity, P.; Bandyopadhyay, U. *Life Sci.* **2007**, *80*, 813-828.

(114) Loup, C.; Lelièvre, J.; Benoit-Vical, F.; Meunier, B. *Antimicrob. Agents Chemother.* **2007**, *51*, 3768-3770.

(115) Pandey, A. V.; Babbarwal, V. K.; Okoyeh, J. N.; Joshi, R. M.; Puri, S. K.; Singh, R. L.; Chauhan, V. S. *Biochem. Biophys. Res. Commun.* **2003**, *308*, 736.

(116) Meshnick, S. R. *Antimicrob. Agents Chemother.* **2003**, *47*, 2712.

(117) Haynes, R. K.; Monti, D.; Taramelli, D.; Basilico, N.; Parapini, S.; Olliaro, P. *Antimicrob. Agents Chemother.* **2003**, *47*, 1175-1175.

(118) Ncokazi, K.; Egan, T. *Anal. Biochem.* **2005**, *338*, 306-319.

(119) Ignatushchenko, M. V.; Winter, R. W.; Bächinger, H. P.; Hinrichs, D. J.; Riscoe, M. K. *FEBS Lett.* **1997**, *409*, 67-73.

(120) Huy, N. T.; Kamei, K.; Yamamoto, T.; Kondo, Y.; Kanaori, K.; Takano, R.; Tajima, K.; Hara, S. *J. Biol. Chem.* **2002**, *277*, 4152-4158.

(121) Iyer, J. K.; Shi, L.; Shankar, A. H.; Sullivan, D. J., *Mol. Med.* **2003**, *9*, 175-182.

(122) Chong, C.; Sullivan, D. *Biochem. Pharm.* **2003**, *66*, 2201-2212.

(123) Egan, T.; Ncokazi, K. *J. Inorg. Biochem.* **2005**, *99*, 1532-1539.

(124) Portela, C.; Afonso, C. M. M.; Pinto, M. M. M.; João Ramos, M. *Bioorg. Med. Chem.* **2004**, *12*, 3313-3321.

(125) Egan, T. J.; Chen, J. Y.; de Villiers, K. A.; Mabotha, T. E.; Naidoo, K. J.; Ncokazi, K. K.; Langford, S. J.; McNaughton, D.; Pandiancherri, S.; Wood, B. R. *FEBS Lett.* **2006**, *580*, 5105-5110.

(126) Leed, A.; DuBay, K.; Ursos, L. M. B.; Sears, D.; De Dios, A. C.; Roepe, P. D. *Biochemistry* **2002**, *41*, 10245-10255.

(127) Tripathi, A. K.; Gupta, A.; Garg, S. K.; Tekwani, B. L. *Life Sci.* **2001**, *69*, 2725-2733.

(128) Egan, T. J.; Hunter, R.; Kaschula, C. H.; Marques, H. M.; Misplon, A.; Walden, J. *J. Med. Chem.* **2000**, *43*, 283-291.

(129) Cheruku, S. R.; Maiti, S.; Dorn, A.; Scorneaux, B.; Bhattacharjee, A. K.; Ellis, W. Y.; Vennerstrom, J. L. *J. Med. Chem.* **2003**, *46*, 3166-3169.

(130) Vippagunta, S. R.; Dorn, A.; Matile, H.; Bhattacharjee, A. K.; Karle, J. M.; Ellis, W. Y.; Ridley, R. G.; Vennerstrom, J. L. *J. Med. Chem.* **1999**, *42*, 4630-4639.

(131) O'Neill, P. M.; Ward, S. A.; Berry, N. G.; Jeyadevan, J. P.; Biagini, G. A.; Asadollaly, E.; Park, B. K.; Bray, P. G. *Curr. To.p Med. Chem.* **2006**, *6*, 479-507.

(132) Egan, T.; Marques, H. *Coord. Chem. Rev.* **1999**, *190-192*, 493-517.

(133) Blauer, G.; Akkawi, M.; Bauminger, E. R. *Biochem. Pharmacol.* **1993**, *46*, 1573-1576.

(134) Kaschula, C. H.; Egan, T. J.; Hunter, R.; Basilico, N.; Parapini, S.; Taramelli, D.; Pasini, E.; Monti, D. *J. Med. Chem.* **2002**, *45*, 3531-3539.

(135) De, D.; Krogstad, F. M.; Cogswell, F. B.; Krogstad, D. J. *Am. J. Trop. Med. Hyg.* **1996**, *55*, 579-583.

(136) Madrid, P.; Sherrill, J.; Liou, A.; Weisman, J.; DeRisi, J.; Guy, R. K. *Bioorg. Med. Chem. Lett.* **2005**, *15*, 1015-1018.

(137) Barrett, A.; Rawlings, N.; O'Brien, E. *J. Struct. Biol.* **2001**, *134*, 95-102.

(138) Sajid, M.; McKerrow, J. H. *Mol. Biochem. Parasitol.*, **2002**, *120*, 1-21.

(139) Olaya, P.; Wasserman, M. *Biochim. Biophys. Acta* **1991**, *1096*, 217-221.

(140) Wickham, M. E.; Culvenor, J. G.; Cowan, G. M. *J. Biol. Chem.* **2003**, *278*, 37658-37663.

(141) Lasonder, E.; Ishihama, Y.; Andersen, J. S.; Vermunt, A. M.; Pain, A.; Sauerwein, R. W.; Eling, W. M.; Hall, N.; Waters, A. P.; Stunnenberg, H. G.; Mann, M. *Nature* **2002**, *419*, 537-542.

(142) Goh, L. L.; Loke, P.; Singh, M.; Sim, T. S. *Protein Expr. Purif.* **2003**, *32*, 194-201.

(143) Goh, L. L.; Sim, T. S. *Biochem. Biophys. Res. Commun.* **2004**, *323*, 565-572.

(144) Goh, L. L.; Sim, T. S. *Biochem. Biophys. Res. Commun.* **2005**, *335*, 762-770.

(145) Dhawan, S.; Dua, M.; Chishti, A. H.; Hanspal, M. *J. Biol. Chem.* **2003**, *278*, 30180-30186.

(146) Dasaradhi, P. V. N.; Mohmmed, A.; Kumar, A.; Hossain, M. J.; Bhatnagar, R. K.; Chauhan, V. S.; Malhotra, P. *Biochem. Biophys. Res. Commun.* **2005**, *336*, 1062-1068.

(147) Go, M. L.; Liu, M.; Wilairat, P.; Rosenthal, P. J.; Saliba, K. J.; Kirk, K. *Antimicrob. Agents Chemother.* **2004**, *48*, 3241-3245.

(148) Singh, N.; Sijwali, P. S.; Pandey, K. C.; Rosenthal, P. J. *Exp. Parasitol.* **2006**, *112*, 187-192.

(149) Rosenthal, P. *Int. J. Parasitol.* **2004**, *34*, 1489-1499.

(150) Singh, N.; Sijwali, P.; Pandey, K.; Rosenthal, P. *Exp. Par.*, **2006**, *112*, 187-192.

(151) Sijwali, P.; Koo, J.; Singh, N.; Rosenthal, P. *Mol. Biochem. Parasitol.* **2006**, *150*, 96-106.

(152) Otto, H. -.; Schirmeister, T. *Chem. Rev.* **1997**, *97*, 133-172.

(153) Babine, R. E.; Bender, S. L. *Chem. Rev.* **1997**, *97*, 1359-1472.

(154) Mutus, B.; Wagner, J.; Talpas, C.; Dimmock, J.; Phillips, O.; Reid, R. S. *Anal. Biochem.* **1989**, *177*, 237-243.

(155) Dimmock, J.; Phillips, O.; Wonko, S.; Hickie, R.; Tuer, R.; Ambrose, S.; Reid, R. S.; Mutus, B.; Talpas, C. *Eur. J. Med. Chem.*, **1989**, *24*, 217-226.

(156) Sijwali, P. S.; Rosenthal, P. J. *Proc. Natl. Acad. Sci. U. S. A.* **2004**, *101*, 4384-4389.

(157) Lyon, J. A.; Haynes, J. D. *J. Immunol.* **1986**, *136*, 2245-2251.

(158) Debrabant, A.; Delplace, P. *Mol. Biochem. Parasitol.* **1989**, *33*, 151-158.

(159) Domínguez, J. N.; López, S.; Charris, J.; Iarruso, L.; Lobo, G.; Semenov, A.; Olson, J. E.; Rosenthal, P. J. *J. Med. Chem.* **1997**, *40*, 2726-2732.

(160) Torres, J. A.; Rodriguez, M. H.; Rodriguez, M. C.; Hernandez-Hernandez, F. d. l. C. *Exp. Parasitol.* **2005**, *111*, 255-259.

(161) Roush, W.; González, F.; McKerrow, J.; Hansell, E. *Bioorg. Med. Chem. Lett.* **1998**, *8*, 2809-2812.

(162) Marquis, R. W.; Yamashita, D. S.; Ru, Y.; LoCastro, S. M.; Oh, H. J.; Erhard, K. F.; DesJarlais, R. L.; Head, M. S.; Smith, W. W.; Zhao, B.; Janson, C. A.; Abdel-Meguid, S. S.; Tomaszek, T. A.; Levy, M. A.; Veber, D. F. *J. Med. Chem.* **1998**, *41*, 3563-3567.

(163) Venkatraman, S.; Kong, J.; Nimkar, S.; Wang, Q. M.; Aubé, J.; Hanzlik, R. *Bioorg. Med. Chem. Lett.* **1999**, *9*, 577-580.

(164) Du, X.; Guo, C.; Hansell, E.; Doyle, P. S.; Caffrey, C. R.; Holler, T. P.; McKerrow, J. H.; Cohen, F. E. *J. Med. Chem.* **2002**, *45*, 2695-2707.

(165) Raventos-Suarrez, C.; Pollack, S.; Nagel, R. L. *Am. J. Trop. Med. Hyg.* **1982**, *31*, 919-922.

(166) Gordeuk, V. R.; Thuma, P. E.; Brittenham, G. M.; Zulu, S.; Simwanza, G.; Mhangu, A. *Blood* **1992**, *79*, 308-312.

(167) Gordeuk, V. R.; Thuma, P. E.; Brittenham, G. M.; Biemba, G.; Zulu, S.; Simwanza, G. *Am. J. Trop. Med. Hyg.* **1993**, *48*, 193-197.

(168) Scheibel, L. W.; Stanton, G. G. *Mol. Pharmacol.* **1986**, *30*, 364-369.

(169) Loyevsky, M.; Gordeuk, V. R.Iron chelators; Rosenthal, P. J., Ed.; In *Antimalarial Chemotherapy: Mechanisms of Action, Resistance, and New Directions in Drug Discovery*; Humana Press: Totowa, New Jersey, 2001; pp 307-324.

(170) Wrigglesworth, J. M.; Baum, H. The biochemical functions of iron; Jacobs, A., Worwood, M., Ed.; *Iron in Biochemistry and Medicine II*; Academic Press: New York, 1980; pp 29-86.

(171) Bezkorovainy, A.; Czajka-Narins, D. M. In *Biochemistry of Nonheme Iron;* Plenum: New York, **1980**.

(172) Scheibel, L. W.; Sherman, I. W. Metabolism and organellar function during various stages of the life cycle: proteins, lipids, nucleic acids and vitamins; Wernsdorfer, W., McGregor, I., Eds.; In *Malaria: principles and practice of Malariology*; Churchill Livingstone: New York, 1988; pp 219.

(173) Bonday, Z. Q.; Taketani, S.; Gupta, P. D.; Padmanaban, G. *J. Biol. Chem.* **1997**, *272*, 839-846.

(174) Pradines, B.; Ramiandrasoa, F.; Basco, L. K.; Bricard, L.; Kunesh, G.; Le-Bras, J. *Antimicrobial Agents Chemother.* **1996**, *40*, 2094-2098.

(175) Moormann, A. M.; Hossler, P. A.; Meshnick, S. R. *Mol. Biochem. Parasitol.* **1999**, *98*, 279-283.

(176) Scheibel, L. W.; Adler, A. *Mol. Pharmacol.* **1980**, *18*, 320-325.

(177) Scheibel, L. W.; Rodriguez, S. *Prog. Clin. Biol. Res.* **1989**, *313*, 149.

(178) Hershko, C.; Theanacho, E. N.; Spira, D. T.; Peter, H. H.; Dobbin, P.; Hider, R. C. *Blood* **1991**, *77*, 637-643.

(179) Cabantchik, Z. I.; Glickstein, H.; Golenser, J.; Loyevsky, M.; Tsafack, A. *Acta Haematol.* **1996**, *95*, 70-77.

(180) Scott, M. D.; Ranz, A.; Kuypers, F. A.; Lubin, B. H.; Meshnick, S. R. *Br. J. Haematol.* **1990**, *75*, 598-602.

(181) Ponka, P.; Baker, E.; Edward, J. T. *Biochim. Biophys. Acta* **1988**, *967*, 122-129.

(182) Ponka, P.; Grady, R. W.; Wilczynska, A.; Schulman, H. M. *Biochim. Biophys. Acta* **1984**, *802*, 477-489.

(183) Mouralian, C.; Buss, J. L.; Stranix, B.; Chin, J.; Ponka, P. *Biochem. Pharmacol.* **2005**, *71*, 214-222.

(184) Staines, H. M.; Ellory, J. C.; Chibale, K. *Comb. Chem. High Throughput Screen.* **2005**, *8*, 81-88.

(185) Wagner, M. A.; Andemariam, B.; Desai, S. A. *Biophys* **2003**, *84*, 116-123.

(186) Huber, S. M.; Uhlemann, A. C.; Gamper, N. L.; Duranton, C.; Kremsner, P. G.; Lang, F. *EMBO J.* **2002**, *21*, 22-30.

(187) Egée, S.; Lapaix, F.; Decherf, G.; Staines, H. M.; Ellory, J. C.; Doerig, C.; Thomas, S. L. *J. Physiol. (Lond.)* **2002**, *542*, 795-801.

(188) Tanneur, V.; Duranton, C.; Verena, B. B.; Sandu, C. D.; Akkaya, C.; Kasinathan, R. S.; Gachet, C.; Sluyter, R.; Barden, J. A.; Wiley, J. S.; Lang, F.; Huber, S. M. *FASEB J.* **2006**, *20*, 133-135.

(189) Krugliak, M.; Ginsburg, H. *Exp. Parasitol.* **2006**, *114*, 253-258.

(190) Saliba, K. J.; Horner, H. A.; Kirk, K. *J. Biol. Chem.* **1998**, *273*, 10190-10195.

(191) Desai, S. A.; Bezrukov, S. M.; Zimmerberg, J. *Nature* **2000**, *406*, 1001-1005.

(192) Fayolle, M.; Ionita, M.; Krishna, S.; Morin, C.; Patel, A. P. *Bioorg. Med. Chem. Lett.* **2006**, *16*, 1267-1271.

(193) Gero, A. M.; Wood, A. M.; Hogue, D. L.; Upston, J. M. *Mol. Biochem. Parasitol.* **1991**, *44*, 195-206.

(194) Rowena, E. M.; Kirk, K. *Blood* **2007**, *109*, 2217-2224.

(195) Kanaani, J.; Ginsburg, H. *J. Cell. Physiol.* **1991**, *149*, 469-476.

(196) Cranmer, S. L.; Conant, A. R.; Gutteridge, W. E.; Halestrap, A. P. *J. Biol. Chem.* **1995**, *270*, 15045-15052.

(197) Lew, V. L.; Tiffert, T.; Ginsburg, H. *Blood* **2003**, *101*, 4189-4194.

(198) Gero, A. M.; Bugledich, E. M.; Paterson, A. R. P.; Jamieson, G. P. *Mol. Biochem. Parasitol.* **1988**, *27*, 159-170.

(199) Ginsburg, H.; Kutner, S.; Krugliak, M.; Cabantchik, Z. I. *Mol. Biochem. Parasitol.* **1985**, *14*, 313-322.

(200) Singh, S.; Puri, S. K.; Sing, S. K.; Srivastava, R.; Gupta, R. C.; Pandey, V. C. *J. Biol. Chem.* **1997**, *272*, 506-513.

(201) Kirk, K.; Horner, H. A.; Elford, B. C.; Ellory, J. C.; Newbold, C. I. *J. Biol. Chem.* **1994**, *269*, 3339-3347.

(202) Gero, A. M.; Upston, J. M. *Parasitol. Today* **1992**, *8*, 283-286.

(203) Kirk, K.; Horner, H. A.; Spillet, D. J.; Elford, B. C.; Ellory, J. C. *FEBS Lett.* **1993**, *323*, 123-128.

(204) Puljak, L.; Kilic, G. *Biochim. Biophys. Acta* **2006**, *1762*, 404-413.

(205) Bouyer, G.; Eg,e, S.; Thomas, S. L. *Blood Cells Mol. Dis.* **2006**, *36*, 248-254.

(206) Desai, S. A. *Curr. Drug Targets Infect. Disord.* **2004**, *4*, 79-86.

(207) Alkhalil, A.; Cohn, J. V.; Wagner, M. A.; Cabrera, J. S.; Rajapandi, T.; Desai, S. A. *Blood* **2004**, *104*, 4279-4286.

(208) Verloo, P.; Kocken, C. H.; Van der Wel, A.; Tilly, B. C.; Hogema, B. M.; Sinaasapel, M. *J. Biol. Chem.* **2004**, *279*, 10316-10322.

(209) Lisk, G.; Kang, M.; Cohn, J. V.; Desai, S. A. *Eukaryot. Cell* **2006**, *5*, 1882-1893.

(210) Desai, S. A.; Alkhalil, A.; Kang, M.; Ashfaq, U.; Nguyen, C. *J. Biol. Chem.* **2005**, *280*, 16861-16867.

(211) Kirk, K.; Horner, H. A. *Biochem. J.* **1995**, *311*, 761-768.

(212) Sharma, R. A.; Gescher, A. J.; Steward, W. P. *Eur. J. Cancer,* **2005**, *41*, 1955-1968.

(213) Rasmusen, H. B.; Christensen, S. B.; Kuist, L. P.; Karazami, A. *Planta Med.* **2000**, *66*, 396-398.

(214) Reddy, R. C.; Vatsala, P. G.; Keshamouni, V. G.; Padmanaban, G.; Rangarajan, P. N. *Biochem. Biophys. Res. Commun.* **2005**, *326*, 472-474.

(215) Nandakumar, D. N.; Nagaraj, V. A.; Vathsala, P. G.; Rangarajan P.; Padmanaban, G. *Antimicrob. Agents Chemother.* **2006**, *50*, 1859-1860.

(216) Martinelli, A.; Rodrigues, A. L. *Exp. Parasitol.* **2008**, *119*, 304-307.

(217) Araujo, C. A.; Alegrio, L. V.; Gomes, D. C.; Lima, M. E.; Gomes-Cardoso, L.; Leon, L. L. *Mem. Inst. Oswaldo Cruz* **1999**, *94*, 791-794.

(218) Koide, T.; Nose, M.; Ogihara, Y.; Yabu, Y.; Ohta, N. *Biol. Pharm. Bull.* **2002**, *25*, 131-133.

(219) Gomes, D. de C F.; Alegrio, L. V.; de Lima,M. E. F.; Leon, L. L.; Araújo, C. A. C. *Arzneim.-Forsch.* **2002**, *52*, 120-124.

(220) Gomes, D. de Castro F.; Alegrio, L. V.; Leon, L. L.; de Lima,M. E. F. *Arzneim.- Forsch.* **2002**, *52*, 695-698.

(221) Koide, T.; Nose, M.; Ogihara, Y.; Yabu, Y.; Ohta, N. *Biol. Pharm. Bull.* **2002**, *25*, 131-133.

(222) Alves, L. V.; de Canto-Cavalheiro, M. M.; Cysne-Finkelstein, L.; Leon, L. *Biol. Pharm. Bull.* **2003**, *26*, 453-456.

(223) Nose, M.; Koide, T.; Ogihara, Y.; Yabu, Y.; Ohta, N. *Biol. Pharm. Bull.* **1998**, *21*, 643-645.

(224) Borsari, M.; Ferrari, E.; Grandi, R.; Saladini, M. *Inorg. Chim. Acta* **2002**, *328*, 61.

(225) Jiao, Y.; Wilkinson, J.; Christine Pietsch, E.; Buss, J. L.; Wang, W.; Planalp, R.; Torti, F. M.; Torti, S. V. *Free Radic. Biol. Med.* **2006**, *40*, 1152-1160.

(226) Bilmen, J. G.; Khan, S. Z.; Javed, M.; Michelangeli, F. *Eur. J. Biochem.* **2001**, *268*, 6318-6327.

(227) Go, M.-L.; Liu, M.; Wilairat, P.; Rosenthal, P. J.; Saliba, K. J.; Kirk, K. *Antimicrob. Agent Chemother.* **2004**, 48, 3241-3245.

(228) Ghatak, N.; Basu, N. *Indian. J. Exp. Biol.* **1972**, *10*, 235-236.

(229) Rao, T. S.; Basu, N.; Siddiqui, H. H. *Indian J. Med. Res.* **1982**, *75*, 574-578.

(230) Mohan, K.; Sam, H.; Stevenson, M. M. *Infect. Immun.* **1999**, *67*, 513-519.

(231) Aldieri, E.; Atragene, D.; Bergandi, L.; Riganti, C.; Costamagna, C.; Bosia, A.; Ghigo, D. *FEB Lett.* **2003**, *552*, 141-144.

(232) Hugossona , E.; Montgomery, S. M.; Premjid, Z.; Troye-Blomberge, M.; Björkmana, A. *Acta Trop.* **2006**, *99*, 75-82.

(233) Huang, M. T.; Lysz, T.; Ferraro, T.; Abidi, T. F.; Laskin, J. D.; Conney, A. H. *Cancer Res.* **1991**, *51*, 813-819.

(234) Ammon, H. P.; Anazodo, M. I.; Safayhi, H.; Dhawan, B. N.; Srimal, R. C. *Planta Med.* **1992**, *58*, 226-226.

(235) Plummer, S. M.; Holloway, K. A.; Manson, M. M.; Munks, R. J.; Kaptein, A.; Farrow, S.; Howells, L. *Oncogene* **1999**, *18*, 6013.

(236) Rao, C. V. *Adv. Exp. Med. Biol.* **2007**, *595*, 213-226.

(237) Brouet, I.; Ohshima, H. *Biochem. Biophys. Res. Commun.* **1995**, *206*, 533-540.

(238) Chan, M. M.; Huang, H. I.; Fenton, M. R.; Fong, D. *Biochem. Pharmacol.* **1998**, *55*, 1955-1962.

(239) Mohan, R.; Sivak, J.; Ashton, P.; Russo, L. A.; Pham, B. Q.; Kasahara, N.; Raizman, M. B.; Fini, M. E. *J. Biol. Chem.* **2000**, *275*, 10405-10412.

(240) Bierhaus, A.; Zhang, Y.; Quehenberger, P.; Luther, T.; Haase, M.; Müller, M.; Mackman, N.; Ziegler, R.; Nawroth, P. P. *Thromb. Haemost.* **1997**, *77*, 772-782.

(241) Bharti, A. C.; Donato, N.; Aggarwal, B. B. *J. Immunol.* **2003**, *171*, 3863-3871.

(242) Ravindranath, V.; Chandrasekhara, N. *Toxicology* **1980**, *16*, 259-265.

(243) Ravindranath, V.; Chandrasekhara, N. *Toxicology* **1981**, *22*, 337-344.

CHAPTER 2
SYNTHESIS AND CHARACTERIZATION OF DERIVATIVES OF CURCUMIN

2.1 Introduction

This chapter describes the synthesis and characterization of derivatives of curcumin. The main aim was to synthesize a lead compound with improved antiplasmodial activity, oral bioavailability and a longer half-life compared to curcumin. The synthetic procedures used were simple one step reactions which may be scaled up at an industrial level. This was a critical consideration in drug development since complex synthetic procedures are associated with high costs and low yields which reduce the competitiveness of a drug in the market [1, 2]. The chemical modifications were aimed at the carbonyl group of curcumin since it is the most important site of metabolism of the parent compound. It was hoped that this would reduce metabolism and therefore increase the half-life of the derivatives. Chemical modifications involved addition of the following bioactiphores: azoles (**2.2.1** and **2.2.2**, Figure 2-1); sulfonylurea (**2.3**); thiosemicarbazone (**2.5**); quinoline (**2.7**) and acyl hydrazone (**2.9**). These bioactiphores were expected to increase activity against selected molecular targets within *Plasmodium falciparum*. Isomerism of synthetic derivatives was investigated. The synthesized derivatives were evaluated for compliance with the minimum molecular requirements for good oral bioavailability as described by Lipinski *et al.* [3] and Veber *et al.* [4]. These molecular properties include: octanol-water partition coefficient (cLogP); topological surface area (tPSA); molecular weight (mwt.); and the total number of hydrogen bond donors and acceptors. The cLog P, tPSA and Mwt. were calculated using ChemDraw ultra™ Software version 9. Hydrogen bond donors were the sum of all heteroatoms bonded to at least one hydrogen group in a molecule. Though curcumin meets all the minimum aforementioned requirements, it has a poor oral bioavailability due to its poor

water solubility. To overcome this problem, the derivatives were required to have a better water solubility profile than curcumin as indicated by a higher cLogP relative to curcumin.

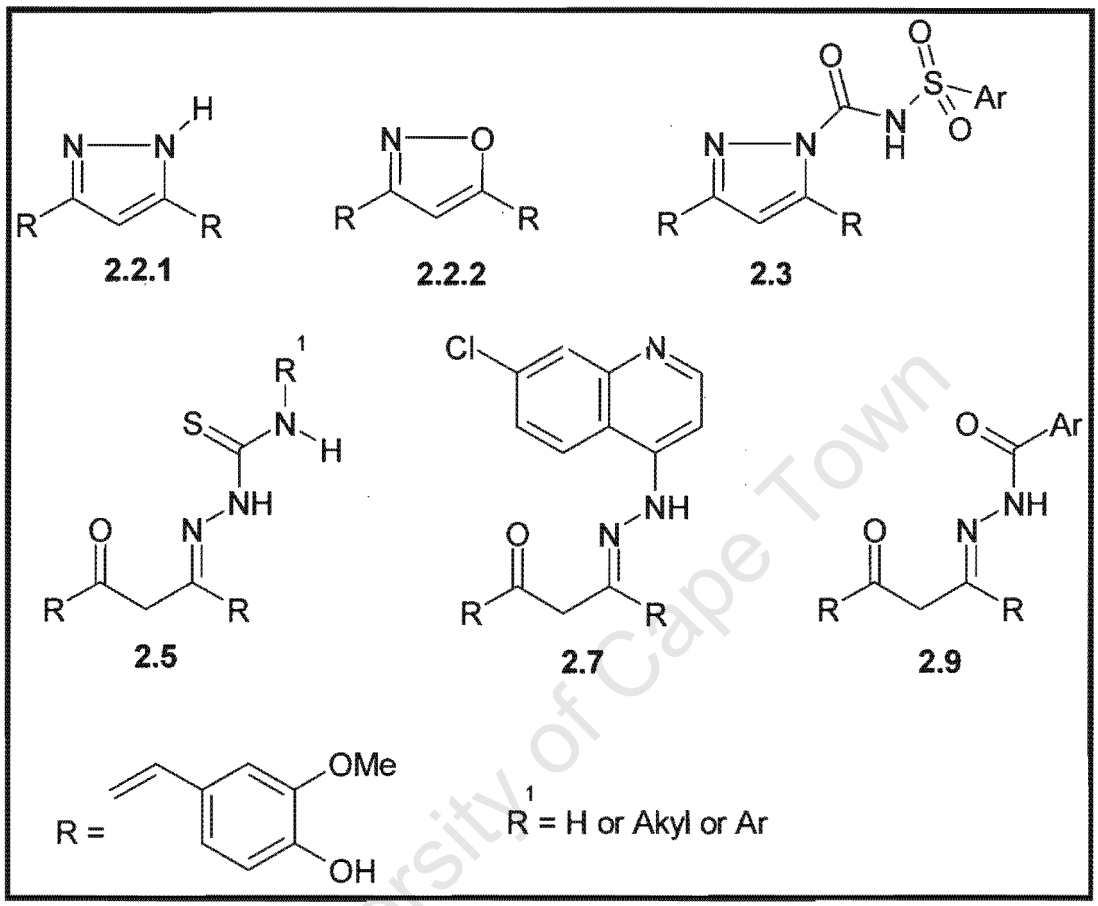

Figure 2 - 1: General structures of the pyrazole: (2.2.1); isoxazole (2.2.2); sulfonylureas (2.3); thiosemicarbazone (2.5); quinoline (2.7) and acyl hydrazone (2.9) derivatives of curcumin.

2.1.1 Reaction mechanisms

Nearly all the synthetic reactions involved 1, 2-nucleophilic attack at the carbonyl groups of curcumin as outlined in Figure 2-2[5]. The carbonyl group is a good electrophile which reacts with nucleophiles at the carbon atom of the carbonyl functional group. The reaction can proceed in either acidic or alkaline conditions. Under acidic conditions, nucleophilic attack was preceded by the protonation of oxygen of the carbonyl group (Figure 2-2). Nucleophilic attack under alkaline conditions began with the deprotonation of nucleophile.

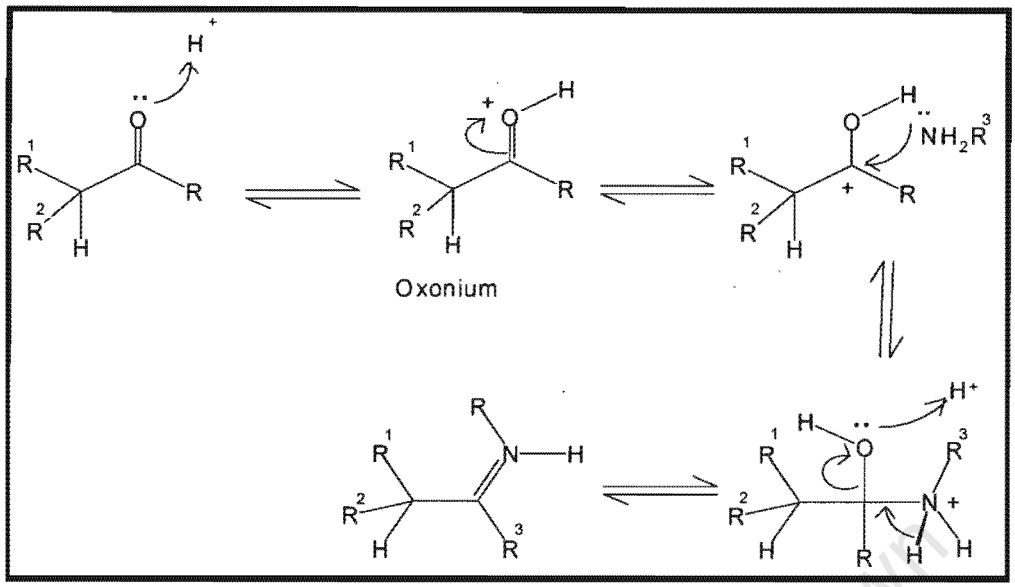

Figure 2 - 2: Mechanism of 1, 2-nucleophilic attack on the carbonyl carbon [5]

In the case of curcumin, a competing mechanism is, 1, 4-conjugate addition where nucleophilic attack takes place on the double bond adjacent to the carbonyl group (Figure 2-3).

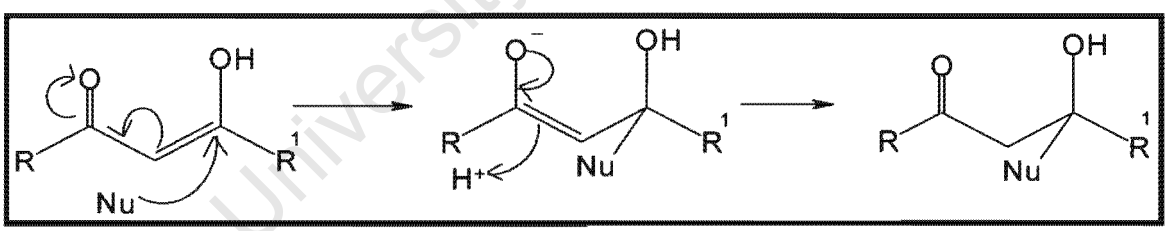

Figure 2 - 3: Mechanism of 1, 4-conjugate addition in α, β unsaturated carbonyl compounds [5]

The former reaction mechanism was expected to predominate since it is faster but is reversible and results in compounds of lower stability [5]. Conjugate addition proceeds slowly compared to 1, 2 nucleophilic addition and its products are more stable. Conjugate addition is irreversible.

2.2 Purification and characterization of curcumin

Curcumin (**2.1.1**) was purified from commercially available technical grade curcumin by flash chromatography on phosphate impregnated silica gel as described by Rasmussen *et al.* [6]. The 1-D and 2-D spectral data of curcumin are presented in Table 2-1. Its physcial and spectroscopic characteristics were in agreement with those previously described in literature [7-9]. An interesting feature in the ^{1}H NMR spectrum of curcumin was the integration due to H-10 which appeared as a single proton confirming the predominance of the enol form as reported in literature [10].

Table 2 - 1: ^{1}H, ^{13}C, HSQC and HMQC spectral data of curcumin (2.1.1B)

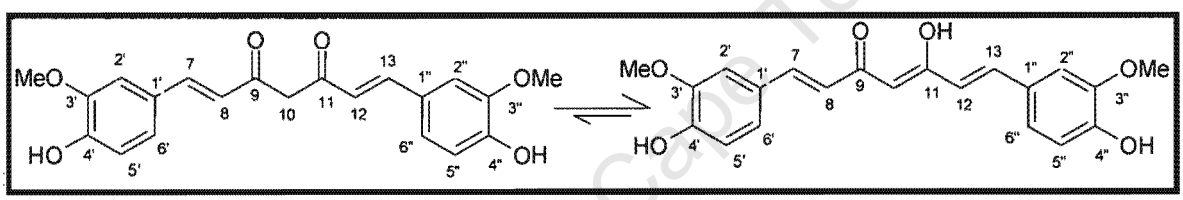

POSITION	δ H	J Value (Hz)	δ C HSQC	HMQC
1', 1"	-		127.7	
2', 2"	7.05	d, 1.8	109.7	C-4', 4", C-1, C-7, C-6',6"
3', 3"	-		146.8	
4', 4"	-		147.9	
5', 5"	6.93	d, 8.1	114.9	C-1',1", C-3', 3"
6', 6"	7.12	dd, 8.1, 1.8	122.9	C-4',4", C-1, 7
7, 13	7.59	d, 15.7	140.5	C-2',2", C-2, 6, C-3
8, 12	6.47	d,15.7	121.8	C-1',1", C-3
9,11	-		183.3	
10	5.80	s	101.1	C-3
2 x OCH_3	3.83		55.0	C-3',3"

2.3 Synthesis of the Azole derivatives of curcumin

2.3.1 Rationale for the antimalarial activity of the azole derivatives

The synthesis of the pyrazole (**2.2.1**, Figure 2-1) and isoxazole (**2.2.2**) derivatives has previously been reported [11-14].

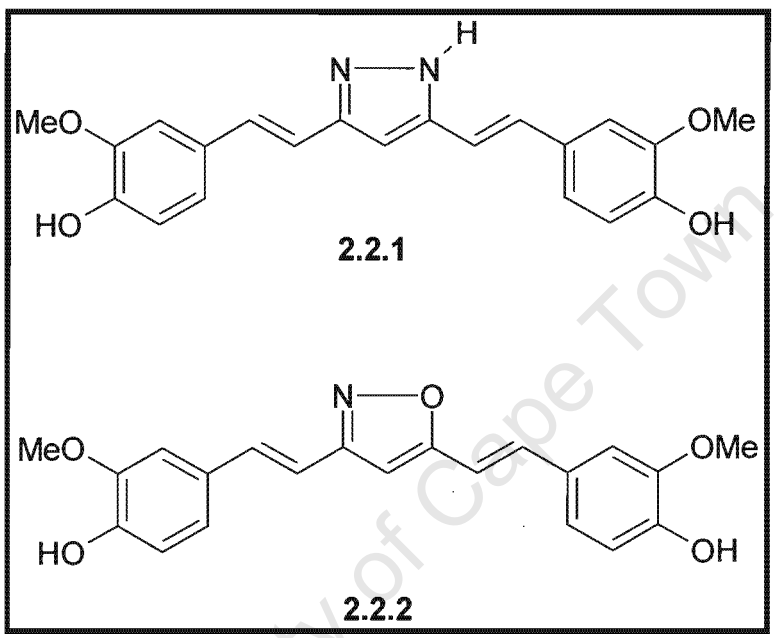

Figure 2 - 4: Structures of the Pyrazole (2.2.1) and Isoxazole (2.2.2) derivatives of curcumin

In this class of derivatives, the diketone moiety was replaced by a rigid pyrazole or isoxazole ring (Figure 2-4). It was envisaged that this modification would improve the antimalarial activity since azole-containing compounds have antiplasmodial activity [15]. This activity is a result of a delocalized π ring system that is capable of interacting with the π rings of hematin thus interrupting hemozoin formation [16]. The protonatable nitrogen group was likely to improve the accumulation of the compound in the parasite's acidic food vacuole. The food vacuole is the site of action of antimalarial agents such as the 4- and 8- aminoquinolines. In addition, azole derivatives have a superior iron chelating ability compared to curcumin and were therefore hypothesized to have better antimalarial activity [17, 18]. The azole derivatives have been shown to have a greater anti-inflammatory activity than the parent compound [17] which is a useful property in the management of malaria [19, 20]. The

introduction of a protonatable nitrogen group was likely to improve the aqueous solubility and thereby improve oral bioavailability. Increasing the rigidity of the heptadiene-dione chain by replacement of the dicarbonyl group with the azole ring was likely to reduce the rate of reductive metabolism of the molecule.

2.3.2 Synthesis and Characterization of isomers of the Pyrazole Derivative (Hydrazinocurcumin)

Curcumin was reacted with hydrazine monohydrate under acidic conditions as described by Selvam *et al.*, [14] and basic conditions (Scheme 2-1).

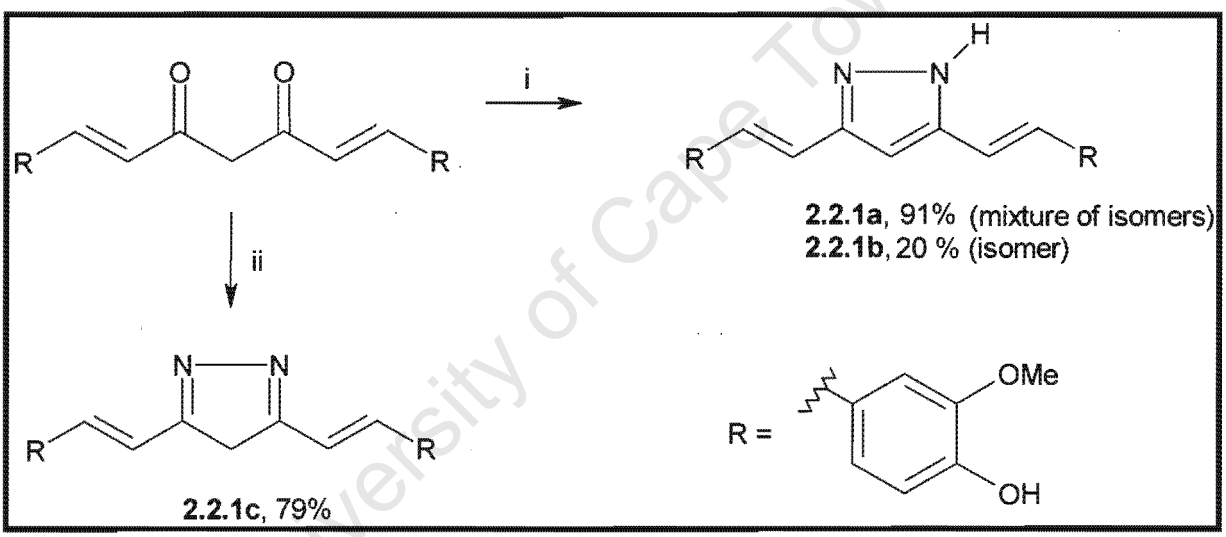

Scheme 2 - 1: *Reagents and conditions* i) NH_2NH_2, acetic acid, rt, 72 h; ii) NH_2NH_2, NaOH, EtOH, 65°C, 15 min.

When synthesis in acetic acid was carried out for 7 hours as described in literature, the reaction yields were low (19 %). The yield increased to 91 % when the reaction was carried out over 72 hours. Though elemental analysis of the reaction product (**2.2.1a**) showed a high degree of purity, HPLC chromatographic separation revealed that it was a mixture of 3 isomers (Figure 2-4).

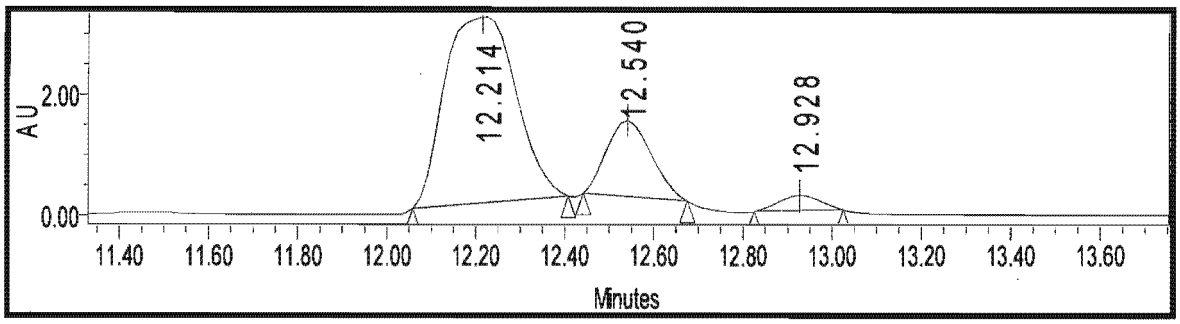

Figure 2 - 5: Expanded HPLC chromatogram of the pyrazole derivative of curcumin - hydrazinocurcumin (2.2.1A)

The mixture was subjected to column chromatography on silica gel and the isomer **2.2.1b** was obtained at a low yield of 20 %. The low yield was attributed to the difficulty in achieving chromatographic separation of the mixture.

The alternative procedure for the synthesis of the pyrazole derivatives by heating curcumin in ethanol at 65°C for 15 minutes using NaOH as a catalyst afforded a red colored isomer **2.2.1c**. When the reaction was carried out for 1 hour instead of 15 minutes, the yellow colored mixture (**2.2.1a**) was obtained. The two products, **2.2.1b and 2.2.1c**, were isomers because they had the same mass charge ratio (*m/z*) of 364 on low resolution mass spectrometry (LRMS). The former compound was yellow in color and had a melting point of 217-218 °C while the later compound had a melting point of 227°C. The mixture (**2.2.1a**) was yellow in color and its melting point (211-212 °C) was similar to that reported by Flynn *et al.* [17]. Interestingly, on crystallization from isopropanol, **2.21b** formed red colored crystals. Though isomers of hydrazinocurcumin have not been reported in literature, different authors report either a red or yellow colored compound [13, 14, 17, 21]. The 1 and 2 D NMR spectral data of **2.2.1b** and **2.2.1c** are presented in Table 2-2 and 2-3 respectively. The ^{1}H NMR spectrum of **2.2.1b** was very similar to that reported by Shim *et al.*, [21]. There were slight differences in the ^{13}C spectra which may have been due to differences in the NMR solvents used. The proton NMR spectrum of **2.2.1c** was similar to that reported to Flynn *et al.* [11].

There were significant differences in the ^{1}H and ^{13}C spectra of **2.2.1b** and **2.2.1c**. In the ^{1}H NMR spectrum of **2.2.1b**, the shift due to H-2 and H-2' appeared as a singlet as opposed to the expected doublet. Secondly, the shifts due to the imine group (C=N) appeared in the ^{13}C spectrum of **2.2.1b** while in the ^{13}C spectrum of **2.2.1c** it did not appear. This indicated that there was limited tautomeric exchange of H-10 in **2.2.1c**. Secondly, the proton shift due to the H-7 and H-13 was more deshielded at δ 7.48 in **2.2.1c** compared to **2.2.1b** where the shifts occurred at δ 7.04. This indicated that resonance was more effective in **2.2.1c**.

Table 2 - 2: The ^{1}H, ^{13}C, HSQC AND HMQC spectral data of the isomer of hydrazinocurcumin (2.2.1B)

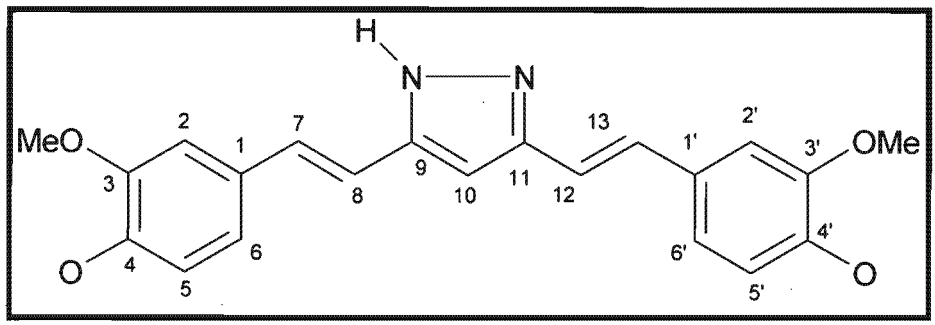

Position	δ ^{1}H	*J* values (Hz)	HSQC	COSY	HMQC
1, 1'	-		128.3[a]		-
2,2'	7.13	d, 1.8	109.6	H-6, H-6'	C 4, 4';C 7,13; C-6,6'
3, 3'	-		146.7[a]		-
4, 4'	-		147.8[a]		-
5, 5'	6.78	d, 8.4	115.6	H-2, H-2', H-6, 6'	C 1, 1'; C 3, 3'
6, 6'	6.90	m	120.0	H-5, H-5'	-
7, 13	7.04	d, 16.5	129.5	-	C-6; C-2
8, 12	6.90	m	-	-	-
9, 11	-		-		-
10	6.05	s	99.3	-	-
2 X OCH_3	3.82	s	55.6		C-3, C-3'

[a] Assignment done using HMQC data and not HSQC data

Table 2 - 3: The ^{1}H, ^{13}C, HSQC AND HMQC spectral data of the isomer of hydrazinocurcumin (2.2.1C)

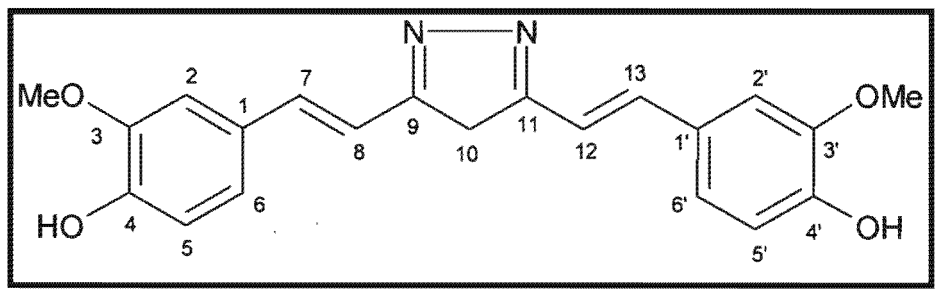

Position	δ ^{1}H	*J* value (Hz)	δC (HSQC)	COSY	HMQC
1, 1'	-		125.8		-
2,2'	7.25	d, 1.9	111.2	H-6, H-6'	C-1, 1'; C 4, 4'; C 7,13; C-6, 6'
3, 3'	-		147.9[a]		-
4, 4'	-		149.1[a]		-
5, 5'	6.78	d, 8.1	116.9	H-2, H-2', H-6, H-6'	C-1, 1'; C-3, 3'; C-6, 6'
6, 6'	7.06	d, 8.6, 1.9	122.7	H-5, H-5'	C-2, 2'; C-5, 5'; C-4, 4'; C-7,13
7, 13	7.48	d, 15.9	144.4	-	C-1, 1'; C-2, 2'; C-6, 6'; C-8,12; C-9,11
8, 12	6.33	d, 15.8	114.6	-	C-1, 1'; C-2, 2'; C-8,12; C-9,11
9, 11	-		167.9[a]		-
10	6.05	s	109.6[a]	-	-
2 x - OCH_3	3.83	s	55.7		C-3, C-3'; C-4, C-4'

[a] Assignment done on the basis of HMQC data and not HSQC data.

On the basis of these observations, it was concluded that **2.2.1b** and **2.2.1c** are tautomers named 1-N-*H*-hydrazinocurcumin and 3-*H*-hydrazinocurcumin respectively. The tautomer, 1-N-*H*-hydrazinocurcumin, had one imine bond and an ethine bond in the pyrazole ring (Figure 2-6). The second tautomer, **2.2.1c**, had two imine bonds in the pyrazole ring.

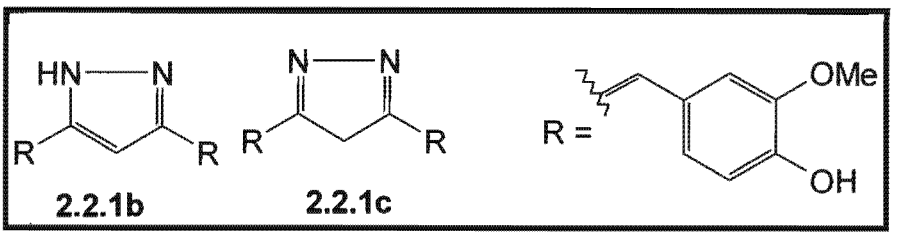

Figure 2 - 6: Chemical structures of tautomers of hydrazinocurcumin.

The differences in the ^{1}H and ^{13}C spectra of **2.2.1b** and **2.2.1c** are best explained by differences in the resonance structures (Figure 2-7).

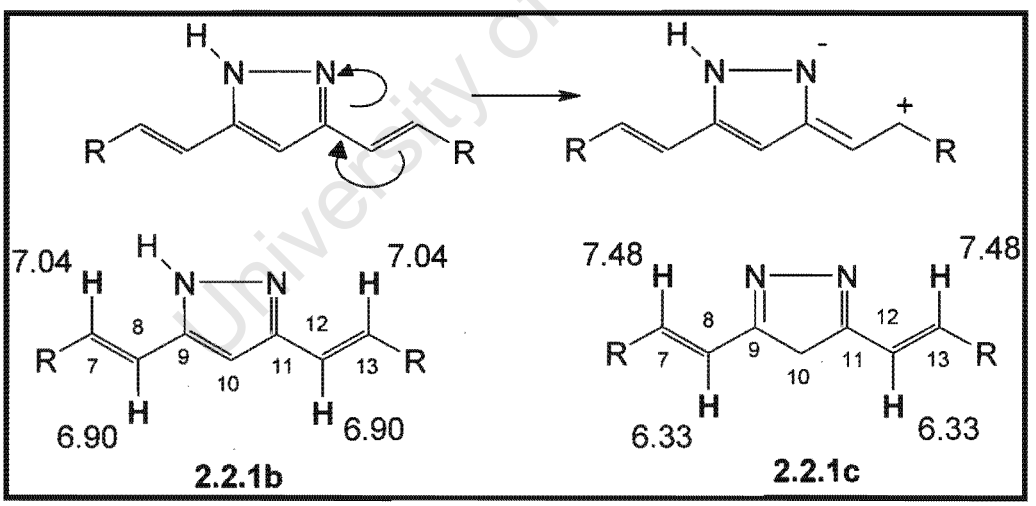

Figure 2 - 7: Key differences in the ^{1}H shifts of tautomers of hydrazinocurcumin

In **2.2.1c**, resonance is more effective because of the presence of two imine bonds hence the affected protons (H-7, 13 and H-8, 12) are more deshielded or shielded. Crystals of **2.2.1b** and **2.2.2c** have been submitted for X-ray crystallography to confirm the structures of the different isomers. The

tautomer, **2.2.1b** is more thermodynamically stable because it is major reaction product when reaction time was prolonged. In the ^{13}C NMR spectrum of **2.2.1b**, the carbon shifts due to C-9 and C-11 were not observed due to rapid tautomerism of the proton H-10 [21] (Figure 2-8).

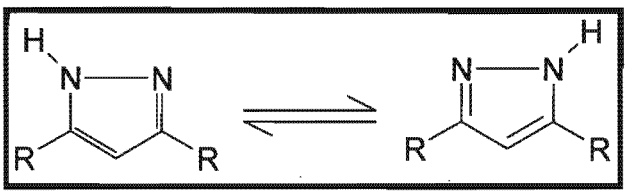

Figure 2 - 8: Tautomeric exchange in 1-N-*H*-hydrazinocurcumin (2.2.1b) [21]

2.3.3 Synthesis and Characterization of Isomers of the Isoxazole derivative of Curcumin

The isoxazole derivatives were synthesized using the method described by Selvam *et al.* [14] (Scheme 2-2).

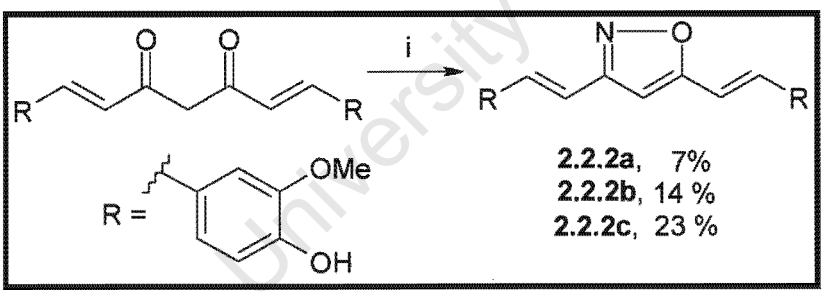

Scheme 2 - 2: *Reagents and Conditions*. NH_2OH, acetic acid, 85°C, 48 h.

On column chromatography, three reaction products were obtained whose molecular ions had the same mass charge ratio of 366.4. The isomers had different colors and melting points (Table 2-4). The most abundant isomer was white as reported in literature [22].

Table 2 - 4: The Physical Characteristics of Isomers of the Isoxazole derivative of Curcumin

Isomer	Color	Yield	%age purity	R_f (EtOAc: CH_2Cl_2 1:19)	m.p. (°C)
2.2.2a	Dull yellow	7 %	88 ($t_{R'}$ = 14.956)	0.3	168-169
2.2.2b	Off white	23 %	88 ($t_{R'}$ = 14.952)	0.26	173
2.2.2c	Bright yellow	14%	97 ($t_{R'}$ = 14.929)	0.3	169-170

Unlike, hydrazocurcumin and curcumin, the ^{1}H NMR spectra of the isoxazole derivative was more complex and this was due to loss of compound symmetry. There were subtle differences in the coupling constants and chemical shifts of the ^{1}H NMR spectra of the different isomers (Table 2-5). Unlike **2.2.2a**, the shifts due to the methoxy groups, phenolic OH groups and protons H-7 and H-13 were equivalent for isomers **2.2.2b** and **2.2.2c**. It was difficult to deduce the differences in the structures of the isomers using the ^{1}H NMR spectrum alone. The isomers have been submitted for X-ray crystallographic evaluation and results are being awaited.

Table 2 - 5: Comparison of the Chemical Shifts of ^1H Spectra of Isomers of the Isoxazole derivative of Curcumin (2.2.2)

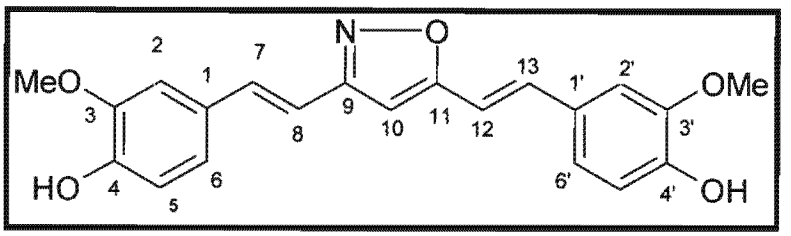

	2.2.2b	**2.2.2a**	**2.2.2c**
POSITION	Yellow	Dull yellow	White
4- Ar-OH	9.37 (s)	9.36 (s)	9.31 (2H,s)
4'- Ar-OH (s)	9.30 (s)	9.29 (s)	
H-2 (d)	7.29 (*J* 1.8)	7.28 (d, *J* 1.6)	7.29 (d, *J* 1.8)
H-2' (d)	7.27 (d, *J* 1.8)	7.27 (*J* 1.6)	7.28 (*J* 2.1)
H-5 (d)	6.80 (*J* 8.4)	6.80 (*J* 8.4)	7.05 (*J* 9.3)
H-5'	6.80 (d, *J* 8.0)	6.78 (d, *J* 8.0)	7.05 (d, *J* 9.3)
H-6, H-6' (dd)	7.07 (*J* 8.2, 1.8)	7.06 (*J* 8.2, 1.6)	6.81 (*J* 8.1, 2.4)
H-7 (d)	7.28 (*J* 16.4)	7.07 (*J* 16.8)	7.28 (2H, *J* 16.5)
H-13 (d)		7.04 (*J* 16.4)	
H-8	7.07 *J* 16.4)	7.07 *J* 16.4)	7.07 (*J* 16.8)
H-12	7.05 (d, *J* 16.8)	7.05 (d, *J* 16.8)	7.05 (d, *J* 16.8)
H-10 (s)	6.83	6.83	6.84
4 -OCH_3	3.84 (6H,s)	3.83 (3H,s)	3.85 (6H, s)
4' -OCH_3		3.82 (3H,s)	

2.3.4 The predictive bioavailability molecular properties of the Azole derivatives

The pyrazole and isoxazole derivatives meet all the minimum requirements for good oral bioavailability as outlined by Lipinski *et al.* [3, 23] (Table 2-6). The clogP values of the pyrazole and isoxazole derivative were greater than that of curcumin indicating the derivatives had higher water solubility and were therefore more likely to have a better absorption profile.

Table 2 - 6: Molecular Properties of the Azole Derivatives (2.2.1 and 2.2.2) that Predict Oral Bioavailability

	cLog P	tPSA	H-bond donors	H-bond acceptors	Mwt.	Criteria met
Rule	< 5	< 140	< 5	< 10	< 500	
Curcumin (enolic form)	2.939	121.9	3	6	368.39	5
2.2.1	3.989	99.9	3	9	364.14	5
2.2.2	3.869	80.28	2	6	365.39	5

2.4 Synthesis and characterization of Sulfonylurea Derivatives of Curcumin

2.4.1 Rationale for the synthesis of Sulfonylurea Derivatives

Sulfonylureas are anionic channel inhibitors and are used clinically for the management of diabetes [24]. Sulfonylureas have anticancer activity [25]. The sulfonylureas, glibenclamide and meglitinide have antimalarial and antileishmanial activity [26, 27]. Their antimalarial activity is attributed to inhibition

of parasite induced anionic channels on the host red blood cell. They inhibit the transport of low molecular weight solutes into the infected erythrocytes. In addition they inhibit formation of beta-hematin and cysteine proteases [28]. It was envisaged that the addition of the sulfonylurea pharmacophore to hydrazinocurcumin would increase its antimalarial activity by imparting the ability to inhibit anionic channels. Retention of the pyrazole pharmacophore would confer the ability to inhibit hemozoin formation. The sulfonylurea pharmacophore was likely to improve the water solubility and thus enhance bioavailability by improving dissolution in the gut.

2.4.2 Synthesis of sulfonylurea derivatives

The sulfonylurea derivatives of curcumin were synthesized by reacting hydrazinocurcumin (**2.2.1**) with an arene sulfonyl isocyanate [29] (Scheme 2-3).

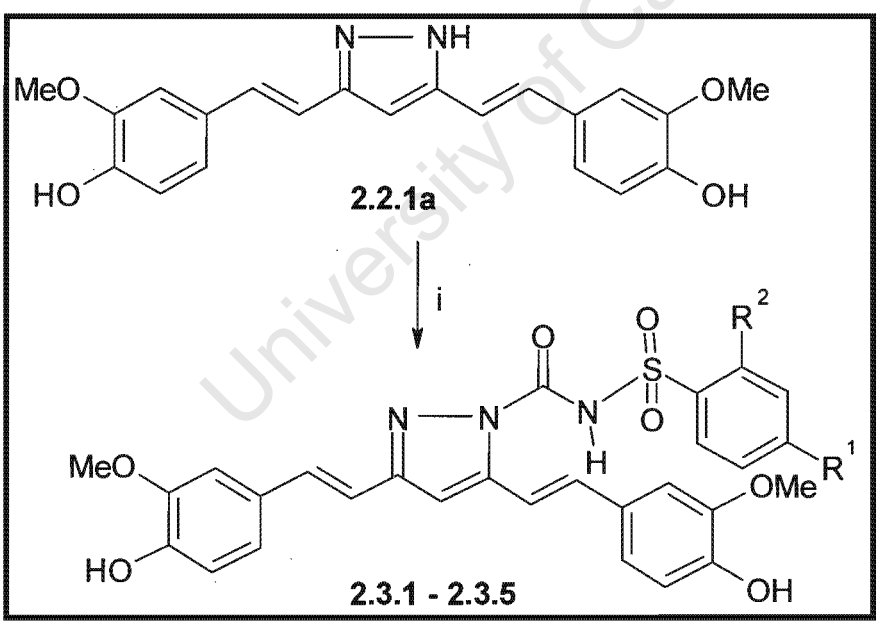

Scheme 2 - 3: *Reagents and conditions* i) arene sulfonyl isocyanate, DMF, 65°C, N_2, 24 h

The reaction involved nucleophilic attack of the pyrazole amine group on the isocyanate carbon group. The reaction was performed under nitrogen in an aprotic solvent, *N*, *N*-dimethyl formamide.

The isocyanates were used in excess. The yields, purity and melting points of the reaction products are presented in Table 2-7.

Table 2 - 7: The yields of the sulfonylurea derivatives of curcumin.

Compound	R^1	R^2	Melting Point (°C)	HPLC Purity	Yield (%)
2.3.1	H	H	140	93 ($t_{R'}$=11.89)	24
2.3.2	CH_3	H	181-2	ND[a]	33
2.3.3	Cl	H	218	93 ($t_{R'}$=11.61)	26
2.3.4	F	H	186-8	100 ($t_{R'}$=11.63)	13
2.3.5	H	CH_3	181-2	100 ($t_{R'}$=11.60)	25

[a] Purity determined by elemental analysis

The presence of a carbonyl shift from δ159 to δ168 in the ^{13}C NMR spectra of the derivatives confirmed the formation of a sulfonylurea. The ^1H NMR of the sulfonylurea urea derivatives was similar to that of pyrazole parent compound except of the appearance of addition peaks due to the phenyl substituents. As was previously observed for the tautomer, **2.2.1b**, the shift due to H-2 and H-2' appeared as singlets as opposed to the expected doublets in the ^1H NMR spectra of **2.3.3** and **2.3.5**.

The sulfonylurea derivatives met only 2 structural requirements for good oral bioavailability (Table 2-8). This class of derivatives may therefore present bioavailability problems. Though the molecular masses of these compounds exceeded 500, this may not be a significant consideration since most anti-infective agents in clinical use have high molecular weights [30].

These compounds had high cLog P values which were consistent with the observation that they are highly soluble in polar solvents like methanol as opposed to solvents with low polarity.

Table 2 - 8: The predictive bioavailability molecular properties of Sulfonylurea derivatives of curcumin

Compound	cLog P	tPSA	H-bond donors	H-bond acceptors	Mwt.	Criteria met
RULE	< 5	< 140	< 5	< 10	< 500	
2.3.1	4.989	169.5	3	8	547.6	2
2.3.2	5.488	169.5	3	8	561.6	2
2.3.3	5.702	169.5	3	9	582.0	2
2.3.4	5.132	169.5	3	9	565.6	2
2.3.5	5.488	169.5	3	8	561.6	2

2.5 Synthesis and characterization of Thiosemicarbazone Derivatives of Curcumin

2.5.1 Rationale for the Synthesis of Thiosemicarbazone Derivatives

The general structure and IUPAC numbering of thiosemicarbazones are presented in Figure 2-9.

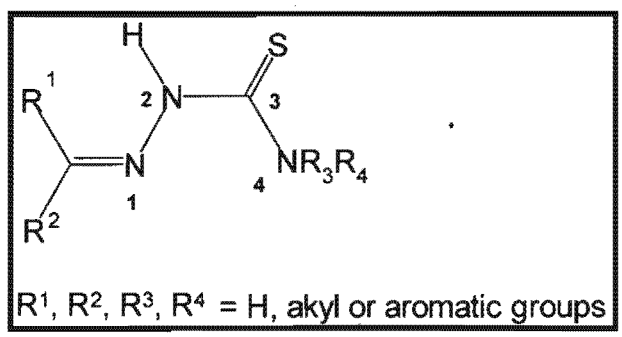

Figure 2 - 9: General Structure and IUPAC numbering of Thiosemicarbazones

Thiosemicarbazones are easy and cheap to synthesize by a Schiff condensation reaction between a ketone and aldehyde with the appropriate thiosemicarbazide [31]. Thiosemicarbazone derivatives exhibit geometric isomerism (Figure 2-8)[32-34].

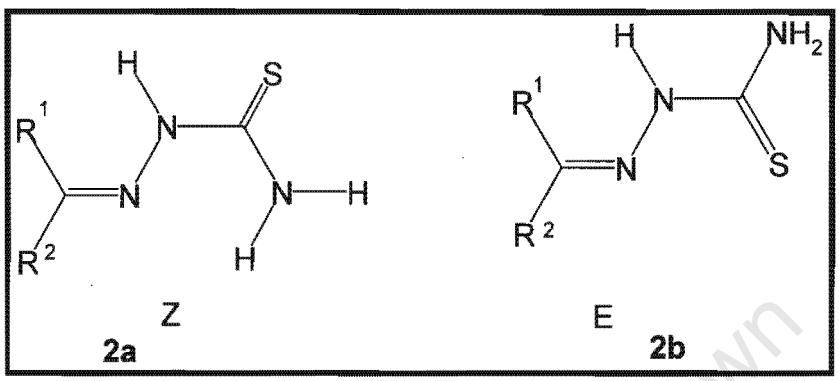

Figure 2 - 10: The general structures of E and Z stereoisomers of thiosemicarbazones

The presence of geometric isomers of thiosemicarbazones is revealed by peak replication in ^{1}H and ^{13}C NMR spectra [35]. In solution, thiosemicarbazones coexist as thione and thiol tautomers (Figure 2-11). Infra-red spectroscopy can be used to determine the predominant form [36].

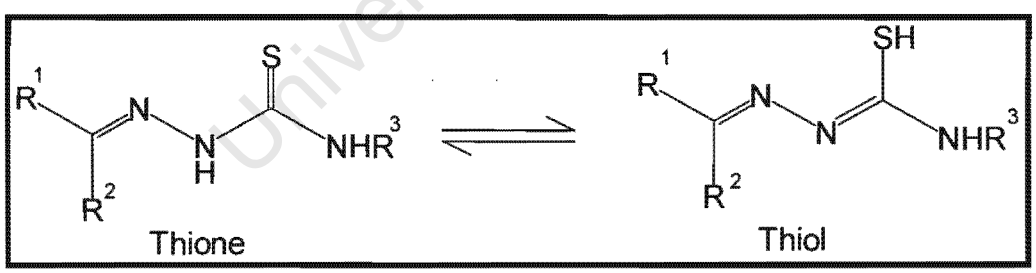

Figure 2 - 11: Thione and thiol tautomers of thiosemicarbazones

Thiosemicarbazones have antitumour [36-38], antiviral [39] antibacterial [40, 41], antiprotozoal [42, 43]; antifungal, anti-inflammatory and anti-HIV activities [43, 44]. The antimalarial activity of thiosemicarbazones was first reported by Klayman et al.[45]. Thiosemicarbazones are potent inhibitors of recombinant falcipain II [46, 47]. The imine (C=N) and thiocarbonyl (C=S) carbons of the

thiosemicarbazone derivatives are electrophilic sites for nucleophilic attack by the thiolate group in cysteine proteases [31]. Attack on the later is favored because the sulphur atom is more electron withdrawing than nitrogen which makes thiocarbonyl carbon a better site for nucleophilic attack. In addition to inhibition of cysteine proteases, thiosemicarbazones are bidendate or tridentate iron chelators. The sulfur and hydrazinic nitrogen atoms are responsible for interaction with the metallic ions. The iron chelating activity of thiosemicarbazones is highly positively correlated with their *in vitro* antimalarial activity [48].

A thiosemicarbazone derivative of curcumin has previously been synthesized [49, 50]. The derivative had metal chelating ability. In this study additional *N*-methyl and *N*-aryl substituted thiosemicarbazone derivatives were synthesized. It was hoped that the derivatives would have good iron chelating and cysteine protease inhibitory abilities which would enhance the antiplasmodial activity of curcumin. The derivatives were expected to have improved water solubility and hence improved oral bioavailability compared to curcumin.

2.5.2 Synthesis of the thiosemicarbazide reagents and the thiosemicarbazone derivatives

Two reagents, phenyl and 4-fluoro phenylthiosemicarbazides, were not commercially available and were therefore synthesized by reacting an isothiocyanate with hydrazine at ambient temperatures as described by Wiles and Suprunchuk [51] (Scheme 2-4).

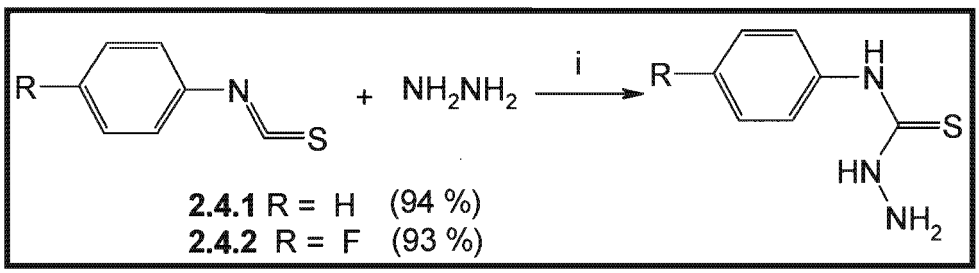

Scheme 2 - 4: *Reagents and conditions* i) diethyl ether, 25°C, 4 h

Two methods were applied for the synthesis of the thiosemicarbazone derivatives. In the first method, curcumin was reacted with the thiosemicarbazide in glacial acetic acid at 85°C. In the second method, curcumin and methyl thiosemicarbazide were heated in acidified isopropanol for 6 hours (Scheme 2-5).

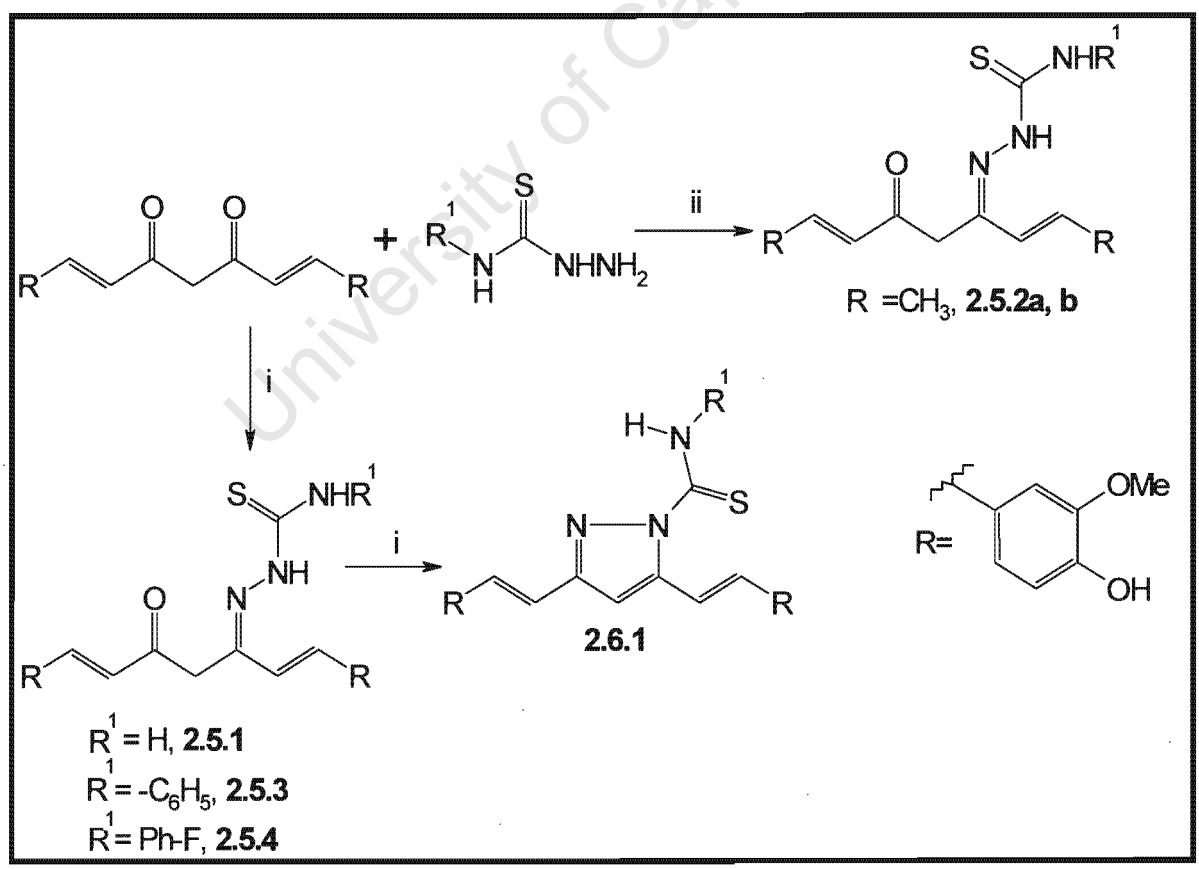

Scheme 2 - 5: *Reagents and conditions* (i) Acetic acid, 85°C, 72 h (i) isopropanol (10 ml), acetic acid (0.5 ml), 65°C, 3 hr

Table 2 - 9: Yields, purity and melting points of thiosemicarbazone derivatives of curcumin

Compound	R	Yield (%)	HPLC Purity (%)	Melting Point (°C)
2.5.1a	H	1	95	163-5
2.5.1b	H	50	96	163-4
2.5.2a	CH_3	10	ND	173
2.5.2b	CH_3	13	81	171-2
2.5.3	Ph	5	3 peaks	185-186
2.5.4	4-Ph-F	3	2 peaks	212-4

The first method gave low yields of less than 5 % because the reactions did not go to completion even after 3 days (Table 2-9). When the reaction duration was increased to 9 days, the yield of **2.5.1** increased from 1 % to 50 %. A second reason for the low yields was the formation of multiple reaction products due to the formation of isomers. The isomers were difficult to separate by column chromatography and prep. TLC.

2.5.3 Characterization of thiosemicarbazone derivatives

The ^{1}H NMR spectra of **2.5.2a** and **2.5.3** had peaks that were replicated 2 or 3 times. This provided evidence for stereoisomerism. This was confirmed by HPLC. Two isomers of N-methyl hydrazine carbothioamide (**2.5.2a** and **b**) were separated by preparative TLC but the yields were quite low. There were significant differences in the ^{1}H and ^{13} C NMR spectra of the isomers. The ^{13}C NMR spectrum of the isomer **2.5.2a** had a peak at δ179 (C=O) which was absent in the spectrum of **2.5.2b.** The isomer, **2.5.2b**, had a peak at δ157 (C=N) which was absent in the spectrum of **2.5.2a**. The differences in the ^{1}H NMR spectra were more subtle.

The ^{1}H NMR spectra of all the thiosemicarbazone derivatives were very similar to that of curcumin with the exception of **2.5.2a** and **2.5.2b**. In these two derivatives, there was loss of symmetry and the ^{1}H NMR spectra were more complex. All the hydrazine carbothioamide derivatives with the exception of *N*-methyl substituted derivatives (**2.5.2a** and **b**) did not form molecular ions on chemical ionization, fast atomic bombardment and electron spray mass spectrometry. The most abundant product ion in the mass spectra of the hydrazine carbothioamides had a mass-charge ratio of 369 which indicated loss of the thiosemicarbazone moiety. Elemental analysis was therefore used to confirm the identity of the compounds.

The IR spectra of all the thiosemicarbazone derivatives, with the exception of **2.5.2a** and **b**, showed the strong thiocarbonyl stretch at about 1277 cm^{-1} and imine stretch at about 1509 cm^{-1}. This was similar to the spectral details reported by Dutta *et al.* [49]. With the exception of the *N*-methyl derivatives (**2.5.2a** and **b**), there was no evidence of a carbonyl group in IR spectra of these compounds.

All the thiosemicarbazone derivatives met at least 4 out of 5 molecular requirements for good oral bioavailability (Table 2-10). This indicated that the thiosemicarbazone derivatives were likely to have good oral bioavailability. All the derivatives had tPSA and clogP values that were greater than that of curcumin indicating that they potentially have a better water solubility profile.

Table 2 - 10: Molecular properties of the thiosemicarbazone derivatives that predict oral bioavailability

	R	cLog P	tPSA	H-bond donors	H-bond acceptors	Mwt.	Criteria met
RULE		< 5	< 140	< 5	< 10	< 500	
2.5.1	H	3.511	145	4	9	441.51	4
2.5.2	CH_3	3.129	135	4	9	455.54	5
2.5.3	Ph	4.574	135	4	9	517.61	4
2.5.4	4-Fluoro Ph	4.719	135	4	9	535.60	4

2.6 Synthesis and Characterization of 7-Chloroquinoline Derivatives of Curcumin

2.6.1 Rationale for the synthesis of 7-chloroquinoline derivatives of curcumin

The 7-chloroquinoline derivatives were synthesized by a condensation reaction between curcumin and 7-chloro-4-hydrazinoquinoline. The rationale for the synthesis of this derivative is presented in Figure 2-12. Cross resistance to the quinoline moiety was likely to be a problem but it was hoped the two aryl groups in curcumin would reverse resistance [52].

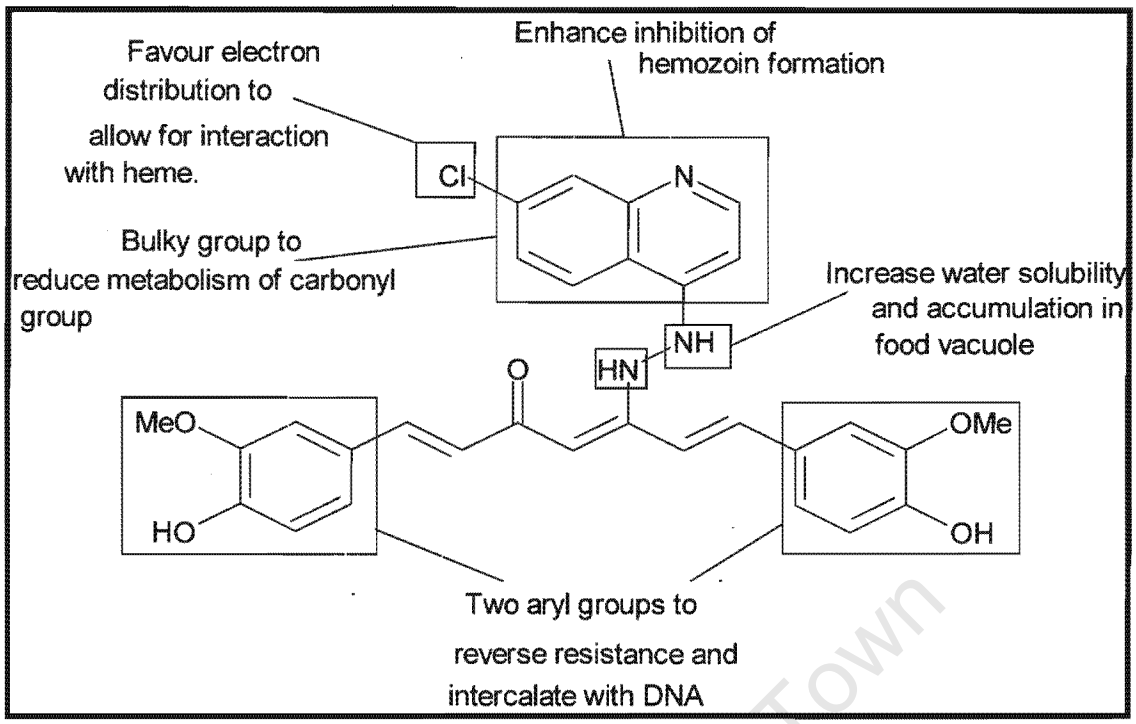

Figure 2 - 12: Rational for the synthesis of 7-chloroquinoline derivative of curcumin

2.6.2 Synthesis of the 7-chloro-quinoline derivatives

The 7-chloroquinoline derivatives were synthesized by a Schiff condensation reaction between curcumin and 7-chloro-4-hydrazinoquinoline under acidic conditions (Scheme 2-6). Both the imine derivative (**2.7.1**) and the pyrazole-based derivatives were obtained (**2.8.1**).

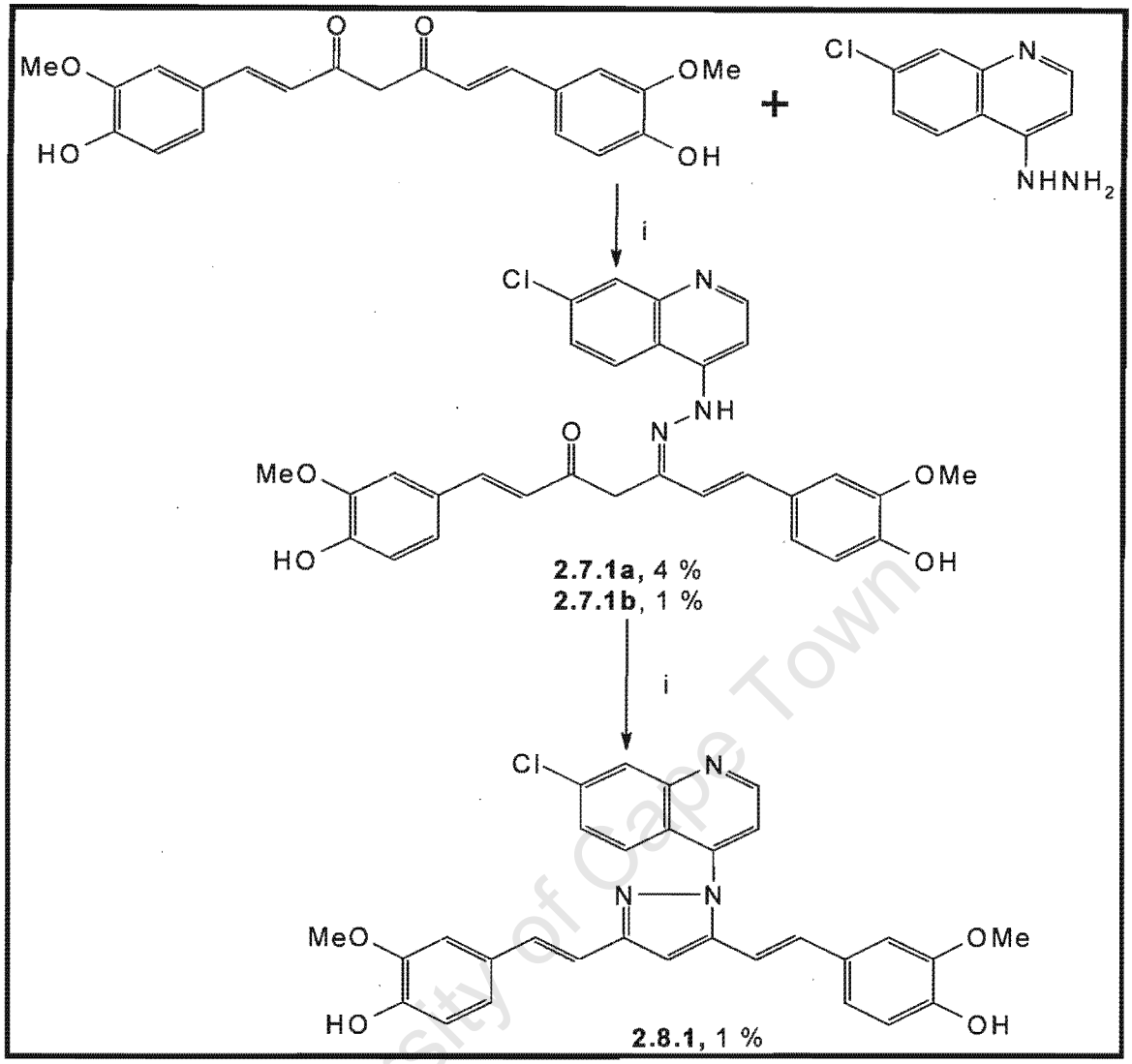

Scheme 2 - 6: *Reagents and conditions* (i) glacial acetic acid, 80°C, 120h

The reaction yields were very low because the reaction did not go to completion despite running the reaction for 120 hrs. Separation of the reaction mixture by column chromatography gave two isomers, **2.7.1a** and **2.7.1b** which had same melting point of 156°C but different colors. The former was bright yellow and the latter was yellow-green in color. Both **2.7.1a** and **2.7.1b** did not form molecular ions on both low and high resolution mass spectrometry. The mass spectra of the two isomers were similar and the most abundant product ions had mass charge ratios of 453.3 and 495. The results from elemental analysis were used to confirm the identity of the compounds.

There were substantial differences in the ^{1}H NMR spectra of **2.7.1a** and **b**. The ^{1}H NMR spectra of **2.7.1a** and **b** were rather unusual since most chemical shifts associated with the 7-chloro-4-hydrazinoquinoline did not appear. This phenomenon was attributed either rapid tautomerism or rapid interchange between two or more conformers [53]. In the case of **2.7.1b**, none of the peaks associated with the quinoline moiety appeared in the ^{1}H NMR spectrum. The appearance of a number of peaks not found in the ^{1}H NMR spectrum of curcumin provided evidence for the successful synthesis of the quinoline derivative. The chemical shift at δ168.3 revealed the presence of an imine double bond.

The ^{1}H NMR spectrum of **2.7.1a** had two peaks due to H-3" and H-5" in addition to those typically associated with curcumin. All the peaks associated with heptadiene dione chain of curcumin (H-7 to H-13) were replicated three or four times.

2.6.3 Characterization of the 1-pyrazole-7-chlor-4-hydrazinoquinoline derivative (2.8.1)

Unlike the 7-chloro-quinoline derivative of curcumin (**2.7.1**), pyrazole based derivative (**2.8.1**), formed a molecular ion on mass spectroscopy. The absence of carbonyl shifts in the ^{13}C NMR and IR spectra confirmed that both carbonyl groups in curcumin had undergone nucleophilic attack. All the proton shifts due to both the 7-chloro-quinoline and curcumin moieties appeared in the ^{1}H NMR spectrum. Though elemental analysis showed a high degree of purity, HPLC separation showed **2.8.1** is a mixture of 3 isomers. Further evidence for stereoisomerism was provided by the ^{1}H NMR spectrum in which most peaks were replicated twice or thrice.

2.6.4 The predicted oral bioavailability of the 7-chloroquinoline derivatives of Curcumin

The 7-chloroquinoline based derivatives met 3 out of 5 requirements for good oral bioavailability (Table 11). This implies that the compounds may have good oral bioavailability.

Table 2 - 11: Molecular properties of the 7chloro-quinoline derivatives that predict oral bioavailability

	cLog P	tPSA	H-bond donors	H-bond acceptors	Mwt.	Criteria met
RULE	< 5	< 140	< 5	< 10	< 500	
2.7.1	6.493	135	3	7	560.1	3
2.8.2	6.663	101.1	2	4	526.0	3

2.7 Synthesis and Characterization of the N-Acyl Hydrazone Derivatives of Curcumin

2.7.1 Rationale for the antiplasmodial activity of the *N*-Acyl hydrazones derivatives

N-Acyl hydrazones are structural analogues of thiosemicarbazones. Like thiosemicarbazones, they inhibit the enzyme cysteine protease and act as iron chelators. The general structure and sites for nucleophilic attack by the cysteine thiolate are presented in Figure 2-12.

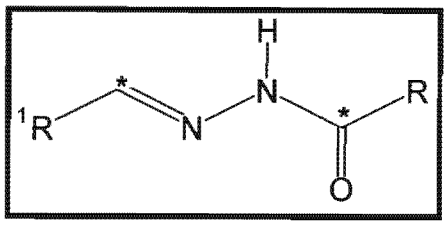

^{1}R, R = Aromatic or heterocyclic substituents.

Figure 2 - 13: The general structure and electrophilic sites of *N*-Acyl hydrazones

An *N*-acyl hydrazone derivative of curcumin, curcuminsemicarbazone, has been previously synthesized [49, 54]. Curcuminsemicarbazone has good metal chelating activity and formed a tridendate complex with copper (II) ions (Figure 2-14)[49]. The stability of the complex was determined by cyclic voltammetry. Differences in the IR spectra of curcuminsemicarbazone and the copper complex showed that imine bond and two carbonyl groups were involved in complexation. The metal chelating ability of the *N*-acyl hydrazone derivatives was likely to improve the antiplasmodial activity compared to the parent compound.

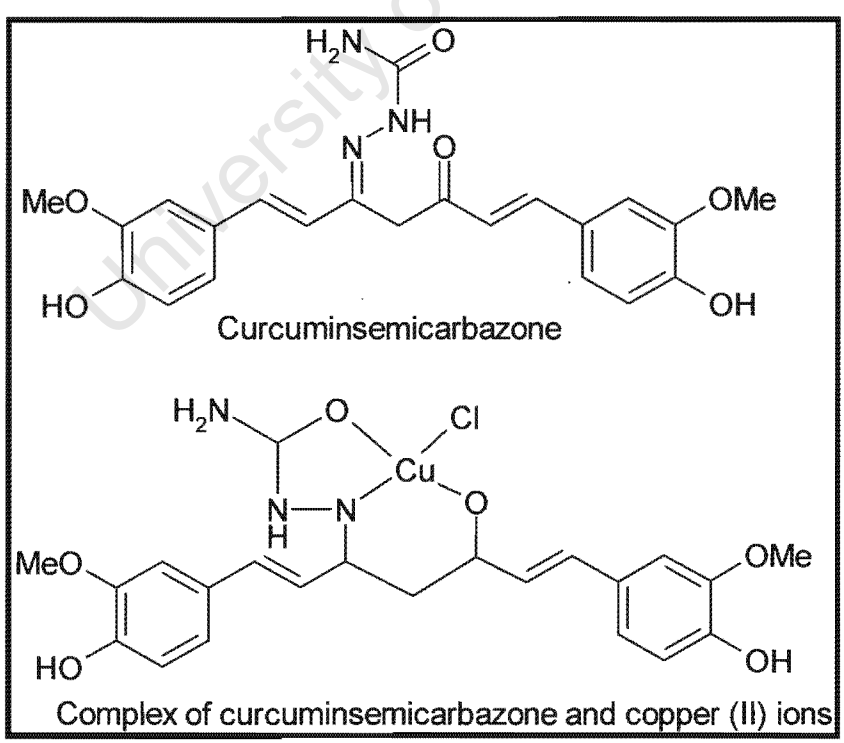

Figure 2 - 14: Structure of curcuminsemicarbazone and its copper complex[49]

N-Acyl hydrazone derivatives are easy to synthesize by nucleophilic attack on the carbonyl group in either acidic or basic conditions (**2.9**). Further nucleophilic addition on the second carbonyl group of curcumin was expected to produce pyrazole-1-yl methanone derivatives (**2.10,** Figure 2-15).

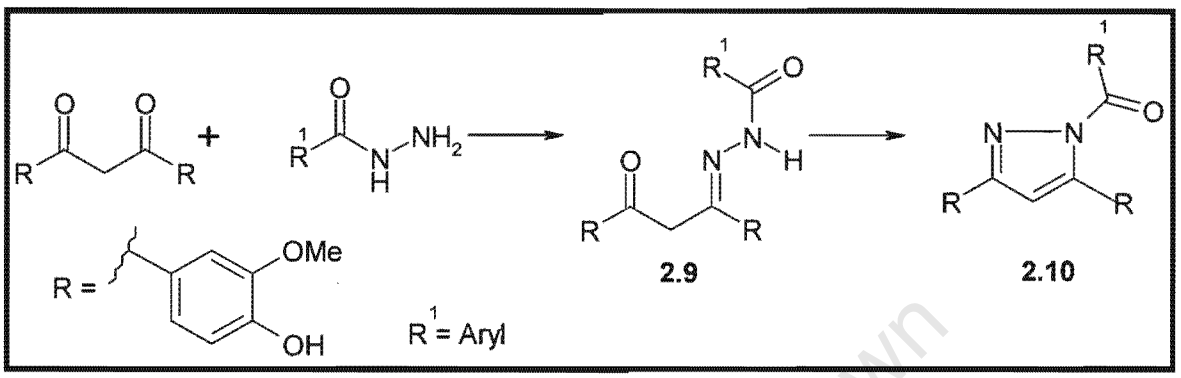

Figure 2 - 15: Aryl hydrazine methanone (2.9) and pyrazole-1-methanone (2.10) derivatives of curcumin.

Stereoisomerism was expected since *N*-acyl hydrazones exist as geometric isomers with the E-isomers being predominant [55]. The E-isomers exist in at least 4 different conformations. The aromatic substituents on the derivatives included isonicotyl, salicylaldehye, furoyl, benzoyl and 4-hydryoxyl benzoyl groups. These groups were selected because they have been reported to play a role in antiplasmodial activities of acyl hydrazones reported in literature [56-58].

2.7.2 Synthesis of the *N*-acyl hydrazone derivatives of curcumin

Two methods were applied in the synthesis of acyl hydrazone derivatives (Scheme 2-7). In the first method, Method A, the acyl hydrazine was heated in acetic acid at 70°C

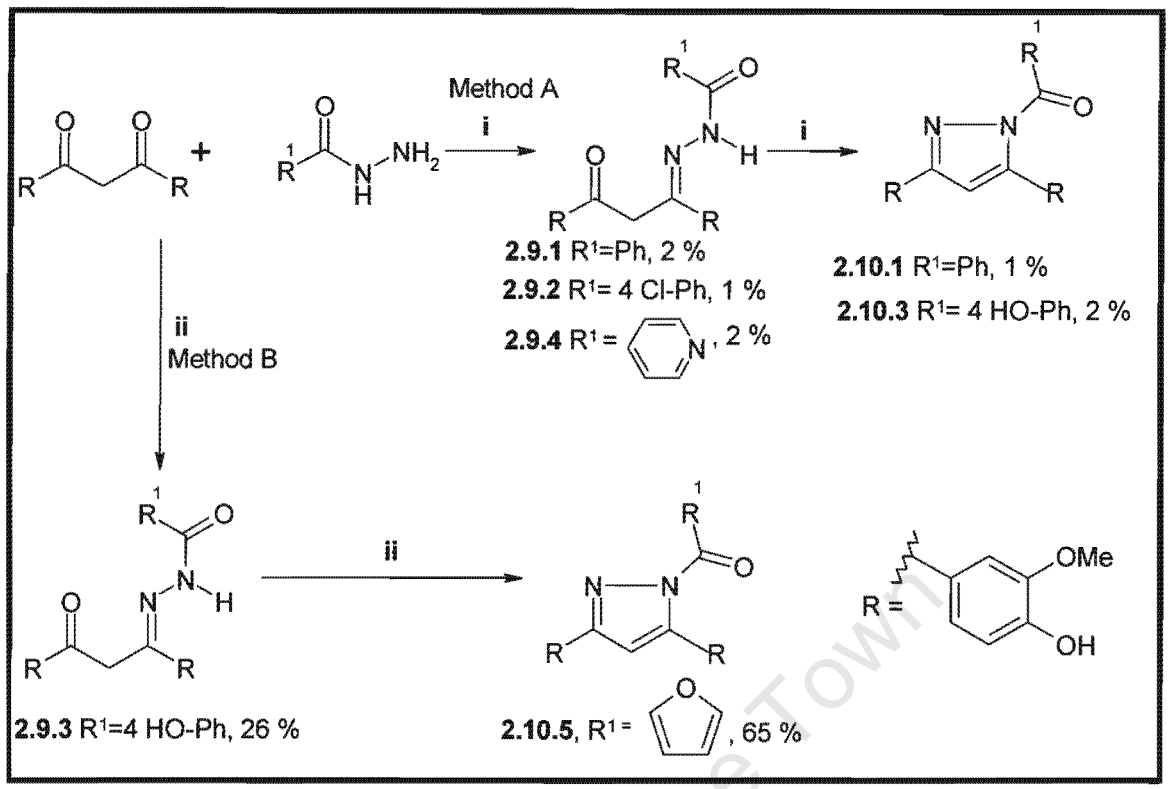

Scheme 2 - 7: *Reagents and conditions* i) Acetic acid, 70°C, 72 h ii) isopropanol, sodium acetate, 65°C, 48 h

Low yields of less than 3 percent were obtained because of the complexity of the reaction mixture due to the presence of aryl hydrazine and pyrazole-1-yl methanone derivatives. Secondly, the reaction did not go to completion. Both aryl hydrazine (**2.9.2** and **2.9.5**) and pyrazole-1-yl methanone derivatives (**2.10.1** and **2.10.3**) were obtained. The second method, Method B, was performed in isopropanol using sodium acetate as the catalyst. This method gave higher reaction yields and the work up was much easier. The precipitate that formed at the end of reaction was simply filtered, washed and dried. The reaction products included the aryl hydrazine methanone derivatives **2.9.1** and **2.9.4** and the 2-furolyl derivative (**2.10.6**).

2.7.3 Characterization of the *N*-acyl hydrazone derivatives

All the aryl pyrazol-1-yl derivatives (**2.10.1** and **2.10.5**) with the exception of **2.10.3** gave molecular ions on mass spectrometry. On the other hand, aryl hydrazine methanone derivatives did not give molecular ions on MS except the isonicotoyl derivative (**2.9.5**).

The ^{1}H NMR spectra of the aryl methanone derivatives (**2.9.1** to **2.9.4**) were similar to that of curcumin. The ^{13}C NMR spectral peaks at about δ183 and δ 157 which confirmed the presence of the curcumin carbonyl bond and the formation of an imine bond respectively. The most abundant product ion in the MS spectra of the aryl hydrazine methanone derivatives has an *m/z* ratio of 369 with relative abundance of 100 %. Though HPLC and peak replication revealed the existence of isomers, none of the isomers were successfully separated.

There was a significant difference in the ^{1}H NMR spectra of the aryl methanone derivative, **2.9.2**, when the spectrum was run in different solvents. When the spectrum was run in *d*-DMSO the peak due to H-2'', 6'' had an integration of about 0.25. The same peak gave an integration of 2 protons when the spectrum was run in *d*-MeOH. The peak due to H-3'', 5'' did not appear when the spectrum was run in *d*-MeOH. The difference in the two spectra seems to suggest that H-2'', 6'' are involved in rapid interconversion between two or more resonance states or conformers which made them appear as a small peak that gives an integration of less than a full proton when the spectrum was run in *d*-DMSO[53]. The other parts of the spectra were similar.

The ^{1}H NMR spectra of the pyrazole-1-yl methanone (**2.10.1**, **2.10.3** and **2.10.5**) derivatives were similar to that of hydrazinocurcumin (**2.2.1**). The appearance of NMR chemical shifts associated with the aryl group was used to confirm formation of the reaction product. The ^{13}C NMR spectrum lacked

the carbonyl shift at about δ183. This confirmed that nucleophilic attack took place on both carbonyl groups of curcumin.

2.7.4 The molecular properties of the *N*-acyl hydrazone derivatives that predict oral bioavailability

All the synthesized *N*-acyl hydrazone derivatives, except **2.9.2,** met at least 3 out of the 5 criteria for good oral bioavailability (Table 2-12). These compounds are therefore likely to have a good absorption profile.

Table 2 - 12: Molecular properties of the *N*-acyl hydrazone derivatives that predict oral bioavailability

R	cLog P	tPSA	H-bond donors	H-bond acceptors	Mwt.	Criteria met
RULE	< 5	< 140	< 5	< 10	< 500	
2.9.1	4.407	144.5	3	8	486.5	4
2.9.2	5.321	144.5	3	8	521	2
2.9.3	4.079	168.3	4	9	520.5	3
2.9.4	3.654	155.8	3	8	487.5	4
2.10.1	6.744	112.1	2	5	468.5	4
2.10.3	5.168	135.9	3	6	484.5	4
2.10.5	5.920	126.2	2	5	458.5	4

2.8 Conclusion

Azole, sulfonylurea, quinoline, thiosemicarbazone and *N*-acyl hydrazone derivatives of curcumin were successfully synthesized by nucleophilic attack on the carbonyl group. In the case of the *N*-acyl hydrazone derivatives, nucleophilic attack also took place on the second carbonyl group of curcumin to yield a series of methanone derivatives. HPLC and ^{1}H NMR revealed the derivatives displayed isomerism. Isomers of azole and quinoline derivatives were successfully separated by column chromatography. More work is required to identify the structural differences between the isomers.

References

(1) Ridley, R. G. *Nature* **2002**, *415*, 686-693.

(2) Ridley, R. G. *Microb. Infect.* **2002**, *4*, 155.

(3) Lipinski, C. A.; Lombardo, F.; Dominy, B. W.; Feeney, P. J. *Adv. Drug Deliv.* **1997**, *23*, 3-25.

(4) Veber, D. F.; Johnson, S. R.; Cheng, H.; Smith, B. R.; Ward, K. W.; Kopple, K. D. *J. Med. Chem.* **2002**, *45*, 2615-2623.

(5) Clayden, G. Nucleophilic substitution at C=O with loss of carbonyl oxygen; In *Clayden, Greeves, Warren & Wothers: Organic chemistry*; Oxford University Press: 2000; pp 114-119.

(6) Rasmusen, H. B.; Christensen, S. B.; Kuist, L. P.; Karazami, A. *Planta Med.* **2000**, *66*, 396-398.

(7) Roughley, P. J.; Whiting, D. A. *J. Chem. Soc. , Perkin Trans.* **1973**, 2379.

(8) Nurfina, A. N.; Reksohadiprodjo, M. S.; Timmerman, H.; Jenie, U. A.; Sugiyanto, D.; van der Goot, H. *Eur. J. Med. Chem.* **1997**, *32*, 321-328.

(9) Mazumder, A.; Raghavan, K.; Weinstein, J.; Kohn, K. W.; Pommier, Y. *Biochem. Pharm.*, **1995**, *49*, 1165-1170.

(10) Karlsen, J.; Mostad, A.; Tønnesen, H. H. *Acta Chem. Scand.* **1988**, *B 42*, 23.

(11) Flynn, D. L.; Belliotti, T. R.; Boctor, A. M.; Connor, D. T.; Kostlan, C. R.; Nies, D. E.; Ortwine, D. F.; Schrier, D. J.; Sircar, J. C. *J. Med. Chem.* **1991**, *34*, 518-525.

(12) Shim, J. S.; Kim, D. H.; Jung, H. J.; Kim, J. H.; Lim, D.; Lee, S.; Kim, K.; Ahn, J. W.; Yoo, J.; Rho, J.; Shin, J.; Kwon, H. J. *Bioorg. Med. Chem.* **2002**, *10*, 2987-2992.

(13) Ishida, J.; Ohtsu, H.; Tachibana, Y.; Nakanishi, Y.; Bastow, K. F.; Nagai, M.; Wang, H.; Itokawa, H.; Lee, K. *Bioorg. Med. Chem.* **2002**, *10*, 3481.

(14) Selvam, C.; Jachak, S. M.; Thilagavathi, R.; Chakraborti, A. K. *Bioorg. Med. Chem. Lett.* **2005**, *15*, 1793-1797.

(15) Huy, N. T.; Kamei, K.; Yamamoto, T.; Kondo, Y.; Kanaori, K.; Takano, R.; Tajima, K.; Hara, S. *J. Biol. Chem.* **2002**, *277*, 4152-4158.

(16) Hempelmann, E.; Marques, H. M. *J. Pharmacol. Toxicol. Methods* **1994**, *32*, 25-30.

(17) Flynn, D.; Belliotti, T.; Boctor, A.; Connor, D.; Kostlan, C.; Nies, D.; Ortwine, D.; Schrier, D.; Sircar, J. *J. Med. Chem.* **1991**, *34*, 518-525.

(18) Vanden Bossche, H. *Curr. Top. Med. Mycol.* **1985**, *1*, 313-351.

(19) Karres, I.; Kremer, J.; Dietl, I.; Steckholzer, U.; Jochum, M.; Ertel, W. *Am J. Physiol. Regul. Integr. Comp. Physiol.* **1998**, *274*, R1058-R1064.

(20) Hugossona , E.; Montgomery, S. M.; Premjid, Z.; Troye-Blomberge, M.; Björkmana, A. *Acta Trop.* **2006**, *99*, 75-82.

(21) Shim, J. S.; Lee, J.; Park, H.; Park, S.; Kwon, H. J. *Chem. Biol.* **2004**, *11*, 1455-1463.

(22) Bera, R.; Sahoo, B. K.; Ghosh, K. S.; Dasgupta, S. *Int. J. Biol. Macromol.*, **2008**, *42*, 14-21 .

(23) Lipinski, C. A.; Lombardo, F.; Dominy, B. W.; Feeney, P. J. *Adv. Drug Deliv. Rev.* **2001**, *46*, 3-26.

(24) Nolte, M. S.; Karam, J. H. Pancreatic hormones and antidiabetic drugs; Katzung, B. G., Ed.; In *Basic and Clinical Pharmacology*; Lange Medical Books/McGraw-Hill: New York, U. S. A., 2001; Vol. 8, pp 711.

(25) Mohamadi, F.; Spees, M. M.; Grindey, G. B. *J. Med. Chem.* **1992**, *35*, 3012-3016.

(26) Kirk, K.; Horner, H. A.; Spillet, D. J.; Elford, B. C.; Ellory, J. C. *FEBS Lett.* **1993**, *323*, 123-128.

(27) Ponte-Sucre, A.; Campos, Y.; V zquez, J.; Moll, H.; Mendoza-Le¢n, A. *Mem. Inst. Oswaldo Cruz* **1997**, *95*, 601-606.

(28) León, C.; Rodrigues, J.; Gamboa de Domínguez, N.; Charris, J.; Gut, J.; Rosenthal, P. J.; Domínguez, J. N. *Eur. J. Med. Chem.* **2007**, *42*, 735-742.

(29) Billeter, O. C. *Ber.* **1904**, *37*, 690.

(30) Zhang, M. Q.;Wilkinson, B. *Curr. Opin. Biotechnol.* **2007**, 18, 478.

(31) Du, X.; Guo, C.; Hansell, E.; Doyle, P. S.; Caffrey, C. R.; Holler, T. P.; McKerrow, J. H.; Cohen, F. E. *J. Med. Chem.* **2002**, *45*, 2695-2707.

(32) Chattopadhyay, D.; Mazumdar, S. K.; Banerjee, T.; Ghosh, S.; Mak, T. C. *Acta Crystallogr. C* **1988**, *44 (Pt 6)*, 1025-1028.

(33) Ota, A. T.; Temperini, M. L. A.; Arêas, E. P. G.; Loos, M. *THEOCHEM,* **1998**, *451*, 269-275.

(34) Cirilli, R.; Ferretti, R.; La Torre, F.; Secci, D.; Bolasco, A.; Carradori, S.; Pierini, M. *J. Chromatogr. A* **2007**, *1172*, 160-169.

(35) West, D. X.; Bain, G. A.; Buthcer, R. J.; Jasinski, J. P.; Li, Y.; Pozdniakiv, R. Y.; Toscano, R. A.; Hern dez-Ortega, S. *Polyhedron* **1996**, *15*, 665-674.

(36) Antonini, I.; Claudi, F.; Franchetti, P.; Grifantini, M.; Martelli, S. *J. Med. Chem.* **1977**, *20*, 447-449.

(37) Agrawal, K. C.; Booth, B. A.; DeNuzzo, S. M.; Sartorelli, A. C. *J. Med. Chem.* **1976**, *19*, 1209-1214.

(38) Hall, I. H.; Lackey, C. B.; Kistler, T. D.; Ives, J. S.; Beraldo, H.; Ackerman, L. J.; West, D. X. *Arch. Pharm. (Weinheim)* **2000**, *333*, 217-225.

(39) Easmon, J.; Heinisch, G.; Holzer, W.; Rosenwirth, B. *J. Med. Chem.* **1992**, *35*, 3288-3296.

(40) Liberta, A. E.; West, D. X. *Biometals* **1992**, *5*, 121-126.

(41) Weller, L. E.; Sell, H. M.; Gottshall, R. Y. *J. Am. Chem. Soc.* **1954**, *76*, 1959-1959.

(42) Dodd, R. H.; Ouannes, C.; Robert-Gero, M.; Potier, P. *J. Med. Chem.* **1989**, *32*, 1272-1276.

(43) Teitz, Y.; Ronen, D.; Vansover, A.; Stematsky, T.; Riggs, J. L. *Antiviral Res.* **1994**, *24*, 305-314.

(44) Bal, T. R.; Anand, B.; Yogeeswari, P.; Sriram, D. *Bioorg. Med. Chem. Lett.* **2005**, *15*, 4451-4455.

(45) Klayman, D. L.; Bartosevich, J. F.; Griffin, T. S.; Mason, C. J.; Scovill, J. P. *J. Med. Chem.* **1979**, *22*, 855-862.

(46) Greenbaum, D. C.; Baruch, A.; Grandier, M.; Bozdech, Z.; Medsihradsky, K. F.; Engel, J.; Derisi, J.; Holder, A. A.; Bogyo, M. *Science* **2002**, *298*, 2002-2006.

(47) Fujii, N.; Mallari, J. P.; Hansell, E. J.; Mackey, Z.; Doyle, P.; Zhou, Y. M.; Gut, J.; Rosenthal, P. J.; McKerrow, J. H.; Guy, R. K. *Bioorg. Med. Chem. Lett.* **2005**, *15*, 121-123.

(48) Walcourt, A.; Loyevsky, M.; Lovejoy, D. B.; Gordeuk, V. R.; Richardson, D. R. *Int. J. Biochem. Cell Biol.* **2004**, *36*, 401-407.

(49) Dutta, S.; Murugkar, A.; Gandhe, N.; Padhye, S. *Met. -Based Drugs* **2001**, *8*, 183.

(50) Dutta, S.; Padhye, S.; Priyadarsini, K. I.; Newton, C. *Bioorg. Med. Chem. Lett.*, **2005**, *15*, 2738-2744.

(51) Wiles, D. M.; Suprunchuk, T. *Can. J. Chem.* **1968**, *46*, 1865.

(52) van Schalkwyk, D. A.; Egan, T. J. *Drug Resist. Updat.* **2006**, *9*, 211-226.

(53) Casy, A. F. *The steric factor in medicinal chemistry: disymmetric probes of pharmacological receptors;* Plenum Press: New York, U. S. A., 1993; .

(54) Dutta, S.; Padhye, S.; Priyadarsini, K. I.; Newton, C. *Bioorg. Med. Chem. Lett.* **2005**, *15*, 2738-2744.

(55) Ifa, D. R.; Rodrigues, C. R.; de Alencastro, R. B.; Fraga, C. A. M.; Barreiro, E. J. *THEOCHEM,* **2000**, *505*, 11-17.

(56) Golenser, J.; Tsafack, A.; Amichai, Y.; Libman, J.; Shanzer, A.; Cabantchik, Z. I. *Antimicrobial Agents Chemother.* **1995**, *39*, 61-65.

(57) Cabantchik, Z. I.; Glickstein, H.; Golenser, J.; Loyevsky, M.; Tsafack, A. *Acta Haematol.* **1996**, *95*, 70-77.

(58) Golenser, J.; Domb, A.; Mordechai-Daniel, T.; Leshem, B.; Luty, A.; Kremsner, P. *J. Parasitol.* **2006**, *92*, 170-177.

CHAPTER 3

IN VITRO ANTIPLASMODIAL ACTIVITY AND CYTOTOXICITY OF DERIVATIVES OF CURCUMIN

3.1 Introduction

After synthesizing derivatives of curcumin, it was necessary to determine if the chemical modifications had resulted in compounds with improved antiplasmodial activity. The derivatives were tested for their in *vitro* antiplasmodial activity against the chloroquine sensitive (CQS) D10 and chloroquine resistant (CQR) K1 strains of *Plasmodium falciparum* using the Parasite Lactate Dehydrogenase (pLDH) assay [1, 2]. The cut off for good *in vitro* activity was an IC_{50} of less than 1 μM [3]. In addition, the cytotoxicity against the Chinese Hamster Ovarian (CHO) cells was determined using the MTT assay [4]. The cytotoxicity was used to determine the selectivity of the compounds for Plasmodium as opposed to mammalian cells. Selected compounds were tested for their ability to inhibit the formation of beta-hematin using the pyridine hemichrome inhibition assay [5]. This test was deemed important since ability to hemozoin formation is linked to the activity of 4-aminoquinoline antimalarials [6].The beta-hematin assay has been successfully used in pharmaceutical industry in high throughput drug discovery [7]. The cut off for good activity was an IC_{50} of less than 200 μM or 5 equivalents of heme.

The *in vitro* activities of derivatives were compared with that of the curcumin. The selectivity index (SI) was used to access the specificity of action of the test compounds. It was also used to access the lack of toxicity to mammalian cells at concentrations where the test compound was effective against *P. falciparum*. It was calculated by dividing the CC_{50} against the CHO cells by the IC_{50} against the CQR strain ($SI = CC_{50}/IC_{50}$) by the CC_{50} .

The resistance index (RI) was used to access activity against the CQR strains. It predicts the likelihood of development of resistance if a compound were in clinical use. It was calculated by dividing the IC_{50} against the CQR strain by the IC_{50} against the CQS strain.

3.2 Results and Discussion

3.2.1 The *in vitro* biological activities of curcumin and the azole derivatives

Although the antiplasmodial activity of curcumin has been reported, no comparison between the activity against CQS and CQR has been made. In this study curcumin was found to be equally active against both the CQS and CQR strains with IC_{50} values of 1.674 and 1.647µg/ml respectively. The resistance index (RI) was 1. The IC_{50} values of curcumin were similar to values reported in literature [8, 9]. The ability of curcumin to act against the CQR strain may have been due to the α, β-unsaturated carbonyl groups within curcumin. The α, β-unsaturated carbonyl groups have been shown to confer the ability to inhibit multidrug resistance proteins thus overcoming drug resistance [10]. Curcumin showed no cytotoxicity against the CHO cells (CC_{50} > 100 µg/ml). However, this finding was interpreted with caution since compounds with antioxidant and chelating activity are known to interfere with MTT assay to give false negative results [11-13].

The antiplasmodial activities of isomers of pyrazole derivative of curcumin were compared (Table 3-1). The mixture of isomers, **2.2.1a,** and the tautomer, **2.2.1b**, had a 9-fold greater activity against the CQS compared to curcumin. The IC_{50} values were 0.183 and 0.085 µg/ml respectively. The enhanced antiplasmodial activity of the pyrazole derivative was attributed to the azole ring which conferred the ability to inhibit beta-hematin formation. However, the isomer **2.2.1c** had an IC_{50} of 1.084 µg/ml and its activity was comparable to that of curcumin. The superior antiplasmodial activity of the tautomer, **2.2.1b**,

may have been due to the presence of the amine group (N-H) which enhanced solubility and the ability to accumulate in the parasitic food vacuole by pH ion trapping.

The antiplasmodial activities of the different isomers of the isoxazole derivative were compared (Table 3-2). There was no difference in the activities of the isomers of the isoxazole derivatives. The IC_{50} values of the isomers, **2.2.2a**, **b** and **c**, were 1.573, 2.180 and 1.866 µg/ml respectively. There was comparable *in vitro* activity between isomers.

Table 3 - 1: ***In vitro*** **antiplasmodial and cytotoxicity of the isomers of the pyrazole derivative of curcumin / hydrazinocurcumin**

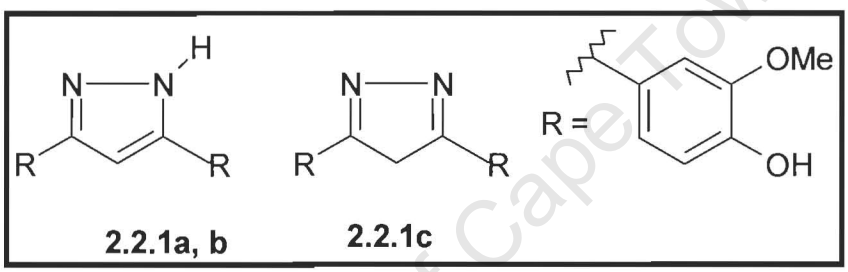

2.2.1a, b **2.2.1c**

	IC_{50} [a] µg/ml (µM)		CC_{50} [a] µg/ml (µM)		
	D10	**K1**	**CHO**	**SI[b]**	**RI[c]**
CQ	5.521 ± 1.547 [d]	182.523 ± 10.253	ND	ND	33.1
Emetine	ND	ND	0.067 ± 0.011	ND	ND
Curcumin	1.674 ± 0.708 (4.545 ± 1.922)	1.657 ± 0.496 (4.496 ± 1.346)	> 100	ND	0.99
2.2.1a	0.183 ± 0.082 (0.502 ± 0.227)	1.832 ± 0.731 (5.030 ± 2.008)	2.151 ± 0.4264 (5.908 ± 1.171)	1.17	10.01
2.2.1b	0.0850[e] (1.909)	…	…		…
2.2.1c	1.084 ± 0.143 (2.976 ± 0.394)	5.790 ± 1.771 (15.900 ± 4.864)	…		5.34

[a] mean ± SD, n=3, [b] SI selectivity index, [c] RI Resistance Index, [d] ng/ml, [e] Only one assay was performed due to low amounts of material.

Table 3 - 2: *In vitro* antiplasmodial and cytotoxicity of the isomers of isoxazole derivative of curcumin

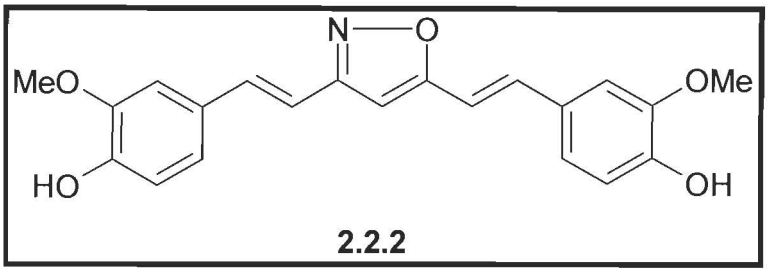

2.2.2

	IC_{50}[a] µg/ml (µM/ml)		CC_{50}[a] µg/ml (µM/ml)		
	D10	**K1**	**CHO**	**SI**	**RI**
CQ	5.521 ± 1.547 [b]	182.523 ±10.253[b]	ND	ND	33.1
Emetine	ND	ND	0.067 ± 0.011	ND	ND
2.2.2a	1.573 ± 0.703 (4.305 ± 1.924)	3.173 0. ± 688 (8.690 ± 1.884)	…		2.02
2.2.2b	2.180 ± 0.833 (5.967 ± 2.278)	3.018 ± 0.070 (8.266 ± 0.191)	…		1.38
2.2.2c	1.866 ± 0.503 (5.105 ± 1.375)	3.921 ± 0.618 (10.739 ± 1.694)	11.339 ± 0.854 (31.032 ± 2.336)	2.89	2.10

[a]mean ± SD, n=3,

The pyrazole derivative (**2.2.1a** and **b**) had greater antiplasmodial activity against the CQS strain compared to isoxazole derivative (**2.2.2**) (Figure 3-1). The activity of the latter was comparable to that of curcumin.

All the azole derivatives had reduced activity against the CQR strain (Figure 3-1). The activity against the CQR strain was less than that of curcumin.

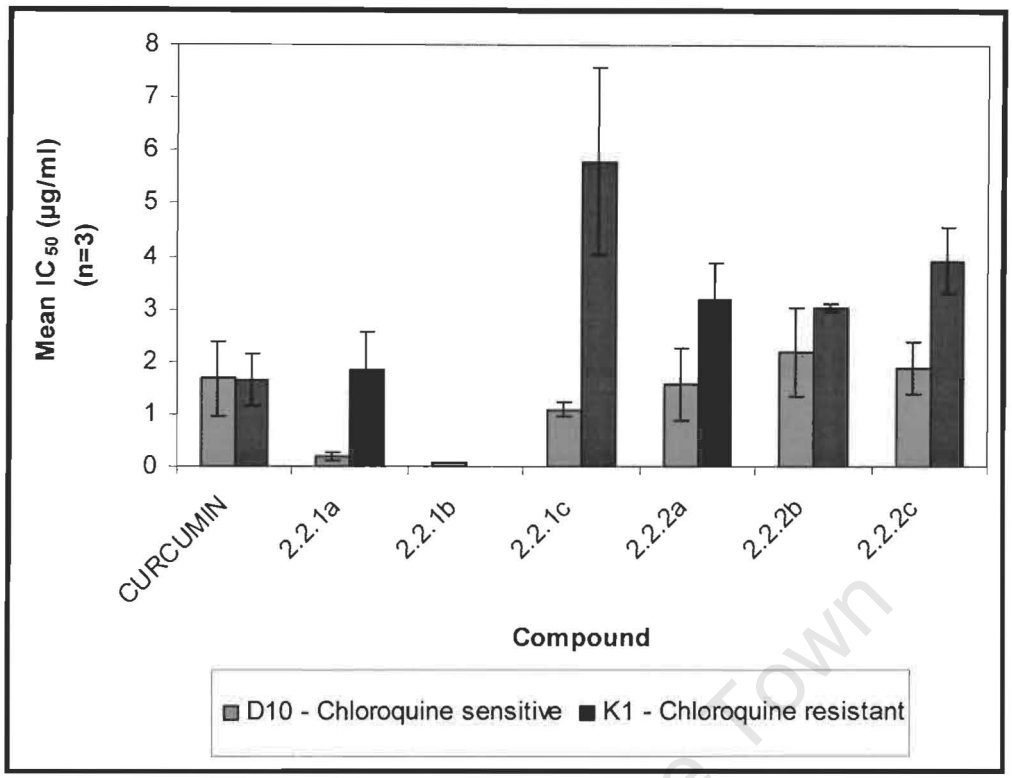

Figure 3 - 1: Comparison of the *in vitro* activities of the azole derivatives against the CQS and CQR strains of *Plasmodium falciparum*

The diminished activity against the CQR strain may suggest that carbonyl groups on curcumin were responsible for activity against the resistant strains. The RI of the isoxazole derivative was much lower than that of the pyrazole derivatives.

Unlike curcumin, the pyrazole (**2.2.1a**) and isoxazole (**2.2.2c**) derivatives inhibited the formation of beta-hematin with IC_{50} values of 0.832 ± 0.1 and 1.054 ± 0.1 equivalent of hematin respectively. In this regard, they had superior inhibitory activity compared to chloroquine diphosphate which had an IC_{50} of 1.91 equivalents. However, chloroquine had a much higher *in vitro* antiplasmodial activity than these derivatives.

The low selectivity indices of the pyrazole and isoxazole derivatives (1.17 and 2.89 respectively), implied that they have a non-specific mechanism of action. They were highly cytotoxic as previously reported [14, 15].

Introduction of an azole ring improved the antiplasmodial activity of curcumin. However, further chemical modifications are required to reduce the cytotoxicity and improve activity against resistant strains.

3.2.2 The *in vitro* biological activities of the sulfonylurea derivatives of curcumin

The sulfonylureas differed in the nature of the substituent at the *para* and *ortho* position. The *in vitro* activity against the CQS strain of the sulfonylureas derivatives was comparable to that of curcumin with IC_{50} values ranging from 1.753 to 7.578 µM (Table 3-3). The sulfonylurea derivatives were less active than the pyrazole derivative. This suggested that bulky substituents on the pyrazole ring diminished antiplasmodial activity. Activity against the CQR strain was considerably reduced and was less than that of curcumin (Figure 3-2). Resistance to the sulfonylureas was probably mediated by the P-glycoprotein homologue 1 (Pgh1) which causes the efflux of drugs from the cytoplasm. [16, 17]. This transporter, which belongs to the ATP-binding-cassette (ABC) transporter family, has been shown to cause resistance to sulfonylureas in isolates of Leishmania [18, 19].

All the sulfonylurea derivatives were highly cytotoxic with CC_{50} values ranging from 3.164 to 9.716 µg/ml. They were more toxic to the CHO cells compared to the CQR strain of *P. falciparum* with SI values ranging from 0.31 to 1.18 (Table 3-3). The CQR strain of *P. falciparum* was probably protected from the cytotoxic effects of the sulfonylureas by efflux of the sulfonylurea from the cytoplasm or by other cellular processes that confer drug resistance. The halide substituted derivatives (**2.3.3** and **2.3.4**) had the highest cytotoxic and antiplasmodial activities. This indicated that the biological activity may be determined by electronic interactions of the phenyl moiety with a receptor target. However, more derivatives need to be synthesized in order to delineate meaningful structure-activity relationships.

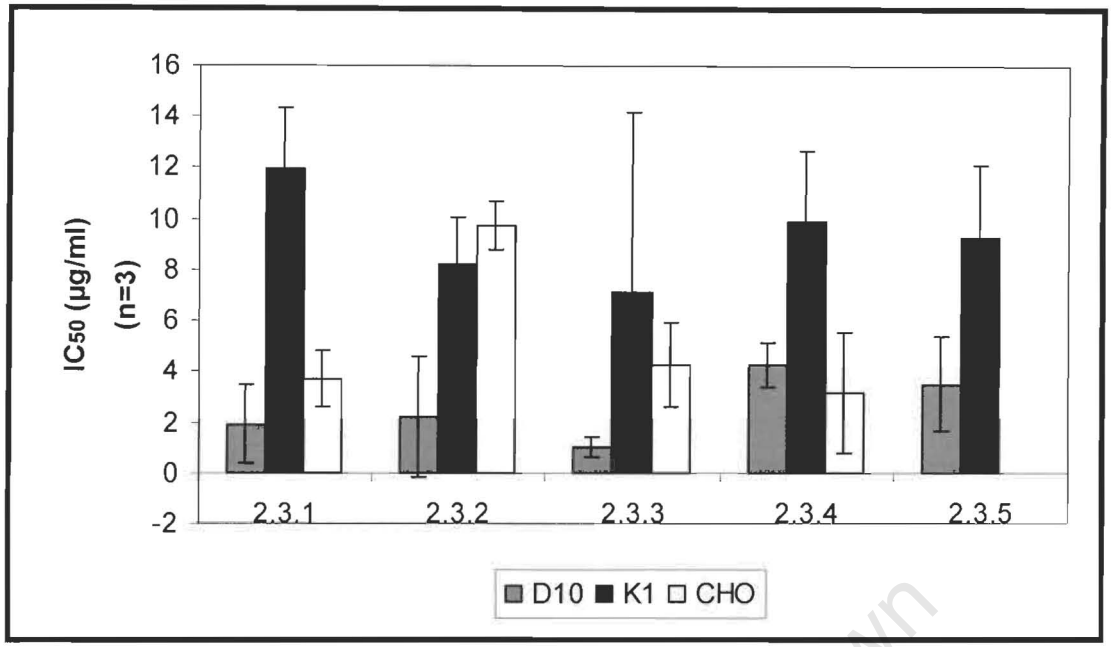

Figure 3 - 2 : Biological activities of sulfonyl urea derivatives of curcumin

Table 3 - 3: *In vitro* antiplasmodial and cytotoxicity of the sulfonylurea derivatives of curcumin

	IC_{50} [a] µg/ml (µM)		CC_{50} [a] µg/ml (µM) [a]		
	D10	**K1**	**CHO**	**SI**	**RI**
2.3.1	1.920 ± 1.556 (2.946 ± 2.231)	11.995 ± 2.304 (15.212 ± 11.968)	3.725 ± 1.117 (6.803 ± 2.034)	0.31	6.25
2.3.2	2.203 ± 2.367 (3.923 ± 4.214)	8.227 ± 1.787 (14.650 ± 3.181)	9.716 ± 0.970 (17.300 ± 1.726)	1.18	3.73
2.3.3	1.031 ± 0.402 (1.753 ± 0.490)	7.086 ± 7.066 (12.175 ± 12.141)	4.253 ± 1.666 (7.308 ± 2.863)	0.60	6.87
2.3.4	4.286 ± 0.866 (7.578 ± 1.531)	(9.864 ± 2.819) (12.216 ± 9.711)	3.164 ± 2.371 (5.594 ± 4.193)	0.32	2.30
2.3.5	3.499 ± 1.838 (6.230 ± 3.273)	9.296 ± 2.787 (11.628 ± 9.222)	ND		2.66

2.3.1 R = H, **2.3.2** R = CH_3, **2.3.3** R = Cl, **2.3.4** R = F, **2.3.5** R = CH_3 (ortho), [a]mean ± SD, n=3

Sulfonylurea derivatives inhibited the formation of beta-hematin (Table 3-4). They had greater inhibitory activity than chloroquine, which had a greater antiplasmodial activity. Sulfonylureas have been shown to inhibit beta-hematin formation [20]. This activity may have been due to the presence of the pyrazole ring. The chloro substituted sulfonylurea derivative had highest beta-hematin inhibitory activity amongst the three derivatives tested which is consistent with the fact that in quinoline derivatives the chloro group alters distribution of eletrons to favor interaction with heme [21].

Table 3 - 4: The IC_{50} values for the inhibition of β-hematin formation by sulfonylurea derivatives of curcumin

	IC_{50} (equivalents of hematin)
CQ	1.91 ± 0.3
2.3.1	0.530 ± 0.1
2.3.3	0.320 ± 0.09
2.3.5	0.631 ± 0.3

[a]mean ± SD, n=3

The sulfonylurea derivatives may not be good lead compounds for antimalarial drugs because of poor activity against the CQR strain and their high cytotoxicity. They, however, could be investigated further as cytotoxic agents for the development of new anticancer drugs.

3.2.3 The *in vitro* biological activities of the thiosemicarbazone derivatives of curcumin

The *in vitro* antiplasmodial activities of the thiosemicarbazone derivatives are presented in Table 3-5.

Table 3 - 5: *In vitro* antiplasmodial and cytotoxicity of the thiosemicarbazone derivatives of curcumin

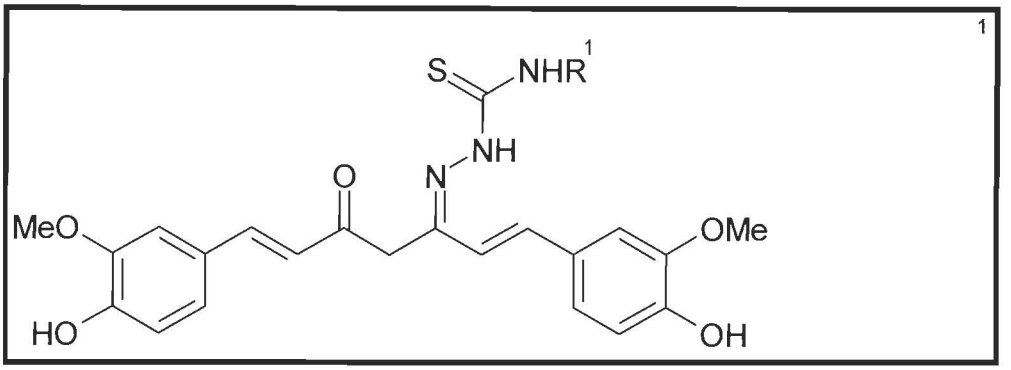

	IC_{50} [a] µg/ml (µM)		CC_5 [a] 0 µg/ml (µM)		
	D10	**K1**	**CHO**	**SI**	**RI**
CQ	5.521 ± 1.547 [b]	182.523 ± 10.253[b]	ND	ND	33.1
2.5.1	2.353 ± 1.018 (5.334 ± 2.307)	...	69.032 ± 0.893 (105.08 ± 89.05)	29.34[c]	...
2.5.2b	3.159 ± 1.894 (5.355 ± 4.016)	2.763 ± 1.277 (6.064 ± 2.804)	71.528 ± 8.868 (157.02 ± 19.47)	25.89	0.87
2.5.3	2.448 ± 1.053 (4.728 ± 2.034)	3.094 ± 0.811 (5.978 ± 1.567)	80.309 ± 34.106 (155.15 ± 65.89)	25.96	1.26
2.5.4	2.307 ± 1.089 (4.308 ± 2.032)	16.368 ± 0.800 (30.561 ±1.493)	59.745 ± 14.985 (111.55 ± 27.98)	25.89[c]	7.09

2.5.1 R = H, **2.5.2b** R = CH_3, **2.5.3** R = Ph, **2.5.4** R = 4-Fluro Ph, [a]mean ± SD, n=3, [b]ng/ml

[c]Calculated using IC_{50} against D1O as the denominator

The antiplasmodial activity of the thiosemicarbazone derivatives against the CQS strain was comparable to that of curcumin. Activity was not affected by the type of substituent at the thioamide bond. Addition of the thiosemicarbazone group did not improve the antiplasmodial activity of these compounds. All the thiosemicarbazone derivatives were equally active against the CQS and CQR strains with the exception of **2.5.4** (Figure 3-3).

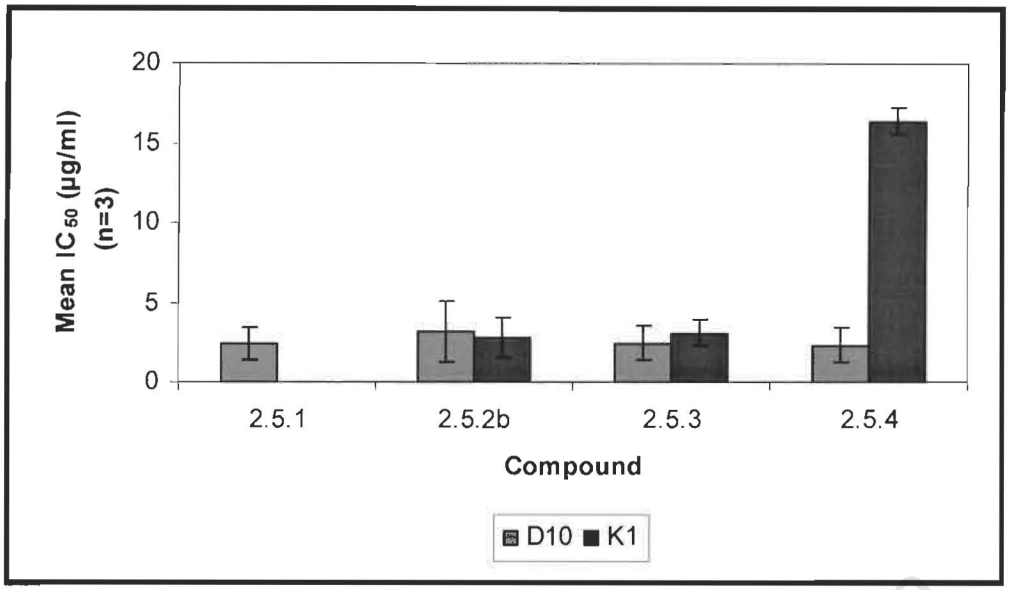

Figure 3 - 3: Comparison of the *in vitro* activities of the thiosemicarbazone derivatives of curcumin against the CQS and CQR strains of *Plasmodium falciparum*

The ability of thiosemicarbazone derivatives to overcome drug resistance may have been due to the presence of the α, β unsaturated carbonyl group [10] or the innate ability of thiosemicarbazones to act against CQR strains [22]. The thiosemicarbazone derivatives were not cytotoxic and had high selectivity indices of above 25 (Table 3-5).

3.2.4 The *in vitro* biological activities of the 7-chloroquinoline derivatives of curcumin

Two types of derivatives were obtained: hyrazino 7-chloroquinoline derivative (**2.7.1a** and **b**, Table 3-6) and the pyrazole-7-chloroquinoline derivative (**2.8.1**).

Table 3 - 6 : *In vitro* antiplasmodial and cytotoxicity of the 7-chloroquinoline derivatives of curcumin

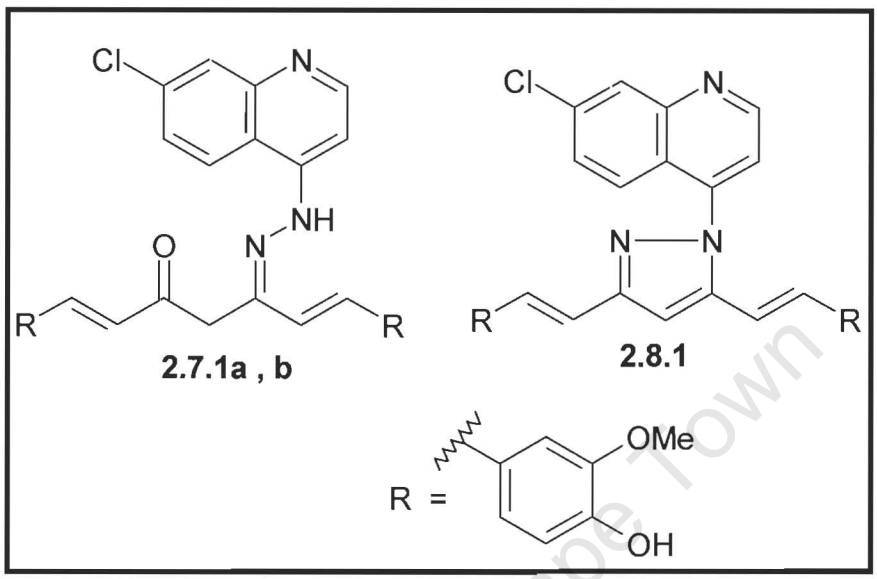

	IC_{50} [a] µg/ml (µM)		CC_{50} [a] µg/ml (µM)		
	D10	**K1**	**CHO**	**SI**	**RI**
2.7.1a	0.968 ± 0.102 (1.728 ± 0.182)	28.080 ± 4.156 (50.138 ± 7.420)	ND	ND	29.01
2.7.1b	2.779 ± 1.211 (4.962 ± 2.162)	4.244 ± 2.606 (7.578 ± 4.653)	>100	ND	1.53
2.8.1	0.412 ± 0.208 (0.784 ± 0.396)	1.671 ± 1.044 (3.177 ± 1.985)	>100	ND	4.06

[a]mean ± SD, n=3

The derivative containing the pyrazole group (**2.8.1**, Table 3-6) had the highest activity against the CQS and CQR strains. The antiplasmodial activity of **2.8.1** was about 4 times that of curcumin. Unlike hydrazinocurcumin, **2.8.1** was not cytotoxic to the CHO cells. This implied that the introduction of bulky substituents on nitrogen atoms of the pyrazole ring abolished the cytotoxicity of the pyrazole based derivatives of curcumin.

The two isomers of **2.7.1** had different *in vitro* activities. The isomer, **2.7.1a** was less active than **2.7.1b** against the CQR. The resistance indices were 29.01 and 1.53 respectively. The isomer, **2.7.1b**, was not cytotoxic to the CHO cells. The diminished activity against the CQR strain was surprising considering that **2.7.1** contained an α, β-unsaturated carbonyl group. The bulky subsituent on the α, β unsaturated carbonyl group may have impaired the ability to overcome the effects of proteins responsible for drug resistance. Resistance may also have been due to cross resistance since the derivative contained the quinoline ring.

The 7-chloroquinoline derivatives were10 times more active than chloroquine at inhibiting the formation of beta-hematin. The IC_{50} values for **2.7.1a** and **2.8.1** were 0.173 ± 0.1 and 0.449 ± 0.05 equivalents of hematin respectively compared to CQ which had an IC_{50} of 1.91 ± 0.3 equivalents of hematin. Despite this, chloroquine had a much greater *in vitro* antiplasmodial activity.

The most promising compound in this class of derivatives was **2.8.1** which had an IC_{50} of less than 1μM against the CQS strain. It lacked cytotoxicity. It may be used to develop other lead compounds if subjected to chemical modifications that impart the ability to overcome resistance.

3.2.5 The *in vitro* biological activities of the *N*-acyl hydrazone derivatives of curcumin

Two types of *N*-acyl hydrazone derivatives were synthesized: the aryl hydrazine methanone derivatives and the pyrazole-1-yl methanone derivatives. The biological activities of these two classes of compounds are presented in Table 3-7 and 3-8 respectively.

Table 3 - 7: *In vitro* antiplasmodial and cytotoxicity of the aryl hydrazine methanone derivatives of curcumin

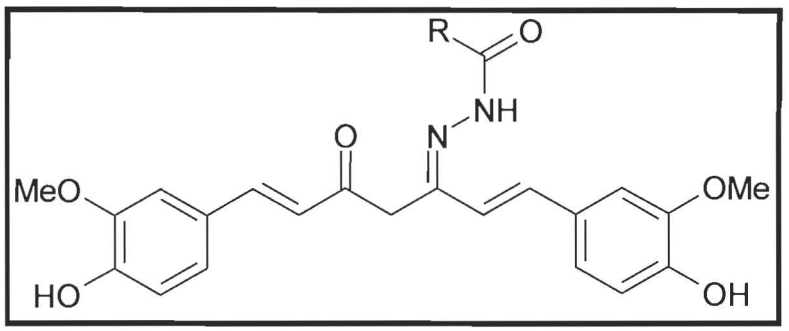

	IC_{50} [a] µg/ml (µM)		CC_{50} [a] µg/ml (µM)		
	D10	**K1**	**CHO**	**SI**	**RI**
2.9.1	0.382 ± 0.121 (1.208 ± 0.755)	ND	84.900 ± 26.154 (174.50 ± 53.76)	ND	ND
2.9.2	2.206 ± 0.893 (4.235 ± 1.715)	3.075 ± 0.484 (5.902 ± 0.929)	33.510 ± 21.715 (43.52 ± 46.55)	15.19	1.39
2.9.4	0.610 ± 0.149 (1.251 ± 0.306)	1.307 ± 0.418 (2.472 ± 0.708)	>100	ND	2.14

2.9.1 R= Ph, **2.9.2** R= 4 chloro Ph, **2.9.4** R= 2 hydroxyl Ph, **2.9.5** R= isonicotyl, [a]mean ± SD, n=3

Table 3 - 8: ***In vitro*** **antiplasmodial and cytotoxic activities of the aryl pyrazole-1-methanone derivatives of curcumin**

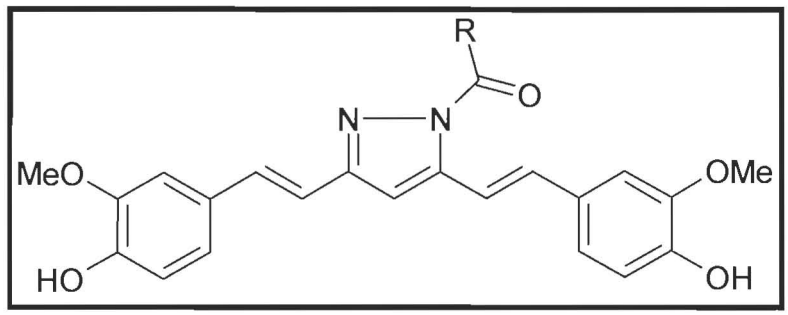

	IC_{50}[a] µg/ml (µM)		CC_{50}[a] µg/ml (µM)[a]		
	D10	**K1**	**CHO**	**SI**	**RI**
2.10.1	1.467 ± 0.820 (2.799 ± 1.364)	8.704 ± 3.487 (18.577 ± 7.442)	1.467 ± 0.820 (2.799 ± 1.364)	1.00	5.93
2.10.3	0.290 ± 0.044 (0.599 ± 0.090)	1.896 ± 1.252 (3.913 ± 2.583)	10.129 ± 1.790 (20.905 ± 3.695)	34.93	6.54
2.10.4	1.512 ± 0.269 (3.214 ± 0.572)	2.963 ± 0.702 (4.896 ± 2.624)	32.186 ± 12.390 (66.02 ± 25.414)	21.29	1.96
2.10.5	0.437 ± 0.157 (0.952 ± 0.342)	7.476 ± 6.415 (16.306 ± 13.991)	26.478 ± 21.661 (57.752 ± 47.246)	60.59	17.1

2.10.1 R= Ph, **2.10.3** R= 4 hydroxy Ph, **2.10.4** R= Isonicotyl, **2.10.5** R= 2-furoyl, [a]mean ± SD, n=3

The most active hydrazine aryl methanone derivatives against the CQR strain were **2.9.1** and **2.9.4** with IC_{50} values of about 1.208 and 1.251µM respectively. They had phenyl and isonicotyl substituents respectively.

Amongst the pyrazole-1-methanone derivatives, **2.10.3** and **2.10.5** were the most active with IC_{50} values of less than 1 µM against the CQS strain. The former had a 4-hydroxyl phenyl substituent while the latter had a furoyl substituent. Unfortunately antiplasmodial activity against the CQR of all the *N*-acyl hyrazone derivatives was substantially reduced with resistance indices ranging from 1.39 to 17.1 (Figure 3-4).

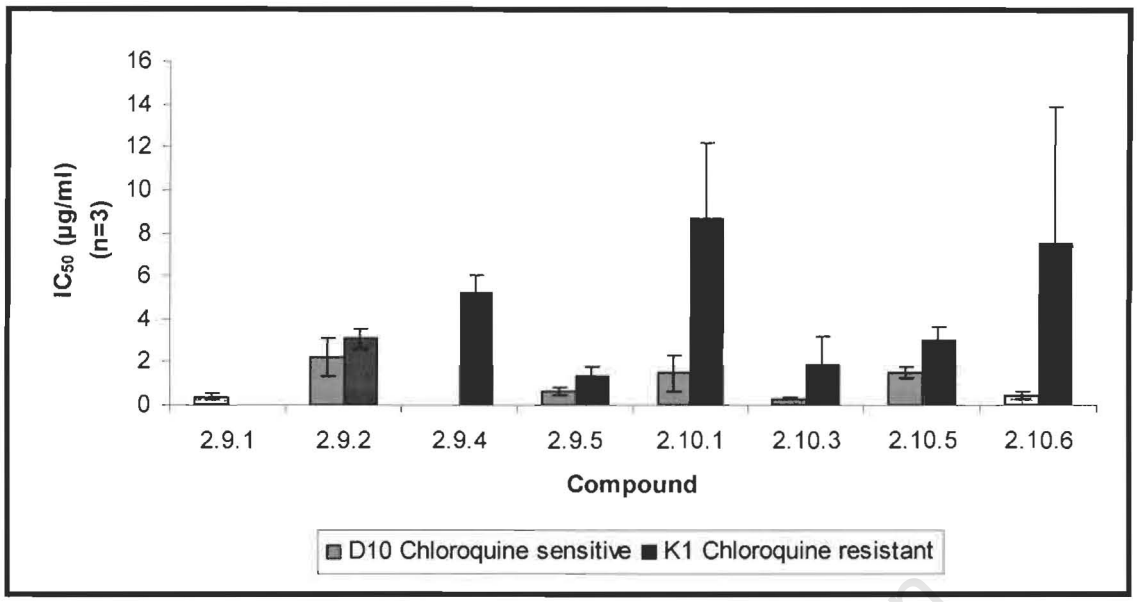

Figure 3 - 4: Comparison of the *in vitro* activities of the *N*-acyl hydrazone derivatives of curcumin against the CQS and CQR strains of *Plasmodium falciparum*

The pyrazole-1-yl methanone derivatives had greater cytotoxicity against the CHO cells compared to the aryl hydrazine derivatives (Figure 3-5).

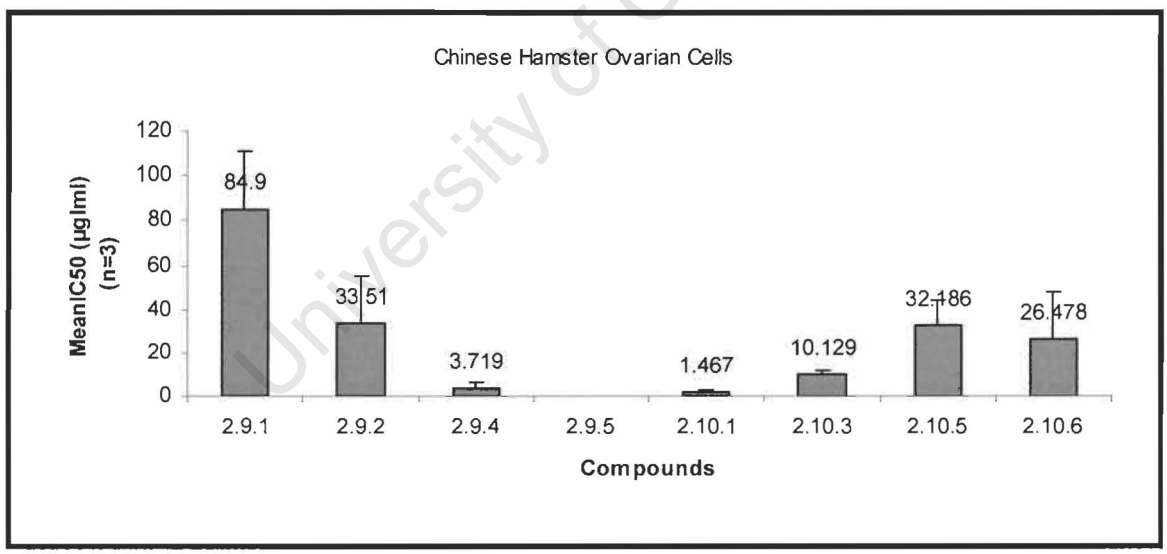

Figure 3 - 5: The cytotoxicity of the *N*-acyl hydrazone derivatives of curcumin against the Chinese Hamster Ovarian cells

The high cytotoxicity of the pyrazole-1-methanone derivatives was attributed to the pyrazole ring [14, 15]. The most cytotoxic compounds in this group, **2.10.1** and **2.10.3**, had phenyl and 4-hydroxylphenyl substituents respectively. Derivatives that had heterocyclic subsituents (isonicotyl in **2.10.4** and furoyl in **2.10.5**) had a lower cytotoxicity. All the hydrazine methanone derivatives had a low cytotoxicity. The high cytotoxicity of the hydroxyl phenyl substituted derivatives (**2.10.3**) may have been due to their ability to undergo tautomeric rearrangements that result in the formation of a quinone intermediate [23]. Quinones are Michael acceptors and cause cellular death by forming adducts with DNA and proteins [24-27].

All the *N*-acyl hydrazone derivatives inhibited formation of beta-hematin (Table 3-9).

Table 3 - 9: IC_{50} for inhibition of beta-hematin formation by *N*-acyl hydrazone derivatives of curcumin.

Compound	IC_{50} (equivalents of hematin)
CQ	1.91 ± 0.3
2.9.1	ND
2.9.2	0.798 ± 0.09
2.9.3	ND
2.9.4	0.826 ± 0.2
2.10.1	ND
2.10.3	0.504 ± 0.05
2.10.4	0.254 ± 0.05
2.10.5	0.614 ± 0.06

3.3 Conclusion

Curcumin was found to be equally active against both the CQS and CQR strains with IC_{50} values of 1.674 and 1.647µg/ml respectively. The resistance index was 1. All synthetic derivatives had reduced activity against the CQR strain except the thiosemicarbazone derivatives. The most active derivatives tended to have a pyrazole ring. Derivatives with IC_{50} values of less than 1 µM against the CQS strain were: **2.2.1a**, **2.8.1**, **2.10.3** and **2.10.6**. The diminished activity against the CQR strain may be improved by chemical modifications that impart the ability to reverse resistance. All the derivatives inhibited the formation of beta-hematin. The azole and sulfonylurea derivatives were highly cytotoxic against the CHO cells.

3.4 Materials and Methods

3.4.1 *In vitro* Test for Antimalarial Activity

3.4.1.1 Materials

Dimethyl sulfoxide (DMSO), absolute ethanol and Giemsa stain were purchased from BDH chemicals. RPMI-1640 with glutamate and without bicarbonate (GibcoBRL) and Albumax II (lipid rich bovine serum albumin) were obtained from InVitrogen Life Technologies, New Zealand. HEPES (N-[2-Hydroxethyl]-piperazine-N'-[2-ethanosulphonic acid]), glucose, sodium bicarbonate, calcium lactate hydrate, chloroquine diphosphate, hydrochloric acid, D-sorbitol, phenazine ethosulphate (PES), Nitro Blue Tetrazolium (NBT) and Triton-X-100 were obtained from Sigma-Aldrich. Gentamycin ampoules for injection (80 mg/2ml) were obtained from Micro Healthcare Pharmaceuticals, RSA. Heparinised O+ human blood was obtained from Western Province Blood Transfusion service, Groote Schuur, Hospital, SA.

Centrifuge tubes, sterile and non-sterile flat bottomed 96 well plates and 50 ml culture flasks were obtained from Greiner.

Absorbance was read at 620 nm using a 7520 Microplate Reader (Cambridge Technologies, Inc.). All glassware and equipment were sterilized by autoclaving and all solutions were sterilized by membrane filtration before use. All reagents were of cell culture grade.

3.4.1.2 Preparation of culture medium, reagents and stock solutions

Culture medium without serum (CMS) was prepared by dissolving RPMI-1640 with glutamate and without bicarbonate, hypoxanthine (44mg), HEPES buffer (6 g), glucose (4g), and gentamycin (50 mg/l) in 1 liter of millipore water. The pH was adjusted to 7.4. Complete culture medium (CM) was prepared by adding Albumax II (10 % v/v) to CMS. Before use bicarbonate solution (17 ml) was added to CMS and CM (400 ml).

To obtain leukocyte free erythrocytes, heparinised O^+ human blood added to an equal volume of CMS and centrifuged at 1250 rcf for 5 minutes. The supernatant layer and the upper buffer layer of cells were discarded. This process was repeated twice. The cells were stored at 4^oC for a maximum of 30 days.

The detection reagent had a similar composition to Malstat Reagent™ (Flow Inc.). It was prepared by dissolving 400 µl of Triton X100, 4g of lithium lactate, 1.32 g of TRIS buffer and 22 mg of APAD in 1 liter of water. The pH was adjusted to 9 using HCl. NBT solution was prepared by dissolving 160 mg of NBT and 8 mg of PES in 100 ml of Millipore water. The solution was protected from light since the reagents were photosensitive. All solutions and reagents were stored at 4^oC for a maximum of 1 month.

Stock solutions (2 mg/ml in 10 % v/v DMSO or EtOH) of the test compounds were prepared weekly. The test compounds (2 mg) were dissolved in DMSO or ethanol (100 µl) and Millipore water (900 µl) in that order. Chloroquine was dissolved in water. The stock solutions were stored at 4°C for a maximum of one week. The blank was 10 % v/v DMSO or EtOH in water.

3.4.1.3 Parasite culture

Plasmodium falciparum was cultured according to the method described by Trager and Jensen [28]. The parasite strains used were D10 which is chloroquine sensitive and K1 which is resistant to both chloroquine and pyrimethamine. These strains are well characterized and originated from Papua New Guinea and Thailand respectively [29].

Parasites were grown in human erythrocytes (5 % haematocrit) suspended in culture medium at 37°C in microaerophilic conditions (93 % N_2, 4 % CO_2 and 3 % O_2 gas mixture) in 50 ml culture flasks. The medium was changed daily to remove toxic metabolic wastes. The level of parasitemia was monitored daily by light microscopic examination of giemsa stained thick smears of the culture. The parasitemia was maintained at 2 to 5 %. When the parasitemia exceeded 5 %, it was reduced by subculturing and adding uninfected erythrocytes.

The parasite culture was synchronized according to the method described by Lambros and Vanderbeg [30]. The culture was centrifuged at 750 rcf for 3 minutes and the supernatant discarded. The RBC pellet was incubated with five volumes of 5 % w/v D-sorbitol aqueous solution at room temperature for 15 minutes. D-sorbitol selectively killed the ring stage of the parasite and the trophozoites were not affected. Sorbitol was removed by centrifugation and the supernatant was discarded.

3.4.1.4 The Plasmodium Lactate Dehydrogenase Assay (pLDH assay)

The assay was performed as described by Makler and Hinrichs [2, 31]. It is a colorimetric assay in which activity for the parasite enzyme lactate dehydrogenase is used as a proxy measure for number of viable parasites. The specificity of the assay is based on the parasite's enzyme ability to utilize 3-acetyl pyridine adenine dinucleotide (APAD) as a co-factor. The human enzyme cannot utilize APAD. In the presence of APAD, parasite lactate dehydrogenase converts NBT to a blue colored formazan product. In the process, APAD is converted to 3-acetyl dihydropyridine dinucleotide (APADH). The absorbance of the formazan product at 620 nm is used as a proxy indicator of the percentage of viable parasites.

The test was performed on a 96 well plate, made up of 8 rows labeled A to H and 12 columns numbered 1 to 12. Each test compound was tested in duplicate on two rows of the plate. Four compounds were tested on each plate. CM (100 µl) was added to each well the plate except the third column. The stock solution of the test compound was diluted with CM to a concentration of 200 µg/ml. The diluted solution of the test compound (200 µl) was added to two wells in the third column. Using a multichannel pipette, the drug solution was serially diluted two-fold across each row. Each well contained 100 µl of drug solution in CM.

Parasited RBCs (100 µl, 2 % parasitemia, 2 % haematocrit) were added to all the wells except column one. Non-parasitized RBCs (100 µl, 2 % haematocrit) were added to each well in column one. The final parasitaemia and haematocrit in each well was 1 %. The plates were incubated for 48 hours at 37°C in a gassed modular chamber.

After incubation the red blood cells in each well were suspended by thorough mixing using a multichannel pipette. The suspended red blood cells (15 µl) were transferred to 96 well plate containing Malstat™ (100 µl). NBT (25 µl) solution was added to each well. The plate was placed in a dark cupboard for

about 15 minutes to allow for the formation of the formazan derivative. The plates were read in a microplate reader at 620 nm.

3.4.1.5 Data Analysis

The absorbances of the wells in the first column were used to correct for background noise. The absorbance of the wells in column 2, where the parasites were grown without any drug, were used as the denominator as they represented the maximum possible growth of the parasites. Microsoft Excel XP™ was used to calculate the percentage parasite growth in each well using the following formula:

$$\%\text{age of maximum growth in well} = \frac{\text{Absorbance in well}_{ij} \times 100}{\text{Absorbance in well}_{i2}}$$

i = row number, j = column number, $well_{i2}$ = the well in row i in the 2nd column

The IC_{50} was obtained by extrapolation from a sigmoidal plot of log of well drug concentration against percentage parasite growth. The graph was fitted by the least square method using GraphPad Prism software [32]. The mean and standard deviation of three determinations of the IC_{50} was calculated using Microsoft Excel. The resistance index was calculated by dividing the IC_{50} against the CQR strain by the IC_{50} against the CQS strain.

3.4.2 MTT Cytotoxicity Assay

The method used was as described by Mosman *et al.* [4]. This assay tests the ability of compounds to kill mammalian cells. It is a colorimetric assay in which the number of viable cells is measured by the conversion of the yellow water-soluble (3-[4,5-Dimethylthiazol-2-yl]-Diphenyltetrazolium bromide) (MTT) to the water insoluble purple formazan product by non-mitochondrial and

mitochondrial hydrogenases [33] . The mammalian cells used in this assay were the Chinese Hamster Ovarian (CHO) cells which were kindly donated by S. Schwager of the Department of Medical Biochemistry, University of Cape Town.

3.4.2.1 Materials

Dulbeco Modified Eagles Medium (DMEM) was purchased from Invitrogen Incorporation (New Zealand). Nutrient HAMS-12 powder, sodium bicarbonate and MTT were purchased from Sigma-Aldrich, St. Loius, USA. All reagents were of cell culture grade.

3.4.2.2 Preparation of culture medium and detection reagent

Phosphate Buffer Solution (PBS) was prepared by dissolving one tablet of the buffer salt mixture in 100 ml of water and warmed to 37^0C for 30 minutes in a water bath before use. Dulbeco Modified Eagles Medium (DMEM) was prepared by dissolving 13.53 g of powder, 500 µl of gentamycin and 3.7 g of sodium bicarbonate in 1 liter of Millipore water. The pH was adjusted to 7.1.

HAMS F-12 solution was prepared by dissolving one bottle of nutrient HAMS-12 powder, 1.176 grams of bicarbonate and 500 µl of gentamycin in one liter of Millipore water. The pH was adjusted to 7.1. Fetal calf serum (FCS) was heat inactivated at 56°C for 30 minutes. Trypsin solution (0. 1% w/v) was prepared by dissolving 0.10 g in 100 ml of PBS. The solution was pre-warmed to 37°C in a water bath before use. All solutions were stored at 4°C for a maximum of 2 months.

3.4.2.3 Cell culture

Cryofrozen cells were thawed in a water bath at 37°C. An equal volume of thawing medium (30% FCS, 35 % DMEM, 35 % HAMS F-12) was added to the thawed cells and the mixture was centrifuged for 5 minutes at 750 rcf. The supernatant was discarded and the pellet transferred to a 50 ml culture flask containing 9 ml of thawing medium. The cells were cultured at 37°C in 5 % carbon dioxide in air humidified atmosphere for 48 hours after which medium was changed to culture medium (10% FCS, 45 % DMEM, 45 % HAMS F-12). Thereafter, the culture medium (CM) was changed every 2 to 3 days. The cells were sub-cultured for a maximum of 10 times when they attained confluence.

3.4.2.4 The cytotoxicity assay

Stock solutions of the test compounds (2 mg/ml in 10 % DMSO) were prepared as previously described for the parasite lactate dehydrogenase assay. The stock solution was diluted ten fold in eppendroff tubes using culture medium to obtain the 6 ten fold dilutions with concentrations ranging from 200 µg/ml to 2ng/ml.

When the culture had attained confluence, culture medium was aspirated, rinsed twice with pre-warmed PBS solution (10 ml) and the cellular matrix of the culture was digested by exposing to pre-warmed trypsin solution (5 ml) for 2 minutes. After confirming that cells were no longer adhering to the flask by examining under a light microscope, the digestive action of trypsin was stopped by the addition of 5 ml CM. The cell suspension was centrifuged at 750 rcf, the supernatant discarded and the cell pellet resuspended in CM (5 ml). The number of cells in 20 µl was determined by counting under a light microscope and this was used to dilute the cell suspension to a count of 10^5 cells/ml of suspension.

The cell suspension (100 µl) was added to each well of a 96 well plate except those in the first row. The plate was incubated for 24 hours at 37°C in a humidified 5 % CO_2-air atmosphere. After confirming that the cells had attained confluence, the medium was carefully aspirated out of the wells and each dilution of the test compounds (100 µl) was added in triplicate to the wells from the third to the eighth row. This was followed by CM (100 µl) so that the final well concentration of the test compounds ranged form 100 µg/ml in the third row to 1ng/ml in the 8 row. An additional 100 µl of CM was added to the first 2 rows. Four compounds were tested in one plate. Emetine (2 mg/ml) was used as the positive control and 10 % v/v DMSO was used as the negative control.

The plate was incubated at 37°C for 48 hours. After incubation, 25 µl of sterile MTT (5 mg /ml in PBS) were added to each well and the plate was further incubated for 4 hours to allow for the formation of the formazan derivative. After 4 hours the plates was centrifuged for 10 minutes at 1200 rpm. The supernatant in each well was aspirated carefully so as not to disturb the formazan precipitate. DMSO (100 µl) was added to each well and the plate vortexed gently for 5 minutes to dissolve the formazan crystals. The plate was read at λ 540 nm on the plate reader. The absorbance of the first row which contained no cells was used to correct for background absorbance.

3.4.2.5 Data Analysis

The absorbance of the culture wells in the first row was used to correct for background absorbance. The absorbance of the culture wells in the second row, where no test compound was added, was used as a denominator to calculate percentage of cell growth in each well. Cell viability in each well was calculated using the following formula:

$$\% \text{ Cell Viability} = \frac{A_{\lambda 540} \text{ test well (cells + drug)}}{A_{\lambda 540} \text{ control well (cells + no drug)}} \times 100$$

Data analysis was performed as described for the antiplasmodial assay. Selectivity index was calculated using the following formula: CC_{50} against the CHO cells/IC_{50} against CQR parasites

3.4.3 The pyridine hemichrome assay for inhibition of beta-hematin formation assay

This assay determines the ability of a compound to inhibit the formation of beta-hematin from hematin. Beta-hematin is the synthetic analogue of hemozoin which is formed in the food vacuole after digestion of hemoglobin by *P. falciparum*. The method used was developed by Ncokazi and Egan [5]. It was a simple colorimetric assay based on the ability of aqueous pyridine to form a low spin complex with hematin.

3.4.3 1 Materials

Bovine hemin, Hepes, chloroquine diphosphate, sodium acetate trihydrate (NaOAc), glacial acetic acid and $NaHSO_4$ were purchased from Sigma-Aldrich, South Africa. Pyridine (AR) was purchased from BDH Chemicals. Sodium chloride (AR) was purchased from Saarchem, South Africa. Methanol (AR) was purchased from Kimix, South Africa. Flat and U- bottomed non sterile 96-well plates were obtained from Greiner. Spectroscopic measurement of the absorbance of the plates was done using an Anthos Labtec HT2 plate reader.

3.4.3.2 Preparation of the stock solutions

A supersaturated solution of sodium acetate trihydrate (100 ml, 12.9 M) was prepared by dissolving 63.14 g of sodium acetate trihydrate in 47.28 ml of glacial acetic acid. Gentle warming and vigorous stirring was done to effect complete dissolution. The pH of the solution was adjusted to 5 and it was stored at room temperature. Before use the solution was incubated at 60°C for one hour.

Hematin stock (1.680 mM) solution was prepared by dissolving 1.680 X 10^{-2} millimoles of bovine hemin in 10 ml of 0.1 M NaOH. The solution was used within 60 minutes of preparation. A stock solution of the test compound (168 mM) was prepared by dissolving 0.168 millimoles of the test compound in 1 ml of 1.0 M HCl or methanol. When methanol was used as the solvent, NaOH solution that was used to dissolve hematin was neutralized by the addition of an equivalent of 1 M HCl. This was done to prevent precipitation of the compound during the assay.

3.4.3.3 The Pyridine hemichrome assay

The assay was performed on a 96 well U bottomed plate. The stock solution (20.4 µl, 168 mM) was added to the 3 wells in first column. The solvent used to dissolve the drug was added to the next 5 wells of each row. Using a multichannel pipette 10.1 µl for stock solution was transferred from the first column on the next column. The multichannel pipette was used to dilute the stock drug solution two-fold in next 4 wells of each row such that each well had 10.2 µl of the test compound. The wells in the 6^{th} and 12^{th} row had no test compound. Hematin stock solution (101.2 µl, 1.680 mM) was added to each well so that the ratio of equivalents of drug to hematin in wells decreased in the following order: 10; 5; 2.5; 1.3; 0.63; and 0.

Pre-warmed acetate solution (58.7 µl, 12.9 M) was added to each well and the plate was incubated for 30 minutes at 60°C to allow for the formation of ß-hematin. After incubation, the detecting reagent, pyridine solution (80 µl, 30 % v/v in 20 mM Hepes, pH 7.5) was added to each well at room temperature. The solids in wells were resuspended by gently vortexing the plate for 5 minutes. The solids were allowed to settle by leaving the plate to stand for 15 minutes at ambient room temperature. The supernatant (38 µl) was transferred to a flat bottomed 96 well plate and diluted to 250 µl by adding 238 µl of pyridine solution. The plate was read using a plate reader at 405 nm.

3.4.3.4 Data analysis

The IC_{50} for ß-hematin formation inhibition was obtained by extrapolation from a sigmoidal plot of log of well drug concentration against absorbance at 405nm. The graph was fitted by the least square method using Graph Pad Prism software [32]. The standard deviation of the mean of three determinations of the IC_{50} was calculated using Microsoft Excel.

References

(1) Trager, W.; Jensen, J. B. *Science* **1976**, *193*, 673-675.

(2) Makler, M. T.; Hinrichs, D. J. *Am. J. Trop. Med. Hyg.* **1993**, *48*, 205-210.

(3) Kalra, B. S.; Chawla, S.; Gupta, P.; Valecha, N. *Indian J. Pharmacol.* **2006**, *38*, 5-12.

(4) Mossman, T. *J. Immunol. Methods* **1983**, *65*, 55-63.

(5) Ncokazi, K.; Egan, T. *Anal. Biochem.* **2005**, *338*, 306-319.

(6) Kumar, S.; Guha, M.; Choubey, V.; Maity, P.; Bandyopadhyay, U. *Life Sci.* **2007**, *80*, 813-828.

(7) Kurosawa, Y.; Dorn, A.; Kitsuji-Shirane, M.; Shimada, H.; Satoh, T.; Matile, H.; Hofheinz, W.; Masciadri, R.; Kansy, M.; Ridley, R. G. *Antimicrob. Agents Chemother.* **2000**, *44*, 2638-2644.

(8) Rasmusen, H. B.; Christensen, S. B.; Kuist, L. P.; Karazami, A. *Planta Med.* **2000**, *66*, 396-398.

(9) Reddy, R. C.; Vatsala, P. G.; Keshamouni, V. G.; Padmanaban, G.; Rangarajan, P. N. *Biochem. Biophys. Res. Commun.* **2005**, *326*, 472-474.

(10) Wortelboer, H. M.; Usta, M.; van Zanden, J. J.; van Bladeren, P. J.; Rietjens, I. M. C. M.; Cnubben, N. H. P. *Biochem. Pharm.*, **2005**, *69*, 1879-1890.

(11) Natarajan, M.; Mohan, S.; Martinez, B. R.; Meltz, M. L.; Herman, T. S. *Cancer Detect. Prev.* **2000**, *24*, 405-414.

(12) Peng, L.; Wang, B.; Ren, P. *Colloids Surfaces B.* **2005**, *45*, 108-111.

(13) Heuser, M.; Kopun, M.; Rittgen, W.; Granzow, C. *Cancer Lett.* **2005**, *223*, 57-66.

(14) Ishida, J.; Ohtsu, H.; Tachibana, Y.; Nakanishi, Y.; Bastow, K. F.; Nagai, M.; Wang, H.; Itokawa, H.; Lee, K. *Bioorg. Med. Chem.* **2002**, *10*, 3481.

(15) Shim, J. S.; Lee, J.; Park, H.; Park, S.; Kwon, H. J. *Chem. Biol.* **2004**, *11*, 1455-1463.

(16) Price, R. N.; Cassar, C.; Brockman, A. *Antimicrob. Agents Chemother.* **1999**, *43*, 2943-2949.

(17) Durrand, V.; Berry, A.; Sem, R.; Glaziou, P.; Beaudou, J.; Fandeur, T. *Mol. Biochem. Parasitol.* **2004**, *136*, 273-285.

(18) Uzcategui, N. L.; Figarella, K.; Camacho, N.; Ponte-Sucre, A. *Comp. Biochem. Physiol. C,* **2005**, *140*, 395-402.

(19) Machuca, C.; Rodríguez, A.; Herrera, M.; Silva, S.; Ponte-Sucre, A. *Exp. Parasitol.* **2006**, *114*, 1-9.

(20) León, C.; Rodrigues, J.; Gamboa de Domínguez, N.; Charris, J.; Gut, J.; Rosenthal, P. J.; Domínguez, J. N. *Eur. J. Med. Chem.* **2007**, *42*, 735-742.

(21) Egan, T.; Ncokazi, K. *J. Inorg. Biochem.* **2005**, *99*, 1532-1539.

(22) Rosenthal, P. J.; P.S. Sijwali; A. Singh; B.R. Shenai *Curr. Pharm. Des.* **2002**, *8*, 1659-1672.

(23) Ifa, D. R.; Rodrigues, C. R.; de Alencastro, R. B.; Fraga, C. A. M.; Barreiro, E. J. *THEOCHEM,* **2000**, *505*, 11-17.

(24) Hillard, E. A.; Pigeon, P.; Vessières, A.; Amatore, C.; Jaouen, G. *Dalton Trans* **2007**, 5073-5081.

(25) Zahid, M.; Saeed, M.; Lu, F.; Gaikwad, N.; Rogan, E.; Cavalieri, E. *Free Radical Biol. Med.* **2007**, *43*, 1534-1540.

(26) O'Hara, K. A.; Wu, X.; Patel, D.; Liang, H.; Yalowich, J. C.; Chen, N.; Goodfellow, V.; Adedayo, O.; Dmitrienko, G. I.; Hasinoff, B. B. *Free Radical Biol. Med.* **2007**, *43*, 1132-1144.

(27) Benites, J.; Valderrama, J. A.; Rivera, F.; Rojo, L.; Campos, N.; Pedro, M.; José Nascimento, M. S. *Bioorg. Med. Chem.* **2008**, *16*, 862-8..

(28) Trager, W.; Jensen, J. B. *Science* **1976**, *193*, 673-675.

(29) Fidock, D. A.; Rosenthal, P. I.; Croft, S. L.; Brun, R.; Nwaka, S. *Nat. Rev. Drug Discov.* **2004**, *3*, 509-520.

(30) Lambros, C.; Vanderberg, J. P. *J. Parasitol.* **1979**, *65*, 418-420.

(31) Makler, M. T.; Ries, J. M.; Williams, J. A.; Bancroft, J. E.; Piper, R. C.; Gibbens, B. L.; Himrichs, D. J. *Am. J. Trop. Med. Hyg.* **1997**, *48*, 739-741.

(32) GraphPad Prism v.4,GraphPad Software Inc , San Diego, CA.

(33) Bernas, T.; Dobrucki, J. *Cytometry* **2002**, *47*, 236-242.

CHAPTER 4

IN VIVO TOXICITY AND ANTIMALARIAL ACTIVITY OF SELECTED CURCUMIN DERIVATIVES

4.1 Introduction

Candidate drugs are tested in animal models to determine the efficacy, toxicity profile and pharmacokinetic properties. *In vivo* tests in animal models is the link between preclinical studies and clinical trials [1]. Information obtained from *in vivo* studies is used to predict the therapeutic index, dose for humans and to identify biomarkers for drug efficacy and disease progression [2]. A major criticism against animal experimentation is that findings in animals cannot always be extrapolated to humans. Secondly, there are ethical concerns about animal experimentation [3, 4]. Despite the shortcomings of animal experimentation, it is an extremely valuable tool in drug discovery because the complexity of an animal cannot be replicated in *in vitro* experiments [4]. It provides a 'proof of concept' before human studies and can be used to predict potential problems in humans. Pre-clinical *in vivo* toxicity study is a mandatory requirement in drug development [5]. The main objective of toxicity tests is not to demonstrate that a chemical substance is safe but rather to characterize what toxic effects the chemical can produce.

This chapter describes a preliminary toxicological investigation of 3 derivatives of curcumin (**2.1.1**, Figure 4-1) aimed at determining the optimal dose for the *in vivo* antimalarial study as well as exploring their intrinsic toxicity. Dose optimization was necessary to rule out drug induced mortality and other related outcomes during the antimalarial study. The study was performed according to the guidelines of the British Toxicology Society (BTS) [6]. Pilot toxicological investigations are qualitative in nature and reveal the type of adverse reactions expected of a compound. They are used to determine the optimal doses for full toxicological investigations using guidelines in Appendix A [7].

The objective of toxicity testing is to classify a test compound as harmful, toxic, very toxic, or unclassified.

The *in vivo* antimalarial efficacy of the test compounds was determined using the method described by de Ferreira-da-Cruz *et al.* [8]. This method was a modification of that described by Peters *et al.* [9]. The key difference between the method used and that earlier described was that parasitemia was monitored for 7 to 9 days instead of only on day 4. This permitted the detection of antimalarial activity of compounds that are slow acting. Secondly, additional outcomes such as survival of infected mice and body mass changes were monitored. These additional outcomes augmented the validity of the *in vivo* efficacy study. Compounds were tested for activity against the chloroquine sensitive strain P. *berghei* ANKA. The main criteria for the selection of the derivatives were high *in vitro* antimalarial activity and high synthetic yields. Each class of derivatives was represented. Structures of the compounds investigated are presented in Figure 4-1. All the derivatives except for **2.2.2a** were N-substituted derivatives of hydrazinocurcumin (**2.2.1a**).

4.1.1 Objectives

The main aim of the study was to test for in vivo efficacy of the test compounds against CQS *Plasmodium berghei* ANKA infected mice. The specific objectives of the study were:

1. Assessment of the intrinsic toxicity of the test compounds.
2. Determination of an optimal dose for the *in vivo* antimalarial assay.
3. Identification of adverse outcomes associated with single and repeated oral doses of the test compounds on body mass and behaviour of the mice.
4. Determination of the effects of the test compounds in the mouse model of malaria on the following outcomes: parasitemia; body mass, survival; and selected clinical signs.
5. Establishment of the dose-response relationship of hydrazinocurcumin (**2.2.1a**) in the mouse model of malaria.

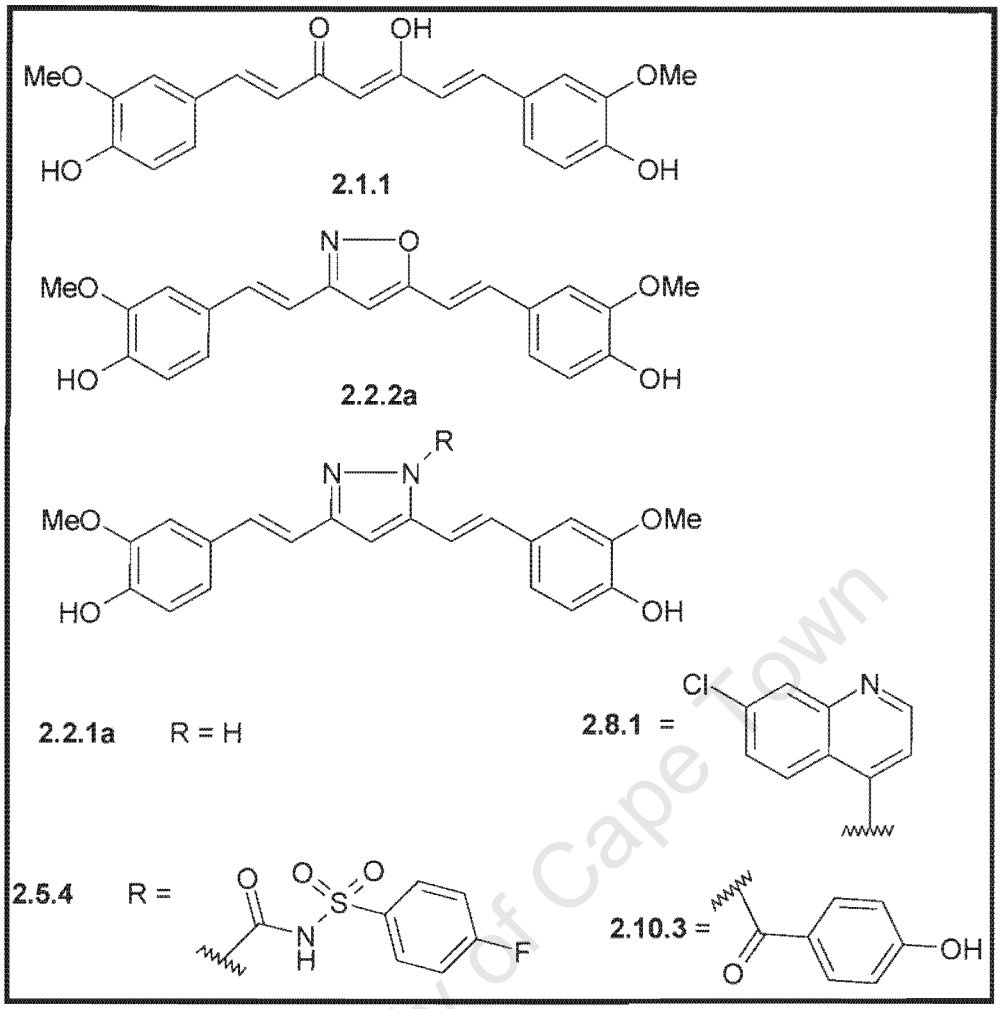

Figure 4 - 1: Structures of compounds tested for *in vivo* antimalarial activity

4.2 Results and Discussion

4.2.1 Pilot Toxicological Investigation

The pilot toxicological investigation was performed on compounds: **2.2.2a**, **2.8.1** and **2.10.3** according to the guidelines set out by the British Toxicological Society [6]. The doses administered ranged from 12.5 to 416 mg/kg of body weight (bwt.) which was within the range typically used in *in vivo* antimalarial studies [10, 11]. A second consideration in the selection of doses was the amount of test material available. There was a 3 to 5 fold

difference in the doses administered across groups. All test compounds were administered orally since this is the ideal route of administration of first line antimalarial agents. As required by the BTS guidelines, each compound was administered to 3 groups of 3 mice with the exception of curcumin (**2.1.1**) and acylhydrazone derivative, **2.10.3**. Curcumin (**2.1.1**) was formulated as a phosholipid complex using the method described by Liu *et al.* [12] and was tested in one group of mice that received a single oral dose equivalent to 200mg/kg of bwt. of the curcumin. Due to limited amounts of test material, the *N*-acyl hydrazone derivative, **2.10.3** tested in only two groups.

The doses administered are presented in Table 4-1.

Table 4 - 1: Doses administered in the pilot toxicological investigation

	Group 1	**Group 2**	**Group 3**
	Daily oral dose[a] (mg/kg of bwt.)	Daily oral dose[a] (mg/kg of bwt.)	Single oral dose (mg/kg of bwt.)
Curcumin	…	…	200
2.2.2a	12.5	62.5	156
2.8.1	25	125	416
2.10.3	12.5	62.5	…

[a]For a duration of 5 days.

The animals were observed for 1 hour after drug administration, 6 hours later and at the end of each day for behavioural and clinical signs of illness such as lethargy, tremors, vocalizations, piloerection and pinocytosis. Mice were weighed daily for 15 days. Body mass loss of more than 20 % of the mass at the start of the study was considered significant. All mortalities were noted.

4.2.1.1 Mortalities and Observed Clinical Signs during the Toxicity Study

No mortalities were observed except for one animal that received a 62.5 mg/kg of bwt. of **2.10.3** daily for 5 days. The animal that died was wasted and had lost about 30 % of its initial body mass by the time it died.

The adverse reactions observed in animals that received the repeated oral doses are listed in Table 4-2. Animals treated with curcumin had the least number of adverse reactions. The only adverse effect was vocalization in distress immediately after drug administration. It may have been due to the constituents of the formulation which may have caused gastrointestinal irritation. To prevent further distress to the mice, curcumin was administered only twice instead of the intended 5 doses. The *N*-acyl hydrazone derivative, **2.10.3** showed the highest frequency and range of adverse reactions. Hypoactivity, unsteadiness and poor motor control were the most frequently observed reactions across all groups except for groups treated with curcumin. The adverse reactions were transient and wore off in 6 hours. The adverse reactions were dose-dependent and were most severe in animals that received **2.10.3**.

The range of adverse reactions observed included: pinocytosis, lethargy and reduced motor function. These observations are subjective and a full well designed toxicological investigation is required to confirm these findings. The observed adverse reactions suggested that the tested compounds may affect the neurological system as has been reported for phenyl pyrazoles [13]. All the test compounds were structurally similar to phenyl pyrazoles.

Table 4 - 2: List of the adverse outcomes observed during the duration of toxicity study

DOSE (mg/kg of bwt.)	OBSERVED CLINICAL AND BEHAVIOURAL CHANGES
2.1.1 - CURCUMIN	
200 mg/kg - two doses	Vocalization immediately after drug administration.
2.2.2a – Isoxazole derivative of curcumin	
12.5 mg/kg daily	No adverse reaction except for transient lethargy on the 4th day of the study.
62.5 mg/kg daily	No adverse reaction except for slight unsteadiness on the 4th day of the study
156 mg/kg single dose	No reaction observed
2.10.3 – N-4'-hydroxyphenyl hydrazone derivative	
12.5 mg/kg daily	Unsteady gait, lethargy. One mouse had contracture of the front right lirnb.
62.5 mg/kg daily	Weakness of the hind limbs, unsteady gait, lethargy, contracture of front left limb in one mouse, pinosis in one eye. One animal died.
2.8.1 – 7-chloro-quinoline derivative	
25 mg/kg daily	No adverse reaction except one animal was lethargic on the 4th day of the study.
125 mg/kg daily	Lethargy, unsteady gait, weakness of hind limbs, vocalizations, piloerection, Intensity of adverse reactions increased daily.
416 mg/kg single dose	Lethargy and unsteady gait. One mouse showed pinocytosis and piloerection. Recovered in 24 hours

4.2.1.2 Effects of the Test Compounds on Body Mass

The most common adverse event was a reversible decrease in body mass. A representative graph of the mean body mass expressed as a percentage of the initial mass plotted against time is presented in Figure 4-2.

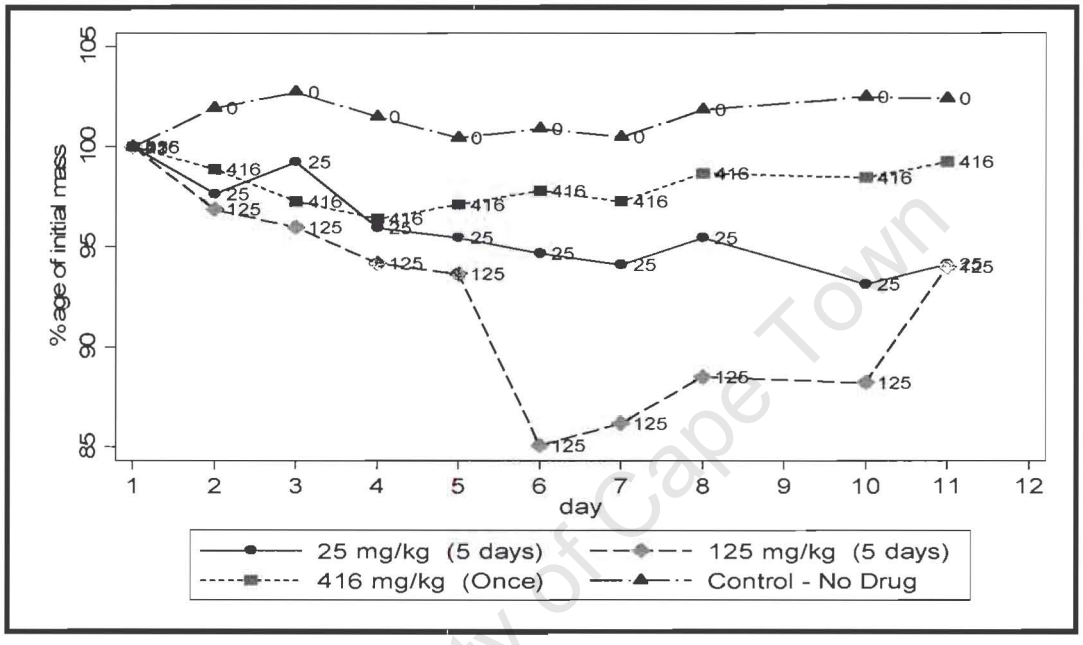

Figure 4 - 2: Effects of different doses of the isoxazole derivative (2.2.2a) on the mass of mice. Mass expressed as a percentage of initial body mass

Mice treated with single oral doses lost less than 6% of their body weight except for mice treated with **2.2.2a** (Figure 4-3). The loss in body mass was not significant.

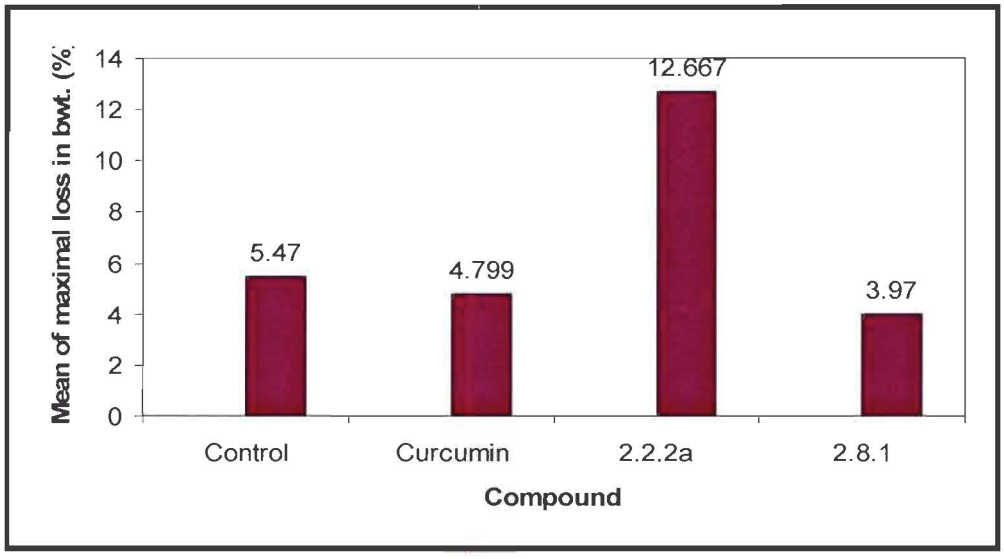

Figure 4 - 3: Single Oral Dose Toxicity Study - Mean of Maximum Percentage Loss of Body Mass (n=3) on administration of **Curcumin** (200 mg/kg), **2.2.2a** (156 mg/kg) and **2.8.1** (416 mg/kg)

Since no mortalities or significant adverse reactions were observed in animals treated with single oral doses, the studied compounds cannot be rated as toxic or very toxic using the guidelines described by Heuvel *et al.* [7] (Appendix A). Using the guidelines, the lowest dose for a full toxicological investigation should be about 500 mg/kg of bwt. The lack of toxicity of curcumin agrees with previous studies [14, 15].

Animals that were treated with repeated oral doses experienced more severe weight loss. The decline in body mass was dose-dependent (Figure 4-4). Animals treated with **2.10.3** experienced the greatest decline in body mass. One animal in each of the groups that received 12.5 and 62.5 mg/kg of **2.10.3** lost over 20 % of its initial body mass.

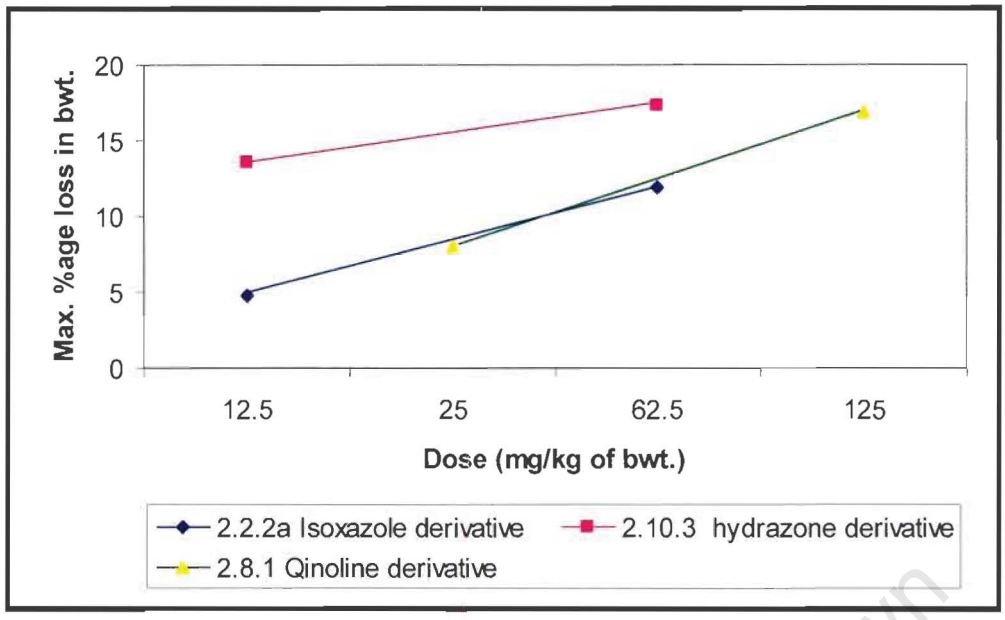

Figure 4 - 4: Repeated Oral Dose Toxicity Study - Mean of maximal Percentage Loss in Body Mass (n=3)

Mice treated with the *N*-acyl hydrazone derivative (**2.10.3**) experienced the most intense and frequent adverse reactions. One mouse treated with this compound died. The toxicity of this compound may have been due to the presence of a phenol group. Phenols are precursors for quinone which is a known toxiphore [16, 17].

4.2.1.3 Dose selection for the *in vivo* antimalarial study

The repeated dose toxicity study was designed to imitate the dosing schedule used in the *in vivo* antimalarial study. Mice in the repeated dose study displayed more adverse reactions compared to mice in the single dose study due to cumulative toxicity. It was observed that severity of adverse reactions was dose dependent. From the dose-response curve for the loss in body mass, it was noted that mice treated with 62.5 mg/kg bwt. of the test compounds lost a least 10 % of their initial body mass (Figure 4-4). This dose seemed to be poorly tolerated since the treated mice displayed many adverse reactions. Mice treated with 12.5 mg/kg of the test compound showed very few adverse reactions while doses of 62.5 mg/kg were poorly tolerated.

To eliminate the risk of drug-induced mortality during the *in vivo* antimalarial study a repeated oral dose of 25 mg/kg of bwt. was considered as safe. This dose was rather conservative and it represented a compromise between the amount of test material available and a maximum tolerated dose.

4.2.2 Determination of the *in vivo* antimalarial activity of curcumin derivatives

The *in vivo* antimalarial activities of the derivatives, **2.2.1.a**, **2.2.2a**, **2.5.4**, **2.8.1** and **2.10.3,** were investigated in C57\BL\6 male mice infected with chloroquine sensitive *Plasmodium berghei*, ANKA strain. The study was approved by the Animal Ethics Committee of the University of Cape Town. Treatment was commenced 24 hours after intraperitoneal infection of mice with 10^7 parasitized red blood cells. A pilot study was performed to compare the *in vivo* efficacy of **2.8.1** when administered orally or subcutaneously. Oral administration of **2.8.1** was found to cause no suppression of parasitemia by day 4 of the study. Subsequently, all the test compounds were administered subcutaneously at a dose 25 mg/kg bwt. every 24 hours for 5 days). A dose response study was performed by treating 3 groups of infected mice with 25, 50 and 100 mg/kg of bwt. of hydrazinocurcumin (**2.2.1a)** respectively. This compound was selected for the dose response study because it was the most abundant and was the easiest to synthesize. The control group did not receive any treatment. Chloroquine diphosphate (10 mg/kg of bwt.) was used as the positive control. The mice were followed for 20 days after which they were sacrificed. The outcomes measured were parasitemia, body mass changes and mortality. Parasitemia was determined by microscopy. Suppression of parasitemia by 20 % on day 4 was considered as a positive indication of *in vivo* antimalarial activity.

4.2.2.1 Effects of the Test compounds on Parasitemia

The scatter plot of log. percentage parasitemia against time showed that parasitemia of the treated mice was lower than that of the controls for the duration of the study (Figure 4-5). The methodology for calculating percentage suppression on Day 4 is presented in Appendix B. All the test compounds suppressed parasitemia on Day 4 by over 50 % with the exception of **2.8.1** (Table 4-3). There was a statistically significant difference in the levels of parasitemia of the test and control mice in animals treated with **2.2.2a, 2.5.4** and **2.10.3**. The ability of the test compounds to suppress parasitemia was inferior to chloroquine (10 mg/kg of bwt) which suppressed parasitemia completely until the 8th day of the study.

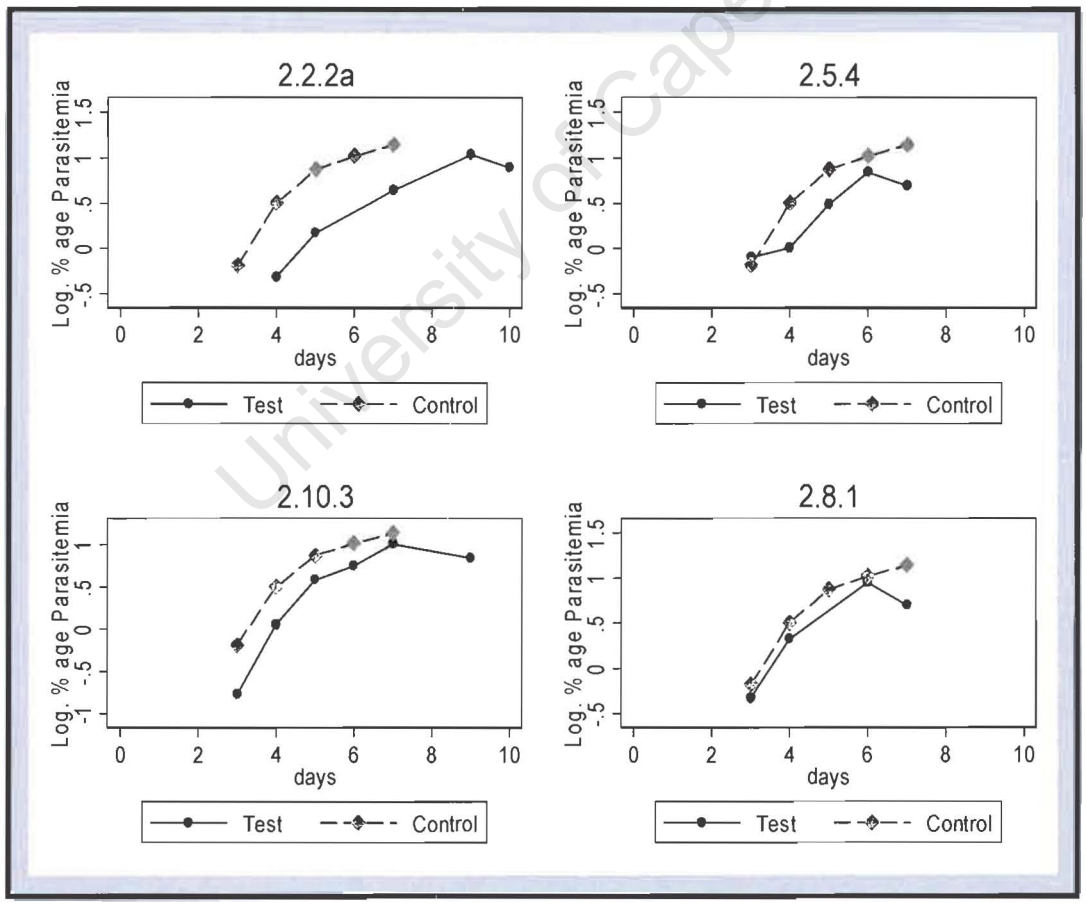

Figure 4 - 5: Mean of Log. Percentage parasitemia against time of *P. berghei* ANKA infected mice.

Table 4 - 3: *In Vivo* Test for Antimalarial Activity - Percentage Suppression of Parasitemia on Day Four

Group	%age suppression	P value[a]
All groups	-	0.003*
2.2.2a vs. control	59.2	0.004*
2.5.4 vs. control	73.0	0.063*
2.8.1 vs. control	20.7	0.144
2.10.3 vs. control	60.8	0.039*
CHLOROQUINE	100	0.000*

*Statistically significant [a]Univariate ANOVA test results for differences in Changes in Log. %age Parasitemia from Days 3 to 5.

4.2.2.2 Effect of Treatment on the Survival of Infected Mice

The percentage mortality and mean survival times of the mice in each group are presented in Table 4-4. The log rank test was used to compare survival of treated groups and the control group. There was no statistically significant difference between survival of animals in the control and treated groups except for the isoxazole derivative (**2.2.2a**) and chloroquine.

Table 4 - 4: *In Vivo* Test for Antimalarial Activity - Group Mortalities by Day 7 and Mean Survival Times

Compound	%age Mortality by day 7	Mean Survival Time (days)[a]	P-value[b]
Control	100	6.4 ± 0.548	-
2.2.2a	0	19	0.002*
2.5.4	80	6 ± 1.225	0.672
2.8.1	60	7 ± 1.000	0.206
2.10.3	80	6.4 ± 1.140	0.869
CHLOROQUINE	0	15	0.002*

*Statistically significant

[a]Data presented as Mean ± S.E. of 5 replicate determinations.

[b]Log Rank test of equality of survivor function. Comparison with the control group

4.2.2.3 Effect of Treatment on the Body Masses of Infected Mice.

A plot of the mean percentage of initial body mass on day one against time showed that there was no difference in changes in the body masses of the treated and untreated groups. The body masses were relatively constant for the first 3 days and then declined sharply thereafter till about day 6 of the study (Figure 4-6). The apparent increase in body mass after day seven observed for mice treated with **2.5.4** and **2.8.1** was an artifact since mean masses represented the masses of 2 or 3 mice that were still surviving. There was no statistically significant difference in the changes in body masses of the derivatives compared to the changes in the mass of the negative control (Table 4-5).

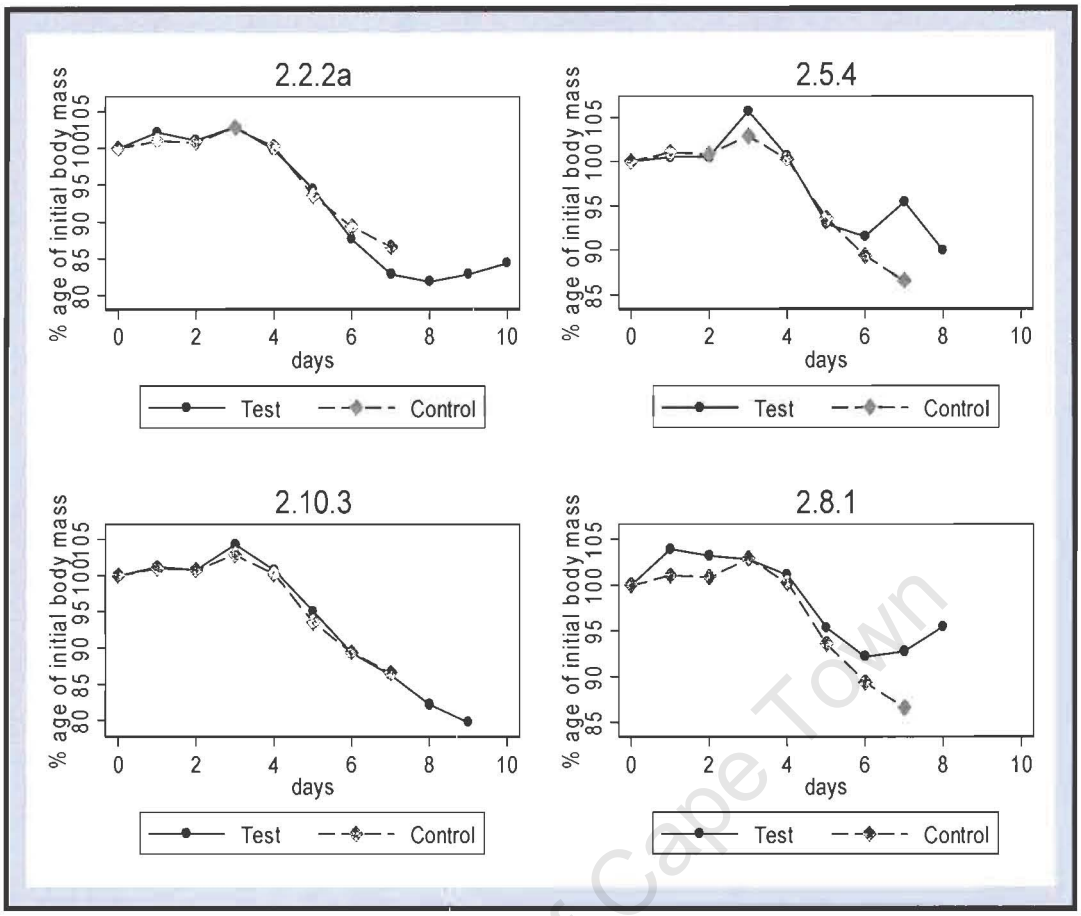

Figure 4 - 6: The mean percentage body masses of *P. berghei* infected mice plotted against time (n=5).

Table 4 - 5: Comparison of Changes in Body Mass between the Treated and Untreated Groups by Univariate ANOVA (n=5)

Groups	P-Value
All groups	0.906
2.2.2a vs. control	0.790
2.5.4 vs. control	0.371
2.6.1 vs. control	0.597
2.8.1 vs. control	0.739
2.10.3 vs. control	0.459

A notable exception in the trend in changes in body mass was the group of mice treated with a single oral dose of chloroquine (Figure 4-7). The mean mass of these mice remained fairly constant at between 97 to 100 % of the initial body mass until day 12 when the mass began to fall. After day 2, there was a significant difference in the changes in body mass of the controls and group treated with chloroquine (P=0.010).

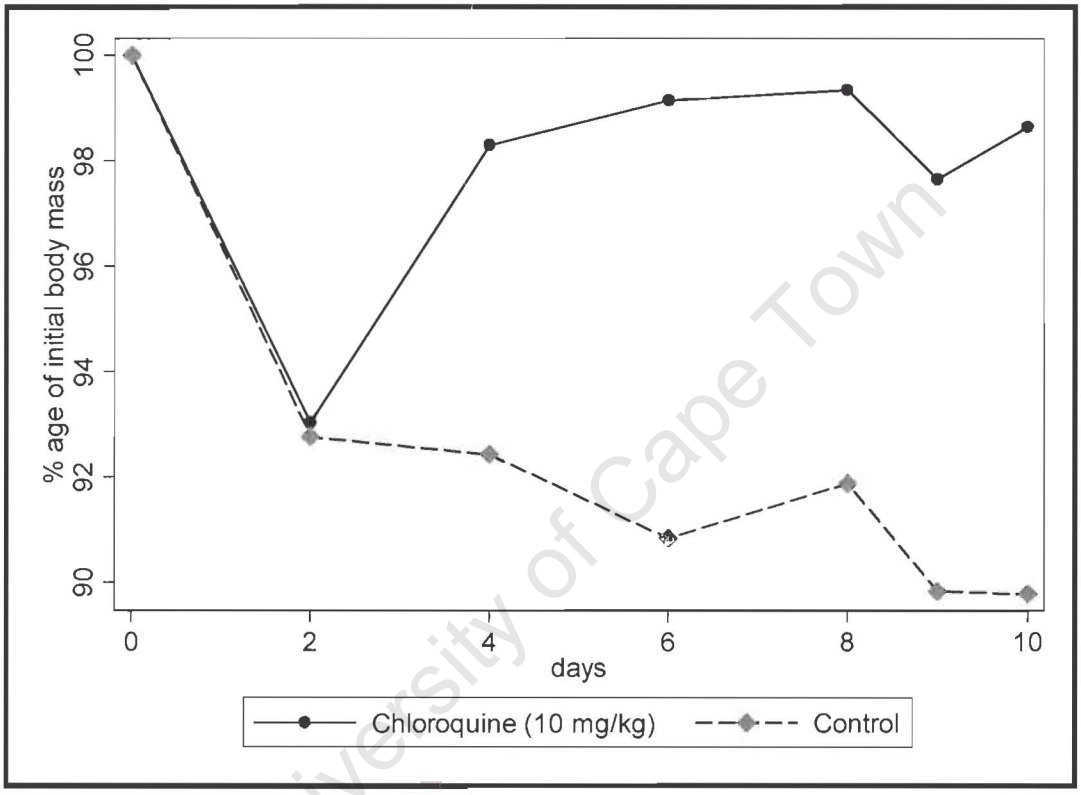

Figure 4 - 7: The percentage body mass of mice infected with *P. berghei* plotted against time. Comparison between chloroquine and the untreated control group (n=3)

A second notable exception in the trend in body mass fluctuations was the group of mice treated with the isoxazole derivative, **2.2.2a**. Like the other test compounds, the body mass declined from day 3 of the study. On the seventh day of the study, it was dramatically clear most mice in the control and other treated groups had died except for mice treated with **2.2.2a**. All the surviving mice were ill and had hypothermia and piloerection.

Readministration of **2.2.2a** (100 mg/kg) 24 hourly for 5 days abolished the clinical signs of rodent infection. The mice looked better although parasitemia was persistently high and the ears and extremities were pale indicating that they were anemic. Interestingly, readministration of **2.2.2a** reversed the decline in mass and the increase persisted for 3 days after administration had stopped (Figure 4-8). The mice fell ill on stopping administration of isoxazole derivative and body mass decline began again on day 17. The mice were sacrificed on Day 19 since they were still infected.

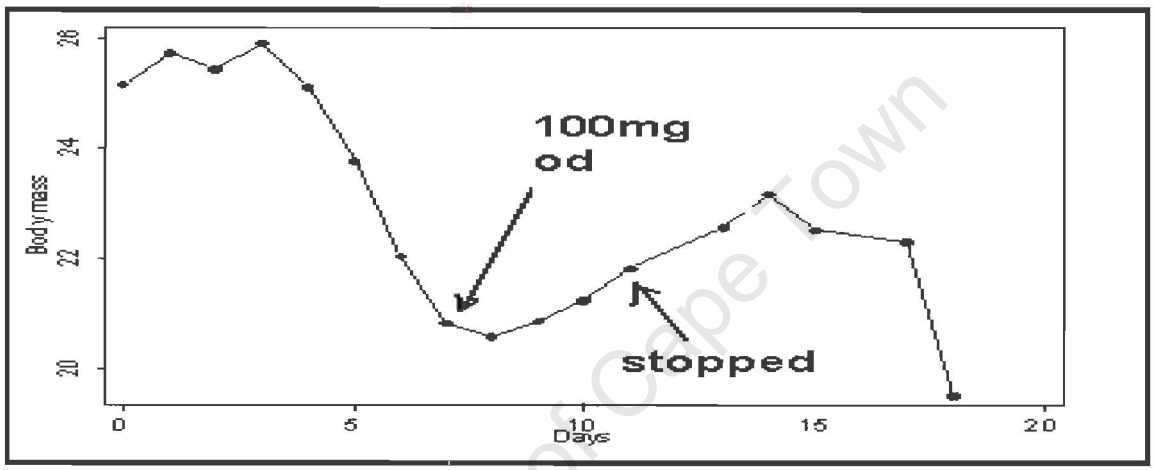

Figure 4 - 8: Scatter plot of mean body mass (g) against time of mice treated with the isoxazole derivative (2.2.2a) (n=5)

The *in vivo* antimalarial effect of **2.2.2a** was rather unusual and merits further investigation. Though **2.2.2a** did not supress parasitemia as effectively as chloroquine but it clearly prolonged survival of infected mice. Curcumin (100 mg/kg bwt. for 5 days) has been noted to prolong the survival of infected mice and in this regard was superior to artesunate and artemether [18]. This effect on animal survival may not be due to a direct antiparasitic effect but may be due to an immunomodulating or anti-inflammatory effect. The immuno-modulating agents such as thalidomide have been shown to improve survival in mice infected with Plasmodium [19, 20]. Immune modulators may have a role in malaria chemotherapy.

4.2.2.4 Dose-Response Study of the Antimalarial Activity of Hydrazinocurcumin

The study found no clear dose-effect relationship on the level of parasitemia following the administration of 25, 50 and 100 mg/kg of bwt. of hydrazinocurcumin to infected mice. The percentage suppression of parasitemia on day 4 was 26, 21 and -3 % respectively (Appendix B). There was no statistically significant difference in the levels of parasitemia between the test and control groups. However, mice that received 100 mg/kg of hydrazinocurcumin had a higher survival time of 10 days compared to the other groups. The mean survival times of mice treated with 25 and 50 mg/kg was 7.6 ± 0.163 and 6 ± 0.213 days respectively.

4.2.3 Over*all* synthesis of the Cytotoxicity and *in vitro* and *in vivo* antimalarial activities of synthetic derivatives of curcumin

A summary of the cytotoxicity and in vitro and in vivo antimalarial activities of synthetic derivatives of curcumin is presented in Table 4-6. There was a clear lack of correlation between *in vitro* and *in vivo* activity . Though **2.2.1a** had almost the highest *in vitro* antiplasmodial acitivity, it had no antiparasitic effects *in vivo*. Though **2.2.2a** and **2.5.4** had about ten-fold less *in vitro* antiplasmodial activity compared to **2.2.1a** they had a higher antiparasitic effect *in vivo*. Lack of correlation between *in vitro* and *in vivo* antiplasmodial activity has b previously been demonstrated [21].

There was also lack of correlation between *in vivo* antiparasitic activity and the survival of infected mice. Though **2.5.4** and **2.10.3** caused a significant reduction of parasitemia, they did not improve survival of infected mice. This

Table 4 - 6: The cytotoxicity, *in vitro* and *in vivo* antimalarial activities of synthetic derivatives of curcumin

	***In vitro* activity IC_{50} (µg/ml)**		**Cytotoxicity CC_{50} (µg/ml)**	***In vivo* antimalarial activity**	
	D10	**K1**	**CHO**	**%age suppression**	**%age survival**
CQ	5.521[d]	182.523[d]	ND	100	100 %
Curcumin	1.674	1.657	> 100	…	…
2.2.1a	0.183	1.832	2.151	-3%	100 %
2.2.1c	1.084	5.790	…	…	
2.2.2a	1.573	3.173 0.	…	59.2*	100 %
2.2.2b	2.180	3.018	…	…	…
2.2.2c	1.866	3.921	11.339	…	…
2.3.1	1.920	11.995	3.725		
2.3.2	2.203	8.227	9.716		
2.3.3	1.031	7.086	4.253		
2.3.4	4.286	9.864	3.164		
2.3.5	3.499	9.296	ND		
2.5.1	2.353	…	69.032		
2.5.2b	3.159	2.763	71.528		
2.5.3	2.448	3.094	80.309		
2.5.4	2.307	16.368	59.745	73.0*	20 %
2.7.1a	0.968	28.080	ND		
2.7.1b	2.779	4.244	>100		
2.8.1	0.412	1.671	>100	20.7	40 %
2.9.1	0.382	ND	84.900		
2.9.2	2.206	3.075	33.510		
2.9.4	ND	5.253	3.719		
2.9.5	0.610	1.307	>100		
2.10.1	1.467	8.704	1.467		
2.10.3	0.290	1.896	10.129	60.8 %*	20%
2.10.5	1.512	2.963	32.186		
2.10.6	0.437	7.476	26.478		

4.3 Conclusion

The toxicological study investigated a narrow range of potential adverse reactions on a small sample size. Nonetheless the propensity of the selected derivatives to cause adverse reactions was demonstrated. A more rigorous toxicological investigation is required. More toxicological studies should be done in other species since the toxic effects observed in one species are not always observed in a different species [5]. The pilot toxicological study provided information for the design and selection of dose levels for future acute and chronic toxicological investigations. The derivatives except **2.10.3** may have a low intrinsic toxicity since single oral doses of 156 or 416 mg/kg did not cause severe adverse reactions. From the pilot study, the optimal dose for the *in vivo* antimalarial study was determined to be 25 mg/kg of body weight.

The test compounds, **2.2.2a**, **2.5.4** and **2.10.3,** suppressed parasitemia significantly. However, their *in vivo* antimalarial activity was inferior compared to that of chloroquine which suppressed parasitemia completely for 7 days. The inferior activity of the test compounds may have been due to short half-lives and a poor intrinsic activity against *P. berghei*. The isoxazole derivative (**2.2.2a**) of curcumin had the most interesting effect on mice infected with *P. berghei*. It improved survival of infected mice. Its beneficial effects may not be due to a direct antiparasiticidal effect but may have been due to immunomodulation.

Typically, body mass is not monitored during *in vivo* antimalarial studies. This study demonstrated that it is a useful outcome to follow since a compound with high efficacy like chloroquine delayed loss in body mass of infected mice. It is an easier outcome to measure compared to parasitemia. Survival was a useful indicator for picking up compounds that may act through mechanisms unrelated to a direct parasiticidal effect.

The lack of correlation between *in vitro* and *in vivo* antiplasmodial activity and survival of infected mice demonstrated the importance of *in vivo* tests.

4.4 Materials and Methods

4.4.1 Materials

4.4.1.1 Chemicals and Reagents

The test compounds were synthesized in the Department of Chemistry of University of Cape Town. Their purity and identify were determined using chromatographic and spectroscopic methods as earlier described. Phosphate buffered saline tablets were obtained from Sigma-Aldrich. Tween 80 and ethanol were obtained from Merck, Darmstadt, Germany. Soya bean lecithine was obtained from BDH, Poole, England. Chloroquine diphosphate salt was obtained form Sigma (St. Louis, MO, USA). Giemsa solution was obtained from Merck and Co., Inc. (Whitehouse Station, New Jersey, USA). Soya bean lecithine was obtained from BDH, Poole, England. PBS buffer solution was prepared by dissolving 5 tablets in 1 liter of Millipore water.

4.4.1.2 Animals and Parasites

Specific pathogen free C57/BL/6 male mice of age 6 to 11 weeks and weighing 25 ± 5g were obtained from the Animal Unit, University of Cape Town. They were fed on a diet of mice pellets and tap water *ad libitum*. The animal house was maintained at a temperature of about 22°C and a relative humidity of 50 – 70 %. A top loading balance model TS120 from Ohaus was used to weigh the mice. The parasite strain used was chloroquine sensitive *Plasmodium berghei*, ANKA strain.

4.4.2 Preparation of Solutions of the Test Compounds for the Toxicological Study

Solutions of the test compounds administered to the animals were designated low, medium and high dose solutions. For all the compounds, the high dose solution was prepared by dissolving 39.0625 mg of the test compound in Tween 80 (200 µl), ethanol (300 µl) and Millipore water (500 µl) in that order. Dissolution was aided by sonication.

The medium dose solutions of **2.2.2a** and **2.10.3** (9.765 mg/ml) were prepared by dissolving 39.0625 mg of the test compound in ethanol (1 ml) followed by Tween 80 (100 µl and Millipore water (3 ml) in that order. To prepare, the lowest dose solution (1.9513 mg/ml), 1 ml of medium dose solution was diluted with 4 ml of 25 % v/v ethanol in water to obtain a solution of concentration. The medium and low dose solutions of **2.8.1** were prepared similarly except that 78.125 mg of **2.8.1** were weighed instead 39.063 mg. The solutions were stored at 4°C for a maximum of 5 days.

4.4.3 Preparation of solutions of test compounds for the *in vivo* antimalarial study

Chloroquine diphosphate (1 mg) was dissolved in 1ml Millipore water to obtain a concentration of 1 mg/ml. The test drugs, **2.2.1a**, **2.2.2b**, **2.5.4**, **2.8.1** and **2.10.3,** were first dissolved in 1 ml of ethanol and sonicated for 30 minutes. Five hundred microliters of Tween 80 was added to the ethanol solution and followed by 3.5 ml of PBS to obtain a final volume of 5 ml. The solutions were stored at 4°C for a maximum of 5 days.

4.4.4The Toxicological Study

The mice were divided into 4 groups of three. The mice in the high dose groups received a 200 µl of the high dose solution orally for one day (312.5 mg/kg of bwt.). The mice in the medium and low dose groups received 200 µl of the respective test solutions orally once daily for 5 days. The doses administered are presented in Table 4-7.

Table 4 - 7: Doses administered the mice in the pilot toxicological study

	Group 1	Group 2	Group 3
	Daily oral dose[a] (mg/kg of bwt.)	Daily oral dose[a] (mg/kg of bwt.)	Single oral dose (mg/kg of bwt.)
Curcumin	-	-	200
2.2.2a	12.5	62.5	156
2.8.1	12.5	62.5	...
2.10.3	25	125	416

The body masses were recorded daily and the mice were observed daily for 15 days for subjective changes in animal behavior. All mortalities were noted.

4.4.5 Determination of *in Vivo* Antimalarial Activity

A cryotube of infected erythrocytes was thawed at room temperature. The contents were diluted with an equal volume of PBS. Two hundred microliters of the thawed erythrocytes were used to infect a mouse intraperitoneally. About 5 days later when the parasitemia of the infected mouse was about 30 % it was bled by nicking the tail vein slightly. Four to five drops of blood were added to an eppendroff tube containing 1 ml of PBS solution. Five hundred microliters were used to infect a second mouse. After five days, the parasitemia of the infected mouse was determined by microscopy. The total number of red blood cells suspended in the PBS was determined by counting

in a haemocytometer. The volume required to infect a mouse with one million infected red blood cells was calculated. Each experimental mouse was infected with one million parasites by intraperitoneal injection.

The mice were divided into groups of 5 each of the same sex. Treatment was commenced 24 hours after infection. The treated group received 200 µl (100 mg/kg of bwt.) of the test drug subcutaneously every 24 hours for 5 days. The control group received the test compound only. The mice were followed up for a minimum of nine days. The parasitemia of each mouse was determined on the 3rd and 4th day of infection and subsequently on alternate days. Blood samples for microscopic examination were obtained from the tail vein. The thin blood smears were fixed with methanol and stained with Giemsa stain. The mice were weighed on alternate days and all deaths were noted.

4.4.6 Data Analysis

Data was analysed using Stata® version SE 8. Body masses obtained in the toxicological and *in vivo* antimalarial studies were expressed as a percentage of initial body mass on day 1 when the test compound was administered. Scatter plots were used to examine the daily changes in body mass. For each group the mean daily body mass was calculated. Univariate ANOVA was used to compare the changes in body mass of the animals that received the test compounds with the changes in the control group. The percentage suppression of parasite growth on day 4 of the study was calculated using the formula: 100 [1 – (mean parasitemia of test group/mean parasitemia of control group)].

For the in vivo antimalarial study, scatter plots were used to examine the daily changes in log. of parasitemia. Univariate analysis of variance was used to test if there was a difference between the log. of parasitemia of the test and control groups. The analysis was restricted to days 3 to 5 of the study. Similarly ANOVA was used to test for differences in changes in the body mass up to day 7 of the study. The mean and standard error of the survival

time of the animals in each group was calculated. The Log rank test was used to test for differences in the survival of the animals in the test groups and the untreated group. P-values of less than 0.05 were considered statistically significant.

References

(1) Unger, E. *J. Am. Coll. Cardiol.* **2007**, *50*, 738-740.

(2) Sultana, S.; Roblin, D.; O'Connell, D. *Drug Discov. Today* **2007**, *12*, 419-425.

(3) DiBernardo, A.; Cudkowicz, M. *Biochim. Biophys. Acta – Mol. Basis Dis.* **2006**, *1762*, 1139-1149.

(4) Spedding, M.; Jay, T.; Costa e Silva J.; Perret, L. *Nat Rev Drug Discov.* **2005**, *4*, 467-478.

(5) Baldrick, P. *Drug Discov. Today* **2003**, *8*, 127-133.

(6) British Toxicology Society *Hum. Toxicol.* **1984**, *3*, 85-92.

(7) van den Heuvel,M J.; Dayan, A. D.; Shillaker, R. O. *Hum. Toxicol.* **1987**, *6*, 279-291.

(8) de Ferreira-da-Cruz, M.; Adami, Y. L.; da Espinola-Mendes, E.; Figueiredo, M. R.; Daniel-Ribeiro, C. T. *Exp. Parasitol.* **2000**, *94*, 243-247.

(9) Peters, W.; Robinson, B. L.; Ellis, D. S. *Ann. Trop. Med. Parasitol.* **1987**, *81*, 639-646.

(10) Fidock, D. A.; Rosenthal, P. I.; Croft, S. L.; Brun, R.; Nwaka, S. *Nat. Rev. Drug Discov.* **2004**, *3*, 509-520.

(11) Kalra, B. S.; Chawla, S.; Gupta, P.; Valecha, N. *Indian J. Pharmacol.* **2006**, *38*, 5-12.

(12) Liu, A.; Lou, H.; Zhao, L.; Fan, P. *J. Pharm. Biomed. Anal.* **2006**, *40*, 720-727.

(13) Cole, L. M.; Nicholson, R. A.; Casida, J. E. *Pestic. Biochem. Physiol.* **1993**, *46*, 47-54.

(14) Lao, C. D.; Ruffin, M. T.,; Normolle, D.; Heath, D. D.; Murray, S. I.; Bailey, J. M.; Boggs, M. E.; Crowell, J.; Rock, C. L.; Brenner, D. E. *BMC Complement. Altern. Med.* **2006**, *6*, 10-10.

(15) Chainani-Wu, N. *J. Altern. Complement. Med.* **2003**, *9*, 161-168.

(16) Moridani, M.; Siraki, A.; O'Brien, P. *Chem. Biol. Interact.* **2003**, *145*, 213-223.

(17) Galati, G.; O'Brien, P. *Free Radical Biol. Med.* **2004**, *37*, 287-303.

(18) Reddy, R. C.; Vatsala, P. G.; Keshamouni, V. G.; Padmanaban, G.; Rangarajan, P. N. *Biochem. Biophys. Res. Commun.* **2005**, *326*, 472-474.

(19) Omer, F. M.; de Souza J.B.; Riley, E. M. *J. Immunol.* **2003**, *171*, 5430-5436.

(20) Muniz-Junqueira, M.; Silva, F.; Paula-Júnior, M.; Tosta, C. *Acta Tropica* **2005**, *94*, 128-138.

(21) Houghton, P. J.; Howes, M.-J.; Lee, C. C.; Steventon, G. J. Ethnopharmacol. **2007**, *110*, 391-400.

CHAPTER FIVE
PHARMACOKINETIC PROPERTIES OF HYDRAZINOCURCUMIN IN MICE

5.1 Introduction

5.1.1 Rationale for Pre-Clinical Pharmacokinetic Studies

While a lead compound may be highly selective and highly potent, it may lack the desired pharmacokinetic properties for use in humans. An ideal antimalarial agent should have good oral bioavailability that permits oral dosing, a long half life that allows for once daily dosing and a minimal potential for drug-drug interactions [1]. The pharmacokinetic evaluation of potential antimalarial agents is a critical consideration in the drug development process. Preclinical pharmacokinetic studies include both *in vitro* and *in vivo* studies. The key advantage of *in vitro* pharmacokinetic studies over *in vivo* pharmacokinetic studies in rodents is that they are performed in human cell lines and the findings can be extrapolated to humans using appropriate software. Secondly, many compounds can be screened rapidly. However, some authors feel that over reliance on *in vitro* tests should be avoided since *in vitro* methods may actually slow down the drug development process. Results obtained from *in vitro* studies may be artfactual since they are performed at physiological conditions that do not reflect reality [2] .*In vivo* tests in rodents are more reliable in early identification of compounds with poor pharmacokinetic properties. Some authors feel that *in vivo* pharmacokinetic tests in rodents should precede *in vitro* tests [2]. The main objective of a PK study in animals is to determine PK parameters such as maximum plasma concentration (C_{max}) and area under the curve of the plasma concentration versus time plot (AUC). These parameters can change depending on the route of administration and type of formulation used [3].

Mice are not frequently used in pharmacokinetic studies because they have a small blood volume which limits the volume of blood samples that can be taken. Mice however are easy to breed, occupy a low cage space and are easier to handle. The challenges associated with the use of mice in pharmacokinetic studies are overcome by using LC-MS/MS for the analysis of drug levels in blood or plasma.

5.1.2 Pharmacokinetic Properties of Curcumin

Curcumin has a poor oral bioavailability in rodents, humans and dogs due to pre-systemic metabolism in the gut [4, 5]. In addition, its poor water solubility leads to most of the administered dose being excreted unchanged. Studies in rats showed that 40-89 % of the orally administered dose is excreted unchanged in feces in 72 hours [6-11]. The rate of fecal excretion is highest in the first 48 hours of drug administration [6].

In the human and rat guts, curcumin is metabolized to curcumin glucuronide, curcumin sulfate, tetrahydrocurcumin, and hexahydrocurcumin. Gut metabolism is more extensive in humans compared to rodents [4]. More recently curcumin bisglucuronide and O-demethylated metabolites have been identified [12]. Mouse and human liver microsomal enzymes metabolize curcumin in a similar fashion [12].

In rodents and humans, negligible amounts of curcumin are found in plasma, liver, kidney and fat after oral administration [6, 7] due to its poor absorption, rapid metabolism and rapid biliary excretion. However, when high oral doses of above 2g/kg of body weight are administered, considerable amounts of curcumin can be detected in body tissues after 12 days [8]. Curcumin is mainly excreted through the bile and the major biliary metabolites are the glucuronides of tetrahydrocurcumin and hexahydrocurcumin. The minor metabolites include dihydroferulic acid and ferulic acid [9]. Urinary excretion is negligible at 1-6%.

Curcumin has a short half life since it is rapidly metabolized. When added to suspensions of liver microsomal enzymes curcumin is rapidly metabolized within 30 minutes [9]. The main route of metabolism is reduction of carbonyl groups and the two C=C bonds on the heptadiene chain and glucuronidation and sulphation of the phenolic hydroxyl groups [4]. The key metabolic sites of curcumin are presented in Figure 5-1. In rodents and humans curcumin undergoes successive reduction to dihydrocurcumin, tetrahydrocurcumin, hexahydrocurcumin and hexahydrocurcuminol (Figure 5-2). The reductive products subsequently undergo glucuronidation and sulphation phase II reactions.

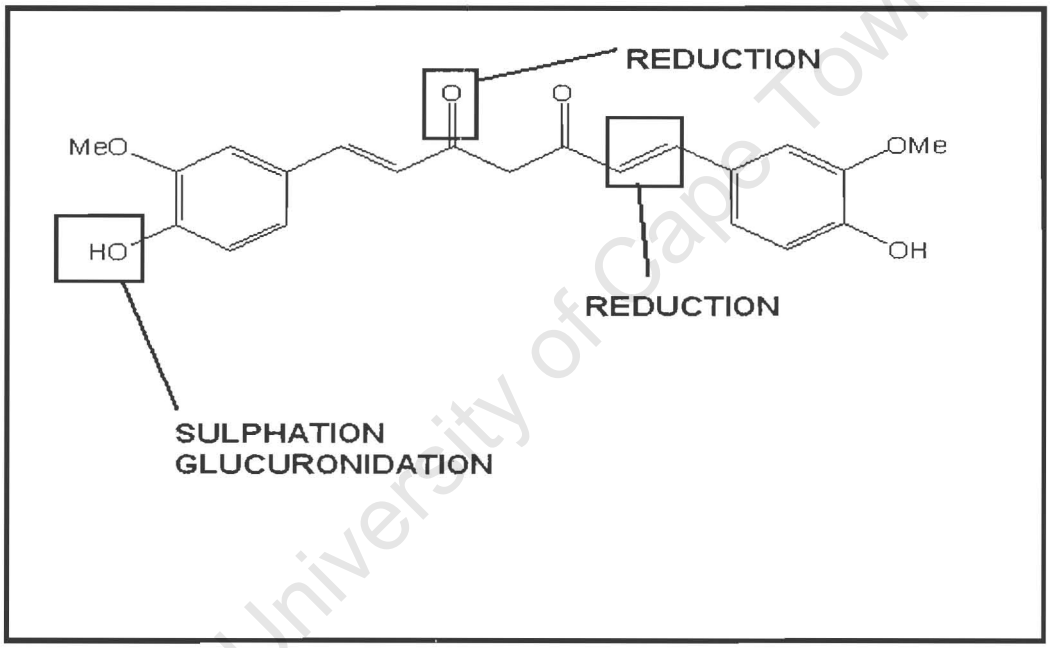

Figure 5 - 1: The key sites of metabolism of curcumin

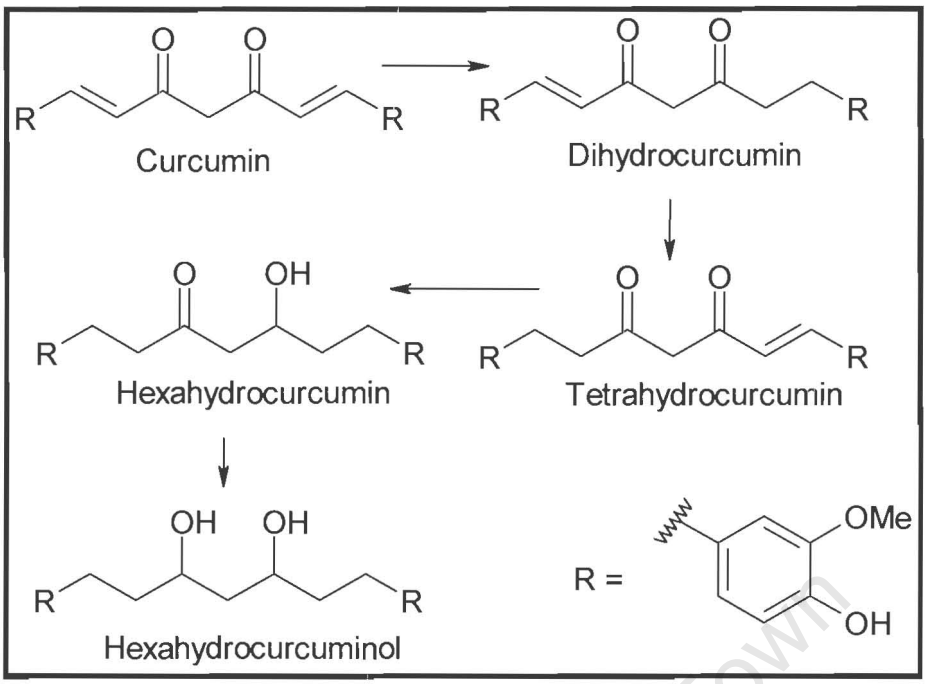

Figure 5 - 2: Key metabolic products of curcumin in rodents and humans

5.1.3 Rationale for the Study of the Pharmacokinetic Properties of Hydrazinocurcumin (2.2.1b)

Out of the number of derivatives synthesized in this work, hydrazinocurcumin was selected for pharmacokinetic investigation (**2.2.1b**, Figure 5-3) because of its high *in vitro* antiplasmodial activity against the chloroquine sensitive strain. Secondly, it was easy to synthesize and gave high yields on synthesis.

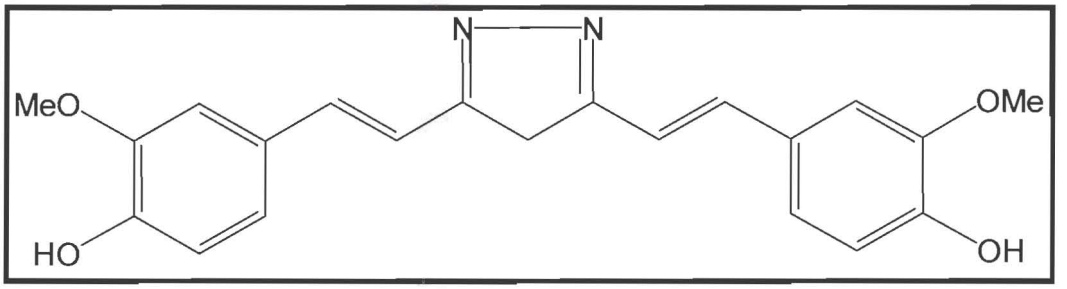

Figure 5 - 3: The structure of hydrazinocurcumin (2.2.1b).

An *in vitro* absorption study showed that hydrazinocurcumin is well absorbed across the isolated rat intestine [13]. No *in vivo* study has been reported on the pharmacokinetic properties of hydrazinocurcumin. It was hoped that hydrazinocurcumin would have a better *in vivo* pharmacokinetic profile compared to the parent compound because the presence of two nitrogen groups on the molecule would increase the water solubility and therefore overcome the problem of low oral bioavailability. Replacement of dicarbonyl groups of curcumin with a pyrazole group was expected to reduce the rate of metabolism by increasing the rigidity of the heptadiene-dione chain which would reduce binding to metabolizing enzymes. Hydrazinocurcumin met all the minimal structural requirements for good oral bioavailability as outlined by Lipinski [14] . Hydrazinocurcumin was expected to have a better water solubility than curcumin since it has a higher octanol-water partition coefficient (cLogP) of 3.989 compared to 2.251 of curcumin. The study focused on the oral route of administration because ideal antimalarial agents should have a good oral bioavailability as well as a long half life.

5.1.4 Aims and Objectives of the Pharmacokinetic Study

The main aim of the pharmacokinetic study was to determine the pharmacokinetic properties of orally administered hydrazinocurcumin in mice.
The specific objectives were:

1. development of an LC-MS/MS method for the assay of hydrazinocurcumin in murine blood. This involved determination of the optimal HPLC and mass spectrometry conditions and a method of extraction of drug from plasma/blood.
2. validation of the analytical procedure.
3. comparison of the bioavailability of orally administered hydrazinocurcumin from 3 different vehicles.
4. determination of the following pharmacokinetic parameters in mice: maximum plasma concentration (C_{max}): area under the curve of the plasma concentration versus time plot (AUC); time taken to reach maximum plasma

concentration (Tmax); half-life in plasma ($t_{1/2}$); and elimination rate constant (K_{el}).

5.2 Results and Discusion

5.2.1 Method Development

5.2.1.1 Instrumentation

The experimental protocol was reviewed and approved by the Animal Ethics Committee of the University of Cape Town. Method development entailed optimization of LC-MS/MS conditions and determination of the optimal extraction method by trial and error. Tandem LC-MS/MS analysis was performed using an Agilent 1200 Series HPLC system (Agilent Technologies, Japan) coupled to a tandem quadruple mass spectrometer (Sciex 3200Q Trap system, Phenomenex, USA). Separation of hydrazinocurcumin was achieved using a Phenomemex Gemini C18 HPLC analytic column (50 X 2.0 mm, 5 µm particle size) maintained at ambient temperatures. The mobile phase consisted of 0.1 % formic acid: acetonitrile (1:1 v/v) at an isocratic flow rate of 0.3ml/minute with a run time of 2 minutes. The injection volume was 10 µl. The retention time was 1.11 minutes. The mobile phase was degassed ultrasonically before use. Detection was done using an MS/MS mass spectrometer. The transition monitored was the fragmentation of the molecular ion to the most abundant product ion (*m/z* 365.2 to *m/z* 349.2) (Figure 5-4). Detection was done in the multireaction monitoring mode (MRM) with a dwell time of 150 msec. Electron spray ionization (ESI) was done in the positive ion mode at a collision energy of 33eV. Voltage of the ion spray needle was 5.5 kV. Nitrogen was used as the auxiliary and nebulizer gas at a flow rate of 60 arbitrary units. The temperature of the source heater was set at 400°C. The flow rate of the curtain gas was 20 arbitrary units. The auto sampler injection needle was cleaned between samples by rinsing for 10 seconds with mobile phase. All mass spectrometric data was processed using Analyst™ software version 1.1.1.

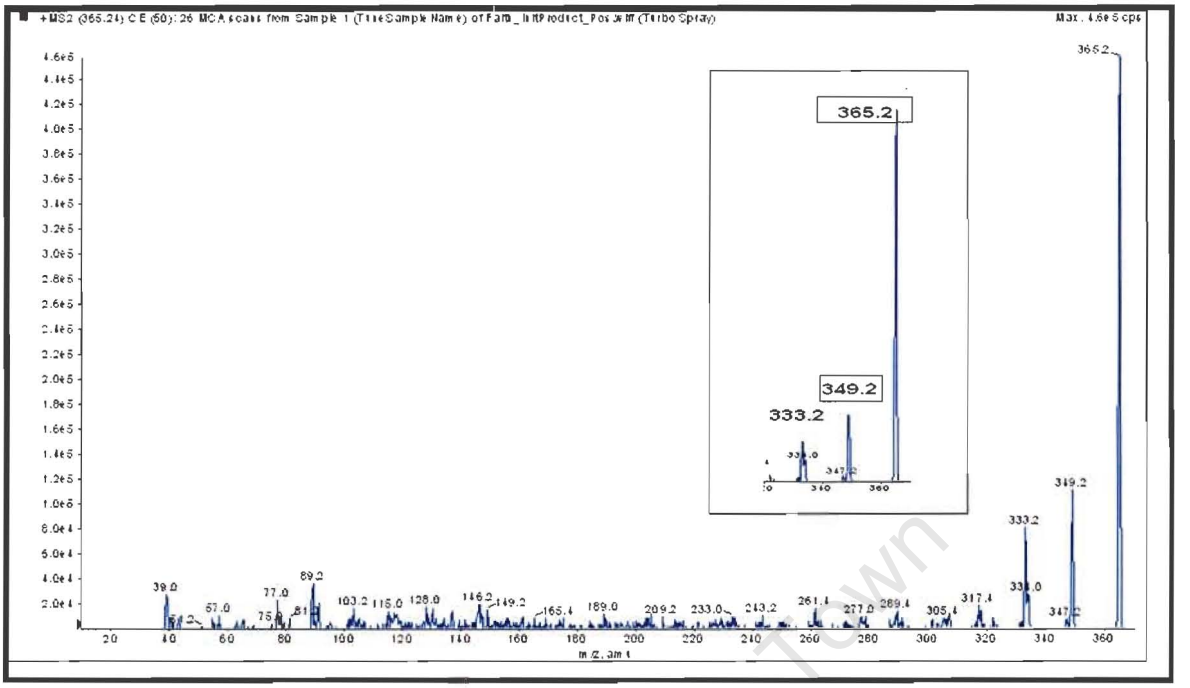

Figure 5 - 4: The mass spectrum of hydrazinocurcumin (2.2.1b).

5.5.1.2 Method of Extraction of Hydrazinocurcumin from Blood/Plasma

Two methods for extracting hydrazinocurcumin from blood were compared: filter paper method as described by Dzinjalamala *et al.* [15] and liquid–liquid extraction. The filter paper method was laborious and had low precision. Liquid-liquid extraction of hydrazinocurcumin from whole blood was the least laborious method and gave a high recovery of 75 %. Extraction was performed by suspending 10 µl of the blood in Britton Robinson universal buffer [16] at pH 10 (50 µl), addition of 250 µl of ethyl acetate, vortexing for 1 min followed by centrifugation. The upper organic layer (215 µl) was removed and evaporated to dryness. The dried extract was stored at -20°C and dissolved in the 100 µl of the mobile phase before analysis.

To determine the optimal pH in which the blood sample was suspended, extraction was performed on spiked blood (10 µg/ml) suspended in a series of Britton Robinson buffers ranging from pH 2-12. Recovery of hydrazinocurcumin was highest when the blood sample was suspended in buffer at pH 10 (Figure 5-5). In basic pH conditions hydrazinocurcumin was

predominantly in the non-ionized form thus favoring dissolution in the organic layer.

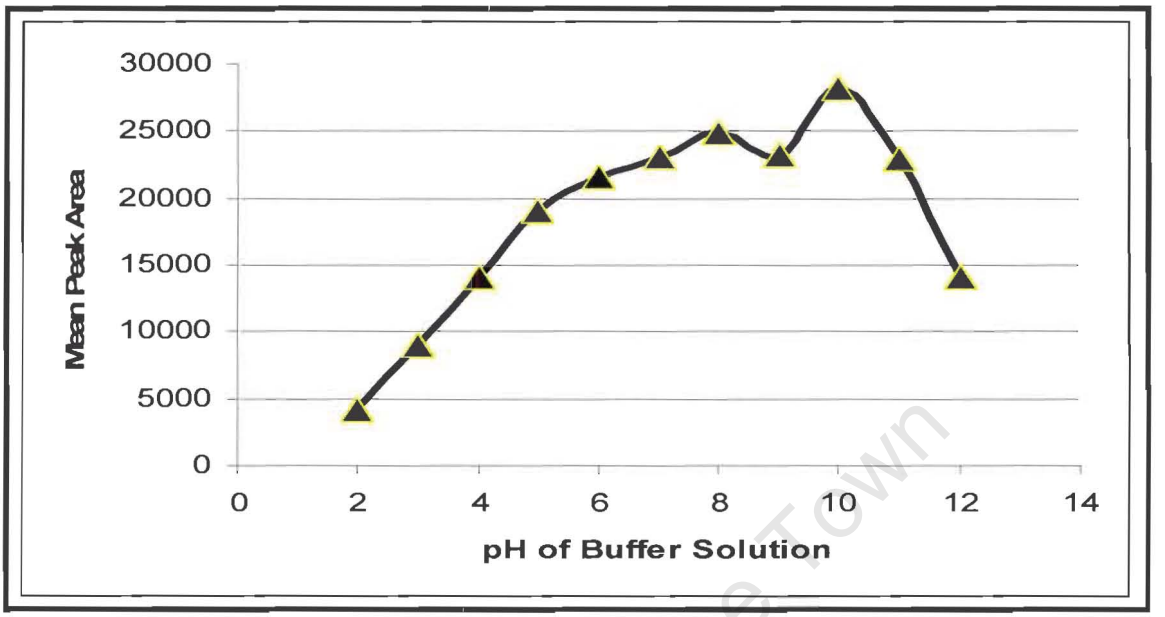

Figure 5 - 5: Determination of the optimal pH for extraction of hydrazinocurcumin from blood. Peak areas at various pH values.

To determine whether extraction from plasma gave a higher recovery compared to extraction from whole blood, a spiked blood sample (10 µg/ml) was centrifuged and separated into plasma and red blood cells. The concentration of hydrazinocurcumin in red blood cell layer was 30.8 times the concentration in plasma. This showed that hydrazinocurcmin may selectively bind to RBCs as opposed to plasma components such as albumin. The accumulation of hydrazinocurcumin in RBC layer did away with the need to centrifuge blood samples to obtain plasma for extraction.

5.2.1.3 The Calibration Curves

The calibration curve, which was used to calculate the concentration of hydrazinocurcumin, was prepared by spiking human blood with hydrazinocurcumin to obtain the following concentrations: 10 µg/ml; 5 µg/ml; 2.5 µg/ml; 1.25 µg/ml; 0.625 µg/ml; 0.313 µg/ml; 0.156; and 0.0781 µg/ml.

The spiked blood samples were extracted as previously described and analyzed by LC-MS/MS. The peak areas were plotted against concentration. Weighted quadratic regression with a weighting of 1/X gave a better fit of the calibration curve compared to linear regression. X represented the nominal concentration of the spiked blood samples.

Since the calibration standards were prepared using human blood as the diluent as opposed to murine blood, it was necessary to compare the calibration curves obtained from the extraction of hydrazinocurcumin from human and murine blood. The two calibration curves were perfectly super imposable with a correlation coefficient of one. Two way paired student t-test showed there was no statistically significant difference in the peaks areas of the two calibration curves (P=0.07).

The calibration curves obtained from spiked human blood and spiked plasma were compared (Figure 5-6). Although the peak areas of the two calibration graphs were highly correlated with a correlation coefficient of 0.974, the peaks areas of the spiked blood samples were 2 to 3 times the peak areas of the spiked plasma samples. Paired one-way student t-test showed the difference in peak areas was statistically significant (P=0.022). This observation validated the extraction of hydrazinocurcumin from human blood as opposed to plasma.

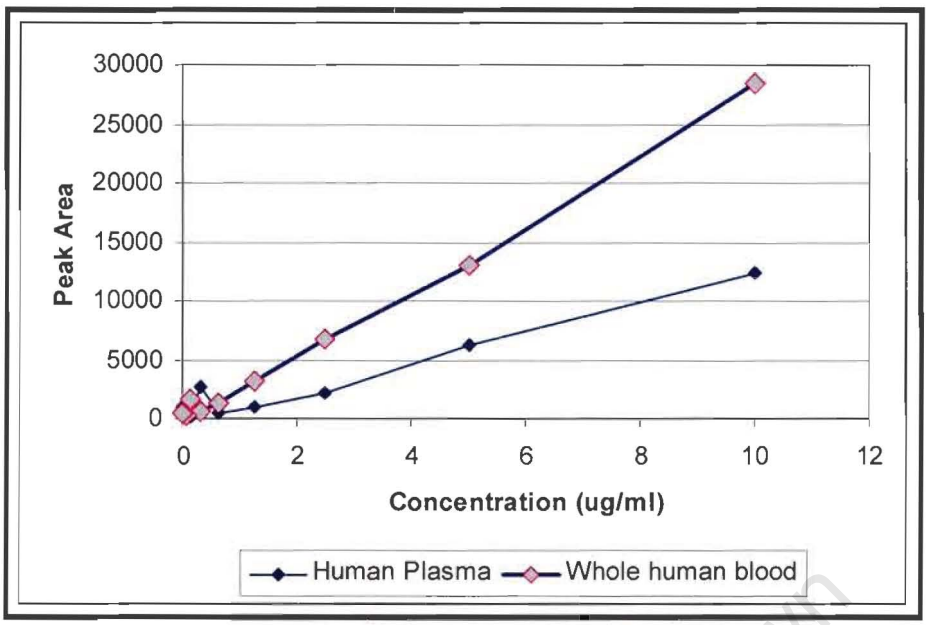

Figure 5 - 6: Comparison of the calibration graphs obtained from whole blood and plasma.

5.2.2 Validation of the LC-MS/MS Method for the analysis of hydrazinocurcumin in blood

Method validation was performed according to the FDA guidelines on validation of bioanalytic methods [17, 18]. However, the sample stability and selectivity was not determined as these are not required for pre-clinical studies. Intra-day accuracy and precision were determined by calculating the relative error (RE) and relative standard deviation (RSD) of 4 replicates of the quality control samples (QC) of concentrations from 10 to 0.156 µg/ml assayed on the same day. Inter-day accuracy and precision were determined by calculating the relative error and coefficient of variation of 4 QC samples assayed on 3 consecutive days. The RE was the percentage deviation of observed concentration (C_{obs}) from the nominal concentration (C_{nom}). The accuracy and precision at the lower limit of quantification (LLOQ) were determined by analyzing 5 replicates of the QC sample one of the validation days. At the lower limit of quantification (LLOQ), a RE of ± 20 % and a CV of 20 % were considered acceptable. For QC samples with a concentration greater than LLOQ, a RE of ± 15 % and a CV of 15 % were considered

acceptable. The limit of detection (LOD) was the lowest concentration at which the signal to noise ratio was 3.

All correlation coefficients of the calibration curves were greater than 0.997. The best fit was obtained by quadratic regression with a weighing factor of 1/X. The LLOQ was determined to be 0.625 µg/ml and the LOD was 0.156 µg/ml. At concentrations above LLOQ, intra- and inter-day accuracy and precision were within accepted limits (Tables 5-1 and 5-2).

Table 5 - 1: The intra-day accuracy and precision of the LC-MS/MS method for the determination of hydrazinocurcumin (2.2.1b) in blood

Nominal concentration (µg/ml)	Observed concentration (µg/ml) (mean ± SD, n=4)	Accuracy (RE %)	Precision (RSD %)
10	10.627 ± 0.917	+ 6.34	9
5	5.49 ± 0.325	+ 9.90	6
2.5	2.513 ± 0.190	+ 0.51	8
1.25	1.363 ± 0.103	+ 9.09	8
0.625	0.692 ± 0.105	+ 10.79	15
0.313	0.452 ± 0.196	+ 45.09	43
0.156	0.755 ± 0.703	+ 387.03	93

Table 5 - 2: The inter-day precision and accuracy of the LC-MS/MS method for the determination of hydrazinocurcumin in blood

	Accuracy (%)	Precision (RSD %)
10	-7	7
5	-8	15
2.5	12	15
1.25	0	11
0.625	+ 5	20
0.313	-5	53
0.156	-20%	219

As expected, intra and inter-day accuracy declined with decreasing concentration of the analyte. The relatively high LLOQ of about 0.625 µl/ml was attributed to the low the sampling volume of 10 µl. The LLOQ could have been improved by increasing the blood sampling volume from 20 to 40 µl which would have still allowed for multiple sampling from a single mouse.

5.2.3 The Pharmacokinetic Properties of Hydrazinocurcumin

Hydrazinocurcumin (100 mg/kg of bwt.) was formulated in 3 different vehicles and administered orally to 3 different groups of mice. The mice had free access to food and water. Vehicle A consisted of 1 % DMSO in 33 % v/v ethanol in water. Vehicle B consisted of 1 % DMSO and 33 % v/v ethanol in buffer at pH 7.4. Vehicle C lacked ethanol as a co-solvent and hydrazinocurcumin was administered in 1 % DMSO in buffer at pH 6. Sampling was done at 5 time points and samples were analyzed by LC-MS/MS. Blood concentrations that were below the lower limit of quantification were noted (Appendix C). Hydrazinocurcumin could not be detected in most of blood samples obtained from animals that received the test compound in vehicle C. Consequently data analysis was restricted to data obtained from

animals that received hydrazinocurcumin in vehicles A and B. Data was analyzed by non-compartmental analysis using WinNonlin software. A scatter plot of the blood concentration – time curve showed that hydrazinocurcumin reached peak plasma concentrations between 0.5 to 1 hour and most of it was cleared from the blood in 5 hours (Figure 5-7).

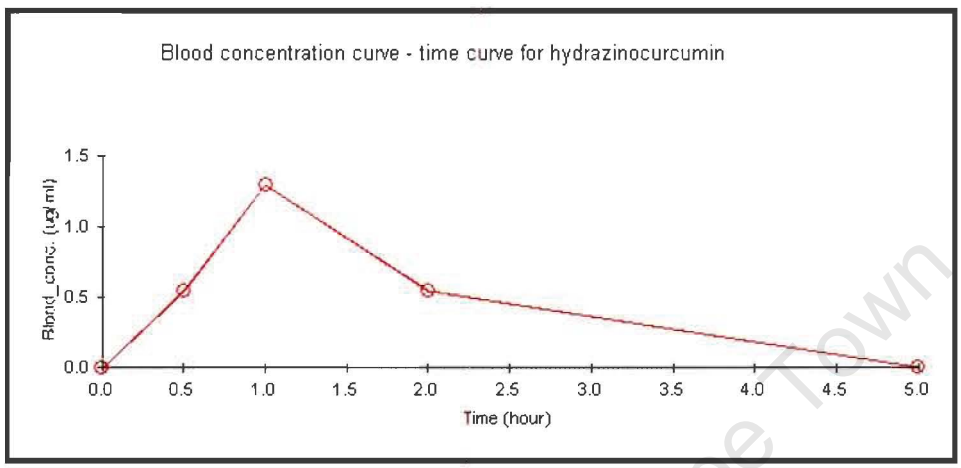

Figure 5 - 7: A typical blood concentration-time curve of hydrazinocurcumin (2.2.1b) in a mouse

Three methods were used to handle values that were below lower limit of quantification (BLOQ) [19, 20]. In the first method all values BLOQ were discarded. This is the most frequently used method for handling values BLOQ but it often results in biased pharmacokinetic parameters [19]. In the second method, all value BLOQ were replaced with a value half of LLOQ. In the third method, all values below the LOD were discarded [20].

The pharmacokinetic parameters calculated using data obtained from mice treated with hydrazinocurcumin in vehicle B were found to be inconsistent as well as varied depending on the method used to handle values BLOQ. (Table 5-3). This was attributed to the fact that a large proportion of the data was BLOQ. The terminal half life and the elimination rate constants could not be calculated.

Table 5 - 3: Pharmacokinetic parameters of hydrazinocurcumin (2.2.1b) in Vehicle B

	First method	Second method	Third method
C_{max} (µg/ml)	0.66 ± 0.438	0.848 ±0.823	0.939 ± 0.341
T_{max} (h)	2	1.3 ± 0.671	1.3 ± 0.3
Terminal Half-life (h)	ND	ND	0.768 ± 0.372
(K_{el}) (h^{-1})	ND	ND	1.601 ±0.537
AUC_{last} $(h*\mu g\ ml^{-1})$	0.33 ± 0.219	0.377 ± 0.450	1.266 ± 0.479
AUC_{all} $(h*\mu g\ ml^{-1})$	1.32 ± 0.875	0.455 ± 0.388	1.937 ± 0.802

Data expressed as mean ± SD, n=5

Due to the inconsistency, pharmacokinetic parameters obtained from hydrazinocurcumin formulated in Vehicle B were not considered reliable. There was more consistency between pharmacokinetic parameters when the 3 different methods were applied to data obtained from mice treated with hydrazinocurcumin in Vehicle A (Table 5-4).

Table 5 - 4: Pharmacokinetic parameters of hydrazinocurcumin (2.2.1b) in Vehicle A

	First method	Second method	Third method
C_{max} (µg/ml)	2.912 ± 1.751	2.91 ± 1.751	2.912 ± 1.751
T_{max} (h)	0.833 ± 0.258	0.833 ± 0.258	0.8333 ± 0.258
Terminal Half-life (h)	0.8333 (n=1)	0.452 ± 0.344	0.377 ± 0.316
(K_{el}) (h^{-1})	2.128 (n=1)	2.220 ± 1.386	2.476 ± 0.717
AUC_{last} $(h*\mu g\ ml^{-1})$	1.414 ± 2.046	2.888 ± 2.315	2.922 ± 0.870
AUC_{all} $(h*\mu g\ ml^{-1})$	2.389 ± 2.193	3.017 ± 2.286	3.076 ± 0.915

Data expressed as mean ± SD, n=5

Since there was greater consistency in the calculated parameters using data obtained from mice treated with hydrazinocurcumin in Vehicle A, greater reliance was placed on this data. The methods used did not influence the parameters C_{max} and T_{max} as opposed to half life, AUC and elimination rate constant. For the purpose of discussion the pharmacokinetic parameters obtained using method 2 in Table 5-4 were used since they represented a compromise between the other two methods. Method three is not popular since parameters obtained using this method has an upward bias.

5.2.3.1 The Half-Life of Hydrazinocurcumin.

The terminal half life of hydrazinocurcumin was short with a mean of 0.452 h. This half-life was less than the reported half-life of curcumin which ranged from 0.74 to 1.96 hrs [21, 22]. The short half may have been due to a high rate of metabolism or rapid excretion. Similar to the parent compound, it is likely that hydrazinocurcumin is metabolized by glucuronidation and sulphation of the phenolic hydroxyl groups and reduction of the double bonds on heptadiene-dione chain. Replacement of hydroxyl groups with halide, alkyl or alkoxy groups may reduce the rate of metabolism of curcumin derivatives. Excessive metabolism may be overcome by incorporating metabolic enzymes inhibitors such as piperine in the molecule. The short half life may explain lack of antimalarial activity observed during *in vivo* antiplasmodial study in *Plasmodium berghei* infected mice.

5.2.3.2 The Bioavailability of Hydrazinocurcumin

The absolute bioavailability of hydrazinocurcumin was not determined since the pharmacokinetic parameters of an intravenously administered dose were not determined. AUC, C_{max} and T_{max} were used as proxy indicators of bioavailability. An *in vitro* study showed that hydrazinocurcumin is well absorbed through a rat intestine [13]. The mean AUC values of hydrazinocurcumin following absorption from vehicle A were almost twice that

when administered in vehicle B. There were large differences in the mean C_{max} and T_{max} values when hydrazinocurcumin was absorbed from vehicle A and B. Absorption from vehicle A was more rapid since T_{max} values ranged from 0.5 to 1 hour while for vehicle B, the T_{max} values ranged from 0.5 to 2 hours.

The C_{max} value of 2.912 µg/ml was above the IC_{50} value of 1.084 µg/ml hydrazinocurcumin against the CQS strain of *Plasmodium falciparum*. This implied that therapeutic concentrations of hydrazinocurcumin were achieved by oral administration of 100 mg/kg in vehicle A. The short half-life of hydrazinocurcumin explained its poor *in vivo* antiplasmodial activity in *Plasmodium berghei* infected mice.

5.2.3.3 Comparison of the Bioavailability of Hydrazinocurcumin from Different Vehicles

The differences in the T_{max} and C_{max} values of hydrazinocurcumin absorption from vehicles A and B were interpreted with caution. The differences may have been due to the differences in amount of food in gut of the animals since they had free access to food and water. A more rigorous comparison of absorption from the vehicles should have been done on fasted animals to eliminate the effect of food on absorption.

In the absence of the effect of food in the gut, any difference in bioavailability profile from the different vehicles may have been due to difference in the pH of the formulations which would have affected the dissolution and diffusion profiles. At a pH of 7.4, hydrazinocurcumin was predominantly in the non-ionized state making it less water soluble but with improved permeability across cellular membranes. In the acidic pH of vehicle C, hydrazinocurcumin was predominately in the ionized state which would have improved its dissolution but retarded diffusion across membranes. This may explain the poor bioavailability associated with vehicle C.

5.2.3.4 Comparison between the Bioavailability of Hydrazinocurcumin and Curcumin

The reported key pharmacokinetic parameters of orally administered curcumin in rats are presented in Table 5-5 [21, 22]. For the sake of comparison an assumption was made that the pharmacokinetic profile of curcumin in mice and rats is similar. The pharmacokinetic parameters of hydrazinocurcumin administered in Vehicle A were included for comparison. An oral dose of hydrazinocurcumin (100mg/kg of bwt.) in vehicle A gave a much higher C_{max} concentrations compared to the parent compound administered at much higher doses. The AUC values of hydrazinocurcumin (100 mg/kg) in vehicle A was greater than that of higher dose of curcumin (1g/kg) (Table 5-5).The superior bioavailability of hydrazinocurcumin was attributed to improved dissolution as a result of the introduction of nitrogen atoms in the molecule or as a result of reduced first pass metabolism in the gut and liver.

Table 5 - 5: Comparison between the pharmacokinetic properties of curcumin and hydrazinocurcumin

	Curcumin [21]	Curcumin [22]	Curcumin [22]	Hydrazinocurcum
Vehicle	Not reported	1 % Tween 20 in water	phospholipid-complex	Vehicle A
Oral Dose	(500 mg/kg)	1g/kg	1g/kg	(100 mg/kg)
C_{max} (µg/ml)	0.06	0.5	1.20	2.91 ± 1.751
T_{max} (hr)	0.692	0.75	1.5	0.833 ± 0.258
Terminal Half-life (hr)	0.74	1.45	1.96	0.452 ± 0.344
(K_{el}) (hr^{-1})	-	0.48	0.35	2.220 ± 1.386
AUC $_{0-t\infty}$ (µg ml^{-1} h)	-	1.68	8.73	2.888 ± 2.315[a]
Bioavailability	1%	ND	ND	ND

[a] AUC_{last}

5.3 Conclusion

The study demonstrated that mice can be used successfully in multiple sampling pharmacokinetic studies. The high sensitivity of LC-MS/MS did away with the need to sacrifice animals at every time point. This was more ethically acceptable. Absolute bioavailability was not determined since the drug was not administered intravenously. Hydrazinocurcumin had a better oral bioavailability than the parent compound reported in literature [21, 22] since higher plasma concentrations and AUCs were attained. The bioavailability of hydrazinocurcumin was affected by the type of formulation. The half life of hydrazinocurcumin was short (0.452 h) and further chemical modifications are required to reduce its metabolism and excretion rate. The short half-life of hydrazinocurcumin may explain its poor *in vivo* activity when administered to *Plasmodium berghei* infected mice. This underlines the importance of performing pre-clinical pharmacokinetic studies hand in hand with *in vivo* investigations for biological in order determine reasons for lack of efficacy.

5.4 Materials and Methods

5.4.1 Materials

5.4.1.1 Chemicals and Regents

Technical grade curcumin, ethyl acetate (HPLC grade), sodium hydroxide pellets and boric acid (Molecular biology grade) were purchased from Sigma-Aldrich. Dimethyl sulfoxide, absolute ethanol, acetic acid, acetonitrile (HPLC grade), formic acid were obtained from Saarchem, MercK Chemicals, Gauteng, South Africa. O-phosphoric acid (analytical grade) was obtained from BDH Chemicals, Poole, England. Hydrazinocurcumin was synthesized by reacting technical grade curcumin and hydrazine hydrate as previously described. Its purity and identity was confirmed by HPLC and spectroscopy methods. Sterile Vacutainer Heparinized PST™ tubes were obtained from Becton Dickinson Vacutainer Systems, Meylan Cedex, France. Human heparinised blood was obtained from the Western Cape Blood Donor Service. It was stored at 4°C for a maximum of two months. Human plasma was

obtained by centrifuging whole blood at 1250 rcf for 10 minutes. The upper supernatant layer was collected and stored at 4°C for a maximum of 2 days

5.4.1.2 Experimental Animals

The experimental protocol was reviewed and approved by the Animal Ethics Committee of the University of Cape Town. Specific Pathogen Free C57/BL/6 mice were obtained from the Animal Unit of the University of Cape Town. The mice were housed in groups of 5-6 in cages at ambient temperatures of 20-25°C with a 12 hour light/dark cycle and free access to water and food. They were allowed to acclimatize in the Pharmacology Animal unit for 2 weeks before the study. Mice blood was obtained by cardiac puncture of anesthetized mice. Mouse blood was stored in heparinized tubes at 4°C for a maximum of 2 days.

5.4.1.3 Instrumentation

Tandem LC-MS/MS analysis was performed using an Agilent 1200 HPLC system (Agilent Technologies, Japan) coupled to a tandem quadrupole mass spectrometer (Sciex 3200Q-Trap). Separation of hydrazinocurcumin was achieved using a Pheromenex Gemini C_{18} HPLC analytic column (50 X 2.0 mm, 5 µm particle size) maintained at ambient temperature. Small blood samples were centrifuged in an Abbot Laboratories centrifuge (Germany, Cat. No. 3530) at 12000 rcf for 5 minutes. Lager volumes of blood samples where centrifuged in an Eppendroff 5804 centrifuge at 1250 rcf for 10 minutes. Samples were vortexed on a Vortex-2-Gen mixer Model G560E from Scientific Industries Inc., Bohemia, New York, USA. Solvents were evaporated in a Cold Trap model 10.10 from Jouan Quality Systems, France.

5.4.2 Preparation of Stock, Reference, Quality Control and Calibration Standard Solutions of Hydrazinocurcumin

All solutions were prepared daily before analysis since hydrazinocurcumin is unstable in solution. A stock solution of hydrazinocurcumin was prepared by dissolving 1 mg in 1 ml of acetonitrile. A secondary stock solution of hydrazinocurcumin was prepared by diluting the stock solution 10 fold to 100 µg/ml using acetonitrile. The reference standard solution was prepared by diluting the secondary stock solution of hydrazinocurcumin with the mobile phase (0.1% FA: ACN, 1:1; v/v) to obtain a solution of concentration 10 µg/ml. The calibration and QC standards were prepared by spiking whole human blood with hydrazinocurcumin to obtain the following solutions with the following concentrations: 10 µg/ml; 5 µg/ml; 2.5 µg/ml; 1.25 µg/ml; 0.625 µg/ml; 0.313 µg/ml; 0.156; and 0.078 µg/ml.

5.4.3 Method Development

5.4.3.1 Optimization of the Mass Spectrometric and Chromatographic Conditions

5.4.3.1.1 MS optimization

The analyte was infused at a concentration of 500 ng/m in mobile phase at a flow-rate of 5 µl/min to obtain a mass spectrum. The molecular ion was selected in Q1 and fragmented in the collision cell using N_2 gas. Q3 was set to scan fro all possible product ions. The most abundant product ion was selected in Q3 and the mass spectrometer was set in the MRM mode. Q1 was set to monitor the molecular ion and Q3 was set to monitor the most abundant product ion.

5.4.3.1.2 Chromatography optimization

The injection solvent and the mobile phase of the HPLC system was optimized which resulted in good peak shapes and a relatively short run time of 2 minutes.

5.4.3.2 Determination of the Optimal Extraction Method from Blood

Three extraction methods for sample preparation from blood were compared:

5.4.3.2.1 Filter paper spotting and direct extraction with ACN-water

Spiked human blood calibration (10 µl) solutions with concentrations ranging from 10 to 0.078 µg/ml were separately spotted on Whatman filter paper No. 542 (110 mm diameter). Each blood spot was dried slowly using a blow dryer held at a distance from the filter paper. The dried blood spot was cut into pieces which were transferred to an eppendroff tube. Water (100µl) and acetonitrile (200µl) were added to the eppendroff tube successively. The eppendroff tube was vortexed for 1 minute and then centrifuged for 5 minutes at 10 900 rpm (10 500 rcf). The supernatant was removed and analyzed by LC-MS/MS.

5.4.3.2.2 Filter paper spotting and direct extraction with ethyl acetate

Spiked human blood calibration solutions (10 µl) were spotted on filter paper, dried and transferred to an eppendroff tube as described above. Millipore water (200 µl) and ethyl acetate (1 ml) were added to the eppendroff tube containing the filter paper. The contents were vortexed for one minute and then centrifuged for 5 minutes. The organic layer (600 µl) was removed and evaporated under vacuum for 40 minutes. The dried residue was dissolved in the mobile phase (100 µl) and analyzed by LC-MS/MS.

5.4.3.2.3 Liquid-liquid extraction using ethyl acetate and determination of the optimal pH for extraction

Universal Britton Robison buffers[16] ranging from pH 2 to 11 were prepared by adjusting the pH of Solution A (0.1 M acetic acid, 0.1 M phosphoric acid; 0.1 M boric acid) to the desired pH using 0.5 M NaOH. Buffer (50 µl), spiked whole blood (10 µl, 10 µg/ml) and ethyl acetate (250 µl) were added to an eppendroff tube in that order. The contents were vortexed for 1 minute and then centrifuged for 5 minutes at 10 900 rpm (10 500 rcf). The upper organic layer (215 µl) was transferred to an eppendroff tube. Ethyl acetate was evaporated under vacuum for 30 minutes and the residue was stored at -20°C till analysis. For each buffer, two replicate extractions were done. The samples were analyzed within 3 days so as to minimize degradation on storage. The dried residues were dissolved in 100 µl of mobile phase before analysis by LC-MS/MS. The mean peak area was plotted against the pH of the buffer. The optimal pH for extraction was the pH at which there was maximal recovery.

5.4.3.3 Comparison of the Recovery from Red Blood Cells and Plasma

Human blood was spiked with the test drug (10 µg/ml, 1 ml) was centrifuged for 10 minutes at 1250 rcf. The upper plasma layer was transferred to an eppendroff tube. The RBCs (30 µl) and plasma (30 µl) were separately transferred to eppendroff tubes containing 150 µl of buffer at pH 10. The RBCs and plasma were separately subjected to liquid-liquid extraction as previously described ethyl acetate (750 µl).The upper ethyl acetate (700 µl) layer were transferred to a glass tube and the solvent was evaporated in a cold trap. The samples were stored at – 20°C until analysis. Before analysis the samples were dissolved in mobile phase (100 µl) and vortexed for 15 seconds. The peak areas obtained were compared.

5.4.3.4 Comparison of Calibration Curves obtained from Spiked Human Blood and Plasma

To obtain the calibration curve, 10 µl of the calibration solutions in human blood were extracted by liquid-liquid extraction with ethyl acetate and buffer at pH 10 as previously described (section 5.4.3.2.3). The organic layer was dried and dissolved in 100 µl of the mobile phase. The solutions were analyzed by LC-MS/MS. The peak areas were plotted against the nominal concentration of the calibration solution. The regression line was fitted by weighted quadratic regression using 1/X as the weighting factor.

Two separate calibration curves were obtained using human and murine blood spiked with hydrazinocurcumin. The correlation between the calibration curves was determined using Pearson's correlation coefficient. The paired student t-test was used to compare the peak areas obtained when extraction was done from either murine or human blood.

5.4.4 Method Validation

5.4.4.1 Determination of LLOQ, LOD, Intra and Inter-Day Accuracy and Precision

Method validation was performed according to the FDA guidelines for validation of bioanalytic methods [17, 18]. However, the sample stability and selectivity was not determined as these are not required for pre-clinical studies. The accuracy of the method was the percentage deviation of observed concentration (C_{obs}) from the nominal concentration and was calculated using the following formula: $[(C_{obs} - C_{nom})]/ C_{nom} \times 100$. The precision was calculated from the relative standard deviation (RSD) of replicate determinations as follows: standard deviation (SD)/C_{obs} X 100. Intra-day accuracy and precision were determined by calculating the relative error (RE) and relative standard deviation (RSD) of 4 replicates of the quality control samples (QC) of concentrations 10 to 0.156 µg/ml assayed on the

same day. Inter-day accuracy and precision were determined by calculating the relative error and coefficient of variation of 4 QC samples assayed on 3 consecutive days. The relative error was the percentage deviation of observed concentration (C_{obs}) from the nominal concentration (C_{nom}). The accuracy and precision at the lower limit of quantification (LLOQ) were determined by analyzing 5 replicates of the QC sample one of the validation days. At the lower limit of quantification (LLOQ), a RE of ± 20 % and a CV of 20 % were considered acceptable. For QC samples with a concentration greater than LLOQ, a RE of ± 15 % and a CV of 15 % were considered acceptable. The limit of detection (LOD) was the lowest concentration at which the signal to noise ratio was 3.

5.4.4.2 Determination of the Recovery Efficiency

Spiked whole human blood (10 µl,10 µg/ml) were extracted by liquid-liquid extraction as described above and analyzed by LC-MS/MS. The recovery efficiency was determined by comparing the peak areas of the recovered calibration solution to the peak area of the reference standard solution (10 µg/ml in mobile phase) using the following formula:

$$\text{Percentage recovery} = \frac{\text{Peak area of extracted sample X F X G X } 100}{\text{Peak area of reference standard}}$$

G is the extraction factor and corrected for the fact that only 215 µl of ethyl acetate was evaporated as opposed to the 250 µl that was used for extraction. The value of G was 1.163. Where F is the dilution factor and corrected for the 10 fold dilution of the extracted sample with mobile phase.

5.4.5 The Pharmacokinetic Study

5.4.5.1 Comparison of the Bioavailability of Hydrazinocurcumin from Different Vehicles

Hydrazinocurcumin was suspended in 3 different vehicles with different pH values. The vehicles were designated A, B and C. The first two vehicles had ethanol as a co-solvent. The third vehicle lacked ethanol as a co-solvent. Vehicle A consisted of 10 % v/v DMSO, 33.3 % v/v ethanol and water in order. Vehicle consisted of 10 % DMSO, 33.3 % v/v ethanol and PBS buffer at pH 7.4. Vehicle C consisted of 10 % DMSO and buffer at pH 6. Hydrazinocurcumin was first dissolved in DMSO with sonication, followed by ethanol (for vehicle A and B) and finally water or the buffer was added.

Male mice weighing between 29 to 34 g were divided in 3 groups of 5 or 6 animals each. Each group of received a single oral dose of hydrazinocurcumin (100 mg/kg of body weight) in different vehicles by gavage. Blood samples (10 µl) were taken from the tail vein at 0, 0.5, 1, 2 and 5 hours post dosing. The blood samples were analyzed for the levels of hydrazinocurcumin.

5.4.6 Data Analysis

The correlation coefficients, means, relative standard deviations and accuracy were calculated using Microsoft Excel ™. The guidelines outlined by Beal [19] and Hennig *et al.* [20] were used to handle values that were below lower limit of quantification (BLOQ). Given that values that are BLOQ may accurately reflect true concentrations discarding them they were used in analysis using 3 different methods. In the first method all values BLOQ were discarded. This is the most frequently method for handling values BLOQ but it often results in biased pharmacokinetic parameters [19]. In the second method, all value BLOQ were replaced with a value half of LLOQ. In the third method, all values below the LOD were discarded [20].

Pharmacokinetic parameters were calculated by Non-compartmental analysis using WinNonlin Standard Edition software version 4.1 (Pharsight Corporation, Mountain View, USA). The area under the curve (AUC) was calculated using the linear trapezoidal rule. AUC from the time of dosing to time to the last measurable concentration was designated AUC_{last}. Area under the curve from the time of dosing to the last time point was designated AUC_{all}. Area under the curve from the time of dosing to the time extrapolated to infinity was designated $AUC_{0-t\infty}$. The terminal half-life (β) was calculated by linear regression of the post-absorption phase/terminal phase of the log concentration vs. time curve. The time points used for the calculating the terminal half life were 0.5 to 2 hours. R^2 (unadjusted for the number of points used to compute the terminal half life) was used to assess the goodness of fit of regression line of the terminal elimination phase. The volume of distribution, mean residence time and clearance were not reported since these could not be accurately determined in the absence of data on fraction of drug absorbed. All pharmacokinetic parameters were reported as the mean and standard error of the mean of five or six individual experiments.

References

(1) Hodgson, J. *Nat. Biotechnol.* **2001**, *19*, 722-726.

(2) Singh, S. S. *Curr. Drug Metab.* **2006**, *7*, 165-182.

(3) Baldrick, P. *Drug Discov. Today* **2003**, *8*, 127-133.

(4) Ireson, C. R.; Jones, D. J.; Orr, S.; Coughtrie, M. W.; Boocock, D. J.; Williams, M. L.; Farmer, P. B.; Steward, W. P.; Gescher, A. J. *Cancer Epidemiol. Biomarkers Prev.* **2002**, *11*, 105-111.

(5) Hao, K.; Zhao, X. P.; Liu, X. Q.; Wang, G. J. *Chromatograhia* **2006**, *64*, 531-535.

(6) Wahlström, B.; Blennow, G. *Acta Pharmacol Toxicol (Copenh).* **1978**, *43*, 86.

(7) Ravindranath, V.; Chandrasekhara, N. *Toxicology* **1980**, *16*, 259-265.

(8) Ravindranath, V.; Chandrasekhara, N. *Toxicology* **1981**, *22*, 337-344.

(9) Holder, G. M.; Plummer, J. L.; Ryan, A. J. *Xenobiotica* **1978**, *8*, 761-768.

(10) Hoehle, S. I.; Pfeiffer, E.; Sólyom, A. M.; Metzler, M. *J. Agric. Food Chem.* **2006**, *54*, 756-764.

(11) Pan, M. H.; Huang, T. M.; Lin, J. K. *Drug Metab. Dispos.* **1999**, *27*, 486-494.

(12) Tamvakopoulos, C.; Sofianos, Z. D.; Garbis, S. D.; Pantazis, P. *Eur. J. Drug Metab. Pharmacokinet.* **2007**, *32*, 51-57.

(13) Rathore, R.; Jain, J. P.; Srivastava, A.; Jachak, S. M.; Kumar, N. *J. Pharm. Biomed. Anal.* **2008**, 46, 374-380.

(14) Lipinski, C. A.; Lombardo, F.; Dominy, B. W.; Feeney, P. J. *Adv. Drug Deliv.* **1997**, *23*, 3-25.

(15) Dzinjalamala, F. K.; Macheso, A.; Kublin, J. G.; Taylor, T. E.; Barnes, K. I.; Molyneux, M. E.; Plowe, C. V.; Smith, P. J. *Antimicrob. Agents Chemother.* **2005**, *49*, 3601-3606.

(16) Methrom Determination of nickel and cobalt in seawater, VA Application Note No. V-69.

(17) U. S. Department of Health and Human Services Food and Drug Administration, Center for Veterinary Medicine (CVM). Guidance for Industry Bioanalytic Method Validation, May **2001**.

(18) Bansal, S.; DeStefano, A. *AAPS J* **2007**, *9*, E109-14.

(19) Beal, S. L. *J Pharmacokinet. Pharmacodyn.* **2001**, *28*, 481-504.

(20) Hennig, S.; Waterhouse, T. H.; Bell, S. C.; France, M.; Wainwright, C. E.; Miller, H.; Charles, B. G.; Duffull, S. B. *Br. J. Clin. Pharmacol.* **2007**, *63*, 438-450.

(21) Yang, K. Y.; Lin, L. C.; Tseng, T. Y.; Wang, S. C.; Tsai, T. H. *J. Chromatogr. B. Analyt Technol. Biomed. Life. Sci.* **2007**, *853*, 183-189.

(22) Maiti, K.; Mukherjee, K.; Gantait, A.; Saha, B. P.; Mukherjee, P. K. *Int. J. Pharm.* **2007**, *330*, 155-163.

CHAPTER SIX
CONCLUSION AND RECOMMENDATIONS FOR FUTURE WORK

A series of derivatives of curcumin were synthesized. These included the azole derivatives, sulfonylureas, chloroquine-based derivatives, thiosemicarbazones and N-acyl hydrazones. These derivatives were designed to act against specific molecular targets in *Plasmodium falciparum*. The derivatives were tested for their *in vitro* activity against the chloroquine sensitive (D10) and resistant (KI) *Plasmodium falciparum* strains. In addition, their ability to inhibit the *in vitro* formation of beta hematin was determined. The parent compound, curcumin, was equally active against the chloroquine sensitive and resistance strains with a resistance index of about 1. The IC_{50} against the sensitive and resistant strains was 4.545 and 4.496 μM respectively. It has a low cytotoxicity with a CC_{50} of over 100 μM against the CHO cell line. Although the antiplasmodial activities of curcumin have previously been reported, its activities against active and resistant strains have never been compared. Some derivatives had improved *in vitro* activity compared to curcumin.

HPLC and ^{1}H NMR revealed that a number of derivatives exist as isomers. Two tautomers of hydrazinocurcumin were synthesized: 1-*N* pyrazole (**2.2.1b**) and the 3-*N* pyrazole tautomer (**2.2.1c**). There were considerable differences in the ^{1}H NMR spectra of the two isomers which were used to establish the structural differences between the tautomers. There was a large difference in *in vitro* antiplasmodial activity of the two tautomers. 1-*N*-pyrazole was 6 times more active than the 3-*N*-pyrazole tautomer with an IC_{50} of 0.502 μM compared to the 3-*N* tautomer that had an IC_{50} of 2.976 μM against the CQS strain. Activity against the CQR strain was reduced. In addition, three isomers of the isoxazole derivative of curcumin were isolated. However, the structural differences of the isomers could not be determined using ^{1}H NMR. The isomers have been submitted for X-ray crystallographic analysis. The *in vitro*

antiplasmodial activities of the isomers were similar and were less active than the pyrazole derivatives.

Sulfonylurea derivatives of curcumin were synthesized by a condensation reaction between an aryl isocyanate and hydrazinocurcumin. The sulfonylureas were active against the CQS strain but activity decreased considerably against the CQR strain. The sulfonylurea derivatives had a high cytotoxicity which indicated that these compounds should be evaluated further as potential anticancer agents. The *in vivo* activity of the most active sulfonylurea was inferior to that of chloroquine.

The thiosemicarbazone and *N*-acylhdrazone derivatives were synthesized by a condensation reaction between a thiosemicarbazide and aryl hydrazide respectively. When the reaction was performed in acetic acid at 70°C the reaction yields obtained were low. HPLC chromatography revealed that thiosemicarbazone and *N*-acylhdrazone derivatives exist as isomers. Unexpectedly, pyrazole-1-methanone derivatives were obtained as a result of nucleophilic attack of the N-2 within aryl hydrazone derivative on the second carbonyl functional group on curcumin. The pyrazole-1-derivatives were more cytotoxic and had better antiplasmodial activity.

The pharmacokinetic profile of the 3-*N* pyrazole tautomer of hydrazinocurcumin was investigated in mice. Blood concentrations of hydrazinocurcumin were assayed by LC-MS/MS. The bioanalytic method was validated. The lower limit of quantification was 0.625 µg/ml and the limit of detection was 0.156 µg/ml. The precision and accuracy of the method was within acceptable limits. Hydrazinocurcumin was administered in 3 different vehicles that had different pH values. Ten microliter blood samples were obtained at 5 different time points. Drug absorption was optimal from the formulation with an acidic pH. Hydrazinocurcumin, however, had a very short half-life of about 0.452 hours. This showed it is rapidly excreted or metabolized and additional chemical modifications are required to improve its pharmacokinetic profile. Hydrazinocurcumin had a better oral bioavailability than curcumin since much higher plasma concentrations and AUC values

were attained compared to values reported in literature. The short half life of hydrazinocurcumin in mice may explain its poor *in vivo* antiplasmodial efficacy.

Conclusion

Derivatives of curcumin with improved *in vitro* antiplasmodial activity were synthesized. Unlike curcumin, some of the derivatives had ability to inhibit beta hematin formation. A pilot toxicological study showed that derivatives were more toxic than curcumin and they may affect the neurological function. Selected derivatives suppressed parasitemia on day 4. Like the curcumin, the pyrazole and isoxazole derivatives were able to prolong survival in infected mice. A pharmacokinetic study done on the pyrazole derivative, hydrazinocurcumin, showed that while it has a better oral bioavailability compared to the parent compound, its half life was too short. This may have accounted for the poor *in vivo* efficacy of the synthetic derivatives.

Recommendations for future work

Though derivatives were designed to act against the molecular targets within *Plasmodium falciparum*: cysteine proteases; iron-dependent enzymes; parasite induced new permeability pathways (NPPs), activity against these targets was not determined. Further work is required to determine if the chemical modifications successfully improved activity against these targets.

HPLC chromatographic separation showed that a large number of the synthetic derivatives of curcumin exist as isomers. These isomers need to be isolated and their three dimensional structure be determined in order to establish the differences between the isomers.

The pilot toxicological investigation showed that selected derivatives of curcumin may affect neurological function. This needs to be investigated further as these agents may find use in management of neurological disease.

The isoxazole and pyrazole derivatives demonstrated an unusual ability to prolong the survival of infected mice. This effect has been noted before for curcumin and a number of compounds. Since such compounds may find use as coadjuvants in the management of malaria and other infections, their effects on the immune response in malaria need to be further investigated.

The pharmacokinetic assay showed that the half-life of the pyrazole ring is too short. This showed that increasing the rigidity of molecule failed to reduce its metabolism or excretion. Further chemical modifications are required that will reduce the metabolic rate and conserve the ability to inhibit growth of the chloroquine resistant strain.

CHAPTER 7

EXPERIMENTAL

7.1 Instrumentation and Materials

Technical grade curcumin, glacial acetic acid, *N, N*-dimethly formamide (DMF) were obtained from Sigma-Aldrich, St. Louis, U.S.A. Hydrazine monohydrate, hydroxylamine hydrochloride, glacial acetic acid and isopropanol were purchased from Merck, Germany. Sodium hydroxide was obtained from Chemical Lab and Suppliers, S. A. Anhydrous sodium acetate was obtained from PAL chemicals, S.A. The arene sulfonyl isocyanates which included p-toluene, benzene, 4-chlorobenzene and 4 flurobenzene sulfonyl isocyanates were obtained from Sigma-Aldrich, Milwaukee, USA. Phenyl thioisocyanate and 4-phenyl thioisocyanate were obtained from Lancaster Synthetics, Morecambe, England. The hydrazides which incluced, semicarbazide hydrochloride, salicyclic acid hydrazide, isonicotinic acid hydrazide, benzoic acid hydrazide, 4-chloro benzoic acid hydrazide, 4-hydroxy benzoic acid hydrazide, 2-furoic acid hydrazide and 7-chloro-4-hydrazinoquinoline, where obtained from Sigma-Aldrich, Milwaukee, USA. Acetonitrile (HPLC grade) was obtained from BDH chemicals. Deuterated solvents for NMR spectroscopy were obtained from Sigma-Aldrich. Reactions were monitored by thin layer chromatography on 0.25 mm silica gel F254 pre-coated aluminum-backed plates (Merck). The plates were visualized using ultraviolet light. The reaction products were purified by gravity column chromatography using silica gel 60 (230-400 mesh) from Merck. Flash chromatography was performed using Silica gel for TLC 60 H GR without a binder obtained from Merck.

Nuclear magnetic resonance spectra (^{1}H NMR) were recorded on a Varian XL-300 spectrometer at 300 MHz, Varian Unity Spectrometer at 400 MHz and at 600 MHz on a Varian Unity Inova spectrometer. ^{13}C NMR spectra were recorded at 75 MHz or 100 MHz on Varian Mercury and Varian Unity spectrometers respectively. The samples were dissolved in either

deuterodimethylsulfoxide or deuteromethanol. The peaks are described in ppm downfield of tetramethylsilane. All the proton NMR shifts and coupling constants were rounded off to one decimal point. The carbon NMR shifts were rounded off to the nearest whole number.

Low resolution mass spectra were recorded using a VG70-SEQ (FAB) operating at 7 kV at the University of Witswatersrand. High resolution mass spectrometry was performed on a VG70-SEQ (FAB) instrument operating at 8kV also at the University of Witswatersrand. Elemental analysis was performed using a Fisons EE 1108 CHNO-S instrument and analyses were within ± 0.4 % of the theoretical values for the specified elements. The samples for purity determination were prepared by dissolving 1mg in DMSO (10µl). Purity was determined by High Performance Liquid Chromatography (HPLC) on a Waters 1525 Instrument with Waters 996 photodiode array detector and an autosampler. The stationary phase was a Discovery® reverse phase C-16 amide column (15 cm by 4.6 mm, 5 µM) (Sulepco) at ambient temperatures. The samples were eluted with acetonitrile-water gradient starting from 20 % acetonitrile in water to 100 % acetonitrile over 30 minutes at a flow rate of 1 ml/min. The peaks were detected at 254 nm and integrated using Millenium^{32} Chromatography Manager Software.

Infra-red spectroscopy was measured using a Perkin Elmer FTIR instrument from 4000 to 450 cm^{-1}. The samples were run as solutions in either dichloromethane or acetonitrile or on potassium bromide (KBr) disks. Melting points were determined on a Gallenkamp hot plate melting point apparatus from Sanyo and are uncorrected.

The octanol-water partition coefficient (cLog P) and typological polar surface area (tPSA) were calculated using ChemDraw ultra™ Software version 9. Hydrogen bond donors were the sum of all heteroatoms bonded to at least one hydrogen group in a molecule. The hydrogen bond acceptors were the sum of all heteroatoms that lacks a formal positive charge. Halogens, pyrrole nitrogen and oxygen and sulfur in aromatic systems were excluded. The total hydrogen bond count was the sum of hydrogen bond acceptors and donors.

7.2 Synthesis, physical and spectral characteristics of derivatives of curcumin

Curcumin/ Diferuloylmethane/ 5-hydroxy-1, 7-bis (4-hydroxy-3-methoxyphenyl) hepta-1, 4, 6-trien-3-one, 2.1.1

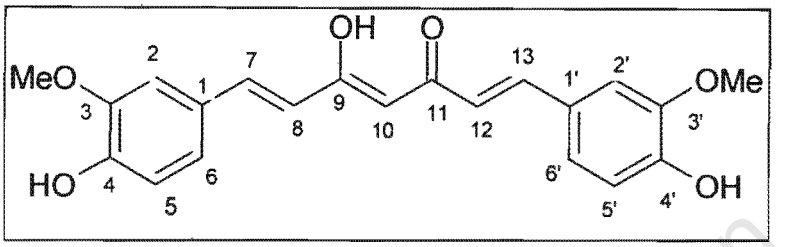

Curcumin was purified from technical grade curcumin using the method described by Rasmussen *et al.*[1]. Silica gel for TLC 60 H without binder (200 g) and potassium dihydrogen phosphate solution (250 ml, 12 % w/v in water) were added to acetone (1 l) and the mixture was stirred for 6 hours. The silica gel was filtered, air-dried and activated by heating overnight in the oven at 80°C before use. Curcumin impregnated silica gel was prepared by adding 40g of silica gel for TLC to a solution of curcumin in DCM (2 g in 1 liter). The mixture was air-dried and eluted by vacuum liquid chromatography with 3 % v/v ethyl acetate in dichloromethane. The fractions by monitored by TLC on phosphate impregnated plates. Red/orange powder (1.48g, 74 %), m. p. 183-184°C [lit. [2] 182-183°C] ; R_f (EtOAc: CH_2Cl_2 4:96) 0.43; IR ν_{max} (CH_2Cl_2) /cm^{-1} 3683 (OH), 3526 (OH), 3060 (C=C-H), 2914 (C-H), 1627 (s, C=C); 1592 (C=O); δ_H (300 MHz, DMSO-d_6) 9.62 (2H, s, Ar-OH), 7.55 (2H, d, *J* 15.9, H-7, H-13), 7.32 (2H, d, *J* 1.8, H-2, H-2'), 7.14 (2H, dd, *J* 1.8, 8.4, H-6, H-6'), 6.83 (2H, d, *J* 8.4, H-5, H-5'), 6.75 (2H, d, *J* 15.9, H-8, H-12), 6.07 (1H, s, H-10), 3.84 (6H, s, Ar-OMe); δ_C (100 MHz, DMSO- d_6)183.3 (C=O), 147.9 (C-4, 4'), 146.8 (C-3, 3'), 140.5 (C-7, 13), 127.7 (C-1, 1'), 122.9 (C-6,6'), 121.8 (C-8, 12), 114.9 (C-5,5'), 109.7 (2, 2'), 101.1 (C-10), 55.0 (C-3 O-Me, 3' O-Me); LRMS (ESI): (M+1) *m/z* 369.3.

(1) **General procedure for the synthesis of pyrazole derivatives.**

The method used was modified from the procedure described by Selvam *et al.* [3] Technical grade curcumin (3 g) and 5 ml hydrazine monohydrate were added to acetic acid (50 ml). The reaction mixture was stirred at ambient temperature for 72 hours. A precipitate formed which was filtered and rinsed with water three times.

4, 4'-(1E, 1'E)-2, 2'-(pyrazole-3, 5-diyl) bis (ethene-2, 1-diyl) bis (2-methoxyphenol) 3- methoxyphenol), 2.2.1a

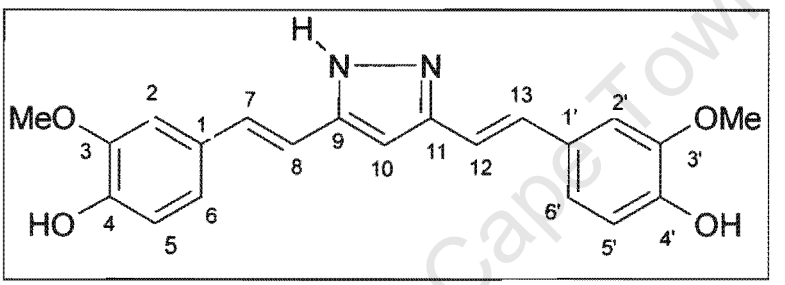

The general procedure for the synthesis of pyrazole derivatives was applied. The precipitate obtained was filtered and washed with water. Pale yellow powder (2.7 g, 90 %) m.p. 211-212°C [lit.[4]211-214°C];. R_f (EtOAc:CH_2Cl_2 1:1) 0.33; IR ν_{max} (KBr) /cm^{-1} 3685 (O-H), 3600 (N-H), 3063 (C=C-H), 2986 (C-H), 1757, 1713, 1606, 1447 (azole ring stretch); δ_H (400 MHz, DMSO- d_6) 12.8 (1H, br s, N-H), 9.12 (2H,s, Ar-OH, 4, 4'), 7.12 (2H, d, *J* 1.7, H-2, 2'), 7.03 (2H, d, *J* 16.5, H-7, H-13), 6.92 (2H, dd, *J* 8.1, 1.7, H-6, 6'), 6.90 (2H, d, *J* 16.5, H-8, H-12), 6.76 (2H, d, *J* 8.1, H-5, 5') / 7.35 (d, *J* 8.5, H-5, 5'), 6.60 (1H, s, H-10), 3.81 (6H, s, Ar-OMe); δ_C (100 MHz, DMSO- d_6) 147.8 (C-4, 4'), 146.7 (C-3, 3'), 129.4 (C-7, 13), 127.6 (C-1, 1'), 119.9 (C-6,6'), 115.6 (C-5, 5'), 109.6 (2, 2'), 99.2 (C-10), 55.6 (C-3 O-Me, 3'O-Me); LRMS (ESI): (M+1) *m/z* 365.2. E.A. Found C, 69.18; H, 5.69; N, 7.59. $C_{21}H_{20}N_2O_4$ requires C, 69.22; H, 5.53; N, 7.69

Isomer of hydrazinocurcumin/ 4, 4'-(1E, 1'E)-2, 2'-(1 *H*- pyrazole-3, 5-diyl) bis (ethene-2, 1-diyl) bis (2-methoxyphenol), 2.2.1b

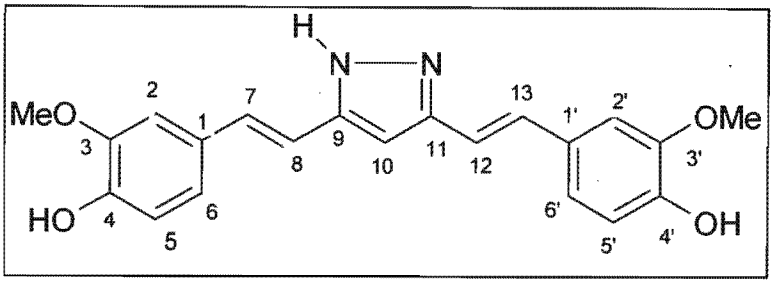

The general procedure for the synthesis of pyrazole derivatives was applied. The precipitate was subjected to column chromatography on silica gel. The column was eluted with ethyl acetate – dichloromethane (1:1) and the compound purified by crystallization from ethanol. Bright yellow needle-like crystals (154 mg, 20 %), m.p. 217-218 °C [lit.[4] 211-214°C]; R_f (EtOAc:CH_2Cl_2 1:1) 0.33; IR ν_{max} (KBr) /cm^{-1} 2913 (C-H), 2848 (C-H), 1447 (azole ring stretch), 1458 ((azole ring stretch); δ_H (300 MHz, DMSO- d_6) 12.8 (1H, s, N-H), 9.12 (2H,s, Ar-OH), 7.13 (2H, s, H-2, 2'), 7.04 (2H,d, *J* 16.4, H-7, H-13), 6.92 (4H, m, H-8, H-12, H-6, 6'), 6.78 (2H, d, *J* 8.2, H-5, 5'), 3.81 (6H, s, Ar-OMe); δ_C (75 MHz, DMSO- d_6) 147.8 (C-4, 4'), 146.7 (C-3, 3'), 129.8 (C-7, 13), 128.3 (C-1, 1'), 120.0 (C-6,6'), 115.6 (C-5, 5'), 109.6 (2, 2'), 99.3 (C-10), 55.6 (C-3 O-Me, 3'O-Me); LRMS (ESI): (M+1) *m/z* 365.2; E.A. Found C, 68.83 ; H, 5.57; N, 7.39. $C_{21}H_{20}N_2O_4$ requires C, 69.22; H, 5.53; N, 7.69; HPLC Purity: 90 %, $t_{R'}$ = 12.315 min.

Isomer of hydrazinocurcumin, 4, 4'-(1E, E'1)-2, 2'- (3 *H*- pyrazole-3, 5-diyl) bis (ethene-2, 1-diyl) bis (2-methoxyphenol), 2.2.1c

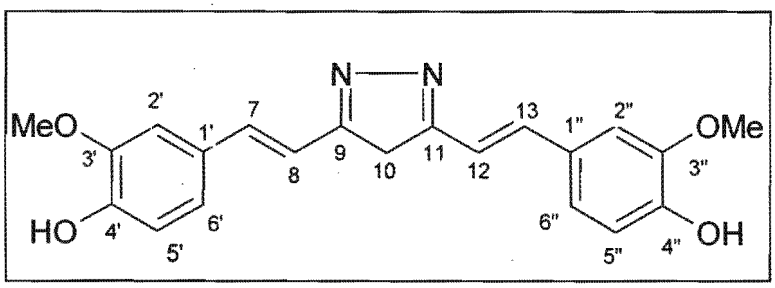

1.36 mmol of sodium hydroxide was dissolved in 50 ml of ethanol with slight warming. An equivalent amount of curcumin (500 mg, 1.36 mmol) and hydrazine monohydrate (0.08 ml) were added to the sodium hydroxide solution. The reaction mixture was stirred for 15 min at 65°C. The reaction was stopped by the addition of 5-6 drops of concentrated hydrochloric acid. A dark red precipitate formed which was filtered and rinsed with water. (388 mg, 79 %), m.p. 227°C [lit. [4] 211-214°C]; R_f (EtOAc:CH_2Cl_2 1:1) 0.38; IR ν_{max} (CH_2Cl_2) /cm^{-1} 3739 (OH), 3362 (N-H/O-H), 2984 (C-H),1462 (azole ring stretch); δ_H (300 MHz, DMSO- d_6) 7.48 (2H, d, *J* 15.9, H-7, H-13), 7.25 (2H, d 1.9, H-2, 2'), 7.06 (4H, dd, *J* 8.6, 1.9, H-6, 6'), 6.78 (2H, d, *J* 8.1, H-5, 5'), 6.33 (2H, d, *J* 15.8, H-8, 12), 4.51 (1H, s, H-10), 3.82/ 3.82/ 3.80 (6H, s, Ar-OMe); δ_C (75 MHz, DMSO- d_6) (major/minor) 167.9 / 169.0 (C-9, 11), 149.1 / 149.4 (C-4, 4'), 147.9 / 147.4 / 146.8 (C-3, 3'),, 144.4 / 144.8 (C-7, 13), 129.7 / 128.4 (C-7, 13), 125.8 / 126.2 / 125.6, 124.8 (C-1, 1'), 122.7 / 123 (C-6, 6') , 120.0 / 120.3, 117.0, 115.6 / 115.6/ 115.3/ 115.0 (C-5, 5'), 114.9 / 114.6/ 114.4 (C-8, 12), 111.3 (C-2, 2'), 109.7, 55.7 / 55.6 (C-3 O-Me, 3'O-Me); LRMS (ESI): *m/z* (M+1) 365.2; HPLC Purity: 85 %, $t_{R'}$ = 12.28 min.

(2) **General method for the synthesis of isoxazole derivatives of curcumin**

The synthesis was as described for the synthesis of pyrazole derivatives except that hydroxylamine hydrochloride was used instead of hydrazine hydrate and the reaction mixture was heated at 85°C for 48 hours. The reaction was stopped by the addition 50 ml of water and extracted with 50 ml portions dichloromethane three times. The dichloromethane extracts were combined and washed with saturated brine solution. The organic extracts were combined, evaporated *in vacuo* and subjected to column chromatography on silica gel. The organic extract eluted column chromatography with dichloromethane. Later fractions were eluted with dichloromethane: ethyl acetate (1:4).

Isomer of 4, 4'-(1E, 1'E)-2, 2'- (isoxazole-3, 5-diyl (ethene-2, 1-diyl) bis (2-methoxyphenol), 2.2.2a

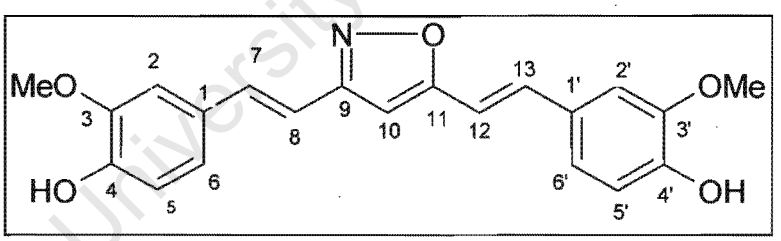

It was obtained from fractions 3-9. Dull Yellow powder (160 mg, 7 %), m.p. 168-169°C [lit. [5] 169-171°C]; R_f (EtOAc:C H_2Cl_2 1:19) 0.3; IR ν_{max} (KBr) /cm^{-1} 3514 (OH), 3341 (O-H), 2957 (C-H), 1642 (C=C), 1588 (azole ring stretch), 1277 (s) (N-O) stretch; δ_H (400 MHz, DMSO-d_6): 9.36 (1H,s br, Ar-OH), 9.29 (lH, s br, Ar-OH), 7.28 (1H, d, *J* 1.6, H-2), 7.27 (1H, d, *J* 1.6, H-2'), 7.27 (2H, d, *J* 16.0, H-7, 13), 7.04 (1H, d, *J* 16.8, H-8), 7.06 (2H, dd, *J* 8.2 , 1.6, H-6,6'), 7.04 (1H, d, *J* 16.4, H-12), 6.83 (1H, s, H-10), 6.80 (1H, d, *J* 8.4, H-5), 6.78 (1H, d, *J* 8.0, H-5'), 3.83 (3H, s, Ar-O-CH_3), 3.82 (3H, s, Ar-O- CH_3); δ_c (100 MHz, DMSO- d_6) 168.3, 162.1, 148.1, 147.9, 147.8, 136.3, 134.7, 127.3,

126.9, 121.6, 121.2, 115.5, 112.6, 110.4, 110.3, 110.1, 97.8, 55.7, 55.6; LRMS (ESI) (M+1): *m/z* 366.2; EA Found C, 68.87; H, 5.40; N, 3.35 $C_{21}H_{19}NO_5$ requires C, 69.03; H, 5.24; N, 3.83 HPLC Purity: 88 % , $t_{R'}$ = 14.96 min.

Isomer of 4, 4'-(1E, 1'E)-2, 2'- (isoxazole-3, 5-diyl (ethene-2, 1-diyl) bis (2-methoxyphenol), 2.2.2b

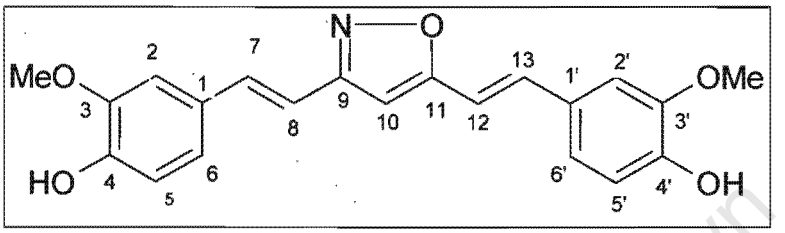

A yellow precipitate that formed from fractions 4 to 12 which was rinsed dichloromethane. Bright yellow (335 mg, 14 %), m.p. 169-170°C [lit. [5] 169-171°C]; R_f (EtOAc:C H_2Cl_2 1:19) 0.3; IR ν_{max} (KBr) /cm^{-1} 3486 (OH), 1642 (C=C), 1508 (C-O), 1426 (azole ring stretch), 1274 (N-O stretch); δ_H (400 MHz, DMSO-d_6) 9.37 (1H,s br, 4Ar-OH), 9.30 (1H, s br, 4' Ar-OH), 7.29 (1H, d, *J* 1.8, H-2), 7.28 (2H, d, *J* 16.4, H-7, H-13), 7.27 (1H, d, H-2', *J* 2.0), 7.07 (1H, d, *J* 16.4, H-8), 7.07 (2H, dd, *J* 8.2, 1.8, H-6,6'), 7.05 (1H,d, *J* 16.8, H-12), 6.83 (1H, s, H-4), 6.80 (1H, d, *J* 8.0, H-5), 6.80 (1H, d, *J* 8.4, H-5'), 3.84 (6H, s, Ar-OMe); δ_c (100 MHz, DMSO-d_6) 168.3, 162.1, 148.1, 147.9, 147.8, 136.3, 134.7, 127.3, 126.9, 121.6, 121.2, 115.6, 115.5, 112.6, 110.4, 110.3, 110.2, 97.8, 55.7, 55.6; LRMS (ESI): (M+1) *m/z* 366.3; EA Found C, 68.70; H, 5.27; N, 3.35 $C_{21}H_{19}NO_5$ requires C, 69.03; H, 5.24; N, 3.83; HPLC Purity: 97 %, $t_{R'}$ = 14.93 min.

Isomer of 4, 4'-(1E, 1'E)-2, 2'- (isoxazole-3, 5-diyl (ethene-2, 1-diyl) bis (2-methoxyphenol), 2.2.2c

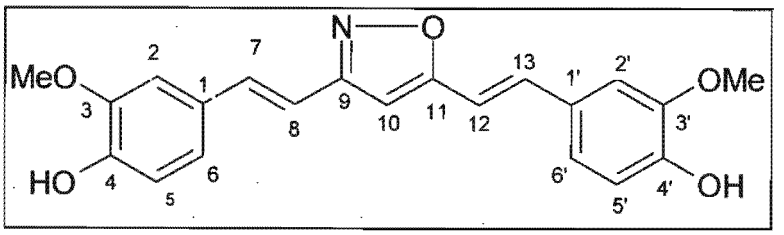

It was obtained from fraction 10. Crystallized from n-butanol. Off-white powder with a yellow-green taint (550 mg, 23.1%), m.p. 173°C [lit.[5] 169-171°C]; R_f (CH_2Cl_2 : EtOAc 19:1) 0.26; IR ν_{max} (KBr) /cm^{-1} 3507 (OH), 3384 (O-H), 1639 (C=C), 1588 (azole ring stretch), 1516 (C-O), 1429 (CH_2/ azole ring stretch), 1364 (C=N), 1274 (s) (N-O); δ_H (300 MHz, DMSO-d_6): 9.31 (2H,s br, 4, 4' Ar-OH), 7.29 (1H, d, *J* 1.8 Hz, H-2/2'), 7.28 (1H, d, *J* 2.1 Hz, H-2/2'), 7.28 (2H, d, *J* 16.5, H-7, H-13), 7.07 (1H, d, *J* 16.8, H-8/12), 7.05 (1H, d, *J* 16.5, H-8/12), 7.05 (1H, d, *J* 9.3, H-5/5'), 7.05 (1H, d, *J* 9.6, H-5/5'), 6.84 (1H, s, H-10), 6.81 (2H, dd, *J* 8.1, 2.4 , H-6,6'), 3.85 (6H, s, Ar-OMe); δ_c (75 MHz, DMSO-d_6) 168.3, 162.1, 148.1/147.9/147.8, 136.3, 134.7, 127.3/126.9, 121.5, 121.2, 115.6, 115.5, 112.6, 110.4/110.3/110.2, 97.8, 55.7, 55.6; LRMS (ESI): (M+1) *m/z* 366.4; HPLC Purity: 88 %, $t_{R'}$ = 14.952 min.

(3) **General method for the Synthesis of Sulfonylurea derivatives**

The arene sulphonyl isocyanate (1 eq) was added to a solution of hydrazinocurcumin (100 mg, 0.275 mmols) in *N, N*-dimethlyformamide. The reaction mixture was stirred at 65°C for 24 hours under nitrogen. The reaction was stopped by the addition of water (10 ml) and the reaction mixture was extracted with ethyl acetate (20 ml) three times. The organic layers were combined, evaporated to dryness and dissolved in about 1 ml of methanol. About 5 ml of water was added to the solution which was extracted again with diethyl ether and toluene in that order.

3, 5-bis-(4-hydroxy-3-methoxystyryl)-*N*-(phenylsuphonyl)-1*H*-pyrazole-1-carboxamide, 2.3.1

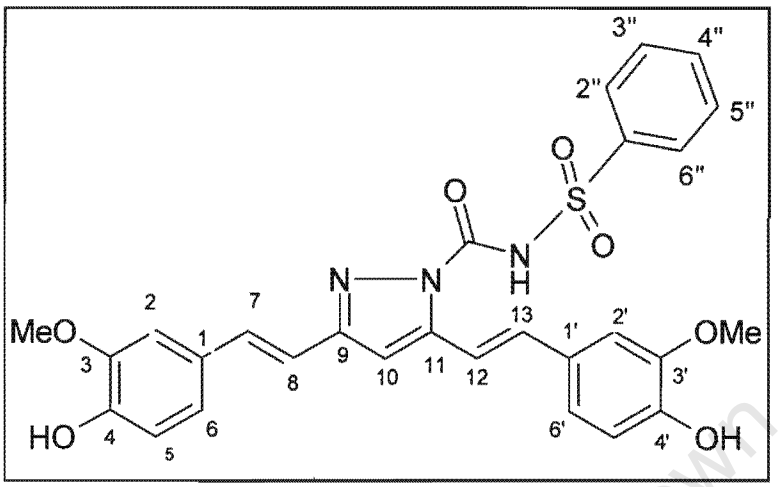

Yellow-brown powder (36 mg , 24 %); m.p. 140°C; R_f (CH_2Cl_2 : EtOAc 1:1) 0.29; IR ν_{max} (ACN) /cm^{-1} 3623 (OH), 3543 (NH), 3159 (C=C-H), 3000 (C=C-H), 2934 (C-H), 1444, 1411, 1358 (S=O stretch) ; 1165 (S=O); δ_H (300MHz, CD_3OD): 7.95 – 7.88 (2H, m, H-2", H-6"), 7.58 – 7.49 (2H, m, H-3", H-5") 7.18 (1H, m, H-4"), 7.14 – 7.04 (4H, m , H-2, H-2', H-7, H-13), 6.96 (4H, m, H-6, H-6',H-8, H-12), 6.79 (2H, d, *J* 8.2, H-5, H-5'), 6.61 (s, H-10), 3.89 (6H, s, -OCH_3); δ_C (75 MHz, CD_3OD) 168.1 (C=O), 149.4/ 149.2 (2C) , 148 (2C), 133.2 (2C), 132.1/ 131.9 (2C), 130.5/ 130/ 129.9/ 128.9/ 129.1 (2C), 127.1 (2C), 126.3 (2C), 121.4 (2C), 116.6/ 116.5/116.4 (2C), 110.5 (1 C), 56.5/ 56.4(2C). HPLC purity: 93 %, t_R 11.89 min.

3, 5-bis-(4-hydroxy-3-methoxystyryl)-*N*-tosyl-1*H*-pyrazole-1-carboxamide, 2.3.2

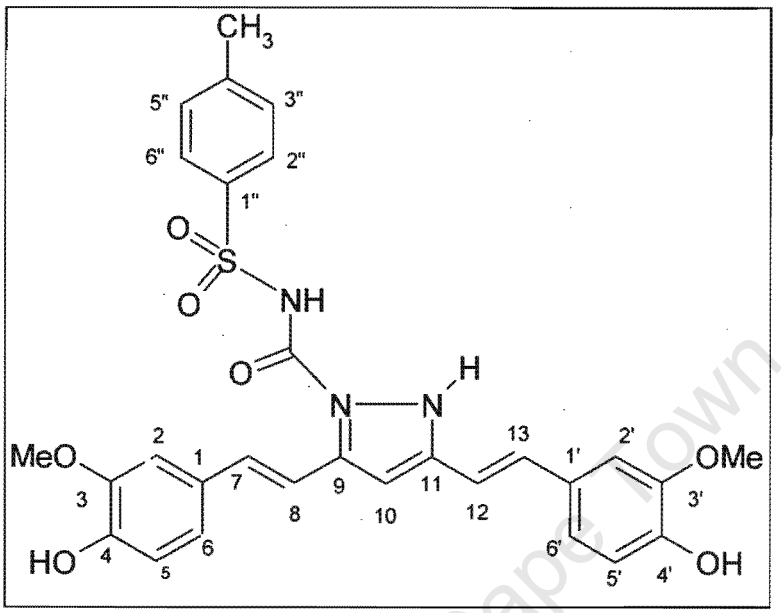

Yellow (51 mg, 33 %); R_f (CH_2Cl_2 : EtOAc 1:1) 0.31; m.p. 181-182°C, IR ν_{max} (ACN) /cm^{-1}: 3616 (NH/ OH), 3536 (NH/ OH), 3159 (Ar-C-H), 2935 (C-H), 1631 (C=C), 1436, 1358 (S=O stretch) ; 1165 (S=O);; δ_H (400MHz; DMSO-d_6): 12.77 (1H, s br, N-H), 9.56 (1H, s br, -C=O-NH), 9.10 (2H, s br, 4' Ar-OH), 7.69 (2H, m, H-2'', 6''), 7.35 (2H, m, H-3'', 5''), 7.22 (1H, s, H-2), 7.12 (1H, d, *J* 0.9, H-2'), 7.02 (2H, d, *J* 16.4, H-7,13), 6.91 (2H, dd, *J* 8.2, 2.0, H-6, 6'), 6.91 (2H, d, *J* 16, H-8, 12), 6.76 (2H, d, *J* 8.0, H-5, H-5'), 6.60 (1H, s, H-10), 3.82 (6H, s, -OCH_3), 2.35 (3H, s, 4''-CH_3); δ_c (100 MHz): 157.0 (HN-CO-NH), 147.8 (C-4, 4'), 147.8 (C-4, 4'), 146.7 (C-3, 3'), 141.8/141.3, 129.2 (C-7, 13), 125.5 (C-1, 1'), 120.0 (C-6,6'), 115.6 (C-5, 5'), 109.6 (2, 2'), 99.3 (C-10), 55.6 (C-3 O-Me, 3'O-Me), 20.29 (4'' Ar-Me) EA Found C 62.26 %, H-5.33 %, N 7.35 % $C_{29}H_{27}N_3O_7S$ requires C 62.02 %, H-4.85 %, N 7.48 % S 5.71 %

_N_-(4-chlorophenylsulfonyl)-3, 5-bis-(4-hydroxy-3-methoxystyryl)-1_H_-pyrazole-1-carboxamide, 2.3.3

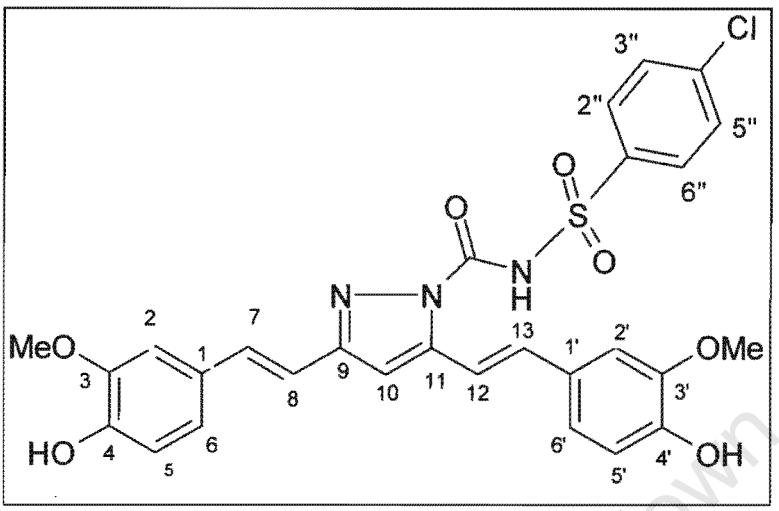

Yellow-brown powder (42 mg, 26 %); m.p. 218°C; R_f (EtOAc:CH_2Cl_2 1:1) 0.31; IR ν_{max} (ACN) /cm^{-1}: 3609 (NH/ OH), 3529 (NH/ OH), 3159 (C=C-H), 2942 (C-H), 1631 (C=C), 1440, 1415, 1375, 1035; δ_H (300MHz, CD_3OD) 7.86 (2H, m, H''-2, H-6''), 7.53 (2H, m, H-3'', H-5''), 7.10 (2H, s, H-2, H-2'), 7.07 (2H, d, *J* 16.5, H-7, H-13), 6.97 (2H, d, *J* 8.1, H-6, H-6'), 6.87 (2H, d, *J* 16.3, H-8, H-12), 6.78 (2H, d, *J* 8.1, H-5, H-5'), 6.62 (s, H-10), 3.90 (6H, s, -OCH_3); δ_c (75 MHz, CD_3OD) 164.8 (NHC=ONH), 158.8 / 158.7 (C=N), 149.2/148.9 (C-4, 4'), 148.1 / 148.0 (C-3, 3'), 139.2, 132.4/ 132.3/ 132.1/ 131.9, 130.4/130.1/129.9/129.8 (C-7, 13), 128.8 (C-1, 1'), 121.4, 120.2 (C-6, 6'), 126.3, 122.3, 121.4, 120.3/ 119.9, 118.6/ 118.3, 116.5 / 116.4 (115.6 (C-5, 5'), 111.0/ 109.2/ 100.2/ 97.3109.6 (2, 2'), 55.8/ 56.5/ 56.4/ 53.5 ((C-3 O-Me, 3'O-Me)); LRMS (FAB): *m/z* 582.4. HPLC purity: 100 %, $t_{R'}$ = 11.61 min.

***N*-(4-flurophenylsulfonyl)-3, 5-bis-(4-hydroxy-3-methoxystyryl)-1*H*-pyrazole-1-carboxamide, 2.3.4**

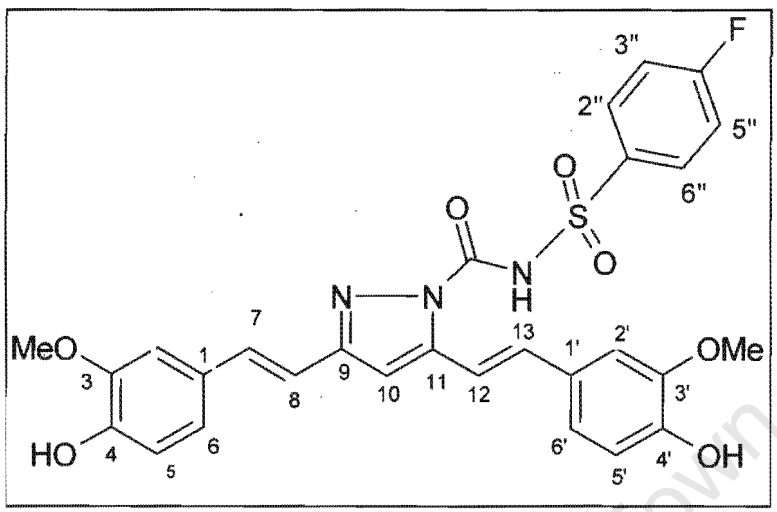

Yellow-green powder (20 mg, 13 %); m.p. 186-188°C ; R_f (EtOAc:CH_2Cl_2 1:1) 0.29 ;IR ν_{max} (ACN) /cm^{-1} 3623 (OH), 3551 (NH), 3203 (C=C-H), 2935 (C-H), 1628 (C=O), 1358 (S=O stretch) ; 1165 (S=O);δ_H (300MHz, CD_3OD): 7.37 (2H, d, *J* 8.7 Hz, H''-2, H-6''), 7.12 (2H, d, *J* 1.5 , H-2, H-2'), 7.08 (2H, d, *J* 16.5, H-7,H-13), 6.98 (2H, dd, *J* 8.25, 1.95, H-6, H-6'), 6.88 (2H, d, *J* 16.8, H-8, H-12), 6.79 (2H, d, *J* 8.4, H-5, H-5'), 6.62 (s, H-10), 3.91 (6H, s, -OCH_3); δ_C (100 MHz, CD_3OD) (major/minor) δ_C (100 MHz, DMSO- d_6) 159.6 (C=O)147.8 (C-4, 4'), 146.7 (C-3, 3'), 141.7 (2 C), 140.2 (2C), 129.4 (C-7, 13), 125.8/125.5 (C-1, 1'), 120.0 (C-6,6'), 115.6 (C-5, 5'), 109.6 (2, 2'), 99.2 (C-10), 55.6 (C-3 O-Me, 3'O-Me); LRMS (ESI): LR FAB MS: *m/z* 565.1. $C_{28}H_{24}N_3O_7SF$ HPLC purity: 100 %, $t_{R'}$ = 11.63 min.

***N*-(2-methyl phenylsulfonyl)-3, 5-bis-(4-hydroxy-3-methoxystyryl)-1*H*-pyrazole-1-carboxamide, 2.3.5**

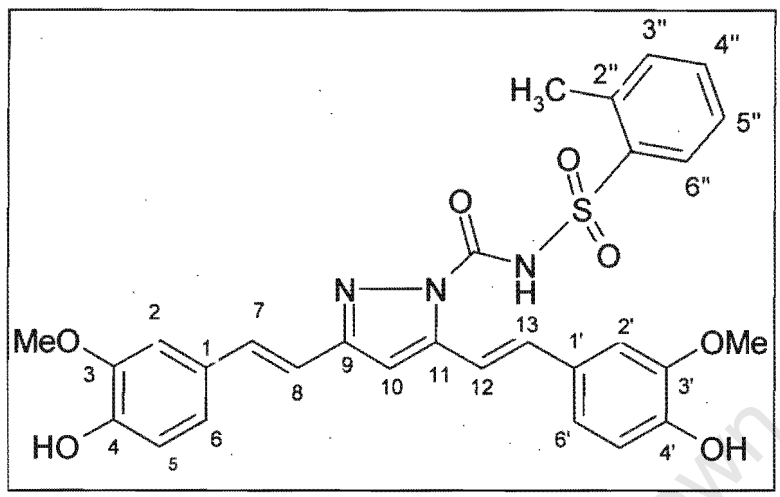

Yellow powder (51 mg, 33 %), m.p. 181-2°C; R_f (EtOAc: CH2Cl2 1:1) 0.31; (ACN) /cm^{-1} 3616 (OH), 3529 (NH), 3167 (C=C-H), 2935 (C-H), 1631 (C=C), 1444, 1418, 1375, 1034; δ_H (400MHz, CD_3OD): 79.4 (1H, m, H-6"), 7.43 (1H, m, H-4), 7.30 (2H, m, H-3",5"), 7.09 – 7.04 (4 H, m, H-2, H-2', H-7, 13), 6.96 (2H, m, H-6, H-6'), 6.86 (2H, d, *J* 16.3, H-8, H-12), 6.78 (2H, d, *J* 8.1, H-5, H-5'), 6.61 (s, H-10), 3.87 (6H, s, 3, 3'-OCH_3); 3.3 (3H, s, 2"-CH_3); 2.91/2.81/2.61 (3H, 2"-CH_3)δ_C (100 MHz, CD_3OD) 158.8 (C=N), 149.5/149.4 (C-4, 4'), 148.1/148.0 (C-3, 3'), 133.4/132.2, 132.5/132.5/132.4/132.1/131.9 (C-7, 13), 130.5/130.2, 128.9/128.5 (C-1, 1'), 127.0 (C-4, 4'), 121.4 (C-6, 6'), 110.5 (C-2, 2'), 100.2 (C-10), 56.4 (-OCH_3), 20.3; HPLC purity: 100 %, $t_{R'}$ = 11.60 min.

(4) **General synthesis of thiosemicarbazide reagents**

The method used was as described by Wiles and Suprunchuk [6]. A solution of hydrazine hydrate (0.022mmol in 25 ml of ethanol) was added drop wise a solution of phenylisothiocyanate or p-flurophenyl isothiocyanate (0.022 mmol in 5 ml diethyl ether). The reaction mixture was stirred gently for one hour at 35°C. The reaction mixture was reduced to about a third its initial volume *in*

vacuo. This lead to the formation of a precipitate which was filtered washed thrice with cooled diethyl ether and twice with ethanol.

4-Phenyl thiosemicarbazide, 2.4.1

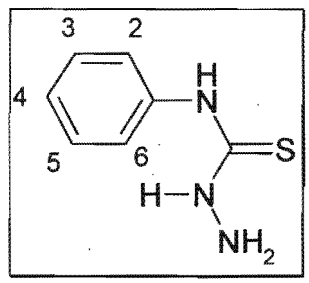

White powder (240 mg, 65 %) m.p. 140°C [lit. [6]141°C]; R_f (EtOAc:CH_2Cl_2 1:1) 0.29; δ_H (400 MHz, DMSO-d_6) 9.84 (1H, s br, N-H), 9.65 (1H, s br, N-H), 7.54 (2H, m, H-2, H-6), 7.33 (2H, m, H-3, H-5), 7.14 (1H, m, H-4), 3.29 (2H, s, $2NH_2$); δ_C (100 MHz, DMSO-d_6) 139.1, 128.1 (2C), 124.8 (2C)

4-Fluorophenyl thiosemicarbazide, 2.4.2

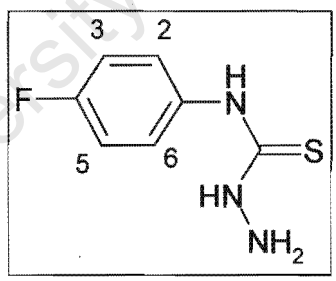

White powder (279 mg, 69 %) m.p. 188-189 [lit. [6] 189 °C]; R_f (EtOAc:CH_2Cl_2 1:1) 0.24; δ_H (400 MHz, DMSO-d_6) 9.08 (1H, s br, NH), 7.6 (2H, m, H-2, H-6), 7.10 (2H, m, H-3, H-5), 4.77 (2H, s br, NH_2) δ_C (100 MHz, DMSO-d_6) 179.8 (C=S), 160.0 (C-4), 157.6 (C-1), 135.6 (2C), 125.8 (2C). E. A. Found C-45.36 %, H-4.49 % N-23.39 %, S-17.19 % $C_7H_8N_3SF$ requires C-45.39 %, H-4.35 % N-22.69 %, S-17.31 % F-10.26 %.

(5) **General Procedure for the synthesis of thiosemicarbazone derivatives**

Technical grade curcumin (3g, 8.15 mmol) was added to a solution of one equivalent of thiosemicarbazide in 50 ml glacial acetic acid. The reaction mixture was stirred at 85°C for 72 hours. The reaction was stopped by the addition 50 ml of water and extracted with 50 ml portions dichloromethane three times. The organic extracts were combined, washed with saturated brine solution and evaporated *in vacuo* and subjected to column chromatography.

1, 7-bis (4-hydroxy-3-methoxyphenyl)-5-oxohepta-1, 6-diene-3-ylidene) hydrazinecarbothioamide, 2.5.1

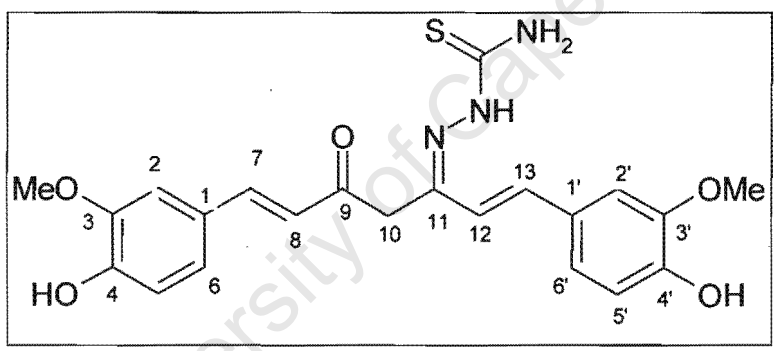

The general procedure for the synthesis for thiosemicarbazone derivatives was applied. The organic layer was eluted with dichloromethane: ethyl acetate (7:3). Fractions yielded an orange-red precipitate (21 mg, 1 %), m.p. 163-165°C; R_f (EtOAC: CH_2Cl_2) 0.43; IR ν_{max} (KBr) /cm^{-1} 3428 (NH, OH), 2891 (C-H), 2826 (C-H), 1631 (C=C), 1509 (C=N), 1277 (C=S stretch); 1140 (C=S); δ_H (400 MHz, DMSO-d_6), 9.59 (2H,s, Ar-OH), 7.54 (2H,d, *J* 16.0, H-7, H-13), 7.31 (2H, d, *J* 2.0, H-2, 2') , 7.14 (2H, dd, *J* 8.0, *J* 2.0, H-6, H-6'), 6.82 (2H, d, *J* 8.4, H-5, H-5'), 6.74 (2H, d, *J* 16.0 , H-8, H-12), 6.06 (1H, s, H-10), 3.83 (6H, s, Ar-OMe), 3.29 (2H, s br, NH_2); δ_C (100 MHz, DMSO-d_6)183.3, 159.7, 149.3, 147.9, 140.6, 140.3, 130.2, 126.3, 125.8, 123.0, 121.0, 115.8,115.6, 100.7, 55.7; HPLC purity: 95 %, $t_{R'}$ = 15.693 min.

Isomer of (*E*)-2-((1*E*, 6*E*)-1, 7- bis (4-hydroxy-3-methoxyphenyl)-5-oxohepta-1, 6-dien-3-ylidene)-*N*-methyl hydrazinecarbothiomide, 2.5.2a

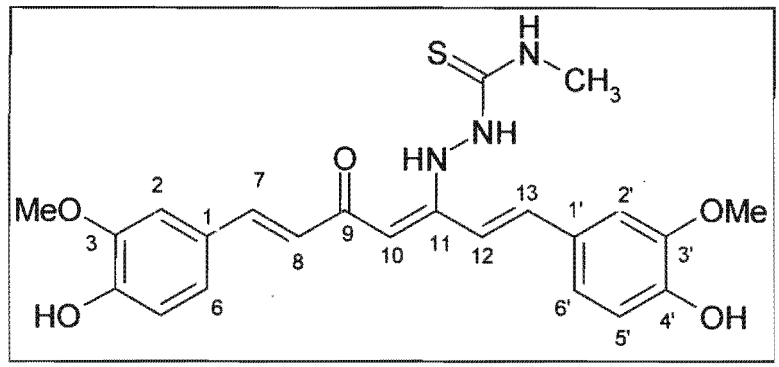

Curcumin (100 mg, 0.272 mmol) was suspended in isopropanol (10ml). Acetic acid (0.5ml) and one equivalent of N-methyl thiosemicarbazide were added to the reaction mixture which was stirred for 6 hours at 65°C. The reaction mixture was reduced to dryness and dissolved in methanol (10ml). A precipitate formed which was dissolved in ethyl acetate and subjected to preparative TLC on silica gel using methanol: DCM (1:39) as the eluent. The fastest moving band with an R_f value of 0.6 afforded an orange colored compound. Orange powder (12 mg, 10%); m.p. 173°C; R_f (EtOAc:CH_2Cl_2 3:97) 0.18; (KBr) /cm^{-1} 3435 (br N-H, O-H), 2884 (C-H), 2826 (C-H), 1631 (C=C);δ_H (400 MHz, CD_3OD) 10.02 (2H, s br, 4,4'-Ar-OH), 8.56 (1H, d, *J* 16.0, H-7/13), 8.07 (1H, d, *J* 16.8, H-7/13), 8.01 (1H, s, H-10), 7.99 (1H, d, *J* 2.0, H-2/2'), 7.82 (1H, d, *J* 16.0, H-8/12), 7.78 (1H, d, *J* 2.0, H-2/2'), 7.74 (1H, d, *J* 16.4, H-8/12) , 7.73 (1H, dd, *J* 8.0,1.6, H-6/6'), 7.69 (1H, dd, *J* 8.4, 2.0, H-6/6'), 7.50 (1H, d, 2.0, H-2/2'), 7.50 (1H, d, *J* 8.0, H-5/5'), 7.49 (1H, d, *J* 8.0, H-5/5'), 4.51 (6H, s, Ar-OMe), 3.31 (3H, s, N-Me); δ_C (100 MHz, CD_3OD): 176.3, 130.4, 126.4, 123.3, 117.9, 112.7, 109.7, 109.5, 99.3, 59.5, 58.3. APCI MS: *m/z* (M+) 455.336

Isomer of (*E*)-2-((1*E*, 6*E*)-1, 7- bis (4-hydroxy-3-methoxyphenyl)-5-oxohepta-1, 6-dien-3-ylidene)-*N*-methyl hydrazinecarbothiomide, 2.5.2b

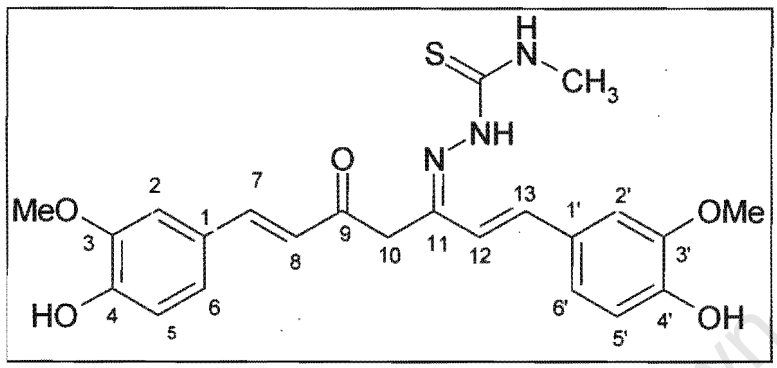

The method used for the synthesis of **2.5.2 a** was applied. The compound was obtained from the second band as a mixture of 2 isomers. Orange/red powder (16 mg, 13 %) m.p. 171-172°C; R_f (EtOAc:CH_2Cl_2 3:97) 0.12; R_f (EtOAc:CH_2Cl_2 3:7) 0.64, 0.80; IR ν_{max} (KBr) /cm^{-1} 3442 (br N-H, O-H), 2891 (C-H), 2826 (C-H), 1631 (C=C); δ_H (300 MHz, DMSO-d_6) 9.30 (1H, s, 4/4'Ar-OH), 9.28 (1H, s, 4/4'-Ar-OH), 7.88 (1H, d, *J* 16.2, H-7/13), 7.39 (1H, d, *J* 16.5, H-7/13), 7.32 (1H, s, H-2/2'), 7.32 (1H, d, *J* 1.5, H-2/2'), 7.14 (1H, d, *J* 16.5, H-8/12), 7.08 (1H, d, *J* 16.0, H-8/12), 7.03 (1H, dd, *J* 8.1, 1.5 H, H-6/6'), 7.00 (1H, dd, *J* 8.0, 2.3, H-6/6'), 6.83 (1H, d, *J* 7.5, H-5/5'), 6.80 (1H, d, *J* 8.1, H-5/5'), 3.86 (3H, m, Ar-OMe), 3.84 (3H, s, Ar-OMe), 2.49/2.49 (3 H, N-Me); δ_C (75 MHz, DMSO-d_6) 153.3, 147.9, 147.8, 147.7, 147.3, 136.3, 133.8, 127.7, 127.6, 121.3, 120.5, 115.8, 115.5, 115.2, 115.1, 110.6, 110.0, 107.0, 55.6; LRMS (ESI): *m/z* (M) 455.3; HPLC purity: 81 %, $t_{R'}$ = 19.88 min.

(*E*)-2-((1*E*, 6*E*)-1, 7- bis (4-hydroxy-3-methoxyphenyl)-5-oxohepta-1, 6-dien-3-ylidene)-*N*-phenyl hydrazinecarbothiomide, 2.5.3

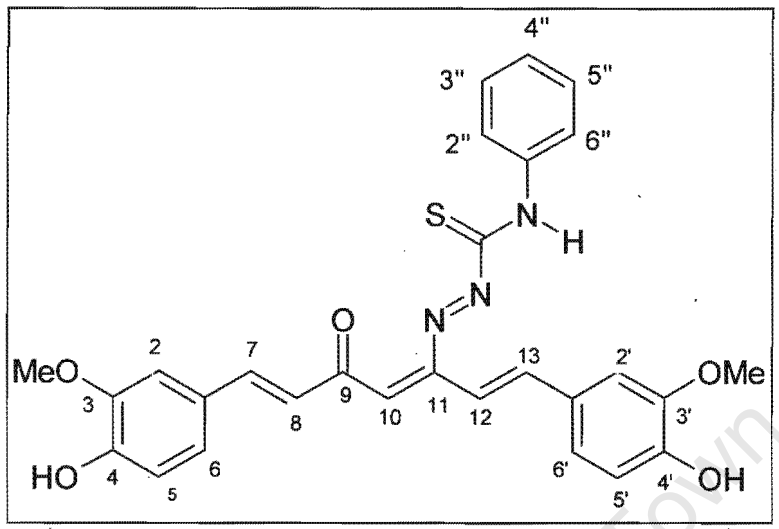

The general method for the synthesis of thiosemicarbazone derivatives was applied. The organic extract was eluted with n-hexane: ethyl acetate (1:1) to give a mixture of three isomers. Orange powder (71 mg, 5 %), m.p. 185-186°C, R_f (n-hexane: EtoAc 1:1) 0.33; IR ν_{max} (KBr) /cm^{-1} 3524 (NH/OH), 3061 (C=C-H), 3054 (C=C-H), 2987 (C-H), 1626 (C=O), 1540, 1511 (C=N), 1277 (C=S stretch); 1135 (C=S); δ_H (300 MHz, DMSO-d_6) Major component 10.15 (1H, s, N-H), 9.75 (2H, s, OH), 7.59 - 7.48 (5H, m, H-2'', H-3'', H-4'', H-5'', H-6''), 7.36 (2H, d, *J* 15.6, H-7, H-13), 7.29 (2H, d, *J* 1.8, H-2, H-2'), 7.13 (2H, dd, *J* 8.7, 2.1, H-6, H-6'), 6.85 (2H, d, *J* 8.4, H-5, H-5'), 6.72 (2H, d, *J* 16.6, H-8, H-12), 6.05 (1H, s, H-10), 3.86 (6H,s, O-CH_3); δ_C (75 MHz, DMSO-d_6) 186.7, 153.1, 150.0, 148.0, 143.6, 140.6, 133.3, 130.9, 129.8, 128.5, 127.3, 126.3, 123.4, 121.1, 117.4, 116.0, 112.2, 100.7, 55.6. Minor component δ_H (300 MHz, DMSO-d_6) 9.99 (IH, s, N-H), 9.58 (2H, s, OH), 7.59 to 7.48 (5H, m, H-2'', H-3'', H-4'', H-5'', H-6''), 7.36 (2H, d, *J* 15.6, H-7, H-13), 7.21 (2H, d, 1.5, H-2, H-2'), 7.10 (2H, dd, *J* 8.1, 1.5, H-6, H-6'), 6.81 (2H, d, *J* 7.8, H-5, H-5'), 6.66 (2H, d, *J* 16.0, H-8, H-12), 6.03 (1H, s, H-10), 3.82 (6H,s, O-CH_3); δ_C (75 MHz, DMSO-d_6) 183.1, 153.1, 149.3, 147.9, 143.6, 140.6, 133.3, 130.2, 129.3, 128.1, , 126.1, 123.0, 121.1, 117.4, 115.8, 111.4, 100.7, 55.6

(*E*)-2-((1*E*, 6*E*)-1, 7- bis (4-hydroxy-3-methoxyphenyl)-5-oxohepta-1, 6-dien-3-ylidene)-*N*-(4-fluorophenyl) hydrazinecarbothiomide, 2.5.4

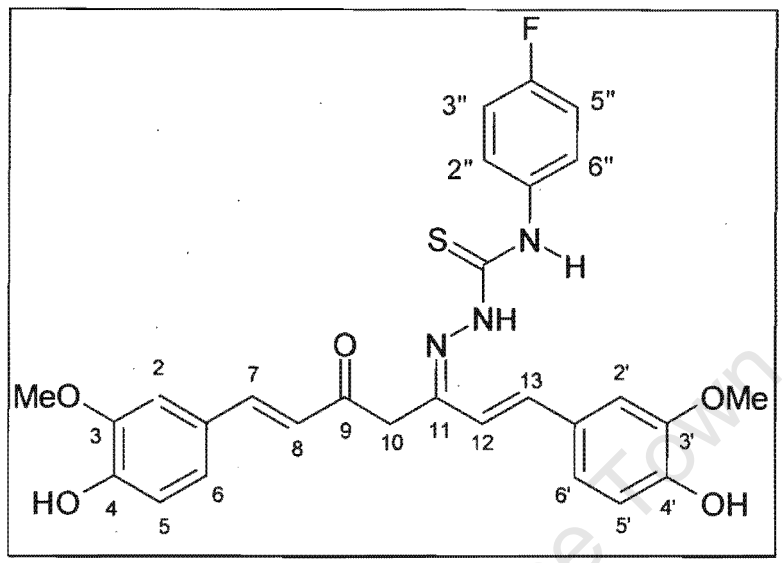

The general method for the synthesis of thiosemicarbazone derivatives was applied. The organic extract eluted on dichloromethane followed by MeoH: DCM (1:9). The product was obtained from fractions which formed a yellow precipitate. The precipitate was rinsed with methanol. Yellow powder (48 mg, 3 %), m.p. 212-214°C; R_f (EtOAc: CH_2Cl_2 3:97) 0.12; IR ν_{max} (KBr) /cm^{-1} 3684 (OH/NH), 3600 (OH/NH), 3061 (C=C-H), 3052 (C=C-H), 2987 (C-C-H), 1606, 1511 (C=N) 1277 (C=S stretch); δ_H (300MHz, DMSO-d_6) 9.81(2H, s, Ar-OH), 9.58 (1H, s, N-H), 7.55 (4H, m, H-6, H-6', H-2", H-6"), 7.52 (2H, *J* 15.9, H-7, H-13), 7.29 (2H, d, *J* 1.2, H-2, H-2'), 7.12 (4H, m, H-6, H-6', H-3", H-5"), 6.81 (2H, d, *J* 8.1, H-5, H-5'), 6.72 (2H, d, *J* 15.9, H-8, 12), 6.05 (1H, s, H-10); δ_c (75 MHz, DMSO-d_6) 183.1, (C=O),158.3 (C=S), 155.7 (C=N), 155.2, 149.3, 148.0, 140.6, 137.6, 126.3 (b), 123.0, 121.1, 118.4/118.3/115.7/115.5/115.2, 111.4, 100.7, 55.7; EA Found C, 62.94; H-4.55; N, 8.24; S, 5.04 $C_{28}H_{26}N_3SFO_5$ requires C, 62.79; H, 4.89; N, 7.85; S-5.99; F, 10.26

5-(2-(7-Chloroquinolin-4-yl)-hydrazino)-3-hydroxyhepta-1, 3, 6-triene-1, 7 –diyl) bis (2-methoxyphenol), 2.7.1a

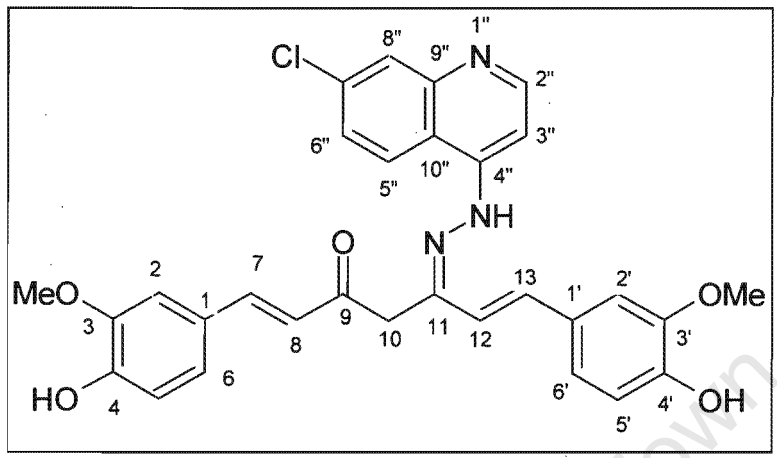

Technical grade curcumin (3g, 8.152 mmol) and 1 equivalent of 7-chloro-4-hydrazinoquinoline were dissolved in 50 ml of glacial acetic acid and heated at 80°C for 5 days with stirring. The reaction was stopped and worked up as previously described for the synthesis of isoxazole derivatives. The organic extract was evaporated *in vacuo* and eluted with dichloromethane using column chromatography. A precipitate formed from one of the factions and was rinsed with ethyl acetate: dichloromethane (1:1). Bright yellow powder (191 mg, 4 %) m.p.156°C; R_f (EtOAc: CH_2Cl_2 3:97) 0.310; IR ν_{max} (KBr) /cm^{-1} 1758 (C=O), 1631 (C=C), 1595 (C=N), 1509 (C=N), 1216 (C-O), 1194 (C=C-OH); 400 MHz, DMSO-d_6) (major/minor/minor/minor/minor) 7.77 (1H, d, *J* 8.4, H-5''), 7.63 /7.64/ 7.64/4.63 (2H, d, *J* 15.6, H-7, H-13), 7.49 (1H, d, *J* 1.6, H-8''), 7.31 (1H, dd, *J* 8.2, 1.8, H-6''), 7.20 (1H, d, *J* 8.8, H-2''/3''), 7.14 (1H, d, *J* 8.0, H-2''/3''), 6.96/6.97/6.91/6.91 (2H, d, *J* 16.0, H-8, H-12); 6.19/6.17/6.17 (1H, s, H-10), 3.85/3.83/3.82 (6H, s, Ar-OMe); δ_C (100 MHz, DMSO-d_6) 183.1 (C=O),169.6/ 169.1(C=N), 152.6, 151.9, 141.7, 140.5/140.1 , 134.4, 133.0, 130.2, 125.3/125.1, 124.0, 123.1, 122.1, 112.8 (C-5,5'), 102.4/ 102.3, 56.7 (C-3 O-Me, 3' O-Me); EA Found C - 66.18 %; H, 5.64 $C_{31}H_{30}N_3O_5Cl$ requires C, 66.48; H, 5.40; N, 7.50; HPLC purity: 91 %, $t_{R'}$ = 18.01 min.

5-(2-(7-Chloroquinolin-4-yl)-hydrazono)-3-hydroxyhepta-1, 3, 6-triene-1, 7 –diyl) bis (2-methoxyphenol), 2.7.1b

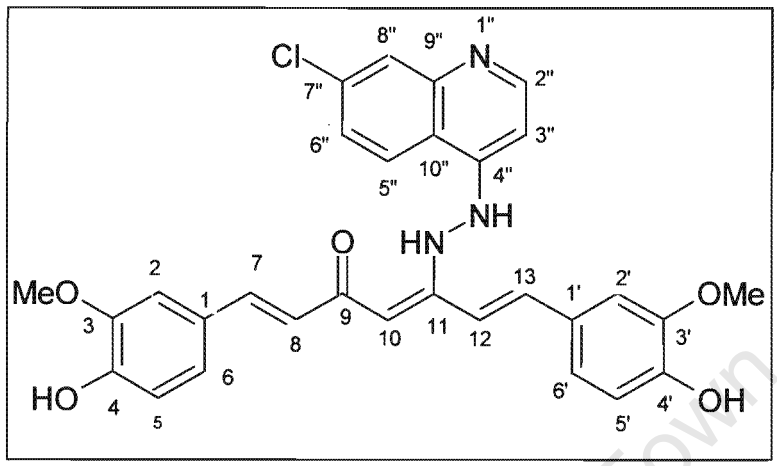

A precipitate that formed was rinsed with ethyl acetate: dichloromethane (1:1). It was obtained as a yellow-green powder (61 mg, 1 %) m.p. 155-156°C; R_f (EtOAc: CH_2Cl_2 3:97) 0.31; IR ν_{max} (KBr) /cm^{-1} 3051 (C=C-H), 2935 (C-H), 2841 (C-H), 1754 (C=O), 1628 (C=C), 1595 (C=N), 1191 (C=C-OH stretch); δ_H (400 MHz, DMSO-d_6) 9.62 (2H,s, Ar-OH), 7.63 (2H, d, *J* 16, H-7, H-13), 7.49 (2H, d, *J* 1.6 Hz, H-2', H-2''), 7.30 (2H, dd, *J* 8.2, 1.8 Hz, H-6, H-6'), 7.14 (2H, d, *J* 8.0, H-5, H-5'), 6.96 (2H, d, *J* 16.0, H-8, H-12), 6.19 (1H, s, H-10), 3.84 (6H, s, Ar-OMe); δ_H (100 MHz, DMSO-d_6) 183.6 (C=O), 168.3 (C=N), 151.1, 140.4, 139.7, 133.6, 124.5, 123.2, 121.3, 112.0, 101.6, 55.9; EA Found C, 66.31; H, 5.36; N, 7.50 $C_{31}H_{30}N_3O_5Cl$ requires C, 66.48 %; H, 5.40; N, 7.50; HPLC purity: 94 %, $t_{R'}$ = 18.09 min.

2, 2'-(1-(7-Chloroquinoline-4-yl)-1*H*-pyrazole-3, 5-diyl) bis (ethane-2, 1-diyl) bis (2-methoxyphenol), 2.8.1

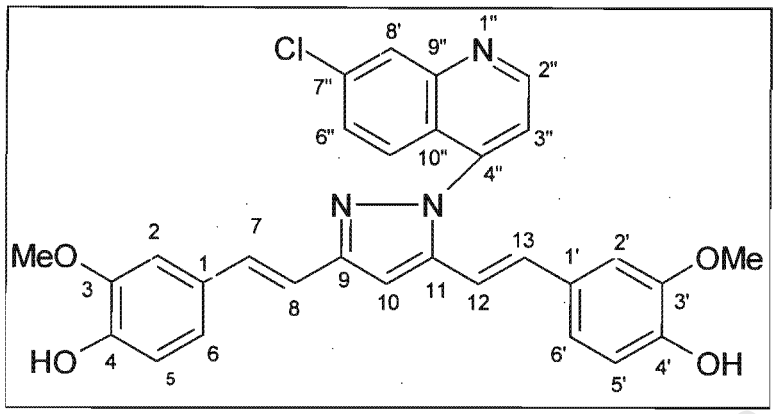

Technical grade curcumin (3g, 8.152 mmol) and 1 equivalent of 7-chloro-4-hydrazinoquinoline were dissolved in 50 ml of glacial acetic acid and heated at 80°C for 5 days with stirring. The reaction was stopped and worked up as previously described for the synthesis of the isoxazole derivatives. The organic extract was evaporated *in vacuo* and eluted with dichloromethane using column chromatography. Fractions were combined, reduced to dryness *in vacuo* and further eluted with petroleum ether: ethyl acetate (5:3). A precipitate formed from the fractions. A mixture of 3 isomers was obtained as a dull yellow precipitate (24 mg, 0.56 %), m.p. 158-161°C; R_f (CH_2Cl_2:EtOAc (6:4) 0.5; IR ν_{max} (KBr) /cm^{-1} 3413 (s, br OH, NH), 1606 (C=C), 1588 (C=N), 1512 (C-O); δ_H (400 MHz, DMSO-d_6) (major/minor/minor) 8.23 (1H, d, *J* 2.0, H-8"), 7.85/7.70/7.70 (1H, d, *J* 9.2, H-5"), 7.71 (1H, dd, *J* 9.0, 2.2, H-6"), 7.62 (1H, d, *J* 4.8, H-2"), 7.44 (1H, d, *J* 8.4, H-3"), 7.22 (2H, s, *J* 4.8, H-2, 2'), 7.22 (2H, d, *J* 16, H-7/ H-13), 7.22 (1H, d, *J* 16.4, H-7/13), 7.06 (1H, d, *J* 16.4, H-8/12), 6.98 (1H, d, *J* 16.0 Hz, H-8/12), 6.98 (1H, m, H-6/6'), , 6.88 (1H, dd, *J* 8.4, 2.0, H-6/6'), 6.79 (1H, d, 8.4 Hz, 5/5'), 6.69/ 6.69 (1H, d, 8.4, 5/5'), 6.60/ 6.59/ 6.56/ 6.55 (1H, s, H-10), 3.83/ 3.70/ 3.69 (6H, s, Ar-OMe); δ_c (100 MHz, DMSO-d_6): (major/minor/minor)152.4/ 152.3 (2C, C=N), 149.6 (1C), 147. 9/ 147.7/ 147.5 (2C, C-4, 4'), 147.0 (2C, C-3, 3'), 144.5 (1C), 142.8 (1C), 134.8 (1C), 133.6 (1C), 131.7 (1C), 128.4/ 128.1/ 127.9/ 127.5 (2C, C-7, 13), 126.1 (2C, C-1, 1'), 122.8 (1C), 120.5/120.4 120.0 (2C, C-6,6'), 119.3 (1C) , 116.9/ 115.6/115.5 (C-5, 5'), 111.3 (1C), 110.7/109. 7/109.6 (2C, 2, 2'), 100.7/99.3

(1C, C-10), 55.6/55.60 (2C, C-3 O-Me, 3'O-Me); LRMS (FAB): *m/z* (M+l) 526.3; EA Found: C, 68.53; H, 4.56; N, 7.58 $C_{30}H_{24}N_3O_4Cl$ requires C, 68.24; H – 4.96; N, 7.96.

(7) **General methods for the synthesis of *N*-acyl hydrazone derivatives**

Method A: One equivalent of the acid hydrazide was added to curcumin (2g, 5.43 mmols) in glacial acetic acid (50ml). The reaction mixture was stirred at 70°C for 72 hours. The reaction was stopped by the addition 50 ml of water and extracted with 50 ml portions dichloromethane three times. The dichloromethane extracts were combined and washed with saturated brine solution. The organic extracts were combined, evaporated *in vacuo* and subjected to column chromatography on silica gel.

Method B: Sodium acetate (0.025 mg) was added to a solution of curcumin (100mg, 271.8 mmols) in isopropanol (10 ml). The reaction mixture stirred for 10 minutes. One equivalent of the aryl acid hydrazide (135.9 mmols) was added to the reaction mixture which was stirred at 65°C for 48 hours. A precipitate formed when the reaction was stopped by the addition of water. It was filtered off and left to dry.

N'-((1E, 6E)-1, 7-bis (4-hydroxy-3-methoxyphenyl)-5-oxohepta-1, 6-dien-3-ylidene) benzohydrazide, 2.9.1

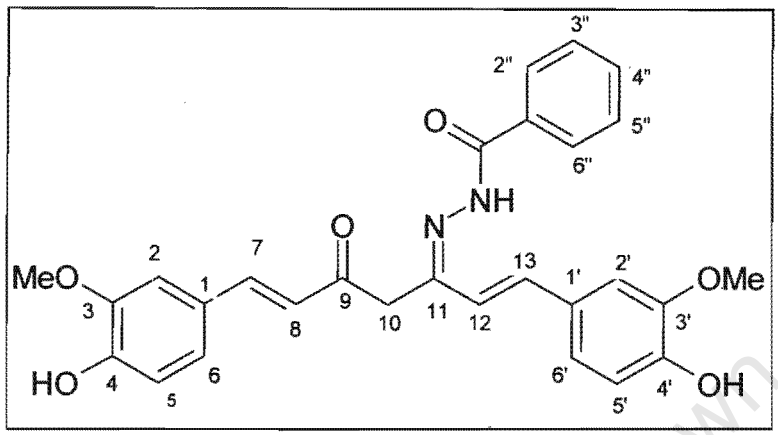

Method A was applied. The organic was eluted on silica gel column using pet. ether: EtoAC (1:3). It was obtained as an orange precipitate (26mg, 2 %), m.p. 165°C;R_f (EtOAc:CH_2Cl_2 3:97) 0.35; IR ν_{max} (CH_2Cl_2) /cm^{-1} 3525 (O-H, N-H), 3051 (s) (C=C-H), 3013 (C=C-H), 2986 (C-H), 2928 (C-H), 1686 (C=O), 1627 (C=C), 1512 (C-O); δ_H (400 MHz, CD_3OH) 7.93 (2H, d, *J* 7.2, H-2", H-6"), 7.56 (2H, d, *J* 15.6, H-8, H-12), 7.43 (3H, m, H-3", H-4", H-5"), 7.19 (2H, s, H-2, H-2'), 7.09 (2H, d, *J* 8.4, H-6, H-6'), 6.82 (2H, d, *J* 8.0, H-5,H-5'), 6.60 (2H, d, *J* 16.0, H-7, H-13), 3.93 (6H, s, Ar-OMe); δ_C (100 MHz, CD_3OH) 184.8, 150.5, 149.4, 142.1, 129.8, 122.9, 116.6, 111.6, 111.8, 56.5; HPLC purity: 100 %, $t_{R'}$ = 14.70 min.

N'-((1E, 6E)-1, 7-bis (4-hydroxy-3-methoxyphenyl)-5-oxohepta-1, 6-dien-3-ylidene)-4-chlorobenzohydrazide, 2.9.2

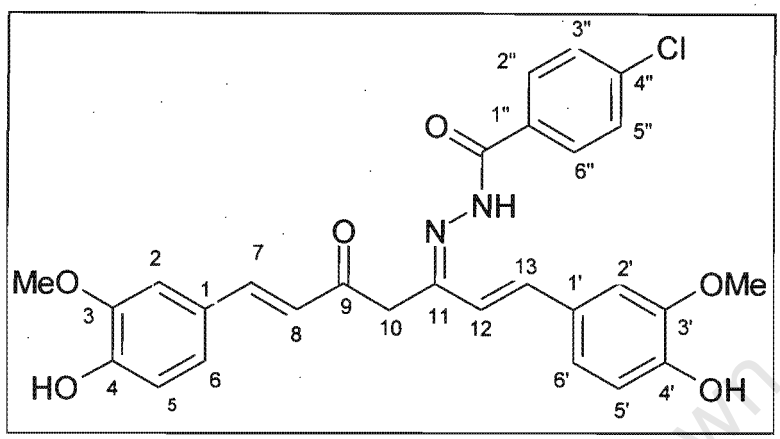

Method A was applied. The reaction mixture was eluted on silica gel using pet. ether: EtoAC (1:3). Fractions formed an orange/red precipitate (22 mg, 1 %) m.p 164-165°C; R_f (EtOAc: CH2Cl2 3:97) 0.22; IR ν_{max} (ACN) /cm^{-1} 3630 (br, OH),3536 (br, NH), 3167 (C=C-H), 2993 (C-H), 1635 (C=O), 497 (C-Cl) ;δ_H (400 MHz, CD_3OD) 7.96 (2H, s, H-2", H-6"), 7.55 (2H, d, *J* 16, H-7, H-13), 7.30 (2H, d, *J* 1.6, H-2, 2'), 7.14 (2H, dd, *J* 6.8, 1.6 Hz, H-6, H-6'), 6.82 (2H, d, *J* 8.0, H-5, H-5'), 6.73 (2H, d, *J* 15.6, H-8, H-12), 3.89 (6H, s, Ar-O-CH_3); δ_C (100 MHz, CD_3OH) 184.6 (1C, C=O), 164.9 (1C, NH-C=O), 150.5 (2C, C-4, 4'), 149.4 (2C, C-3, 3'), 142.1 (2C, C-7, 13), 129.9 (2C, C-2", 6"), 128.6 (2C, C-3", 5"), 124.1 (2C, C-6,6'), 122.3 (2C, C-8, 12), 116.6 (2C, C-5,5'), 111.9 (2C, C-2,2'), 56.5 (2C, C-3, 3' MeO-Ar); δ_H (400 MHz, DMSO-d_6) (major/minor) 7.93 (2H, d, *J* 8.4, H-2", H-6"), 7.67 (2H, m, H-3", H-5")/7.59 (2H, d, 8.4 Hz, H-3," 5"), 7.54 (2H, d, *J* 16, H-7, H-13), 7.30 (2H, d, *J* 1.6, H-2), 7.19 (1H, d, *J* 1.6, H-2'), 7.08 (2H, dd, *J* 6.8, 1.6 Hz, H-6, H-6'), 6.81 (2H, d, *J* 8.4, H-5, H-5'), 6.60 (2H, d, *J* 16, H-8, H-12), 3.89 (6H, s, Ar-O-CH_3)δ_C (100 MHz, DMSO-d_6) 183.1 (1C, C=O), 164.5 (1C, NH-C=O), 149.3(2C, C-4, 4'), 147.9 (2C, C-3, 3'), 140.6 (2C, C-7, 13), 131.4 (2C, C-2", 6"), 128.6 (2C, C-3", 5"),126.3 (2C, C-1, 1'), 123.0 (2C, C-6,6'), 121.0 (2C, C-8, 12), 115.6 (2C, C-5,5'), 111.4 (2C, C-2,2'), 100.7 (1 C, C-10), 55.6 (2C, C-3, 3' MeO-Ar). HPLC purity: 100 %, $t_{R'}$ = 15.68 min.

N'-((1E, 6E)-1, 7-bis (4-hydroxy-3-methoxyphenyl)-5-oxohepta-1, 6-dien-3-ylidene)-4-hydroxybenzohydrazide, 2.9.3

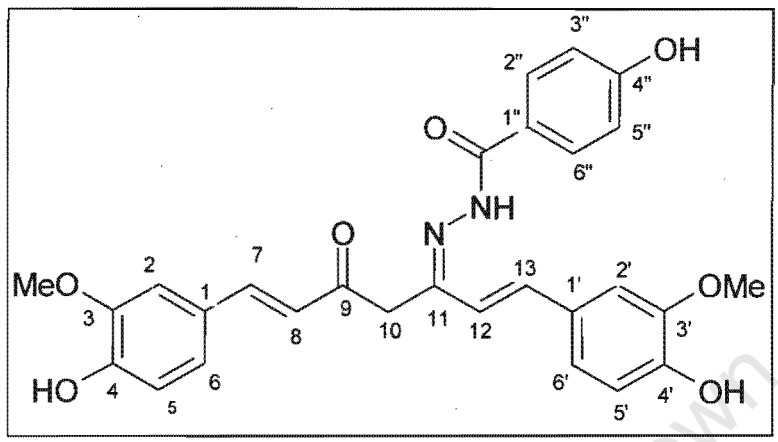

Method B was applied. Orange powder (36 mg, 26 %); m.p. 174°C; R_f (EtOAc:CH_2Cl_2 1:9) 0.42; IR ν_{max} (ACN) /cm^{-1} 3420 (br, NH, OH), 2884 (C-H), 1631 (C=O); δ_H (400 MHz, CD_3OD) (major/minor) 7.66 / 7.74 (2H, d, *J* 9.0, H-3'', H-5''), 7.56 (2H, d, *J* 15.7, H-7,13), 7.20 (2H, d, *J* 1.8,H-2, H-2'), 7.10 (2H, m, H-6, H-6'), 6.82 (4H, m, H-5, H-5', H-2'', H-6''), 6.61 (2H, d, *J* 15.7, H-8, H-12), 5.47 (s, H-10), 3.91 (6H, s, -OCH_3); δ_c (100 MHz, CD_3OD) 193.3, 160.9, 150.5, 149.5, 142.1, 130.1, 128.6, 124.1, 122.3,116.6, 116.2, 111.8, 56.5; EA Found C, 66.58; H, 5.52; N, 5.94 $C_{28}H_{26}N_2O_7$ requires C, 66.92; H, 5.22; N, 5.57.

N'-((1E, 6E)-1, 7-bis (4-hydroxy-3-methoxyphenyl)-5-oxohepta-1, 6-dien-3-ylidene) isonicotinohydrazide, 2.9.4

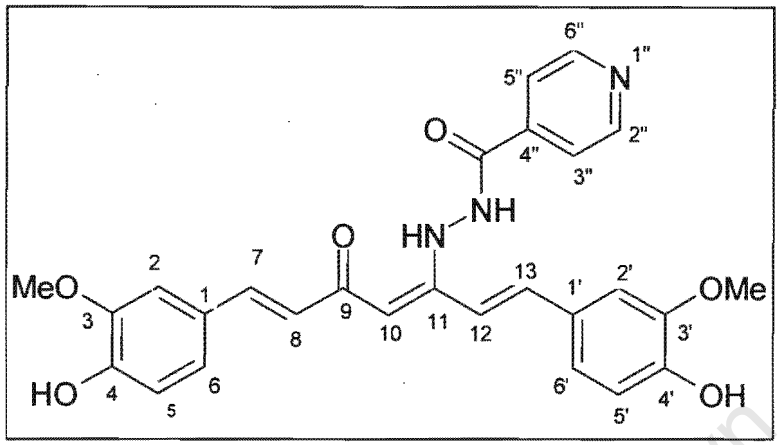

Method A was applied. The organic extract was eluted with pet. ether: EtoAc (1:1). A precipitate was obtained as a mixture of 3 isomers. Orange-red powder (21 mg, 2 %), m.p.155-157°C ; R_f (EtOAc:CH_2Cl_2 3:97) 0.46; IR ν_{max} (KBr) /cm^{-1} 3687 (N-H / O-H), 3599 (N-H / O-H), 3526 N-H / O-H, 3071 (C=C-H), 3051 (C=C-H), 2986 (C-H), 1627 (C=O), 1605 (C=C); δ_H (400 MHz, *d*-DMSO) 7.56-7.47 (4H, m, H-2'', 3'', 4'', H-5''), 7.31 (2H, s, H-2, H-2')/ 7.27 (2H, d, *J* 1.6 H-2, H-2'), 7.14 (2H, dd, *J* 8.2, 1.8, H-6, H-6')/ 7.07 (2H, dd, *J* 8.0, 2.0, H-6, H-6'), 6.82/6.72 (2H, d, *J* 8.0, H-5, H-5'), 6.74/6.74/6.67 (2H, d, *J* 16, H-7, H-13), 6.35/6.28 (2H, d, *J* 16, H-8, H-12), 6.06/6.04/6.03 (1 H, s, H-10), 3.84/3.82/3.81 (6H, s, -OCH_3); δ_c (100 MHz, *d*-DMSO) 183.2/183.1, 167.9, 159.7, 149.3/149, 147.9/149.8, 144.4/144.1, 140.6/140.3, 130.2/130.0, 126.3/125.8, 123.0/122.7, 121.120.8, 115.8/115.7/115.6/115.3, 114.4/111.3/111.2, 107.7, 100.8/100.7, 94.9, 55.6/58.3; LRMS (FAB) *m/z* $(M+1)^+$ 488.2

(3, 5-bis (4-hydroxy-3-methoxystyryl))-1*H*-pyrazol-1-yl (phenyl) methanone, 2.10.1

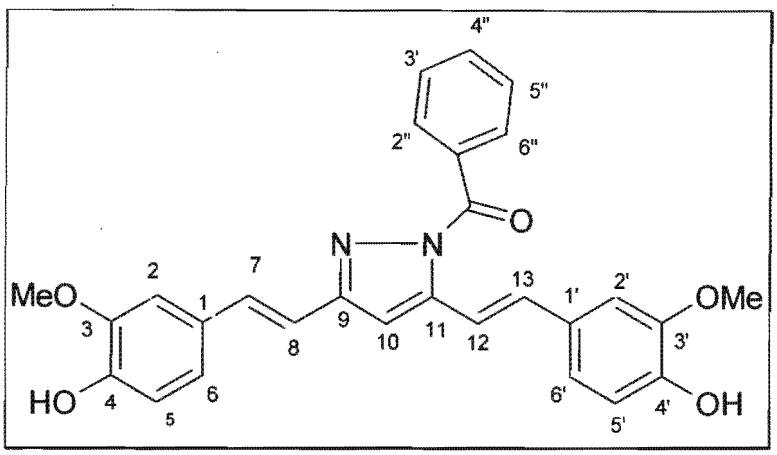

Method A was applied. The organic layer was eluted with petroleum ether: ethyl acetate (1:1) to give the product as an orange-red precipitate (19 mg, 1 %); m.p. 168°C; R_f (EtOAC: CH_2Cl_2 1:1) 0.23; IR ν_{max} (KBr) /cm^{-1} 3428 (O-H, N-H), 2957 (C-H), 2913 (C-H), 1722 (C=O); 1631 (C=C), 1512 (C-O), 1465 , 1375, 1277 δ_H (600 MHz, Acetone-d_6) 7.75 (2H, m, H-2", H-6"), 7.65 (3H, m, H-3", H-4", H-5"), 7.20 (2H, d, *J* 1.8, H-2, H-2'), 7.12 (2H, d, *J* 16.2, H-7, H-13), 7.00 (2H, dd, *J* 9.0, 2.4, H-6, H-6'), 6.99 (2H, d, *J* 16.2, H-8, H-12), 6.83 (2H, d, *J* 8.4 , H-5,H-5'), 6.66 (1H, s br, H-10), 3.92 (6H, s, Ar-OMe); δ_C (150 MHz, Acetone-*d*) 167.1 (C=O), 147.7 (2C, C-4, 4'), 146.8 (2C, C-3, 3'), 132.0, 131.1, 129.7, 129.3 (2 C, C-7, 13), 128.7 (2C, C-1, 1'), 120.3 (2C, C-6,6'), 115.9 (C-5, 5'), 115.1, 109.0 (2C, C-2, 2'), 99.1 (1C, C-10), 55.3 (2C, C-3, 3' Ar-OMe); LRMS (ESI): *m/z* (M+1) 469.5; HPLC purity: 90 %, $t_{R'}$ = 12.34 min.

(3, 5-bis (4-hydroxy-3-methoxystyryl)-1*H*-pyrazol-1-yl (4-hydroxy-phenyl) methanone, 2.10.3

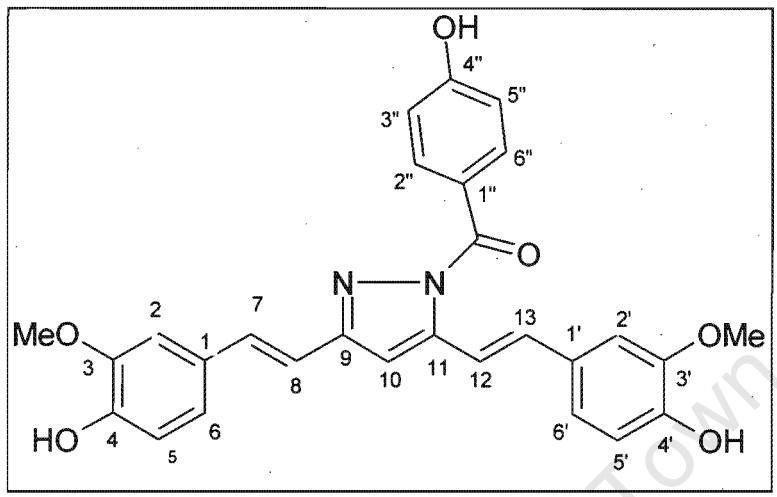

Method A was applied. The organic extract was eluted with methanol: DCM (1:19) to give the compound as a pale yellow precipitate (66mg, 2 %), m.p. 184-185°C, R_f (CH_3OH: DCM 1:19) 0.23 ; IR ν_{max} (KBr) /cm^{-1} 3684 (OH/NH), 3601 (OH/NH), 3534 (OH), 3061 (C=C-H), 3052 (C=C-H), 2987 (C-C-H), 2928 (C-C-H), 1606, 1513, 1275;δ_H (300MHz; DMSO-d_6): 12.65 (1H, s br, 4''-Ar-OH), 9.50 (1H, s br, 4-Ar-OH), 9.15 (1H, s br, 4'-Ar-OH), 7.35 (2H, d, *J* 8.7, H-2'',H-6''), 7.12 (1H, d, *J* 0.9, H-2/2'), 7.03 (2H, d, *J* 16.8, H-7, H-13), 6.93 (1H, d, *J* 0.9, H-2/2'), 6.92 (2H, m, H-6, H-6'), 6.84 (2H, d, *J* 16.5, H-8, H-12), 6.76 (4H, *J* 8.4, H-5, H-5', H-3'', H-5''), 6.60 (s, H-10), 3.83 (6H, s, -OCH_3); δ_c (75 MHz, DMSO-d_6) 157.3 (C=O) , 147.9 (2 C, C-4, 4'), 146.7 (2 C, C-3, 3'), 129.5 (2 C, C-7, 13), 128.3 (2 C), 127.6 (2 C), 120.0 (2 C, C-6,6', C-1, 1'), 115.6 (4 C, C-5, 5'), 109.6 (2 C, 2, 2'), 99.2 (1 C, C-10), 55.6 (2 C, C-3, 3' Ar-OMe); HPLC purity: 70 %, $t_{R'}$ = 12.686 min.

(3, 5-bis (4-hydroxy-3-methoxystryryl)-1*H*-pyrazol-1-yl) furan-2-yl) methanone, 2.10.5

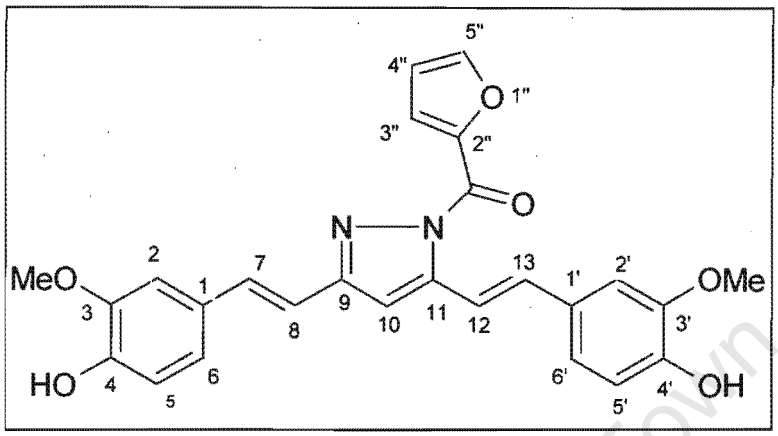

Method B was applied. The precipitate obtained was filtered, rinsed with cooled isopropanol, dissolved in ethyl acetate and extracted with water to get rid of sodium acetate. The organic layer air-dried. A yellow powder was obtained after drying (40 mg, 65 %), m.p. 180-181°C; R_f (EtOAc:CH_2Cl_2 3:97) 0.20; IR ν_{max} (ACN) /cm^{-1} 3627 (O-H), 3540 (N-H), 3238 (w, br), 3166 (C=C-H), 3013 (C=C-H), 2992 (C-H), 2941 (C-H), 1631 (C=C), 1539 (C-O), 1518 (C-O); δ_H (400 MHz, DMSO-d_6) 9.33 (1H, s br, 4-Ar-OH), 9.26 (1H, s br, 4'-Ar-OH), 8.17 (1H, d, *J* 1.6, N-H), 7.99 (1H, d, *J* 3.2, H-2"), 7.62 (1H, d, *J* 16.4, H-7/13), 7.32 (1H, d, *J* 16.4, H-7/13), 7.30 (1H, d, *J* 8.8, H-5/5'), 7.28 (1H, d, *J* 1.6, H-2/2'), 7.27 (1H, d, *J* 16.0, H-8/12), 7.14 (1H, d, *J* 2.0, H-2/2'), 7.08 (1H, d, *J* 16.4, H-8/12), 7.02 (1H, dd, *J* 8.1, 4.2, H-5"), 7.02 (1H, d, *J* 8.0, H-5/5'), 6.84 (1H, s, H-10), 6.83 (2H, dd, *J* 8.4, 1.6, H-6, H-6'), 6.82 (1H, dd, *J* 5.4, 1.8, H-4"), 3.83 (6H, s, 3, 3' Ar-O-CH_3); δ_C (100 MHz, DMSO-d_6) 156.3, 154.1, 149.1, 147.9/147.9, 147.7/147.5 (2C, C-4, 4'), 146.9 (2C, C-3, 3'), 145.0, 134.7, 134.3, 127.7/127 (2C, C-1, 1'),124.1, 121.1/121.0 (2C, C-6,6'), 120.7, 116.6, 115.8/115.7/115.5 (2C, C-5, 5'), 113.5, 112.8,110.3, 109.9 (2C, C-2, 2'), 55.6/55.6 (2C, C-3, 3' Ar- OMe); EA Found: C , 67.57; H, 4.92; N, 5.68 $C_{26}H_{24}N_2O_6$ requires C, 67.52; H, 5.25; N, 6.08; LRMS (ESI): *m/z* 459.6; HPLC purity: 98 %, $t_{R'}$ = 17.63 min.

References

(1) Rasmusen, H. B.; Christensen, S. B.; Kuist, L. P.; Karazami, A. *Planta Med.* **2000**, *66*, 396-398.

(2) Pedersen, U.; Rasmussen, P. B.; Lawesson, S. -. *Liebigs Ann. Chem.* **1985**, 1557.

(3) Selvam, C.; Jachak, S. M.; Thilagavathi, R.; Chakraborti, A. K. *Bioorg. Med. Chem. Lett.* **2005**, *15*, 1793-1797.

(4) Flynn, D.; Belliotti, T.; Boctor, A.; Connor, D.; Kostlan, C.; Nies, D.; Ortwine, D.; Schrier, D.; Sircar, J. *J. Med. Chem.* **1991**, *34*, 518-525.

(5) Bera, R.; Sahoo, B. K.; Ghosh, K. S.; Dasgupta, S. *Int. J. Biol. Macromol.* **2008**, *42*, 14-21.

(6) Wiles, D. M.; Suprunchuk, T. *Can. J. Chem.* **1968**, *46*, 1865.

APPENDICES

Appendix A

Table 1: Pilot Toxicological Investigations - Guidelines for Dose Selection and Classification of Compounds

Test dose (mgkg-1)	Result	Action
5	Less than 90% survival	Classify as very toxic
	90% or more survival but evident toxicity	Classify as toxic
	90% or more survival, no evident toxicity	Retest at 50mgkg-1
50	Less than 90% survival	Classify as toxic Retest at 5mg kg-1 If not already tested At that dosage
	90% or more survival, but evident toxicity	Classify at harmful
	90% or more survival, no evident toxicity	Retest at 500mgkg-1
500	Less than 90% survival, or evident toxicity and no deaths	Classify harmful. Retest at 50mgkg-1 If not already tested At that dose
	No evident toxicity	Unclassified

Source: Van den Heuvel et al (1987)[1]

[1]van den Heuvel, M. J. ; Dayan, A. D. ; Shilaker, R. O.Hum. Toxicol. **1987**, 6, 279-291.

Appendix B

Calculation of the suppression of parasitemia of mice infected with *Plasmodium berghei* ANKA

The percentage suppression of parasite growth on day 4 of the study was calculated using the formula: 100 [1 – (mean parasitemia of test group/mean parasitemia of control group)].

Table 1: Parasitemia and calculation of percentage suppression

Mouse	Control	2.2.2a	2.5.4	2.8.1	2.10.3
1	2.357	1.623	0.571	2.324	0.000
2	4.043	1.958	0.000	4.023	0.199
3	2.840	0.685	1.176	2.843	2.387
4	3.588	0.000	1.523	0.469	2.022
5	3.448	2.375	1.130	3.256	1.774
MEAN	3.255	1.328	0.880	2.583	1.276
IC_{50} test/IC_{50} control	1.000	0.408	0.270	0.793	0.392
%age suppression	**0.0**	**59.2**	**73.0**	**20.7**	**60.8**

Table 2: Parasitemia and calculation of percentage suppression for mice treated with hydrazinocurcumin (2.2.1a)

MOUSE	CONTROL	25 mg/kg	50 mg/kg	100 mg/kg
1	1.299	5.140	3.415	2.614
2	6.604	2.745	2.564	1.667
3	0.656	0.000	2.428	4.068
4	3.970	0.000	2.083	5.010
5		3.692	1.905	2.829
MEAN	3.132	2.315	2.479	3.238
IC_{50} test/IC_{50} control	1.000	0.739	0.791	1.034
%age	**0%**	**26%**	**21%**	**-3%**

Appendix C

Blood Concentrations of Mice Treated with Hydrazinocurcumin (2.2.1b) in the Pharmacokinetic Study

Table 1: Blood concentrations (µg/ml) of mice that received hydrazinocurcumin (2.2.1b) in vehicle A

Time (h)	Mouse One	Mouse Two	Mouse Three	Mouse Four	Mouse Five	Mouse Six
0	0	0	0	0	0	0.0255 [a]
0.5	0.545 [a]	0.822	1.8	0.572 [a]	0.191 [a]	3.33
1	1.3	0.364 [a]	5.75	3.26	3.01	0.159 [a]
2	0.545 [a]	0.116 [a]	0.685	0.169 [a]	0.0703 [a]	0.00818 [a]
5	0	0.171 [a]	0.285 [a]	0.182 [a]	0	0.196 [a]

[a] Below lower limit of quantification

Table 2: Blood concentrations (µg/ml) of mice that received hydrazinocurcumin (2.2.1b) in vehicle B

Time (h)	Mouse One	Mouse Two	Mouse Three	Mouse Four	Mouse Five
0	0.188	0	0	0	0
0.5	0.18	0.252	0.609	0.113	0.145
1	0.0454	0.262	0.16	0.238	0.55
2	2.18	1.12	0.122	0.0833	0.0548
5	0	0.364	0.119	0.133	0

All values except the shaded boxes were BLOQ

Table 3: Blood concentrations (µg/ml) of mice that received hydrazinocurcumin (2.2.1b) in vehicle C

Time (h)	Mouse One	Mouse Two	Mouse Three	Mouse Four	Mouse Five
0	0	0	0	0	0
0.5	0.321	0.0516	0	0	0
1	0	0.117	0	0	0
2	0	0	0	0	0
5	0	0.196	0	0	0